BEHAVIOUR OF AXIALLY RESTRAINED CONCRETE SLABS

HISHAM MOHAMMED AL-HASSANI, B.Sc.(Eng), M.Sc.(Eng)

A THESIS SUBMITTED TO THE UNIVERSITY
OF LONDON FOR THE DEGREE OF
DOCTOR OF PHILOSOPHY

JULY 1978

DEPARTMENT OF CIVIL AND MUNICIPAL ENGINEERING
UNIVERSITY COLLEGE LONDON

TO MY FATHER WITH RESPECT

ABSTRACT

A study is presented of the behaviour of reinforced concrete slab strips under the combined effect of bending and compressive membrane action. The existing methods for allowing for membrane action in predicting the plastic behaviour of reinforced concrete slabs are reviewed and their limitations outlined. A new theory of the plastic behaviour of materials with tension cracks based on 'total strain' and 'strain rate' flow rules is proposed and applied to problems of axially restrained concrete slab strips. The effect of elastic axial strains, flexible restraints and physical gaps at the boundaries are carefully considered. The results of a series of experiments on slab strips designed to test the proposed theory are presented.

ACKNOWLEDGMENTS

I take this opportunity to express my deepest thanks and indebtedness to Professor K.O. Kemp for providing the facilities required to conduct this research. His guidance, sincere efforts and valuable suggestions were important factors in the achievement of this work.

I should like to thank Messrs. D. Vale, J. Ford and Y. Adepoju for their assistance and advice in preparing the experimental programme.

I gratefully acknowledge the financial support given to me by the Iraqi Government - Ministry of Higher Education and Scientific Research.

Particular thanks are due to my parents for their continuous support and encouragement.

Finally I should like to thank Mrs. H. Redgewell for having the patience to type a difficult manuscript.

LIST OF CONTENTS

NOTATION

A_s	Area of bottom reinforcement per unit width of slab
$\bar{A}_s$	Total area of bottom reinforcement in a slab strip
A_s'	Area of top reinforcement per unit width of slab
a	Distance of concentrated load from slab support
b	Breadth of slab strip
C	Compressive force on concrete per unit width of slab
c	Distance of the positive plastic hinge from the centre
d	Overall depth of slab
d_1	Effective depth of slab
d_n	Depth of neutral axis measured from the compressed face of slab
E_c	Modulus of elasticity of concrete
E_s	Modulus of elasticity of steel
e	Plastic axial elongation at mid-depth of slab
e_b	Elastic shortening of slab strip due to membrane force = $\frac{N}{S_b}$
e_e	Value of e at slab ends
e_o	Value of e at centre of slab
e_s	Elastic spread of surround due to membrane force = $\frac{N}{S_s}$
f_{rp}	Modulus of rupture of concrete
f_y	Yield stress of steel reinforcement
h	Vertical distance between the membrane forces at sagging and hogging yield lines
k	Membrane force parameter
k_1k_3u	Average bending compressive stress on concrete at yield
k_2d_n	Depth of resultant compressive force on concrete at yield, measured from the compressed face of slab

L	Span of slab (Long span of rectangular slab)
l	Short span of rectangular slab
M	Yield bending moment per unit width of slab
M_o	Value of M with zero membrane force
m	Ratio of outward movement of restraining body to elastic shortening of the restrained slab element or beam
N	Yield membrane force at mid-depth per unit width of slab
$\bar{N}$	Total yield membrane force in a slab strip acting at mid-depth
P	Concentrated yield load on a slab strip of unit width
$\bar{P}$	Total concentrated yield load on a slab strip of width b
p	Intensity of uniformly distributed loading
P_c	Value of concentrated load at first visible crack
$(P_{max})_E$	Experimental maximum value of P
$(P_{max})_T$	Theoretical maximum value of P
P_y, p_y	Value of P, p corresponding to yield line theory collapse load
R	Radius of circular slab
r	Parameter fixing extent of central tensile membrane
S, $\bar{S}$	Stiffness factors; $S = \lambda S_b$; $\bar{S} = \frac{16k_2}{k_1 k_3} \frac{S}{\frac{L}{d}u}$
S_b	Elastic stiffness of slab strip
S_s	Elastic stiffness of surround
T_o, KT_o	Yield forces in tensile reinforcement per unit width of slab, in orthogonal directions
u	Concrete cube strength
v	Membrane force parameter

w_o Vertical deflection at centre of slab

w_o' Value of w_o when the slab is first cracked throughout its depth OR when the membrane force decreases to zero in slab strip

$(w_o)_{cr}$ Critical value of w_o corresponding to maximum membrane force

$(w_o)_e$ Value of w_o due to elastic deformations

$(w_o)_p$ Value of w_o due to rotation at yield hinges

γ Parameter denoting ratio of reinforcement = $\frac{A_s'}{A_s}$

Δ Initial gap at supports of axially restrained slab

δ Central horizontal movement of slab end

ϵ Total plastic axial strain at mid-depth of slab

η Parameter fixing yield-line pattern

θ Plastic rotation of slab element about the support

$\varkappa$ Total plastic curvature of slab section

λ Degree of the stiffness of the surround = $\frac{\frac{S_s}{S_b}}{1 + \frac{S_s}{S_b}}$

μ Depth of neutral axis measured from mid-depth of slab according to strain rate flow rule

μ' Depth of neutral axis measured from mid-depth of slab according to total strain flow rule

μ_o Value of μ when membrane force is zero

ν, ν_1 Parameters denoting elastic compressibility and elastic extensibility of slab respectively

ρ Coefficient of orthotropy

σ_c Average compressive bending stress on the concrete

Φ Inclination of the line joining the neutral axis position at the centre and support

Ψ Parameter fixing yield-line pattern

CHAPTER I

INTRODUCTION

1.1 YIELD LINE THEORY

The prediction of the collapse loads of reinforced concrete structures using inelastic concepts has been given considerable attention during the past half of this century. Accordingly methods have been developed which take into account the conditions that apply in the structure just prior to failure. One of these methods (yield line theory) which considers the limit state of collapse for reinforced concrete slabs was first proposed in Denmark by Professor K.W. Johansen (1).

In this theory (which forms part of the general theory of limit analysis), the structural elements are assumed to behave in a rigid perfectly plastic manner, and elastic deformations, strain hardening effects, shear stresses as well as membrane stresses, are ignored. Two analytical methods, 'virtual work' and 'equilibrium', can be used in this theory to predict the ultimate flexural strength of a slab once a valid mechanism or a yield line pattern has been postulated for the slab. Yield line theory is simple in concept and amenable to hand computation. Furthermore, its applicability to slabs with complex shapes, boundary conditions and loading have led to extensive use of this theory and its recommendation in Codes of Practice (2).

But despite all these advantages, Johansen's yield line theory gives no information on deflections and little on the moment field at collapse. In addition, the theory grossly underestimates the load carrying capacity of reinforced concrete slabs when they are restrained axially against any lateral movement. It also fails to give the actual physical picture of the behaviour of such slabs since it considers flexure only and neglects membrane action.

1.2 MEMBRANE ACTION - THE CONCEPT

In reinforced concrete slabs, bending is usually accompanied by lateral displacements at the edges of the slab. In axially restrained slabs, such displacements are prevented by the support

restraints and, therefore, compressive membrane forces appear. If the deflection of the slab is small relative to its thickness, such forces at mid span may act above those at the supports and an arching or dome action will be formed. This is known as compressive membrane action and in this way very high loads can be sustained with very small deflections. Tests conducted on slabs restrained against lateral movements have indicated ultimate strengths which are far in excess of those predicted by Johansen's yield line theory because of the development of large compressive membrane forces in the slab which raise the ultimate moments at the yield lines significantly above those occurring in pure flexure.

In axially unrestrained slabs where the collapse mechanism forms a non-developable surface, the load necessary to produce increasing deflection after initial yielding; depends on, and increases with, the deflection. This is known as tensile membrane action. This kind of membrane action will not greatly influence the load at which the yield mechanism forms, but it will raise the load necessary to produce continuing deflection. The increases in strength in unrestrained slabs arise partly from the tensile membrane action produced in the central region of the slab and partly from the increased yield moment in the outer regions where compressive membrane action is caused.

1.3 LOAD-DEFLECTION BEHAVIOUR OF SLABS WITH MEMBRANE ACTION

The results of the previous studies of membrane action (as will be discussed in detail in Chapter 2) show that the effect of membrane action in reinforced concrete slabs is to produce load versus deflection curves of the form given in Fig. (1). These curves are of two types depending on the boundary conditions of the slab.

1.3.1 LOAD-DEFLECTION BEHAVIOUR OF A SLAB AXIALLY RESTRAINED (TYPE I)

If a reinforced concrete slab is restrained completely against any lateral movement and subjected to a transverse loading system, the load-deflection curve will have the shape shown

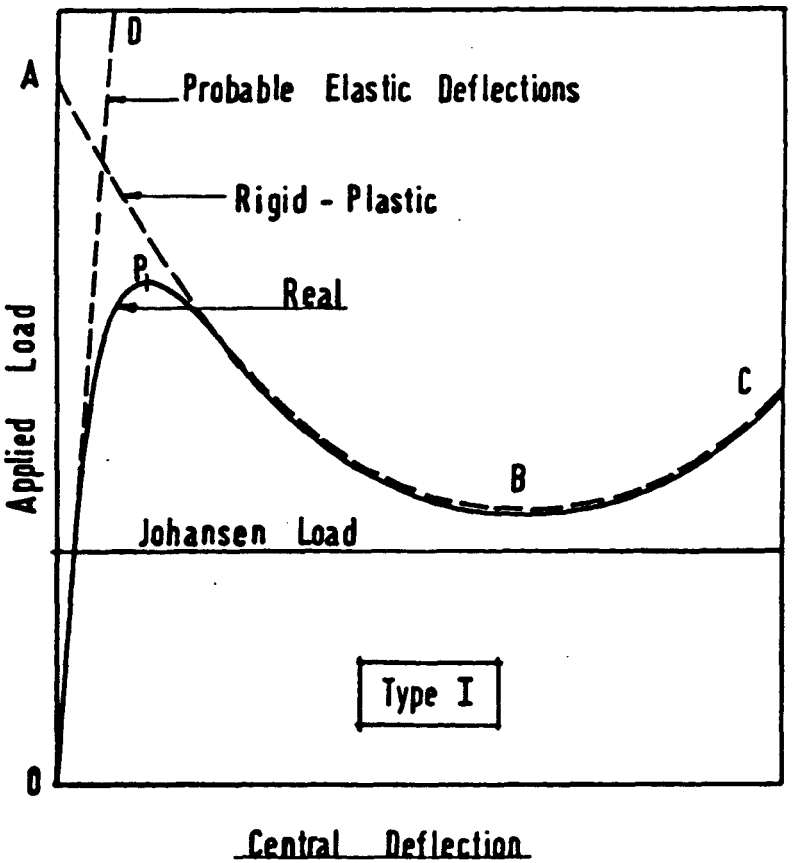

(a) Load - Deflection Behaviour of a Slab Axially Restrained

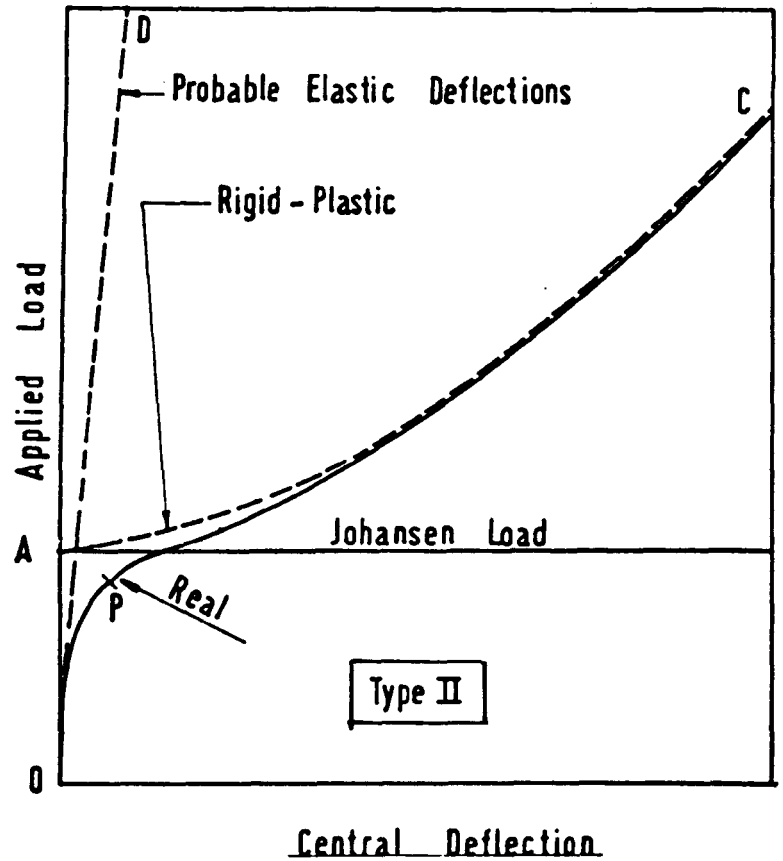

(b) Load - Deflection Behaviour of an Axially Unrestrained Slab

FIG (1)

in Fig (1a).

In this figure, the curve ABC represents the load-deflection characteristics of the slab on the assumption that the slab behaves in a rigid-perfectly plastic manner and that elastic deflections, which include axial strains caused by compressive membrane forces as well as creep and shrinkage strains, are ignored. It has been pointed out by Wood (3) in his solution of the circular slab that, according to these assumptions, the compressive membrane forces as well as the corresponding vertical loads will have their maximum values at the start of collapse (when the central deflection of the slab is zero). This very high initial load, which is many times greater than that predicted by yield line theory, is represented by point A in the figure.

However, if the elastic deflections of the structural member are considered (line OD), the actual ultimate load will be reduced to point P as shown. The experimental tests which have been conducted on such types of slabs have confirmed that the curve OPBC is the most representative behaviour. The initial linearity in this curve, therefore, represents the elastic deformation of the uncracked slab. In fact, considerations of the elastic axial deformations will change the form of the behaviour of the membrane forces as well. In this case, the compressive membrane forces start to increase from zero (point O) to a maximum value that lies somewhere between points P and B. Therefore, the portion OP of the curve may be considered as a region of increasing membrane action.

As the deflection of the slab is increased, the load carried by the slab decreases rapidly due to the compressive membrane forces becoming smaller. A limiting stage is reached at point B when the membrane forces in the central region of the slab commence to change from compression to tension with cracks extending throughout the depth of the concrete due to the large stretch of the slab surface. Unreinforced slabs will carry no further load once this stage is reached.

A reinforced concrete slab can carry some extra load with further increments in deflection beyond point B. Although at this

particular point the concrete in the central region of the slab can carry no more load due to cracks penetrating its full thickness, the stress and deflection of the reinforcement enable the slab to carry load by tensile membrane action. The increase in load with further deflection stops only when the reinforcement begins to fracture (point C in the figure). However, if the slab is heavily reinforced, the load carried by tensile membrane action at point C may well exceed the ultimate flexural load defined by point P.

It is worth commenting here that the load-deflection curve described above is only obtained if a load system is used with sufficient stiffness to allow the descending region P to B of the load-deflection curve to be followed. If the load causing the failure of the slab is the practical case of gravity loading, which remains unchanged as the slab deflects, the load-deflection curve will run from O to P as before and then move dynamically to a point at the same load level on the curve BC. Thus if the point C is not as high or higher than the point P, gravity loading will cause an unstable failure at P.

1.3.2 LOAD-DEFLECTION BEHAVIOUR OF AN AXIALLY UNRESTRAINED SLAB (TYPE II) :

In an axially unrestrained slab, the membrane forces will become significant only when a collapse mechanism forms that has a non-developable surface. Therefore if the slab is assumed to be rigid - perfectly plastic, the initial collapse load, in this case, will be the Johansen load at zero deflection (see point A in Fig. 1b). As the deflection increases, the membrane forces are found to vary linearly with the deflections which, in turn, enable the slab to carry more load with continuing deflection. This is represented by the curve AC in the figure, and if the elastic deflections are introduced, the actual behaviour will be the curve OPC.

It has been found (4) that the enhancement in the load at any value of deflection is proportionately greater for lightly reinforced slabs. This enhancement increases with the deflection due to the appearance of a pure tensile membrane after complete

penetration of the cracks throughout the whole thickness of the slab occurs at the central region. This can be readily seen in Figure (1b) where the shape of the curve becomes steeper at large values of deflection. The slab will continue to carry increasing load until the reinforcing bars begin to fracture leading to collapse.

1.4 AIM AND SCOPE OF WORK

In the review of the previous work on the problem of membrane action in slabs (as will be shown in Chapter 2), it is found that two fundamental assumptions about plastic behaviour; namely, total strain and strain rate, have been adopted in the analyses. These approaches showed different results both in estimating the ultimate strengths and in studying the load-deflection behaviour of such slabs. In this investigation, a careful examination will be made of these two methods to determine the correct assumption.

Chapter 2 of this thesis presents a general critical study of previous work on membrane action in reinforced concrete slabs. The assumptions and limitations upon which each approach was based are stated and equations of the collapse loads are given in their final forms. Comparison is also made between experimental tests and the theoretical predictions.

In Chapter 3, a yield criterion of a slab section under the combined effect of bending and membrane action is derived and a new study of the real significance of total strain and strain rate assumptions and the relevance of cracking is presented.

In Chapter 4, comparison is made between total strain and strain rate approaches when applied to reinforced concrete slab strips laterally restrained against longitudinal expansion. The slab strips in this case are assumed to behave in a rigid - perfectly plastic manner. The comparison is presented to include both the ultimate strengths as well as the load-deflection characteristics.

In Chapter 5, the effects of the axial shortening of the slab member as well as the outward movement of the surround are introduced into the analysis. In this chapter, important conclusions are drawn on the correct analysis to use.

A series of tests on restrained slab strips is presented in Chapter 6 to check the validity of the proposed hypothesis.

Finally, general discussions and conclusions are presented in Chapter 7. Some suggestions and remarks for future research are also given in this chapter.

CHAPTER 2

PREVIOUS STUDIES OF MEMBRANE ACTION

During the last twenty years of this century, intensive studies have been carried out to try to understand and utilize the considerable reserves of strength in reinforced concrete slabs in which membrane action can occur. These studies have not only verified that Johansen's yield line theory grossly underestimates the strength of the slabs but have also given particular attention to the relationship between the load and the deflection in the slab as yield proceeds.

One of the first records of measured ultimate loads being higher than those calculated by yield line theory is found in a report by Thomas (5). This report commented upon the enhanced ultimate strength of beams and slabs which were tested with boundaries restrained against lateral movement.

It was Professor Ockleston (6), in 1955, who made the effect of this type of boundary condition most widely known as a result of the full scale loading tests on a conventional reinforced concrete building (The Dental Hospital at Johannesburg). Some one way and two way slabs were uniformly loaded to failure and the enhanced ultimate strengths obtained were up to about three times the yield line theory load. Ockleston, in his report, attributed the increase to ignoring the effect of tensile strength of concrete in the method of analysis, but in a later paper (7), he showed that this unexpected result can be explained by an arching action due to the development of compressive membrane stresses in the concrete.

About the same time, Powell (8), of Cambridge University, conducted a series of tests on encastré model slabs and the collapse loads were extraordinarily large.

The University of Illinois (9) have reported on the testing of a 1/4 scale model of a 9 panel (3 by 3) slab and beam floor and the supporting beams failed when the load on the interior panel was at approximately twice the yield line theory load. Discounting the tensile membrane action and the strain hardening of

the reinforcement, it was commented that at high deflections the increased bending moment at yield sections due to an apparent increase in the lever arm could account for the high ultimate load.

This conclusive experimental evidence of the beneficial effect of membrane action on the ultimate strength of slabs has attracted many other investigators. Studies have been carried out to find the exact effects of membrane action in different shapes of slabs and boundary conditions. As a result, different methods of approach have been obtained, each based on certain assumptions and subject to certain limitations. It is the aim of this chapter to study critically these methods in detail, identifying their assumptions and limitations, the technique of analysis, presenting the equations for the collapse loads in a common form and, finally, to examine the degree of agreement with the experimental results.

For convenience, the methods are divided into three different types:

1. Methods based on rigid - plastic considerations
2. Methods based on elastic - plastic considerations
3. Strip method

2.1 METHODS BASED ON RIGID - PLASTIC CONSIDERATIONS

A material is assumed to be rigid - perfectly plastic if the material is rigid up to the yield point and then deforms plastically at constant yield stress. This implies ignoring both the elastic deformations and any strain hardening or softening. On this assumption, and some others, analyses have been attempted by several investigators, notably, Wood (3) (on the circular slab), Kemp (4) (on the square slab), Morley (10) (on the polygonal and rectangular) and many others.

But one of the earliest methods of analysis based on such assumptions was attempted by Ockleston (7) on the two way rectangular slab shown in Fig. (2.1e). The attempt was made to explain

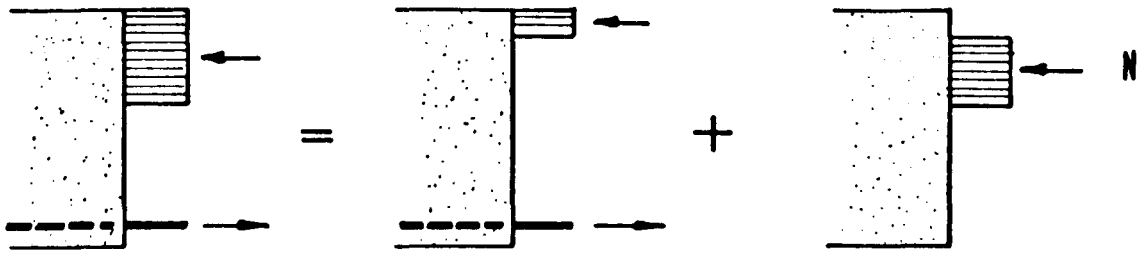

(a) Stress Distribution at a Yield Line

(b) Stress Distribution According to Yield Line Theory

(c) Compressive Membrane Force

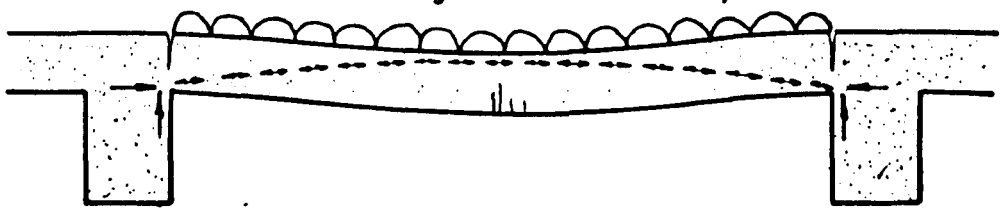

(d) Arching Action in a Slab

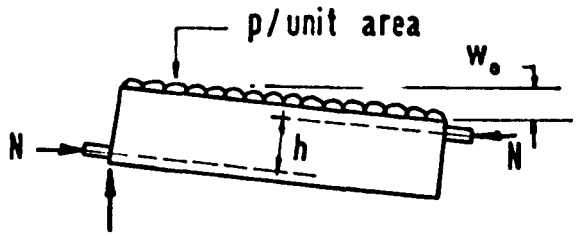

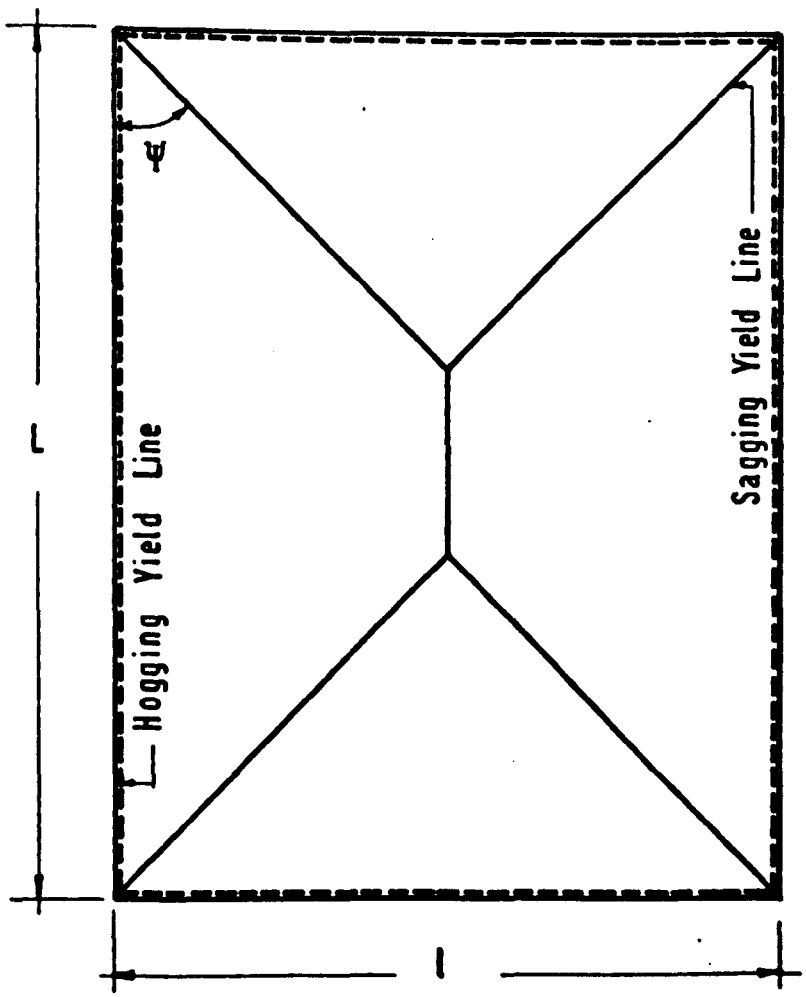

(e) Yield Line Pattern of a Rectangular Slab

FIG. (2.1)

in algebraic form how the phenomenon of membrane action can influence the load carrying capacity of such slabs. In this analysis, the membrane forces were assumed to be constant in all directions and to have no appreciable effect on the mechanism of collapse. Furthermore, the distribution of stress at any yield line (Fig. 2.1a) was regarded as the sum of that considered by the yield line theory (Fig. 2.1b), where the total compression is equal to the total tension in the steel, and the one in Fig. (2.1c) representing the compressive membrane force. In a slab-beam floor system, when the central deflection of the loaded slab is small relative to its thickness, such membrane forces at sagging yield lines will always act above those at boundary hogging yield lines increasing the load carrying capacity of the slab by the resulting arching action (See Fig. 2.1d). Therefore, for any increment of deflection, the energy absorbed at the yield lines due to this action can be equated to the work done by the applied load. In this way Professor Ockleston found that the enhancement in the load has the following expression :

$$\frac{\text{enhancement in p above yield line theory prediction}}{\text{above yield line theory prediction}} = 24\,\frac{N}{l^2}\,\frac{(\frac{L}{l} - \cot\Psi)(h - w_o) + (\tan\Psi + \cot\Psi)(h - \frac{w_o}{2})}{(3\frac{L}{l} - \cot\Psi)} \qquad (2.1)$$

where the compressive membrane force N and the vertical distance between the membrane forces at sagging and hogging yield lines (h) depend on the depth of the compression block.

Since neither the central deflection of the slab (w_o) nor the depth of the compression block at failure can be estimated, equation (2.1) cannot be applied to calculate the enhanced loads. However, this equation was used by Ockleston to explain the high ultimate loads obtained in his tests by introducing the measured deflection of the slab at failure for w_o and assuming the depth of the compression zone to be increased from 4.1 mm (0.16 in) (the value corresponding to bending action only) to 14.2 mm (0.56 in).

Many attempts have been made, since, to establish a formula from which the actual collapse loads can be predicted directly. These attempts appear to have been initiated by R.H. Wood (3), who, in Chapter 7 of his book "Plastic and Elastic Design of Slabs and Plates" and under the heading "The Problem of Minimizing the Reinforcement : Inducing Membrane Action", gave a theoretical solution to the problem of circular slabs (both clamped - axially restrained and simply supported - axially unrestrained). The term "arching action" is not a good enough description in Wood's view. It is rather a change in the yield criterion with compression in the slab. Especially in restrained slabs, where the restraint against lateral expansions provides a kind of self prestressing, the collapse does not usually commence before an appreciable increase in yield moments takes place. Wood's rigid - perfectly plastic approach is, therefore, based on establishing a yield criterion which includes the membrane stresses. For this purpose, a reinforced concrete slab section (Fig. 2.2a) of unit width and in which both materials are assumed to be rigid - perfectly plastic was considered under the effect of a bending moment M and a compressive axial force N, taken to act at the mid-depth of the slab. The moment M and the force N were assumed to be such that on this section the stress distribution of Fig. (2.2b) exists. From equilibrium considerations of longitudinal force and moment, the yield criterion was found to be :

$$\frac{M}{M_o} = 1 + \alpha\left(\frac{N}{T_o}\right) - \beta\left(\frac{N}{T_o}\right)^2 \qquad (2.2)$$

where $$\alpha = \frac{\frac{1}{2}\frac{d}{d_1} - \frac{3}{2}t}{1 - \frac{3}{4}t}$$

$$\beta = \frac{\frac{3}{4}t}{1 - \frac{3}{4}t}$$

$$t = \frac{A_s}{d_1}\frac{f_y}{u}$$

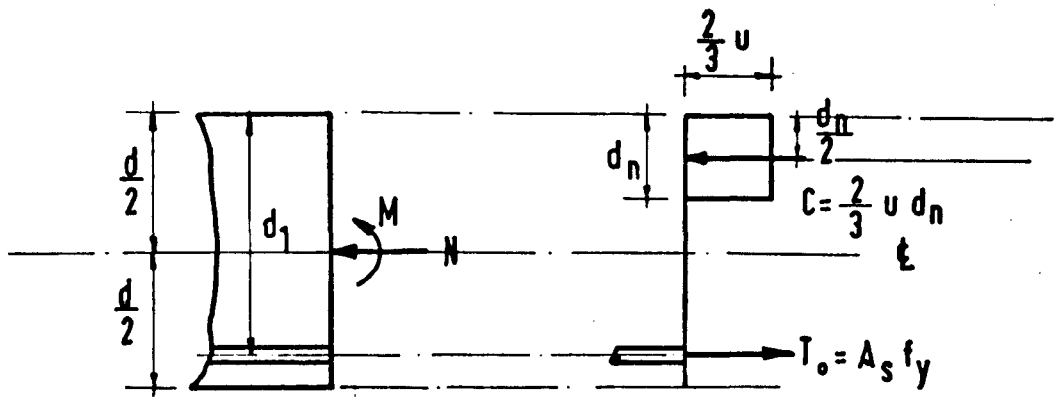

(a) Slab Section at Yield

(b) Stress Distribution on the Slab Section at Yield

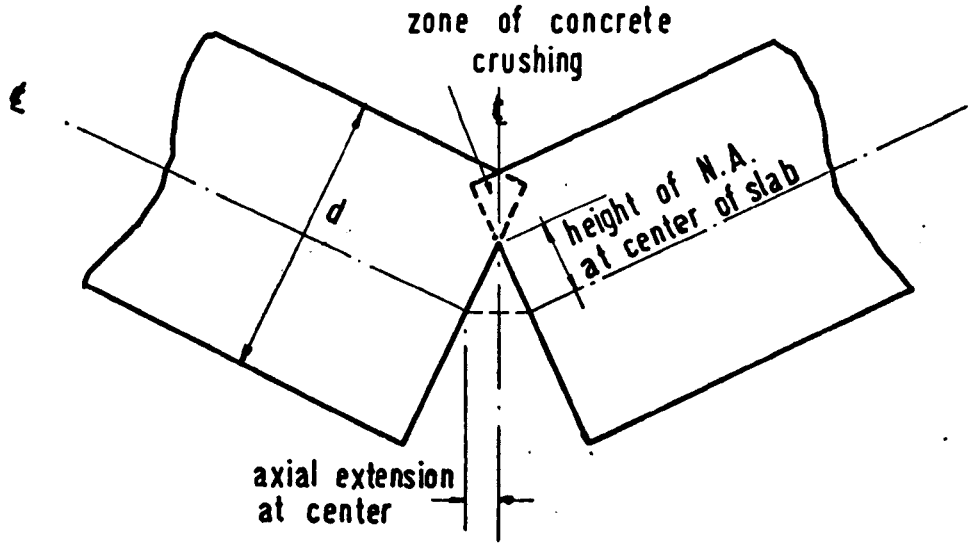

(c) Conditions at the Center of a Slab With a Conical Collapse Mode

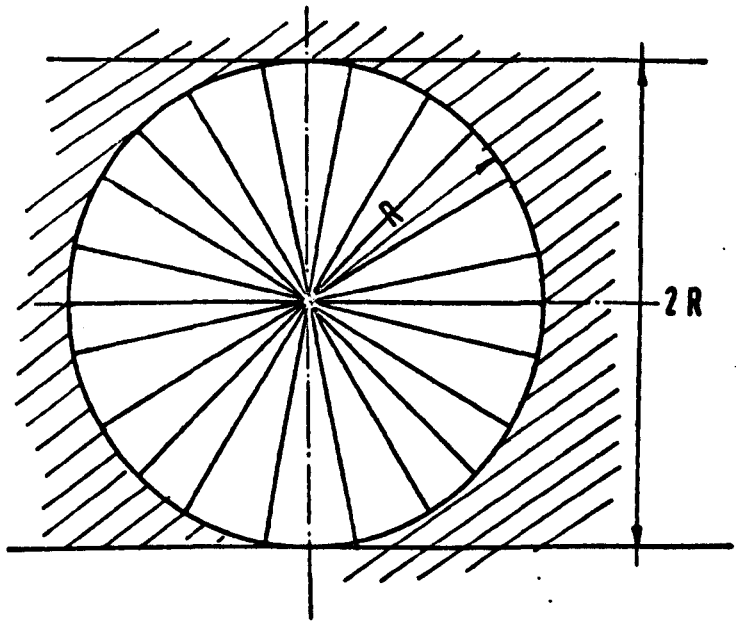

(d) Yield Line Pattern of a Circular Slab

FIG. (2.2)

M_o denotes the moment capacity of the section under bending only and T_o is the tensile yield force of the reinforcing bars.

This yield criterion was used to evaluate the curvature and extension strains of different sections of the circular slab shown in Fig.(2.2d). Following a total strain approach; solutions were presented for an isotropically reinforced and uniformly loaded circular slab with simple and clamped supports.

i. Simply Supported - Axially Unrestrained Circular Slab: This case was treated by Wood in two successive stages.

The first stage represents the development of the cracks from the tension face of the slab to the top surface during which compressive stress act on the concrete. The analysis presented for this stage involved using Timoshenko's (11) definitions for the axial extensions of an infinitesmal element and the assumption of the conical collapse mode shown in Fig.(2.2c). First, the circumferential stretch of any section inside the slab was obtained in terms of both the central axial extension and the central deflection (radial extensions were assumed zero) and by adopting the plastic potential theory and using total strains, the value of this stretch was obtained in terms of the depth of the neutral axis at the centre of the slab. A small element of a circular plate under radially symmetrical loading was then considered and equilibrium equations were derived to find the neutral axis depth at the centre and, subsequently, at any other section inside the slab. The yield criterion given by Eq.(2.2) was used to evaluate moments and membrane forces in the radial and circumferential directions. Boundary conditions were satisfied to find other unknowns and, thus, the ratio of the uniformly distributed load p carried by the slab including the effect of membrane action to the corresponding Johansen's theoretical limit analysis load p_y was found, for this particular stage, to be :

$$\frac{P}{P_y} = 1 + \frac{\beta}{16} \left(\frac{\alpha}{\beta} + 2\right)^2 \left(\frac{w_o}{d}\right)^2 * \qquad (2.3)$$

* This equation is incorrectly given in Wood's book (Eq.210, page 236) and implies a factor 12 in the denominator instead of 16.

where w_o is the central deflection of the slab and other notations are as defined in Eq. (2.2).

The limiting central deflection for this stage was shown to be :

$$\frac{w_o'}{d} = \frac{4}{(\frac{\alpha}{\beta} + 2)} \qquad (2.4)$$

The second stage starts when the central deflection of the slab exceeds the value given by Eq. (2.4). A pure tensile membrane action then starts to spread outwards from the central region as the deflection increases. The behaviour of the slab in this case may be imagined as concrete segments suspended by steel bars. The spreading of the tensile membrane increases with continuing deflection until all the bars commence to fracture. At a certain value of deflection the pure tensile membrane will reach a distance, say r from the centre of the slab (see Fig. 2.3). In Wood's analysis, the circumferential and radial membrane forces at this junction were taken to be equal to the tensile force of the reinforcement, the yield moments were defined by the yield criterion (Eq.2.2) and finally, the axial extension in the two directions were assumed identical. Following the same procedure as in the first stage, the ratio p/p_y for this case was found to be :

$$\frac{p}{p_y} = \frac{1 + \dfrac{1 - 5\frac{r}{R}}{1 - \frac{r}{R}}\beta}{(1 + 2\frac{r}{R})(1 - \frac{r}{R})^2} \qquad (2.5)$$

Thus for any junction radius r between plastic membrane and cone the load is known. The corresponding central deflection was found to be :

$$\frac{w_o}{d} = \frac{4}{(\frac{\alpha}{\beta} + 2)(1 - \frac{r}{R})} + \frac{\frac{3}{4}}{\beta(\frac{\alpha}{\beta} + 2)} (\frac{p}{p_y}) (\frac{r}{R})^2 \qquad (2.6)$$

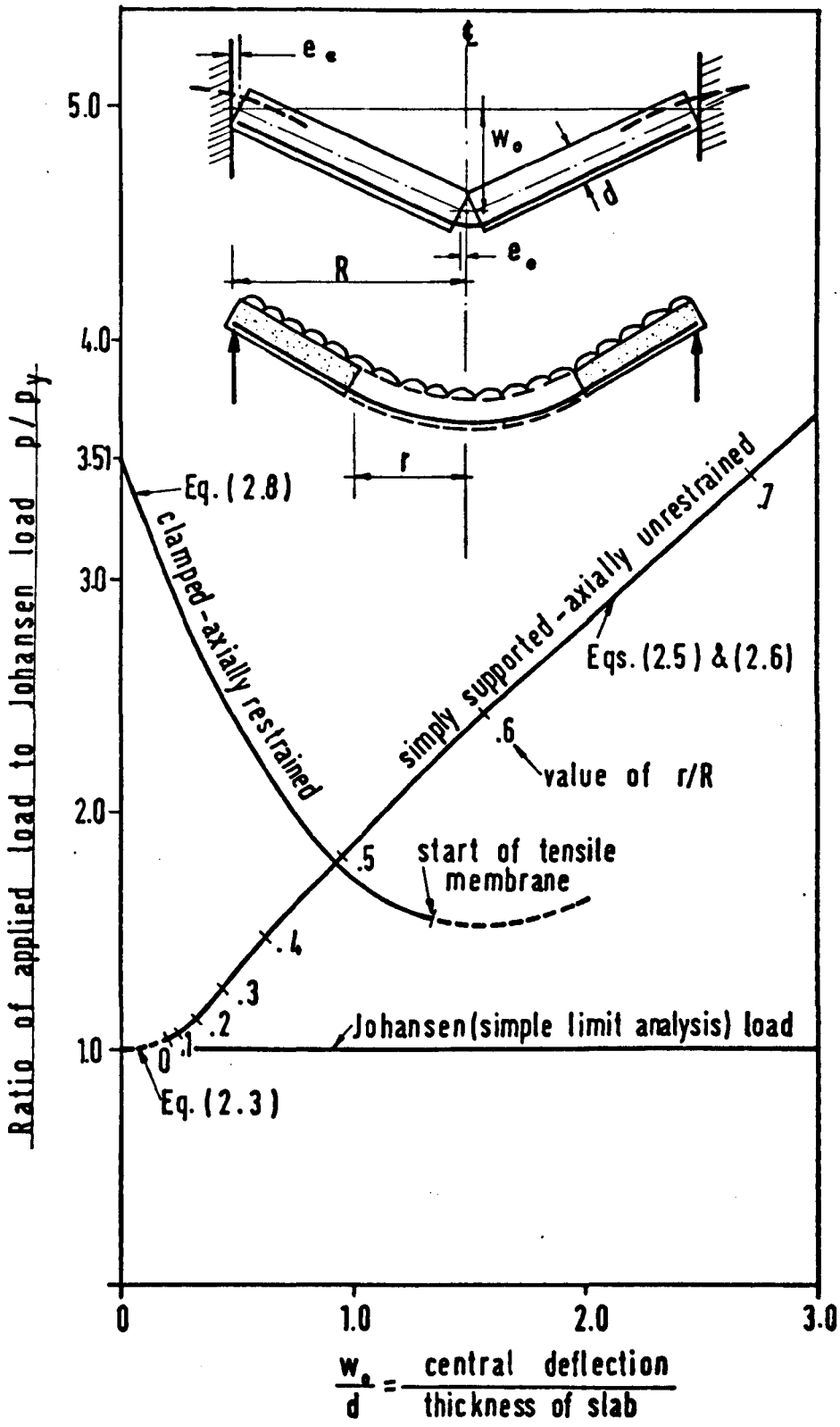

FIG. (2.3) Load - Deflection Relationship of a Circular Concrete Slab [Simply Supported - Axially Unrestrained and Clamped - Axially Restrained]

ii. Clamped - Axially Restrained Circular Slab: Axial restraint at the supports adds another unknown to the problem (the axial extension at the edge) and, hence, one more equation is needed. This difficulty, however, was overcome by considering the conical - deflection collapse mechanism of Fig.(2.3) in which the extra equation taken was the following compatibility equation :

$$R + e_o + e_e = \sqrt{R^2 + w_o^2} \qquad (2.7)$$

where e_o and e_e represent the axial extensions at centre and supports respectively. Following the same steps as in the simply supported case, the ratio p/p_y for clamped circular slabs was found to be :

$$\frac{p}{p_y} = 1 + \frac{\alpha^2}{4\beta} - \frac{\alpha}{4}\left(\frac{\alpha}{\beta} + 2\right)\left(\frac{w_o}{d}\right) + \frac{5}{64}\beta\left(\frac{\alpha}{\beta} + 2\right)^2\left(\frac{w_o}{d}\right)^2 \qquad (2.8)$$

Equation (2.8) represents the first stage in which the slab at the centre is not fully cracked. The limiting deflection for this case was found to be 4/3 times the slab thickness. Wood did not extend his solution to cover the second stage of tensile membrane action other than to point out that the load would be increased thereafter.

Figure (2.3) shows curves of load versus deflection plotted by using Eqs.(2.3), (2.5) and (2.6) for the simply supported - axially unrestrained case and Eq. (2.8) for the clamped - axially restrained case for a slab with the following properties :

$$f_y/u = 10; \quad A_s/d_1 = 0.4\%; \quad d/d_1 = 1.2$$

Wood also conducted some tests on lightly reinforced 1.727m (68 in) square slabs of 57.1 mm (2.25 in) thickness. These slabs were restrained at the boundaries against all movements by a massive reinforced concrete surrounding frame and were uniformly loaded to failure by means of 16 point loadings spaced at 0.457 m

(18 in) centres. The results of these tests, as well as the tests carried out by Powel (8) and Thomas (5), have confirmed that the load falls off rapidly once the ultimate load is reached, but also they showed that Eq.(2.8) overestimates the ultimate load by a considerable margin due to ignoring the elastic shortening of the slab element and the outward movement of the surround in the derivation of the equation.

In 1967, Kemp (4) presented an approach, following Wood, to solve the problem of tensile membrane action in simply supported - axially unrestrained reinforced concrete square slabs which were assumed to be isotropically reinforced, uniformly loaded and to have rigid - perfectly plastic properties.

Kemp's method of analysis, again based on a total plastic strain approach, included the determination of the position of the neutral axis along the yield lines by combination of geometrical considerations and in-plane equilibrium. First, the horizontal translation of the triangular middle surface elements due to a vertical deflection w_o at the centre of the slab was obtained in terms of the axial strain at the centre. A compatibility equation and plastic potential theory were then used to express the height of the neutral axis at any section along the yield lines in terms of the neutral axis depth at the centre of the slab. Thereafter, the neutral axis depths at all sections were obtained by considering the horizontal force equilibrium of a slab segment. The yield criterion was then used to evaluate the yield moments and the membrane forces along the yield lines. The results showed that the membrane forces vary linearly with the central deflection w_o and that when w_o reaches a certain value w_o', which was found to be the same as that given by Wood for circular slabs (Eq. 2.4), the neutral axis will lie outside the slab section in the central region. The slab was then considered to be cracked throughout its depth in this region and the axial force was taken to be the yield force of the reinforcement. With increasing deflection the pure tensile membrane action was considered to spread outwards from the centre of the slab. After

evaluating the yield membrane forces and the yield moments as a function of the central deflection of the slab; the yield loads corresponding to any given central deflection were found by considering the moment equilibrium equation for one of the four rigid triangular elements of the slab. In this moment equilibrium equation, the vertical shear forces and torsional moments along the yield lines were assumed zero because of symmetry arguments. In this way, the ratio p/p_y for simply supported square slabs was found to be as follows :

i. For $0 \leqq \frac{w_o}{d} \leqq \frac{4}{(\frac{\alpha}{\beta} + 2)}$

$$\frac{p}{p_y} = 1 + \frac{\beta}{16}(\frac{\alpha}{\beta} + 2)^2 \, (\frac{w_o}{d})^2 \qquad (2.9)$$

ii. For $\frac{w_o}{d} \geqq \frac{4}{(\frac{\alpha}{\beta} + 2)}$

$$\frac{p}{p_y} = 1 + \beta + \beta \, (\frac{\alpha}{\beta} + 2)(\frac{w_o}{d}) - 2\beta\sqrt{(\frac{\alpha}{\beta} + 2)(\frac{w_o}{d})} \qquad (2.10)$$

The proportional increase in the yield load due to membrane action (Eq. 2.9) is identical with Eq.(2.3) given by Wood for the simply supported circular slabs. For large values of central deflection w_o, the solution given by Eq. (2.10) is different from the corresponding equation developed by Wood (Eq. 2.5) because the assumed yield mechanisms are of different forms after the pure tensile membrane develops. Eq. (2.10) by Kemp predicts rather lower increases in the yield load than Wood's analysis.

The approach adopted by Morley (10) was also based on rigid - plastic theory where deformation fields are straightforward developments of conventional yield-line patterns. Isotropically reinforced concrete slabs under proportional loading normal to the

original plane of their middle surface were considered. Clamped - axially restrained and simply supported - axially unrestrained polygonal slabs and rectangular slabs with all edges fully restrained against lateral movement were included. Analysis of the polygonal slabs covered the range from the initial mechanism to pure tensile membrane action and cracking at large deflections while the solution given for the rectangular slab was only concerned with the initial compression stage. However, in all cases, the load factor at any stage of deflection was assessed by equating the work done by the loads to the energy dissipated plastically within the slab, during a small additional deflection in the assumed mode. Moreover, the stress resultants developed and the energy dissipated in a yield-line were taken to depend only upon the strain rates at that stage, in accordance with the plastic potential 'flow-rule'.

Morley used the technique of searching for the least possible load estimate at a given stage of deflection, for a number of different deformation patterns, since a 'least possible load estimate' is believed to be sufficiently accurate when the assumed range of deformation patterns approximates to the actual collapse mode. By considering a slab with a yield-line pattern, an estimate of the load factor at a given stage of deflection was obtained by using the principle of virtual work.

In deriving the equations for the ratio of the collapse load to yield line theory load, Morley used different parameters for the stress block and the lever arm from those specified by Wood and Kemp. If Morley's results are modified to be consistent with the concrete stress block parameters used by Wood and Kemp, to enable a strict comparison to be made, the load enhancement due to membrane action for a regular q-sided simply supported - axially unrestrained polygon becomes :

i. For $0 \leq \frac{w_o}{d} \leq \frac{2}{(\frac{\alpha}{\beta} + 2)}$

$$\frac{p}{p_y} = 1 + \frac{\beta}{12} (\frac{\alpha}{\beta} + 2)^2 (\frac{w_o}{d})^2 \qquad (2.11)$$

ii. For $\frac{w_o}{d} \geq \frac{2}{(\frac{\alpha}{\beta} + 2)}$

$$\frac{p}{p_y} = 1 + \beta + \beta\,(\tfrac{\alpha}{\beta} + 2)(\tfrac{w_o}{d}) - \tfrac{4\sqrt{2}}{3}\,\beta\sqrt{(\tfrac{\alpha}{\beta} + 2)(\tfrac{w_o}{d})} \qquad (2.12)$$

Equations (2.11) and (2.12) depend neither upon the load distribution nor upon the number q of the sides of the polygon. Therefore, the solution can be applied to any "symmetrically shaped slab" provided the slab is simply supported - axially unrestrained and isotropically reinforced in the bottom face only. However, according to this solution, the pure tensile membrane action will start at the centre of the slab when the deflection ratio w_o/d becomes $2/[(\alpha/\beta) + 2]$, which is one half the limiting value obtained when total strain concepts are used (Eq. 2.4). For deflections less than $2/[(\alpha/\beta) + 2]$ equation (2.11) holds, which predicts higher increases in the yield load than the total strain solutions given by Kemp (Eq. 2.9) and Wood (Eq. 2.3). For greater values of deflection, the predictions of equation (2.12) are similar to the corresponding result obtained by Kemp (Eq. 2.10) except that the last term has a factor 4/3 instead of $\sqrt{2}$ which again provides larger yield loads with continuing deflection. Comparisons of these results are shown graphically in Fig. (2.4). It can be seen from this figure that, at larger stages of deflection, the solution presented by Wood predicts more exaggerated load enhancements than the other two methods given by Kemp and Morley due to using a different mechanism.

Polygonal slabs with axially restrained encastré edges were also analysed for the case of uniform bottom steel only on the central yield lines and equal top steel only at the edges. The final expressions for p/p_y in this case, after modification of the concrete stress block parameters, are :

i. For $0 \leq \frac{w_o}{d} \leq \frac{2}{3}$

$$\frac{p}{p_y} = 1 + \frac{\alpha^2}{4\beta} - \frac{\alpha}{4}\,(\tfrac{\alpha}{\beta} + 2)(\tfrac{w_o}{d}) + \frac{5}{48}\beta(\tfrac{\alpha}{\beta} + 2)^2(\tfrac{w_o}{d})^2 \qquad (2.13)$$

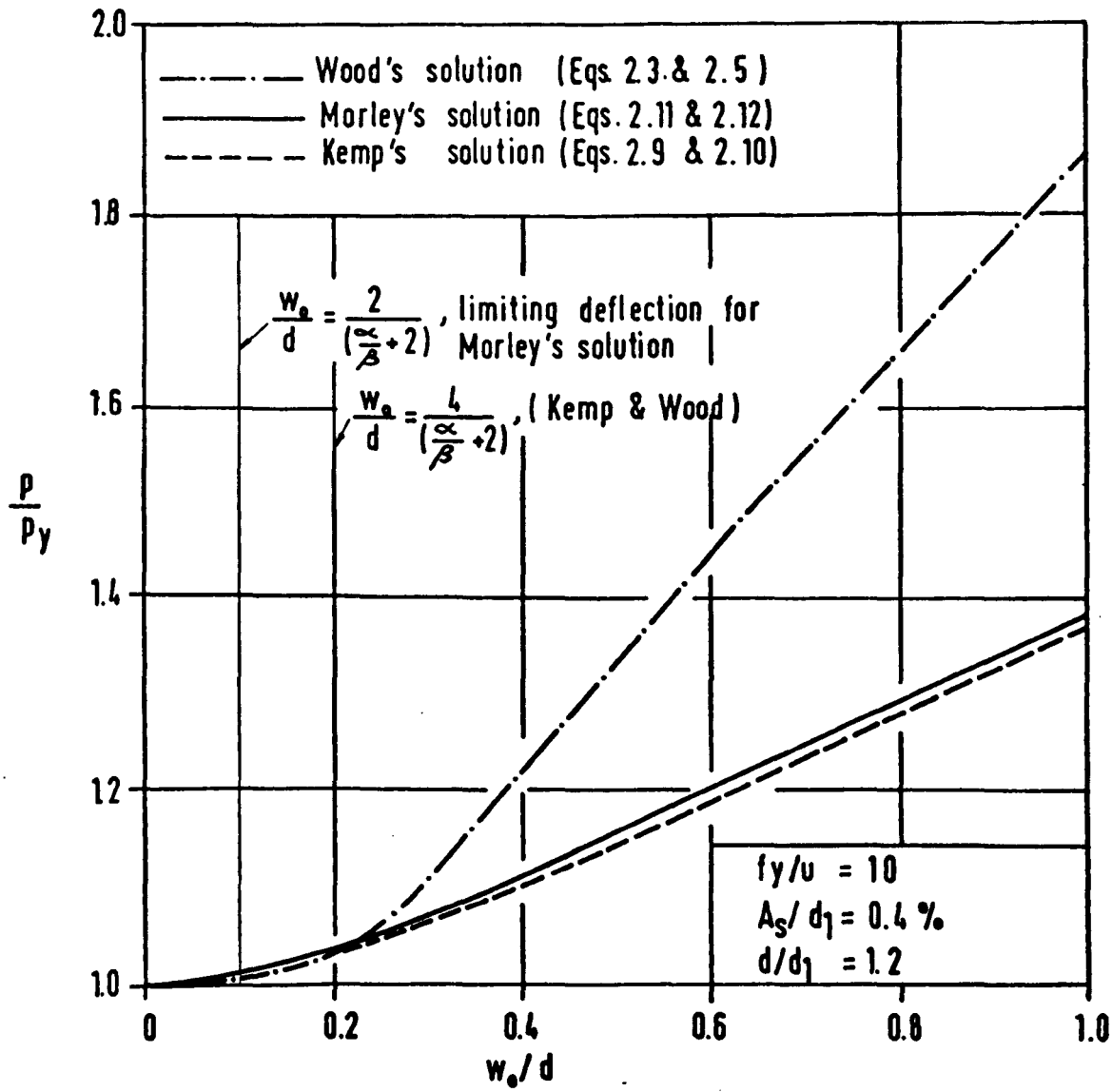

FIG. (2.4) Comparison of Results for a Simply Supported — Axially Unrestrained Slab

ii. For $\frac{w_o}{d} \geq \frac{2}{3}$

$$\frac{p}{p_y} = 1 + \beta + \frac{\alpha}{2}\left(\frac{\alpha}{\beta} + 2\right) + \beta\left(\frac{\alpha}{\beta} + 2\right)\left(\frac{\alpha}{\beta} + \frac{5}{2}\right)\left(\frac{w_o}{d}\right) + \frac{1}{3}\beta\left(\frac{\alpha}{\beta} + 2\right)^2 \left[\left(\frac{w_o}{d}\right)^2 - \sqrt{\left(\frac{w_o}{d}\right)\left(2 + \frac{w_o}{d}\right)^3}\right] \qquad (2.14)$$

Solution (2.13) can be compared with Wood's result (Eq. 2.8) on the clamped - axially restrained circular slab. The two equations are identical except in the factor of the last term. As shown in Fig. (2.5) the initial load factors are the same but the curves diverge as $\frac{w_o}{d}$ increases; again Morley's strain-rate method predicts greater loads than Wood, who uses total strain. According to Morley the pure tensile membrane action starts at deflection $\frac{w_o}{d} = \frac{2}{3}$ while Wood's prediction is $\frac{4}{3}$. For any value of central deflection greater than $\frac{2}{3}$ equation (2.14) holds in Morley's analysis while Wood did not extend his solution any further.

It must be emphasized here that if Morley had used total-strain concepts in his analysis, his solutions would have been exactly the same as those given by Wood and Kemp. The choice of flow rule to be used in such analyses, strain rate or total strain, is therefore of considerable importance.

In the case of rectangular slabs with axially restrained encastré edges, neither the in-plane shear forces nor the in-plane shear displacements were considered in the analysis. This approach gives approximate values for the horizontal displacement rates. Morley claimed that the neglect of work done in shear in his analysis is counterbalanced by using these approximate values of the displacement rates in the wrong equilibrium equations and leads to an overestimate of the load factor due to the condition of 'minimum possible load' being violated. However, a solution was only given for the special case of a rectangular slab with yield lines at 45^0 to its edges and uniform equal top and bottom reinforcement. The expression of the enhanced load is :

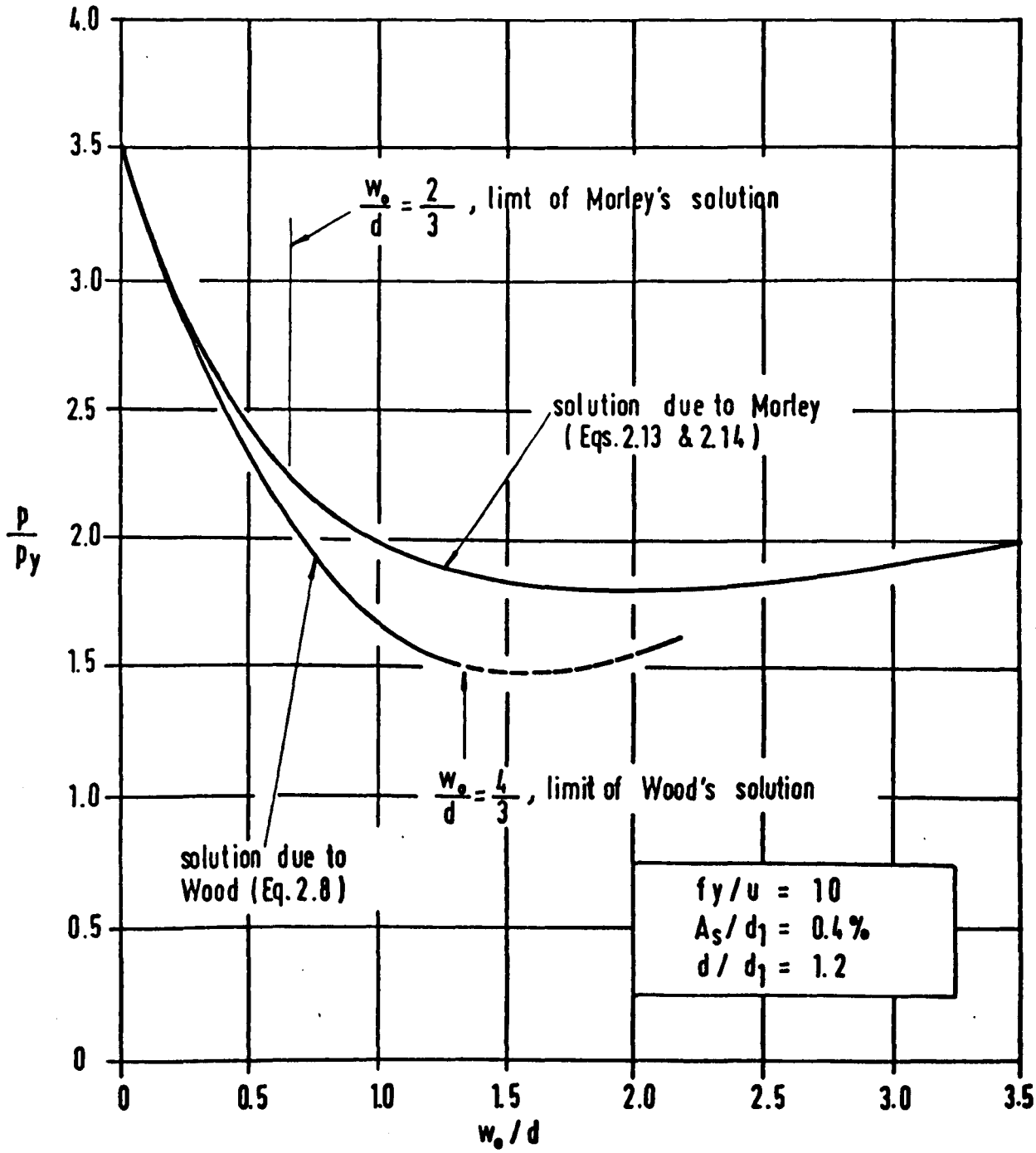

FIG. (2.5) Comparison of Results for an Axially Restrained Clamped Slab

$$\frac{p}{p_y} = 1 + \frac{\alpha'^2}{4\beta'} - \frac{\alpha'^2}{4\beta'} \cdot \frac{2\frac{L}{l}}{\frac{L}{l} + 1} \left(\frac{w_o}{d}\right) + \frac{\alpha'^2}{4\beta'} \cdot \frac{9\left(\frac{L}{l}\right)^2 - 3\left(\frac{L}{l}\right) - 1}{3\left(\frac{L}{l} + 1\right)\left(3\frac{L}{l} - 1\right)} \left(\frac{w_o}{d}\right)^2 \qquad (2.15)$$

where

$$\alpha' = \frac{\frac{d}{d_1}}{4\left(1 - \frac{1}{2}\frac{d}{d_1}\right)}$$

$$\beta' = \frac{\frac{3}{8}\frac{A_s}{d_1}\frac{f_y}{u}}{\left(1 - \frac{1}{2}\frac{d}{d_1}\right)}$$

Equation (2.15) is valid for

$$0 \leq \frac{w_o}{d} \leq \frac{3\left(\frac{L}{l}\right) - 1}{4\left(\frac{L}{l}\right) - 1} \qquad (2.16)$$

when the central section of the slab is not yet fully cracked. The solution, however, was not extended to cover the second stage of pure tensile membrane action at large deflections.

Morley checked his theoretical predictions for the ultimate loads with the experimental results obtained by Wood on 1.727 m (68 in) x 57.1 mm (2.25 in) thick restrained square slabs and by Powell on 0.914 m (36 in) x 0.521 m (20.5 in) x 32.5 mm (1.28 in) thick restrained rectangular slabs by using Park's (12-16) empirical value for the central deflection ($w_o/d = 0.5$) at peak load. The comparison showed a discrepancy in the peak loads with a coefficient of variation of ±13%.

Following a total strain approach; Sawczuk (17), in 1965, presented a kinematical method of analysis of rigid - perfectly plastic plates beyond the bending collapse load in the investigation of the load - deflection relationship for isotropically reinforced simply supported - axially unrestrained rectangular concrete slabs. In this analysis, a collapse mechanism of the yield line theory type

which remains unchanged with continuing deflection was adopted. The tensile membrane action was found to be localized in zones of yielding flexural hinges.

Based on a yield criterion similar to that of Wood (3) and by using virtual work, the analysis assumed three different modes of collapse. One belongs to a plate with edges restrained against sliding but free to rotate. In this case, the yield moments and membrane forces were considered to act perpendicular to the yield lines. The second collapse mode is caused by cracks extending perpendicular to the longer side of the rectangular slab through the thickness of the slab. These cracks were first observed by Wood (3) in some experimental tests on rectangular slabs and was later confirmed by Sawczuk in his own tests. The analysis of this mechanism required the consideration of in-plane bending moments which tend to rotate the slab elements in their own plane. In the third mode of collapse, tension membrane cracks were analysed. The slab in this case was considered to be composed of rigid triangular elements (see Fig. 2.6a) which are subjected to bending moments as well as membrane forces acting along the periphery of the formed triangle and also to axial extension on the tensile crack perpendicular to the longer side of the slab. In all these mechanisms, the virtual work method was adopted to express the load in terms of the deflection. The results showed that the third mode of collapse governs for almost all values of deflection which are large enough to cause the pure tensile membrane to be developed. The enhancement of the load related to this mode of collapse was found to be in the following form :

$$\frac{p}{p_y} = 1 + \frac{2}{3 + \frac{\mu_o}{d}} \left[\frac{1}{1 + 2n\left(\frac{L}{l}\right)^2}\right] \left(\frac{w_o}{d_1}\right) \qquad (2.17)$$

where μ_o denotes the depth of the neutral axis from the mid-depth of the slab when the membrane forces are zero; and n is the parameter controlling the yield line pattern (Fig. 2.6a) so that;

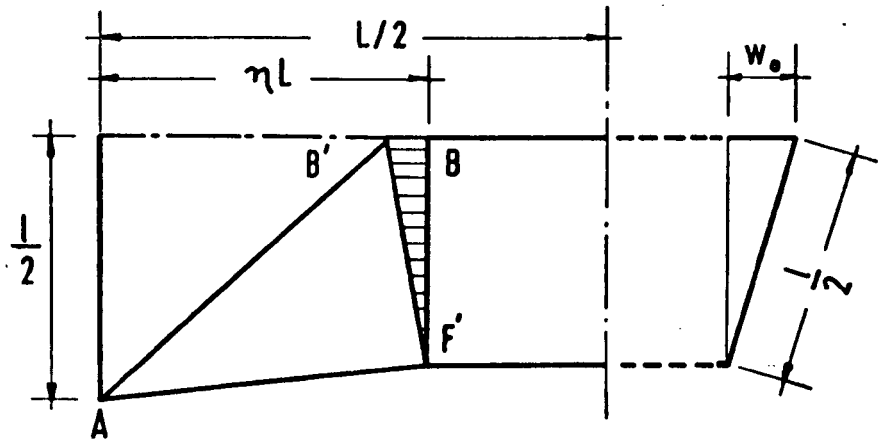

(a) Detail of The Critical Collapse Mode Considered by Sawczuk

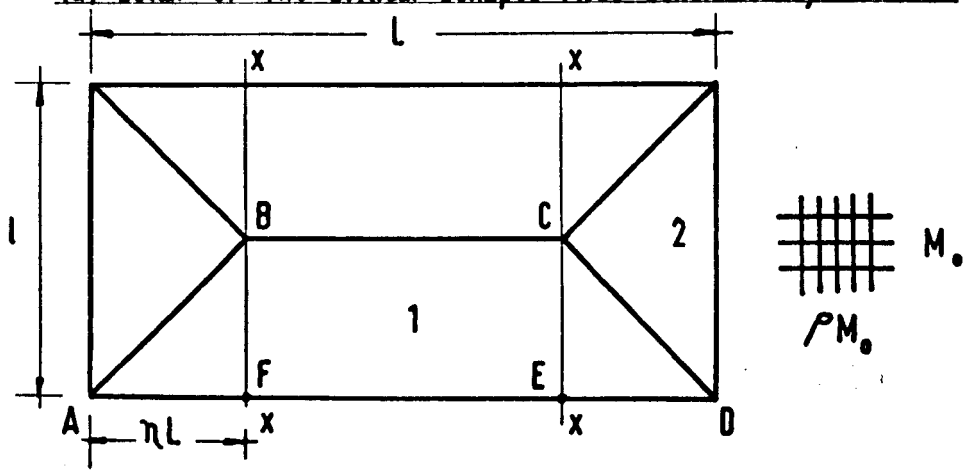

(b) Basic Yield Line Pattern of a Rectangular Slab

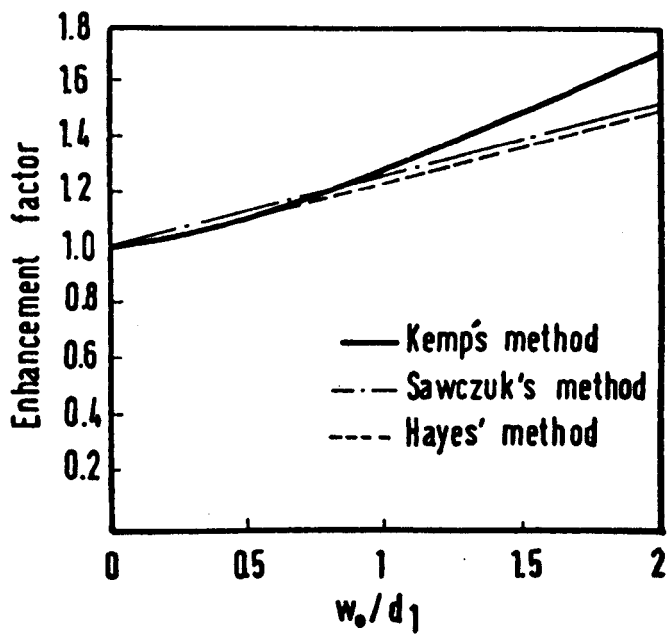

(c) Comparison of Analyses for Simply Supported - Axially Unrestrained Square Slabs (t = 0.04)

FIG. (2.6)

$$n = \frac{1}{2(\frac{L}{l})^2}\left[\sqrt{3(\frac{L}{l})^2 + 1} - 1\right] \qquad (2.18)$$

For a particular slab, the increases in strength obtained from Eq. (2.17) are directly proportional to the central deflection w_o. Such increases become smaller with increasing rectangularity. For the special case of a square slab, Eq. (2.17) may be compared with Kemp's solution (Eq. 2.10). The two equations are different because the assumed collapse modes are of different type. Sawczuk's solution, in fact, predicts lower increases in strength with deflections becoming large.

Some experiments on isotropically reinforced, simply supported - axially unrestrained reinforced concrete rectangular slabs of two sizes; 2.0 m (78.74 in) x 1.0 m (39.37 in) x 30 mm (1.18 in) and 1.6 m (63 in) x 1.1 m (43.3 in) x 30 mm (1.18 in), were carried out by Sawczuk to test his theoretical analysis. The slabs were tested under uniformly distributed load by applying water pressure to the bottom face of the slab. Tensile cracks extending perpendicular to the longer side of the slab through the thickness of the slab were observed in these tests and comparison of the load - deflection behaviour was made by amending the theoretical solution to account for the elastic deflections. In this way a close agreement between the experimental load - deflection relationship and the theoretical predictions was obtained.

A rigid-plastic solution to the problem of orthotropically reinforced simply supported - axially unrestrained rectangular slabs was presented by Hayes (18) in 1968 as an extension to Sawczuk's analysis. The neutral axes along the yield lines were considered to be straight lines and the variation of membrane forces along the yield lines were assumed linear. A critical distribution of membrane forces was found which was just sufficient to cause in-plane bending hinges to form at sections x-x (see Fig. 2.6b).

Two possible stress distributions were investigated, depending on whether or not cracks penetrated to the upper surface of the slab. In this investigation, two membrane force parameters,

(v) and (k), and a parameter (r) fixing the extent of the central tensile membrane were assumed to define the shapes of the in-plane stress distributions along the yield lines in the two cases. The values of these parameters were found by considerations of in-plane equilibrium of the forces* acting along the yield lines of elements 1 and 2 (Fig. 2.6b) and by equating the in-plane moments of these forces about points E or F to the in-plane plastic moment at section CE or BF assuming that all reinforcement along these two sections are yielding. The results obtained were;

$$k = 1 + \frac{4\eta^2 \left(\frac{L}{l}\right)^2 (1 - 2\eta)}{1 + 4\eta^2 \left(\frac{L}{l}\right)^2} \tag{2.19}$$

$$v = \frac{3}{K\left[1 + 4\eta^2 \left(\frac{L}{l}\right)^2\right](2k - 1)} \tag{2.20}$$

$$r = \frac{\frac{3}{K} - 1 + 12\eta^2\left(\frac{L}{l}\right)^2 - 8\eta \left(\frac{L}{l}\right)^2}{2 + 4\eta \left(\frac{L}{l}\right)^2} \tag{2.21}$$

In these equations, K denotes the ratio of the tensile force of the reinforcement in the direction of the shorter side of the rectangular slab to the tensile force of the reinforcement in the longer side direction. η is the parameter controlling the yield line pattern and is given in this case by;

$$\eta = \frac{1}{2\rho \left(\frac{L}{l}\right)^2}\left[\sqrt{3\rho \left(\frac{L}{l}\right)^2 + 1} - 1\right] \tag{2.22}$$

where ρ is the coefficient of orthotropy.

The distribution of in-plane forces having been calculated, moment equilibrium for elements 1 and 2 about their axes of

---

* The forces acting along the yield lines are the resultant tensile force in the central region of the slab, the resultant compressive force near the edges and the shear force along the yield line.

rotation were considered to estimate the load enhancement. However, the action of the in-plane shear, or any vertical shear, on the yield lines were initially ignored in the analysis. The enhancement of the load determined by considering the two portions of the slab were unequal, and an average value was obtained. The contributions to the moment equilibrium due to membrane forces and bending moments were actually determined separately and then combined to give the final equation * for the net enhancement of the load-carrying capacity of the slab for the two cases of compressive membrane action (the early stages of cracking) and the pure tensile membrane action (after cracks penetrate to the upper surface of the slab).

It can be seen from Eq. (2.22) that for a given slab with a given value for the coefficient of orthotropy (ρ) and the ratio of the sides (L/l), the parameter (η) is a fixed quantity. If this value of η is used in Eqs. (2.19), (2.20) and (2.21) the parameters (k, v and r) will be fixed quantities too indicating that the stress distributions along the yield lines are independent of deflections and, consequently, the values of the membrane forces do not change as yield proceeds. One of the basic features of the problem of membrane action in axially unrestrained rigid-plastic slabs is that membrane forces are zero at the start of collapse and increase linearly with continuing deflection. Hayes' solution is not consistent with this and gives no indications of the value of the limiting central deflection which separates the two cases of compressive and tensile membrane action. However, the predicted enhanced loads in both cases were found to decrease with increasing rectangularity (L/l) and coefficient of orthotropy (ρ). Comparison was made by Hayes, apparently by using the equation corresponding to the second stage of pure tensile membrane action, with the solutions presented by Kemp and Sawczuk and the approach was found to have good agreement with the latter (see Fig. 2.6c). Some experimental tests on rectangular slabs were carried out but the load-deflection relationships obtained were not in close agreement with the theoretical predictions.

---

* Eq. (17) page (209) reference (18).

Hayes attributed the differences to ignoring the strain hardening of the reinforcement and the assumption that the material of the slab behaves in a rigid - perfectly plastic manner.

Taylor (19) developed an analysis for predicting the load-carrying capacity of simply supported - axially unrestrained square slabs on the basis of considering the equilibrium of the segments of the slab bounded by the yield lines at any stage of loading (see Fig. 2.7) recognising from tests that tensile membrane action only occurs at large deflections and does not alter the collapse mode. The neutral axis along the yield lines bounding the segments was assumed linear with the central region in tension and the outer region in compression.

Taylor suggested that the load-carrying capacity of the slab could be determined, then, by allowing for the increase in the effective lever arm of the reinforcement brought about by a redistribution of the concrete compression zone. With simplifying assumptions for the shape of the compression zone (by assuming a horizontal line for the neutral axis) and for the stress-block (by using values similar to those in the load factor method in CP 114 - 1957, a simple method of calculating the strength of a slab corresponding to a particular deflection was obtained. From analysis of test data by Maher (20) using a computer programme by Hayes (21) it was argued that such assumptions are reasonable. The method presented predicts a continuously rising strength - deflection characteristics.

Following a strain-rate approach, Janas (22) in 1968 presented a kinematical method to derive the load - deflection relations in cases of uniformly loaded, clamped - axially restrained, strip, square and circular slabs proceeding from the initial compressive membrane action to the overall membrane tension and cracking at large deflections. In this study, the slab was assumed to be rigid - perfectly plastic and the initial collapse mode of each case was taken to be the yield line collapse mechanism which remains unchanged with deformation. An equation for the rate of energy dissipation of an elementary segment of the yield line was derived

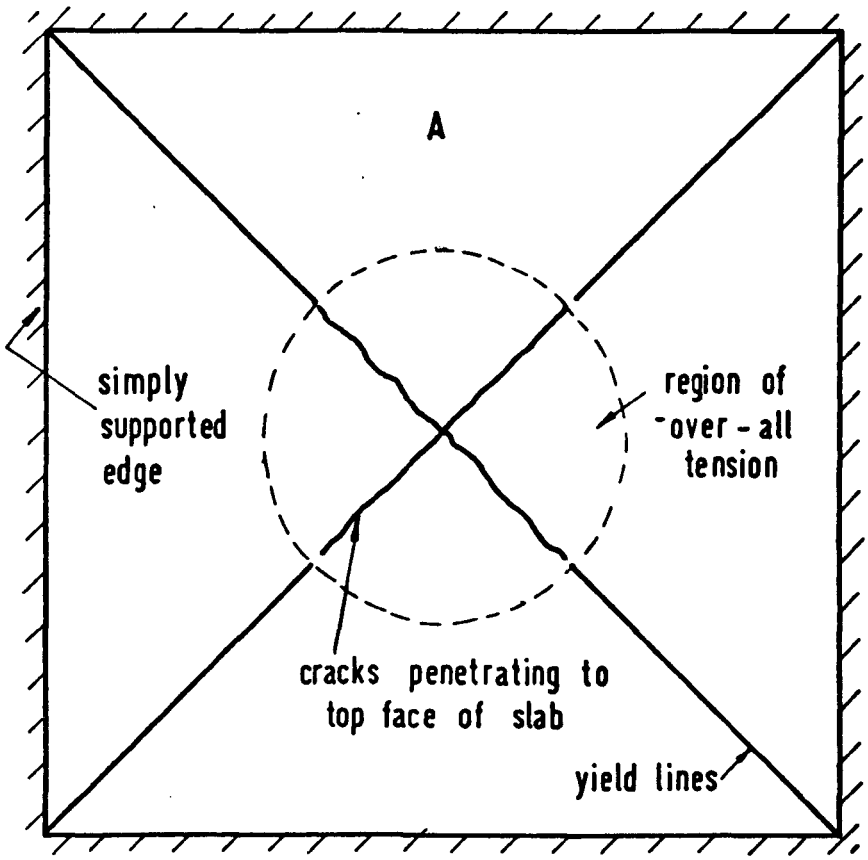

Plan of slab

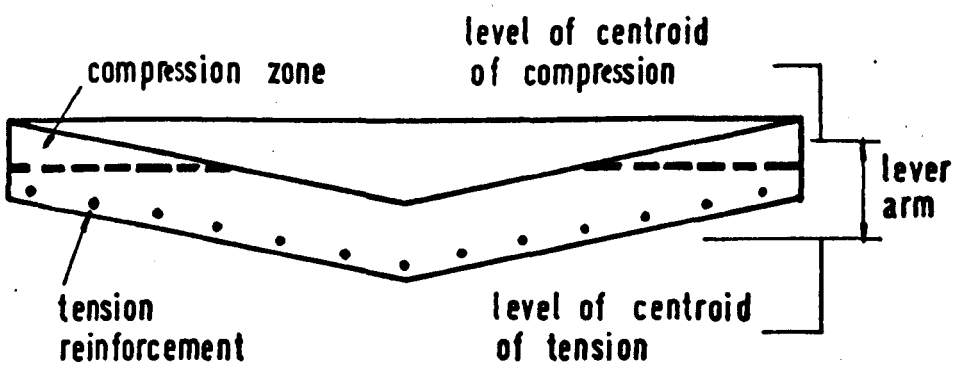

Elevation of segment A

FIG. (2.7) Development of Tensile Membrane Action in a Square Slab at Large Deflections

as a function of the depth of the neutral axis. Then searching for the least upper bound to the collapse load, this equation was minimised to find the position of the neutral axis. The work done by the applied load was, then, equated to the integral sum of the energy dissipation along the yield lines to give the load corresponding to any vertical deflection. This approach seems to have much in common with that adopted by Morley (10). The load - deflection equations for each case in their final form are given as follows:

(1) Clamped - axially restrained strip of unit width with reinforcement γA_s at the top face of the strip and reinforcement A_s at the bottom.

i. For $0 \leqq \frac{w_o}{d} \leqq 1 - 2(1-\gamma)t$

$$\frac{p}{p_y} = 1 + \frac{(1 - \frac{w_o}{d})^2}{4t[(1+\gamma) - (1-\gamma)^2 t]} \qquad (2.23)$$

ii. For $1 - 2(1-\gamma)t \leqq \frac{w_o}{d} \leqq 1$

$$\frac{p}{p_y} = \frac{2\gamma + (1-\gamma)\frac{w_o}{d} + \frac{1}{2t}(1 - \frac{w_o}{d})^2}{(1+\gamma) - (1-\gamma)^2 t} \qquad (2.24)$$

iii. For $\frac{w_o}{d} \geqq 1$

$$\frac{p}{p_y} = \frac{(1+\gamma)\frac{w_o}{d}}{(1+\gamma) - (1-\gamma)^2 t} \qquad (2.25)$$

where $t = (A_s f_y)/(\sigma_c d)$ and σ_c is the compressive stress of the concrete.

The load - deflection relationship was thus given in three successive stages. The first stage (Eq. 2.23) represents the behaviour of the slab strip under compressive membrane action. The maximum enhancement in the load occurs at the start of this stage at $w_o = 0$. The second stage (Eq. 2.24) becomes applicable immediately after cracks penetrate the whole thickness of the slab at one of the yield sections (either the mid-span section or the end sections depending on the value of γ). The third and final stage of behaviour is the stage of pure tensile membrane action (Eq. 2.25) which applies when all the three yield plastic hinges are fully developed and cracks have penetrated through the whole thickness of the slab at these sections.

It must be pointed out that in problems of membrane action in doubly reinforced concrete slabs attention must be given to the conditions at large deflections when the sections of yield are cracked throughout the depth and the neutral axis at these sections lies outside the slab. In this case the 'compression' reinforcement no longer acts in compression since it undergoes tensile strains. Janas did not pay attention to this fact. Neither does his analysis at large deflections satisfy horizontal equilibrium because he assumes that after the slab is cracked throughout the depth at one yield section the concrete stress block at the other yield sections reduce with further increments in deflection until all the three yield sections are fully cracked. This is not valid because horizontal equilibrium requires that the membrane force at all yielding sections has to be the same and since the value of this membrane force at the first fully cracked yield section (after full cracking occurs) remains unchanged with further increments in deflection, the neutral axis should remain fixed at the other yield sections.

However, equations (2.23), (2.24) and (2.25) were derived on the assumption that the reinforcement is placed with no cover. For the special case of equal top and bottom reinforcement ($\gamma = 1$), cover $(d - d_1)$, and $\sigma_c = \frac{2}{3}u$ the corresponding equations for p/p_y

would have been as follows :

i. For $0 \leqq \frac{w_o}{d} \leqq 1$

$$\frac{p}{p_y} = 1 + \frac{\alpha'^2}{4\beta'} \left(1 - \frac{w_o}{d}\right)^2 \qquad (2.26)$$

ii. For $\frac{w_o}{d} \geqq 1$

$$\frac{p}{p_y} = \frac{w_o}{d} \qquad (2.27)$$

where values of α' and β' are defined in Eq. (2.15).

Thus the tensile membrane action, according to Eq.(2.27), will form inside the slab strip when the value of the central deflection w_o is equal to the thickness of the slab. Since equal top and bottom reinforcements are provided, at this value of deflection the slab will be cracked throughout the depth at the mid-span and end sections at the same time. For further increments in deflection the neutral axis at these sections will lie outside the slab strip and the load - deflection relationship will be linear.

(2) Isotropically reinforced, circular, clamped - axially restrained slabs with equal top and bottom reinforcement. (The equations listed below are derived after a slight modification to account for the cover to the reinforcement).

i. For $0 \leqq \frac{w_o}{d} \leqq \frac{2}{3}$

$$\frac{p}{p_y} = 1 + \frac{\alpha'^2}{4\beta'} - \frac{\alpha'^2}{4\beta'} \left(\frac{w_o}{d}\right) + \frac{5}{48} \frac{\alpha'^2}{\beta'} \left(\frac{w_o}{d}\right)^2 \qquad (2.28)$$

ii. For $\frac{2}{3} \leqq \frac{w_o}{d} \leqq 1 + \frac{1}{6}\frac{\alpha'^2}{\beta'}$

$$\frac{p}{p_y} = \frac{\alpha'^2}{2\beta'}(1 - A)^2 + \left[1 + \frac{3}{2}\frac{(A - \frac{w_o}{d})^2}{\frac{w_o}{d}}\right] + \frac{1}{6}\frac{\alpha'^2}{\beta'}\frac{A^3}{\frac{w_o}{d}} \qquad (2.29)$$

where $$A = 2\sqrt{\left[\left(\frac{3\beta'}{\alpha'^2} + \frac{w_o}{d}\right)^2 + 2\left(\frac{3\beta'}{\alpha'^2} + 1\right)\frac{w_o}{d}\right]} - \left(\frac{3\beta'}{\alpha'^2} + \frac{w_o}{d}\right)$$

iii. For $\frac{w_o}{d} \geqq 1 + \frac{1}{6}\frac{\alpha'^2}{\beta'}$

$$\frac{p}{p_y} = 1 + \frac{3}{2}\frac{(1 - \frac{w_o}{d})^2}{\frac{w_o}{d}} + \frac{1}{6}\frac{\alpha'^2}{\beta'}\frac{1}{\frac{w_o}{d}} \qquad (2.30)$$

The three stages given by Eqs. (2.28), (2.29) and (2.30) represent respectively the behaviour of the slab under compressive membrane action, the start of tensile membrane action at the central region of the slab and the final stage of the load - deflection characteristics after the slab is fully cracked along yield lines. However, equation (2.28) may be compared with the corresponding equation (Eq. 2.15) found by Morley for the case of a clamped - axially restrained rectangular slab with equal top and bottom reinforcement. If the span ratio (L/l) in Morley's equation is taken as unity to represent the special case of a square slab the two equations will be identical. This confirms that the enhanced load in "symmetrically shaped slabs" is unique.

(3) Clamped - axially restrained square slabs with bottom reinforcement only at distance d_1 from the compressed face of the slab.

i. For $0 \leq \frac{w_o}{d} \leq \frac{2}{3} \frac{(\frac{\alpha}{\beta} + 4)}{(\frac{\alpha}{\beta} + 2)}$

$$\frac{p}{p_y} = 2(\alpha+\beta) + \frac{\alpha^2}{4\beta} - \frac{\beta}{4} (\frac{\alpha}{\beta} + 2)^2 (\frac{w_o}{d}) + \frac{5}{48}\beta(\frac{\alpha}{\beta} + 2)^2 (\frac{w_o}{d})^2 \quad (2.31)$$

ii. For $\frac{2}{3} \frac{(\frac{\alpha}{\beta} + 4)}{(\frac{\alpha}{\beta} + 2)} \leq \frac{w_o}{d} \leq \frac{1}{4} (\frac{\alpha}{\beta} + 2)$

$$\frac{p}{p_y} = \frac{\beta}{2} (\frac{\alpha}{\beta} + 2)(\frac{\alpha}{\beta} + 6) + \frac{\beta}{2} (\frac{\alpha}{\beta} + 2)(2\frac{\alpha}{\beta} + 9)(\frac{w_o}{d}) + \frac{\beta}{3} (\frac{\alpha}{\beta} + 2)^2 \left[(\frac{w_o}{d})^2 - \sqrt{(\frac{w_o}{d}) \left\{ (\frac{w_o}{d}) + 2 \frac{(\frac{\alpha}{\beta} + 4)}{(\frac{\alpha}{\beta} + 2)} \right\}^3} \right] \quad (2.32)$$

iii. For $\frac{w_o}{d} \geq \frac{1}{4} (\frac{\alpha}{\beta} + 2)$

$$\frac{p}{p_y} = \frac{\beta}{2} (\frac{\alpha}{\beta} + 2)(\frac{w_o}{d}) + \frac{1}{6}\beta (\frac{\alpha}{\beta} + 2)^2 \frac{1}{\frac{w_o}{d}} \quad (2.33)$$

values of α and β as defined in Eq. (2.2).

Again Eq. (2.31) represents the initial stage of compressive membrane action, Eq. (2.32) applies once the slab is fully cracked at the centre and finally Eq. (2.33) holds for the behaviour of the slab at large values of deflection after the slab is fully cracked along the yield lines.

Janas made no attempt to provide experimental evidence in support of his theoretical analysis.

2.2 METHODS BASED ON ELASTIC - PLASTIC CONSIDERATIONS

The methods of analysis discussed in the previous section neglected the effects of both the elastic strains in the slab and any lateral movement of the restraining supports. Accordingly,

the relationship between the load and the deflection was approximately obtained. Moreover, the theoretical peak value of the load, in axially restrained rigid-plastic slabs was found to be higher than the actual collapse load.

One of the earliest attempts to include elastic and support movement effects in the analysis was made by Christiansen (23). Based on a total strain approach, laterally restrained built-in reinforced concrete beams were analysed by assuming plastic hinges to be fully developed at supports and at mid-span. Following Ockleston's (7) explanation of the arching action, an expression was derived for the additional compression (N) at yield sections by equating the outward movement of the support with the lengthening of the beam due to rotation of the plastic hinges less the elastic and plastic shortening of the beam. The expression was determined as a function of the combined deflection (which is the sum of the deflection $(w_o)_e$ due to elastic deformations of the beam and deflection $(w_o)_p$ due to rotation at the hinges).

$$N = \frac{1}{6}\, u.b.d. \; \frac{[2Z_1 - (\frac{w_o}{d})_p]}{[1 + \frac{Z_2}{(\frac{w_o}{d})_p}]} \qquad (2.34)$$

where: $Z_1 = 1 - (\frac{w_o}{d})_e - \frac{3}{2}(1+\gamma)\frac{A_s}{bd}\frac{f_y}{u}$

$$Z_2 = \frac{1}{12}(1+m)\frac{uL^2}{E_c d^2}$$

In this equation, γ represents the ratio of the area of top reinforcement at supports to the area of bottom reinforcement at mid-span; L, b, d are the length, the width and the depth of the beam respectively; E_c is the concrete modulus of elasticity and m is a factor denoting the ratio of the outward movement of

the support to the elastic shortening of the beam. Other notations are as defined previously.

The moment due to N about the support was found to be :

$$\text{moment due to } N = N.d\left[Z_1 - \left(\frac{w_o}{d}\right)_p - \frac{3}{2}\frac{N}{u.d}\right] \qquad (2.35)$$

From Eqs. (2.34) and (2.35) the load carried by arching at any value of deflection can then be determined. The maximum load was found to occur at a deflection $(w_o)_p$ given by;

$$3\left(\frac{w_o}{d}\right)_p^4 + (8Z_2 - 4Z_1)\left(\frac{w_o}{d}\right)^3 + (6Z_2^2 - 12Z_1Z_2)\left(\frac{w_o}{d}\right)_p^2 - 12Z_1Z_2^2\left(\frac{w_o}{d}\right)_p + 4Z_1^2Z_2^2 = 0 \qquad (2.36)$$

Therefore solution of Equation (2.36)together with Eqs. (2.34) and (2.35) lead to the maximum load carried by arching. It was pointed out by Christiansen that the above analysis can also be used to predict the collapse loads of two-way slabs by estimating separately the load carried by arching across the shorter span and the load carried by bending from the yield line method and adding the resulting loads.

The analysis was supplemented by tests on four reinforced concrete beams restrained laterally by a welded steel frame and subjected to a single concentrated load at mid-span. The results showed slightly higher ultimate loads than the theory predicts. The discrepancy in the results was attributed to the effect of biaxial stresses occurring at the mid-span section (under the applied load) and also to the assumption that the plastic hinges are fully developed at all stages whereas the ultimate loads given by the theory were found to occur at deflections which are too small

to develop full plasticity at the hinge positions.

In 1969, Roberts (24) presented an experimental and theoretical study for the behaviour of axially restrained simply supported reinforced concrete slab strips. In this study, the effects of both the elastic shortening of the elemental strip as well as the outward movement of the surround were considered. The theoretical analysis follows Wood's approach very closely. Using the yield criterion given by Wood (Eq. 2.2) and plastic potential theory based on total strain, the positions of the neutral axis at mid-span and supports were expressed in terms of the membrane force N. Then by considering compatibility of the deformed strip of unit width and length L, the membrane force N was expressed in terms of the central deflection w_o. The resulting equation was given in the following form;

$$\frac{N}{T_o} = \frac{\frac{1}{2}\left[\left(\frac{\alpha}{\beta}+1\right) - \frac{1}{2}\left(\frac{\alpha}{\beta}+2\right)\frac{w_o}{d} - \frac{1}{2}\left(\frac{\alpha}{\beta}+2\right)\frac{\frac{\Delta}{d}\frac{L}{d}}{\frac{w_o}{d}}\right]}{\left[1+\frac{1}{\bar{S}}\frac{1}{\frac{w_o}{d}}\right]} \qquad (2.37)$$

in which Δ is an assumed initial gap at the supports and

$$\bar{S} = \frac{6\,S}{\frac{L}{d}\,u} \qquad (2.38a)$$

S is a stiffness factor which can be related to the stiffness of the surround S_s and the stiffness of the strip S_b in the following expression :

$$\frac{1}{S} = \frac{1}{S_s} + \frac{1}{S_b} \qquad (2.38b)$$

where S_s has to be found experimentally and

$$S_b = \frac{2dE_c}{L} \qquad (2.38c)$$

The value of E_c (concrete modulus of elasticity) was taken by Roberts to be

$$\left.\begin{aligned} E_c &= \frac{\sqrt{u}}{180.6} \times 10^6 \quad N/mm^2 \\ \text{or} \\ E_c &= \frac{\sqrt{u}}{15} \times 10^6 \quad lb/in^2 \end{aligned}\right\} \qquad (2.38d)$$

Having determined N for any given central deflection w_o, the value of the load can then be found from equilibrium. The equation was given in the following form :

$$\frac{p}{p_y} = 1 + 2\beta\left[\left(\frac{\alpha}{\beta} + 1\right) - \left(\frac{\alpha}{\beta} + 2\right)\frac{w_o}{d}\right]\left(\frac{N}{T_o}\right) - 2\beta\left(\frac{N}{T_o}\right)^2 \qquad (2.39)$$

Roberts made no attempt to find an explicit solution for (w_o/d) corresponding to the peak load but used Eqs. (2.37) and (2.39) to plot load - deflection curves from which the ultimate loads were obtained graphically.

The theoretical analysis was performed on restrained slab strips under uniformly distributed load but in the experimental tests, the elemental strips were subjected to a four point loading system. However, the analysis was assumed to be valid since the collapse mechanisms of both cases are the same.

36 slab strips were tested in the form of beams 0.229 m (9 in.) in width and 1.461 m (4 ft. 9½ in.) in length. The thickness of 20 of these beams was 50.8 mm (2 in.) and the remaining 16 beams were 76.2 mm (3 in.) deep. The specimens to be tested were inserted in a very stiff reinforced concrete surround (Fig. 2.8) and were 9.5 mm (3/8 in.) shorter than the interior length. These specimens were supported at the ends on steel plates and the gap between the specimen and the surround was filled with a rich mix of cement mortar. In each test, readings were taken for the applied load, the central deflection and the outward thrust (the membrane force). The latter was measured by semi-

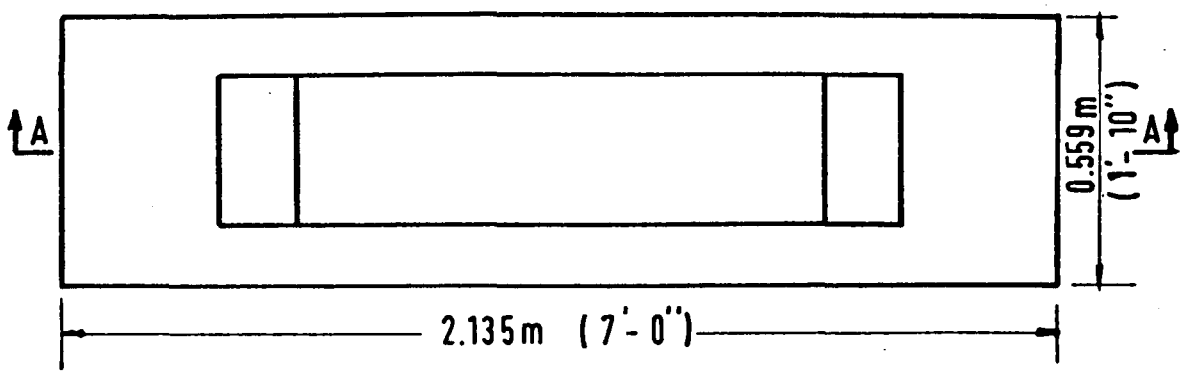

Plan of surround before beam is inserted

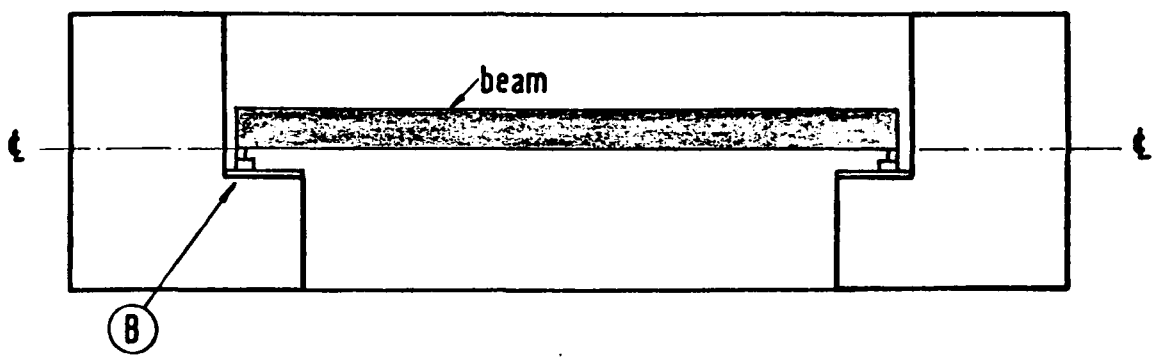

Section A-A with beam inserted into position

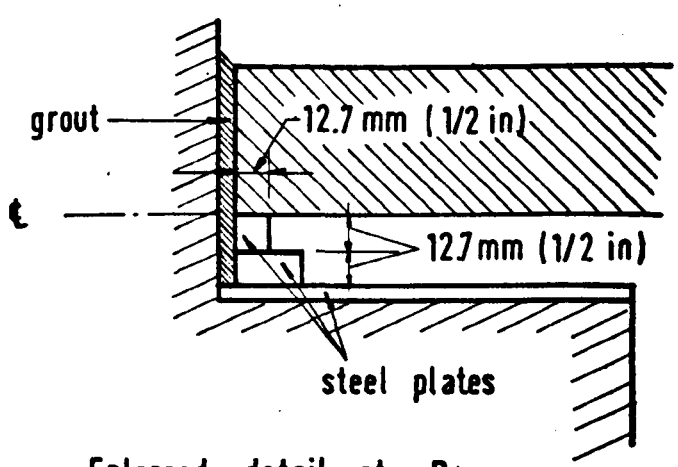

Enlarged detail at B

FIG. (2.8) The Rig Used by Roberts (24)

conductor strain gauges mounted at the middle of the surround. The results of these tests showed discrepancies in both the ultimate loads and the maximum membrane forces when compared with the theoretical predictions. The experimental peak loads were found in some tests to be higher (up to 55%) than the corresponding theoretical values and in other tests they were 25% lower. Roberts attributed the differences to the crushing strength of the concrete in the tested beams being greater than the cube strength. Supplementary tests on wedge shaped specimens were provided in support of this explanation. This explanation is not entirely convincing and the differences may be due to the following;

(1) From Fig. (2.8), it can be seen that the condition of the supports allows a friction force to develop at the interface between the steel plate and the beam, which can be quite considerable at peak loads. This force was not accounted for in the analysis.

(2) Equations (2.37) and (2.39) were derived on the assumption that the mean yield stress of the concrete is 2/3 of the cube strength. A better agreement with the experimental results would have been obtained if the parameters $k_1 k_3$ and k_2 suggested by Hognestad, Hanson and McHendry (25), which depend on the cube strength of the concrete, had been used in defining the shape of the concrete stress block. It will be seen in Chapters 4 and 5 that the choice of the parameters for the stress block is of great importance.

(3) The arrangement of the rig does not ensure that the gap between the specimen and the surround can be fully grouted. A very small gap will cause a considerable reduction in both the peak load and the maximum value of the membrane force. This point will be studied in detail in Chapter 5.

Following a 'strain-rate' approach, Janas (26) in 1973 modified his original solution for the problems of rigid axially restrained clamped strips and axially restrained square slabs to account for the elastic axial compressibility in such members. The slab strip in this case was assumed to be subjected to a concentrated load at mid-span, and to be reinforced in the bottom face only at middle sections and in the top face only at supports. Using plastic potential theory and a strain rate flow rule, the internal moments and membrane forces at the locations of the plastic hinges, i.e. the mid-span and end sections of the slab strip, were expressed in terms of the depth of the neutral axes at these sections. It was assumed that these axes lie on the same horizontal level, and by satisfying horizontal equilibrium their position was computed. The value of the membrane force (N) was given in the following expression;

$$\frac{N}{T_o} = \frac{1}{t}\left[\left(1 - e^{-\nu\frac{w_o}{d}}\right)\left\{1 - (1+\gamma)t + \frac{1}{\nu}\right\} - \frac{w_o}{d}\right] \qquad (2.40)$$

where ν describes the elastic compressibility of the slab,

$$\nu = \frac{8E_c\, d^2}{\sigma_c\, L^2} \qquad (2.41)$$

and other notations are as defined previously.

The current limit load (P) was found from equilibrium to be;

$$\frac{P}{P_y} = 1 + \frac{1}{A}\left[1 - (1+\gamma)t - \frac{w_o}{d}\right]^2 - \frac{1}{A}\left[1 - (1+\gamma)t - \left(1 - e^{-\nu\frac{w_o}{d}}\right)\left\{1 - (1+\gamma)t + \frac{1}{\nu}\right\}\right]^2 \qquad (2.42)$$

where $A = 4t\left[(1+\gamma) - \frac{1}{2}t\,(1+\gamma^2)\right]$

However, the above solution (Eq. 2.42) is valid only when the membrane force is compressive (i.e. for all values of deflection less than w_o' defined from Eq. (2.40) with $\frac{N}{T_o} = 0$). For $w_o > w_o'$ the axial force will be tensile and therefore the analysis has to be modified by introducing a new coefficient of extensibility ν_1 . In this case,

$$\frac{P}{P_y} = 1 + \frac{1}{A}\left[1 - (1+\gamma)t - \frac{w_o}{d}\right]^2 - \frac{1}{A}\left[1 - (1+\gamma)t - \left(\frac{w_o'}{d}\right) - \left\{1 - e^{-\nu_1\left(\frac{w_o}{d} - \frac{w_o'}{d}\right)}\right\}\left\{1 - (1+\gamma)t + \frac{1}{\nu_1} - \frac{w_o'}{d}\right\}\right]^2 \tag{2.43}$$

Equations (2.42) and (2.43) were used by Janas to plot load - deflection curves for different percentages of reinforcement and by assuming $\nu_1 = \nu/4$. These curves gave loads less than the rigid plastic solution ($\nu = \infty$) with one common point with rigid plastic corresponding to maximum axial compression. The latter was found to take place at the deflection

$$\left(\frac{w_o}{d}\right)_{cr} = \frac{1}{\nu} \ln\left[1 + \{1 - (1+\gamma)t\}\nu\right] \tag{2.44}$$

Based on numerical data, the ultimate peak load was taken to correspond to deflection $w_o/d \approx 0.5\,(w_o/d)_{cr}$. Therefore this value was introduced in Eq. (2.42) and the ultimate peak load P_u was found to be :

$$\frac{P_u}{P_y} = 1 + \frac{1}{A}\left[1 - (1+\gamma)t - \frac{1}{2}\left(\frac{w_o}{d}\right)_{cr}\right]^2 - \frac{1}{A\nu^2}\left[\sqrt{1 + \nu\{1 - (1+\gamma)t\}} - 1\right]^2 \tag{2.45}$$

The method outlined above was thence applied to uniformly loaded built-in square slabs with reinforcement distributed only in the tensile zones and edges axially restrained against lateral movement. The traditional yield line mechanism with diagonal plastic

hinges was taken to be the collapse mode of these slabs which remains unchanged with deformation. The position of the instantaneous neutral axis in the positive hinge was defined in terms of the axial strains in the two directions of the slab which again include elastic and plastic strain rates. Assumption was made that the elastic deformations in both directions of the slab are proportional to the mean value of the axial forces at positive and negative plastic hinges. With these assumptions and for virtual rotations around supports the position of the neutral axis in the positive hinge was related to the corresponding value in the negative hinge. Then by equating the integral sum of the membrane forces along the yield lines of one of the four panels of the slab to zero, the position of the neutral axis and consequently the membrane forces were obtained. By considering the moment equilibrium of one panel, the current collapse load p was found to have the following expression :

$$\frac{p}{p_y} = 1 + \frac{1}{A}\left[1 - (1+\gamma)t\right]^2 - \frac{1}{A}\frac{w_o}{d}\left[1 - (1+\gamma)t - \frac{5}{12}\frac{w_o}{d}\right]$$

$$- \frac{1}{A}\left[1 - (1+\gamma)t - (1 - e^{-\nu\frac{w_o}{d}})\left\{1 - (1+\gamma)t + \frac{1}{2\nu}\right\}\right]^2$$

$$- \frac{1}{6\nu^2}(1 - e^{-\nu\frac{w_o}{d}})^2 \qquad (2.46)$$

Solution (2.46)represents the behaviour of the slab under compressive membrane action and, therefore, it is valid for all values of deflection less than w_o' defined from the equation

$$\frac{w_o'}{d} + e^{-\nu\frac{w_o'}{d}}\left[\frac{2}{3}\left\{1 - (1-\gamma)t\right\} + \frac{1}{\nu}\right] = \frac{1}{\nu} + \frac{2}{3}\left[1 + (1-\gamma)t\right]$$

For larger deflections, a pure membrane tension zone will appear in the central region of the slab. Janas could not extend his solution to cover this stage because of the algebraic complexity and instead he suggested that the following formula, which was

obtained from rigid - plastic considerations, could be used as an alternative.

$$\frac{p}{p_y} = \frac{1}{A}\left(2 + \frac{w_o}{d}\right)(1 + \gamma)t + \frac{1}{A}\left[2 + \frac{w_o}{d} + 2(1 - \gamma)t\right]$$

$$\left[\frac{4}{3}\frac{w_o}{d}\left\{1 - \sqrt{1 + \frac{2}{\frac{w_o}{d}}(1 + t - \gamma t)}\right\} + 1\right] + \frac{1}{3A}\frac{w_o}{d}\left[1 + 7(1 - \gamma)t\right]$$

(2.47)

Yee (27) in 1973 presented an approximate method of estimating the ultimate load carrying capacity of square concrete slab-beam panels taking into account the compressive membrane action resulting from the non-rigid lateral restraint provided by the supporting beams. The panels were assumed to carry load by two actions; the flexural action of the slab itself and the membrane action induced by the existence of the surround. Two limits were given for the ultimate load depending on whether or not the surrounding beams might collapse first. The lower limit is represented by the maximum load carried by membrane action only (the case when the flexural capacity of the slab is exhausted before cracking of the restraining elements takes place) and the upper limit is given by the sum of the maximum loads carried by both flexural and membrane actions (the case when these actions reach their respective maximum value at the same time). It was stated that the ultimate load should lie between these two limits. However, the analysis furnished a solution for the maximum load carried by membrane action only while the load carried by flexure was taken as the cracking load of the slab panel based on elastic analysis. Critical assumptions were made that the membrane force is constant along the span of the slab, its position is a fixed quantity that does not change with deformation (assumed to be at a distance 1/10 of the slab thickness below the compressed face) and the moment along the yield lines is constant. With these assumptions, the analysis began by first finding an expression for the membrane force in terms of the modulus of rupture of concrete. This was done by equating the latter to

the sum of the direct tensile stress, the flexural tensile stress and the tensile stress due to eccentricity, all caused by the effect of the axial membrane force (N) acting alone on the restraining beam. The result was given in the following form :

$$N = \frac{2\, b^2\, d\, f_{rp}}{L(3.7b + L)} \qquad (2.48)$$

where, b : Width of the restraining beam
d : Thickness of the slab
f_{rp} : Modulus of rupture of concrete
L : Slab span

The second step was to find the lateral movement of one of the restraining beams. This was taken equal to the extension of the beam in the perpendicular direction acting as a tie plus the deflection of the centre of the restraining beam relative to its ends. The total movement δ was thus found to be :

$$\delta = \frac{NL^2(L^2 + 29.6\, b^2)}{32E_c\, b^3 d} \qquad (2.49)$$

(E_c being the concrete modulus of elasticity)

By considering the compatibility of a strip passing through the centre of the slab, the movement δ was related to the central deflection of the panel according to the following expression :

$$w_o = \frac{L}{2d}\left(\delta + \frac{NL}{2dE_c}\right) \qquad (2.50)$$

From geometrical consideration of the strip the vertical distance between the membrane forces at centre and end of the slab was defined and therefore the moment that these forces make around the edge of the slab was obtained to be :

$$M_{mem} = N\left(0.8d - \frac{w_o}{d}\right) \qquad (2.51)$$

Similar to the yield-line theory, the load was given as

$$p_{mem} = \frac{24}{L^2} M_{mem} \qquad (2.52)$$

Therefore from Eqs. (2.48), (2.49), (2.50), (2.51) and (2.52) the following expression for the load carried by membrane action was obtained.

$$p_{mem} = 48 \frac{\frac{b^2}{L^2}\frac{d^2}{L^2} f_{rp}}{3.7\frac{b}{L} + 1}\left[0.8 - 0.5 \frac{\frac{b^2}{d^2}\frac{f_{rp}}{E_c}}{3.7\frac{b}{L} + 1}\left\{\frac{1}{16}\frac{L^3}{b^3}\left(1 + 29.6\frac{b^2}{L^2}\right) + 1\right\}\right] \qquad (2.53)$$

Five small model square slabs of approximately 16.5 mm (0.65 in.) thickness spanning 0.254 m (10 in.) and subjected to a point load at the centre of the slab were tested to check the validity of the proposed method. The variable in this series of five slabs was the size of the restraining edge beam which ranged from 25.4 mm (1 in.) wide by 101.6 mm (4 in.) deep to 101.6 mm (4 in) by 101.6 mm (4 in.). The results of all these tests showed higher ultimate loads than the theoretical upper limit given by $p_{mem} + p_{flexure}$. The differences could be attributed to the critical assumptions made in the analysis. The membrane force was assumed to act at a fixed distance from the compressed face of the slab section whereas a slight shift in the position of this force will result in a considerable change in the value of the ultimate load. The latter is also influenced by the assumption of constant moment along the yield lines since membrane forces usually vary from one section to another along the yield line which result in changing the value of the moment accordingly.

2.3 STRIP METHOD

A strip method was used by Park (12-16) in his analysis of the problem of uniformly loaded rectangular concrete slabs which have either all or three edges restrained against lateral movement.

The slab according to this method is considered to be composed of strips running in the x and y directions which have the same depth as the slab (Fig. 2.9). The x direction strips contain only the x direction steel and the y direction strips contain only the y direction steel. These strips are divided into portions located between the yield lines of a given collapse mechanism and have yield sections which are at right angles to the direction of the steel. The portions of the strip between the yield sections are assumed to remain straight at all stages of deformation. Analysis of the slab by this method involves finding the position of the neutral axis along the yield lines by combination of geometrical considerations of the deformed strip (based on total-strain) and horizontal equilibrium. Membrane forces and yield moments can be evaluated once the positions of the neutral axis are found. Thereafter the end portions of the slab strips may be given a small virtual rotation and the total internal work at the yield sections of all the x and y direction strips can be equated to the external work done by the applied load. In this way, an expression for the relationship between the applied load and the central deflection can be obtained.

However, the strip method requires the use of empirical values for the central deflection at which the peak collapse loads occur. These values were found to vary from one slab to another depending on the shape of the slab and the boundary conditions. Park has supplied values for these deflections for the case of a rectangular slab with all edges fully restrained against all movement (the value of the central deflection at peak load in this case is 0.5 times the slab thickness) and the case of a slab with three edges restrained and the other edge free to move laterally (in this case the value is only 0.4 times the slab thickness). Therefore, if the strip method is to be applied to other problems, experimental tests must be performed to find the critical values for these deflections.

It is worth commenting here that in slabs with all edges fully restrained against rotation and horizontal translation, the

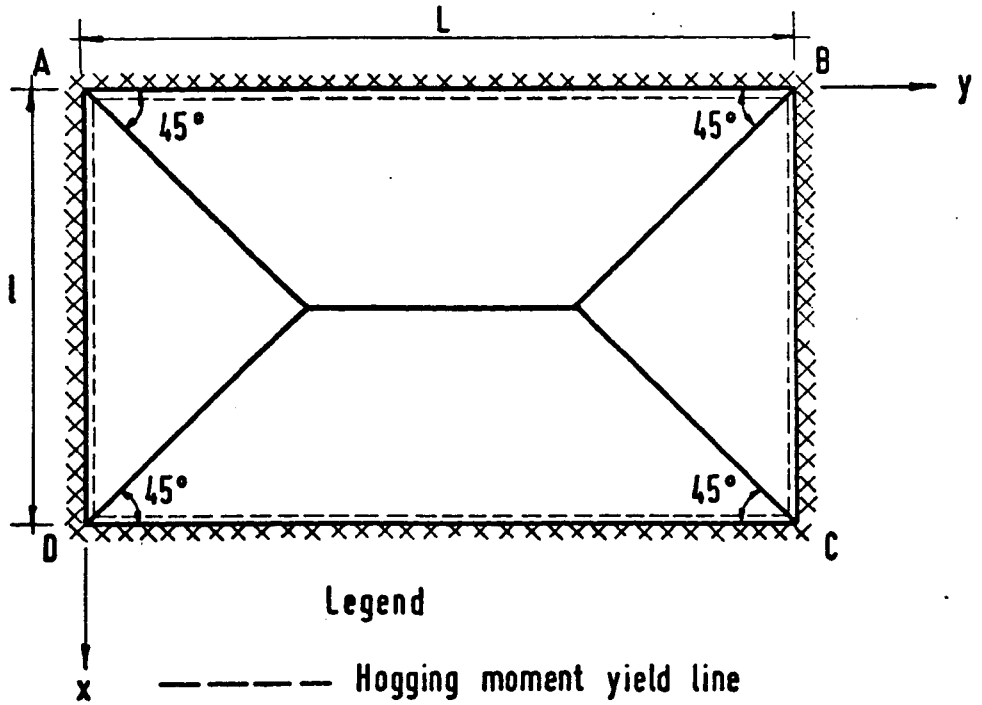

Yield line pattern of actual slab

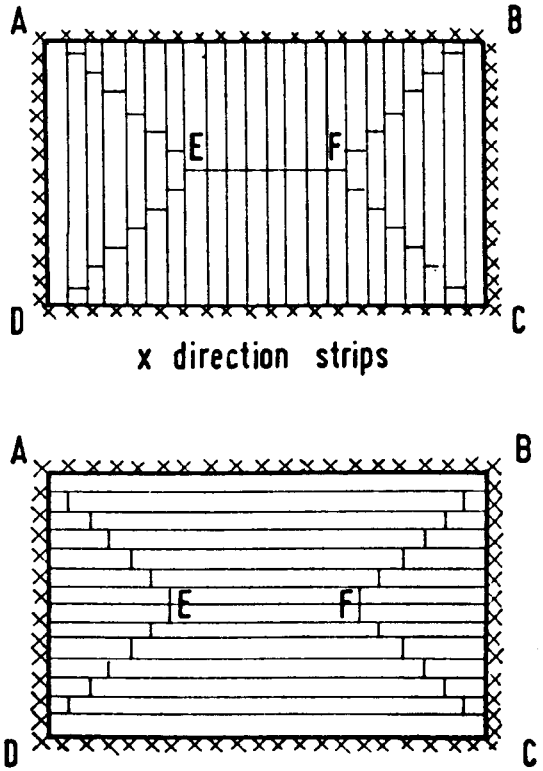

Strips of equivalent slab

FIG. (2.9) Strip Method Applied to Rectangular Slabs

strip method like the previously discussed methods considers membrane forces to generate in both directions of the slab. But in slabs with three edges fully restrained and the remaining edge free to move laterally, the method ignors any membrane forces in the direction of the span at right angles to the unrestrained edge. This is due to the assumption that each slab strip must be in horizontal equilibrium and, therefore, if a strip has one end free to move laterally no membrane force can occur. Accordingly, in the cases of corner panels in a slab-beam floor system where the two interior adjacent edges of these panels are the only edges that are restrained laterally, no membrane forces would be predicted in such slabs and the ultimate loads would simply be Johansen's loads.

Park presented his strip analysis for the problem of orthotropically reinforced rectangular slabs with lateral restraint by considering two cases. These are slabs under short-term and long-term uniform loading. The analysis of the slabs under short-term loading was based on a rigid-plastic strip approximation whereas in the analysis of the slabs under long-term loading, effects of axial strains in the slab and the lateral displacements at the boundaries were considered. The axial strains were taken to be the sum of creep, shrinkage and axial elastic strains caused by the induced compressive membrane forces. The behaviour of a slab as a tensile membrane at large deflections was also investigated and the results showed that heavily reinforced slabs can carry loads by tensile membrane action which exceed the ultimate flexural load. Park checked his theoretical predictions with some experimental tests conducted on 1.524m (60 in.) x 1.016 m (40 in.) reinforced concrete slabs and thickness ranging between 1 inch and 2 inches and the results showed that the maximum load can be predicted reasonably but the theoretical and the corresponding experimental load - deflection curves were not in good agreement.

Some more experimental data on this subject was provided in 1975 by the Indian Institute of Technology (28). Tests on nineteen single-panel square slab-beam models were reported and a

method of analysis, based on Park's strip method and total strain considerations,was presented to explain the enhancement in the ultimate loads obtained. In the analysis, the bowing of the surrounding beams was considered but the elastic shortening of the slab itself was neglected. Again the method, following Park, required the use of empirical values for the deflection corresponding to the ultimate load.

2.4 SUMMARY AND CONCLUSIONS

This review of existing research shows that there is conclusive experimental evidence of the beneficial effect of membrane action on the ultimate strength of slabs, and that, several theoretical methods have been developed to explain this phenomenon. Each one of these methods has a different approach and is based on different assumptions. The various approaches may, however, be summarized as follows :

i. Approximate approaches:

These are represented by the methods given by Ockleston (who assumes constant membrane force in all directions of a rectangular slab), Taylor (who uses a horizontal line for the neutral axis), Yee (who assumes that the value of the membrane force is a fixed quantity which does not change with deformation, and also that the distributions of both the membrane force and the moment along the yield lines are constant), Sawczuk (who considers in-plane bending hinges) and finally Hayes (whose analysis shows that the values of the membrane forces along the yield lines do not change as yield proceeds).

ii. Approaches using equilibrium and compatibility but a total strain flow rule

These are represented by the methods given by Wood, Kemp, Roberts and Christiansen. The strip method adopted by Park and the Indian Institute of Technology can also be categorised under the same heading but in addition they require the use of empirical values for the deflection corresponding to the ultimate load.

iii. Approaches using equilibrium and compatibility but a strain rate flow rule

These are represented by the methods given by Morley and Janas.

The general picture which emerges from this review of existing research is one of considerable confusion and there is certainly a need for clarification, particularly of the most appropriate theoretical model. Almost all the discussed methods agree that the yield line theory does not accurately predict the collapse load of reinforced concrete slabs largely due to membrane action. The approximate methods of Ockleston and Yee and the more rigorous methods of Wood, Roberts, Christiansen, Park, Morley, Janas and the Indian Institute of Technology have shown that due to compressive membrane action in axially restrained slabs, very high loads can be sustained with very small deflections. In axially unrestrained slabs where the collapse mechanism forms a non-developable surface, the approximate methods of Taylor, Sawczuk and Hayes and the more rigorous methods of Wood, Kemp and Morley have shown that due to tensile membrane action, the load necessary to produce increasing deflection after initial yielding; depends on, and increases with, the deflection.

CHAPTER 3

YIELD CRITERION AND FLOW RULE FOR HOMOGENEOUS AND CRACKED SECTIONS

In this chapter, a yield criterion is derived for a reinforced concrete slab section under the combined effect of bending moment and direct compressive force. The plastic potential theory defining the flow rule of a rigid perfectly plastic material is stated and the concepts of total strain and strain rate theories are presented. The validity and applicability of these theories in homogeneous and cracked sections are discussed.

3.1 YIELD CRITERION

Consider a concrete slab of unit width and depth d, Fig. (3.1a), reinforced with steel bars of area A_s and yield stress f_y. The reinforcing bars are placed at distance d_1 from the compressed face of the slab. It is assumed that this slab yields when it is subjected to a bending moment M and a direct compressive force N applied at the mid-depth of the section as shown in Fig. (3.1a).

Let the moment M and the force N be such that on the slab section at yield, the strain and stress distributions of Figs. (3.1b) and (3.1c) exist. It can be seen from these figures that the neutral axis is located at a distance d_n from the compressed face of the slab and that the shape of the compressive stress block of the concrete is curved but assumed rectangular fixed by the parameters k_1k_3 and k_2. The values of these coefficients were determined by Hognestad, Hanson and McHenry (25) in terms of the crushing strength of a 152.4 mm (6 in) x 304.8 mm (12 in) cylinder but were modified and related elsewhere (29) to the crushing strength u of a 152.4 mm (6 in) cube by assuming the cylinder strength to be equivalent to 0.78 of the cube strength. Values of k_1k_3 and k_2 in SI units* are;

$$k_1k_3 = \frac{3040 + 31u}{3200 + 113u} \qquad (3.1a)$$

---

* The units of the cube strength u in these equations are N/mm^2.

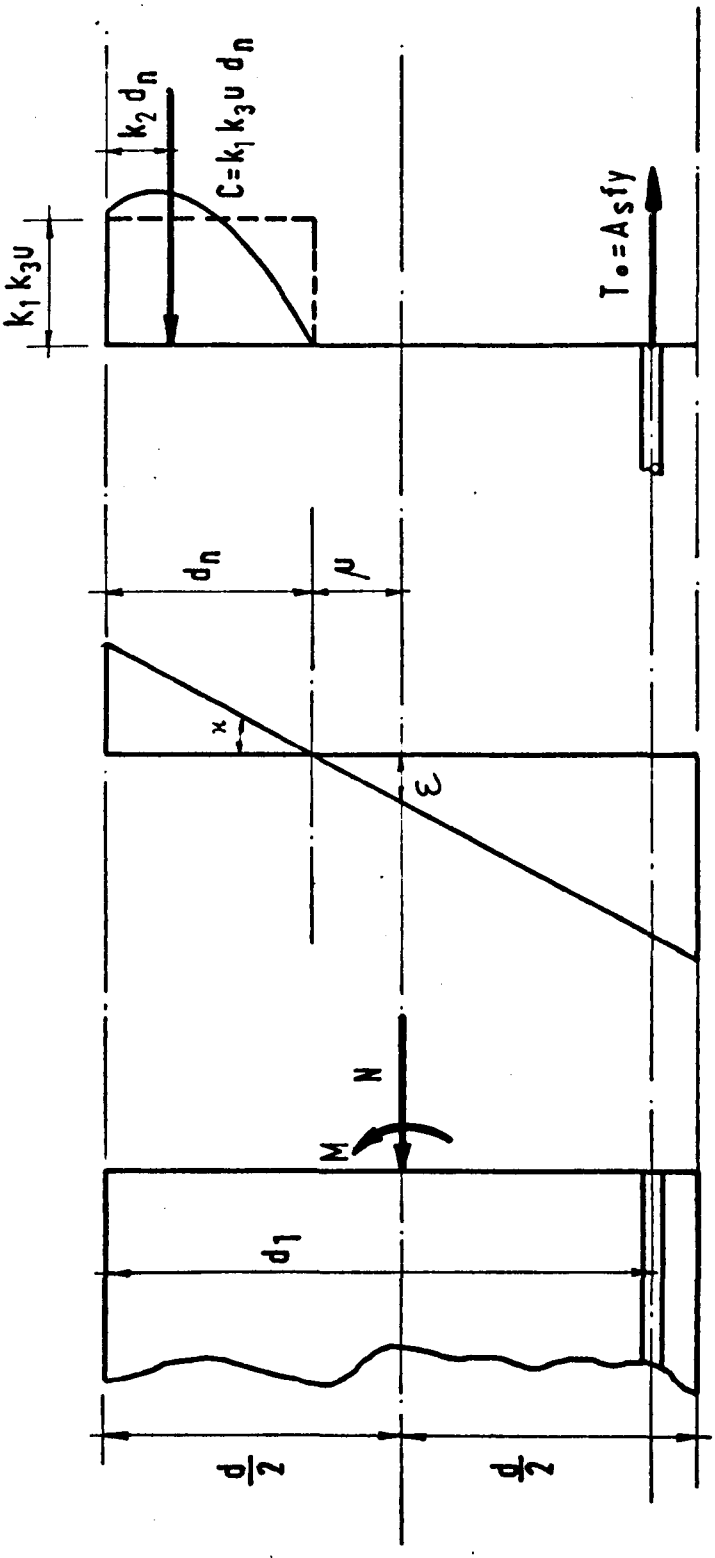

FIG.(3.1) Stress Distribution on a Slab Section at Yield

$$k_2 = 0.5 - \frac{u}{707} \tag{3.1b}$$

Referring to Fig. (3.1c) the magnitudes of the compressive force in the concrete C and the tensile force in the reinforcement T_o are respectively $k_1 k_3 u d_n$ and $A_s f_y$. Equating horizontal forces on the section gives;

$$N = C - T_o = k_1 k_3 u d_n - A_s f_y \tag{3.2}$$

The applied moment M is equal to the sum of the moments of C and T_o about the mid-depth of the section. Therefore,

$$M = k_1 k_3 u d_n \left(\frac{d}{2} - k_2 d_n\right) + A_s f_y \left(d_1 - \frac{d}{2}\right) \tag{3.3}$$

Substitution of the neutral axis depth d_n obtained from equation (3.2) into equation (3.3) leads to the yield criterion

$$M = A_s f_y \left(d_1 - \frac{k_2}{k_1 k_3} \frac{A_s f_y}{u}\right) + N \left(\frac{d}{2} - \frac{2k_2}{k_1 k_3} \frac{A_s f_y}{u}\right) - N^2 \frac{k_2}{k_1 k_3 u}$$

The yield moment corresponding to N = 0 is;

$$M_o = A_s f_y \left(d_1 - \frac{k_2}{k_1 k_3} \frac{A_s f_y}{u}\right) \tag{3.4}$$

and the yield criterion, in non-dimensional form, becomes

$$\frac{M}{M_o} = 1 + \alpha \left(\frac{N}{T_o}\right) - \beta \left(\frac{N}{T_o}\right)^2 \tag{3.5}$$

where

$$\alpha = \frac{\left(\frac{1}{2} \frac{d}{d_1} - \frac{2k_2}{k_1 k_3} \frac{A_s}{d_1} \frac{f_y}{u}\right)}{\left(1 - \frac{k_2}{k_1 k_3} \frac{A_s}{d_1} \frac{f_y}{u}\right)}$$

and $$\beta = \frac{\frac{k_2}{k_1 k_3} \frac{A_s}{d_1} \frac{f_y}{u}}{\left(1 - \frac{k_2}{k_1 k_3} \frac{A_s}{d_1} \frac{f_y}{u}\right)}$$

are constants for a particular slab section.

For an isotropically reinforced slab, the above yield criterion is valid for moments and axial forces acting in any direction relative to the reinforcement directions and is assumed independent of the moments and axial forces acting transversely to the slab section.

In equation (3.5), the maximum moment is obtained when;

$$\frac{N}{T_o} = \frac{\alpha}{2\beta} \tag{3.6a}$$

giving $$\frac{M_{max}}{M_o} = 1 + \frac{\alpha^2}{4\beta} \tag{3.6b}$$

The minimum moment corresponds to $N = -T_o$ when the concrete stress block vanishes and the section is fully cracked;

$$\frac{M_{min}}{M_o} = 1 - \alpha - \beta \tag{3.7}$$

and this marks the terminating point on the yield curve.

To show the relationship between the moment M and the axial force N graphically, a typical reinforced concrete slab section is considered with the following properties : percentage of reinforcement $A_s/d_1 = 0.004$ or 0.4% steel, $f_y = 276$ N/mm^2 (40,000 lbf/in^2), $u = 27.6$ N/mm^2 (4000 lbf/in^2) which gives

$$k_1 k_3 = \frac{3040 + 31 \times 27.6}{3200 + 113 \times 27.6} = 0.616$$

$$k_2 = 0.5 - \frac{27.6}{707} = 0.461$$

Suppose the cover makes $d/d_1 = 1.2$. Therefore,

$$\alpha = \frac{0.6 - 2 \times \frac{0.461}{0.616} \times 0.004 \times \frac{276}{27.6}}{1 - \frac{0.461}{0.616} \times 0.004 \times \frac{276}{27.6}} = \frac{0.6 - 0.06}{0.97} = 0.557$$

and $\beta = \frac{0.03}{0.97} = 0.0309$. Thus, the yield criterion is;

$$\frac{M}{M_o} = 1 + 0.557 \left(\frac{N}{T_o}\right) - 0.0309 \left(\frac{N}{T_o}\right)^2$$

This equation is plotted in Fig. (3.2) and represents a parabola. The form of this parabola is important indicating that there can be considerable divergence from $M = M_o$, the simple Johansen criterion, ranging from $M_{min} = 0.412\ M_o$ at full tension ($N/T_o = -1$) to $M_{max} = 3.51\ M_o$ when $N/T_o = +9.0$.

3.2 FLOW RULE AND THE CONCEPTS OF 'STRAIN RATE' AND 'TOTAL STRAIN'

For a rigid perfectly plastic material the flow rule is normally assumed to be defined by the plastic potential theory. To present this theory let us assume that, at a given state of stress on the yield locus, plastic strain rates with components $d\varkappa$ (plastic curvature strain rate in the direction of M) and $d\varepsilon$ (plastic axial strain rate in the direction of N) occur at the mid-depth of the concrete slab section in Fig. (3.1a). The combined effect of these two plastic strain rate components is a vector which according to plastic potential theory is normal to the yield locus (See Fig. 3.2). The direction of this vector describes the sign of the axial strain rate $d\varepsilon$. If the vector is pointed to the north-east; $d\varepsilon$ is tensile and when the vector is pointed to the north-west; $d\varepsilon$ is compressive. In other words, when the slab section is subjected to a bending moment M and a direct compressive force N such that on the yield locus this point is located to the right of the peak point

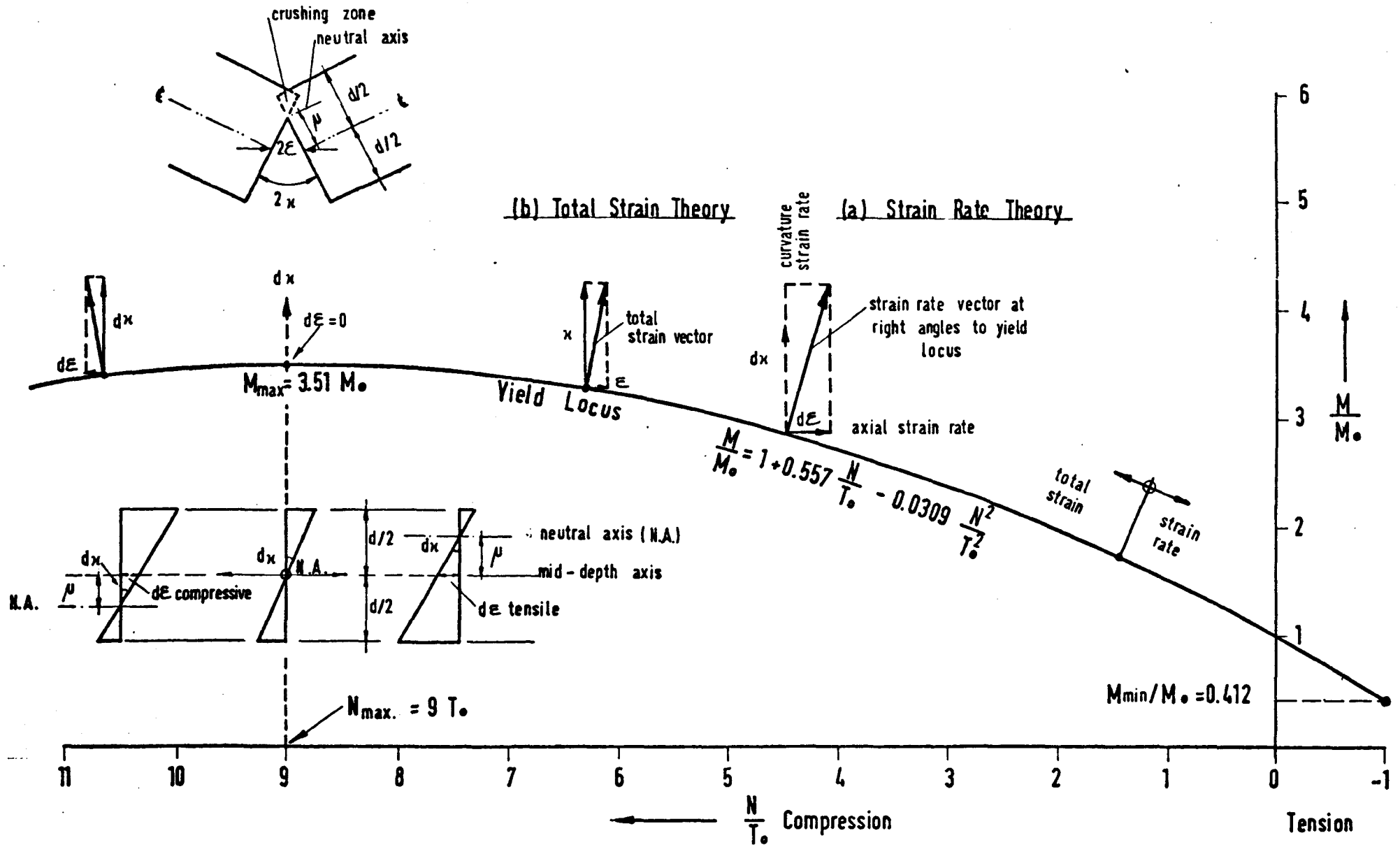

FIG. (3.2) Yield Criterion For a Typical Slab Section

representing M_{max} the mid-depth of the slab section undergoes tensile axial strain rate but if this point lies to the left of M_{max} the axial strain rate is compressive. The limiting case is attained at the peak point (M_{max}) when the vector normal to the yield locus is directed exactly to the north indicating that the mid-depth of the slab section undergoes a plastic curvature strain rate $d\varkappa$ with no axial strain rate.

If f is the plastic potential function assumed equal to the yield criterion given by equation (3.5) so that;

$$f(M, N) = 0$$

the plastic flow according to strain rate theory relates the two plastic 'strain rate' components $d\varepsilon$ and $d\varkappa$ such that

$$\frac{d\varepsilon}{d\varkappa} = \frac{\partial f/\partial N}{\partial f/\partial M} \tag{3.8}$$

Strictly, the ratio $d\varepsilon/d\varkappa$ defines the position of the neutral axis μ for the instantaneous stress state (see Fig. 3.3a). This is actually based on the assumption that plane sections before bending remain plane after bending, i.e. the distribution of the strain across the depth of the section is linear. Therefore,

$$\frac{d\varepsilon}{d\varkappa} = \mu \tag{3.9}$$

Equations (3.8) and (3.9) together give;

$$\mu = \frac{\partial f/\partial N}{\partial f/\partial M} \tag{3.10}$$

It has been demonstrated by Wood (30) that unless the coefficient $k_2 = 1/2$ the neutral axis position determined by plastic potential theory (Eq. 3.10) is not consistent with the corresponding one obtained from equilibrium (Eq. 3.2).

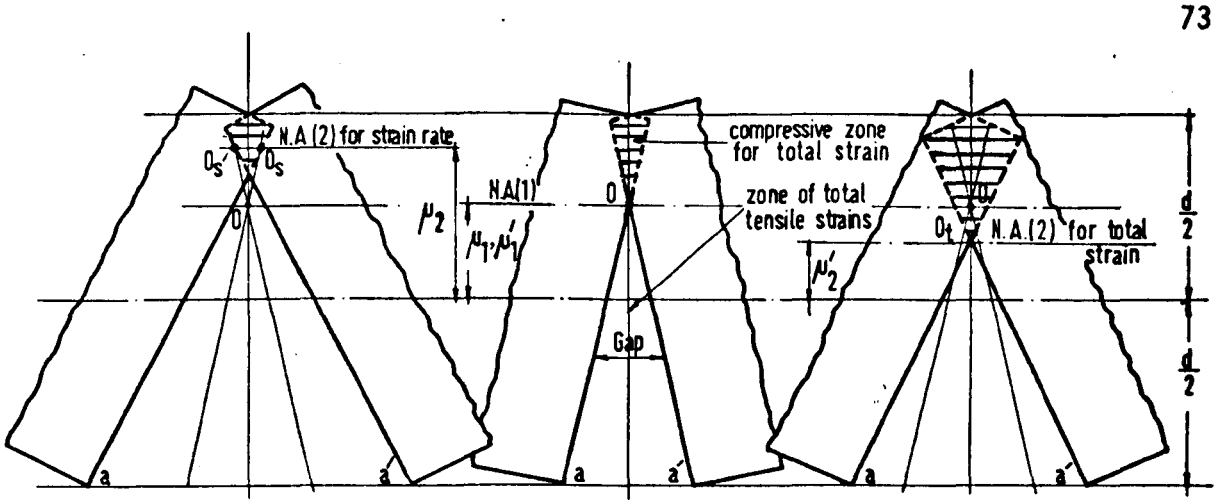

(c) N.A. For Strain Rate Moving Into Compressive Zone For Total Strain

(b) A Cracked Section

(d) N.A. For Strain Rate Moving Into Zone of Total Tensile Strains

(b),(c),(d) Determining The Position of The Neutral Axis In Cracked Sections

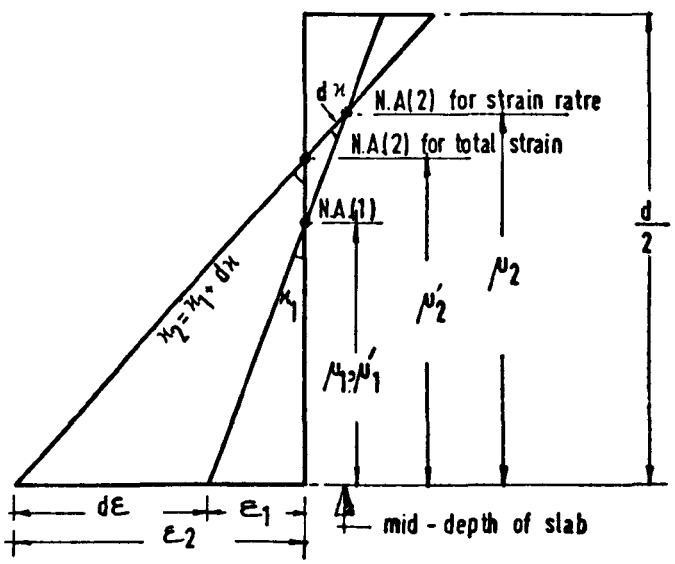

(a) Determining The Position of the Neutral Axis by Strain Rate & Total Strain

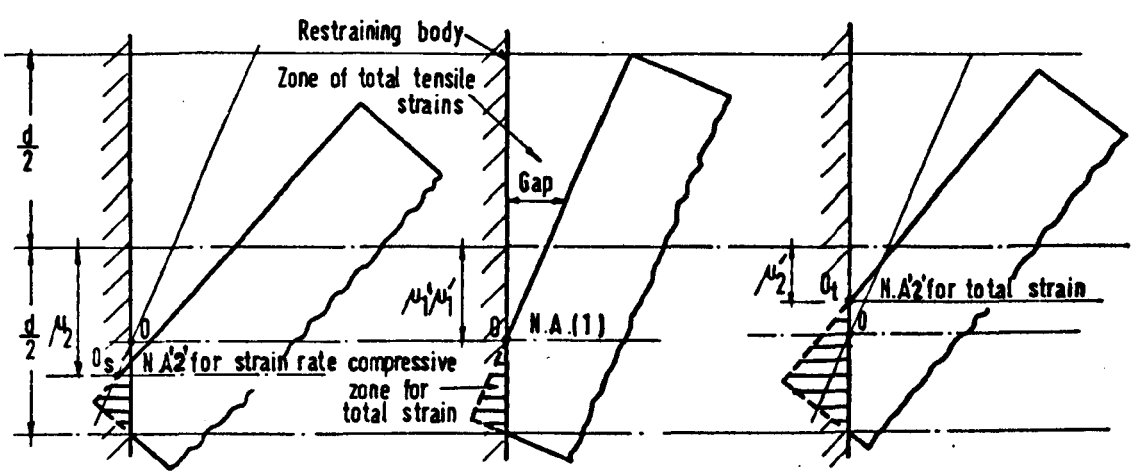

(f) N.A. For Strain Rate Moving Into Compressive Zone for Total Strain

(e) An Axially-Restrained End

(g) N.A. For Strain Rate Moving Into Zone of Total Tensile Strains

(e),(f),(g) Determining The Position of The Neutral Axis In Axially Restrained Ends

FIG.(3.3)

From equations (3.5) and (3.10),

$$\mu = \alpha \frac{M_o}{T_o} - 2\beta \frac{M_o}{T_o} \frac{N}{T_o}$$

Introducing the α, β and M_o functions into this equation leads to

$$\mu = \frac{d}{2} - \frac{2k_2}{k_1 k_3} \frac{(N + A_s f_y)}{u} \qquad (3.11)$$

From the horizontal equilibrium represented by Eq. (3.2), by noting that $d_n = \frac{d}{2} - \mu$;

$$\mu = \frac{d}{2} - \frac{1}{k_1 k_3} \frac{(N + A_s f_y)}{u} \qquad (3.12)$$

If equations (3.11) and (3.12) are compared, it will be seen that they are identical only when $k_2 = 1/2$ whereas experimental tests on reinforced concrete beams usually indicate values of k_2 rather less than 0.5. To be consistent with the plastic potential theory the neutral axis depth μ will be assumed to be given by Eq. (3.11). However, the inconsistency between the plastic potential theory and the equilibrium method refers to the modification of the shape of the compressive stress block of the concrete which is curved in reality but assumed to be rectangular for the convenience in analysis. The effect of the discrepancy in k_2 will be shown in Chapter 4.

In contrast to the strain rate theory the 'total strain theory' associates the 'accumulated' or total plastic strain components ϵ and $\varkappa$ with the current state of stress. This implies using the ratio $\epsilon/\varkappa$ to represent a new definition for the neutral axis depth μ' so that

$$\mu' = \frac{\epsilon}{\varkappa} = \frac{\partial f/\partial N}{\partial f/\partial M} \qquad (3.13)$$

Equation (3.13) has been adopted by some authors, Wood (3) and Kemp (4), for convenience in analysis but with no physical justification. However, the definition of the neutral axis for total strain by the instantaneous stress state is not generally valid and the total strain theory can only furnish similar prediction to the neutral axis depth with the strain rate theory when the stress state remains constant. This can be shown mathematically as follows;

From equation (3.13);

$$\epsilon = \mu' \kappa$$

Differentiating both sides of the equality gives

$$d\epsilon = \mu' d\kappa + \kappa \, d\mu'$$

or $$\frac{d\epsilon}{d\kappa} = \mu' + \kappa \frac{d\mu'}{d\kappa}$$

which together with equation (3.9) becomes

$$\mu = \mu' + \kappa \frac{d\mu'}{d\kappa} \qquad (3.14)$$

Equation (3.14) shows that the neutral axis depth μ' predicted by total strain theory can only be identical with that obtained by strain rate theory μ when there is no change in the stress state (i.e. when $d\mu'/d\kappa = 0$).

This conclusion could be derived in a different way. Let the slab section of Fig. (3.1a) at yield undergo, for a certain state of stress, a plastic axial strain of value ϵ_1 (see Fig. 3.3a) and a plastic curvature strain κ_1. Assume that when the state of stress is changed the values of these plastic strain components will be changed by $d\epsilon$ and $d\kappa$ respectively. The strain rate theory states that the position of the neutral axis μ_2 for the new state of stress is given by;

$$\mu_2 = \frac{d\epsilon}{d\kappa} \qquad (3.15)$$

while the total strain theory suggests that this axis will be located at a depth μ_2' so that;

$$\mu_2' = \frac{\varepsilon_1 + d\varepsilon}{x_1 + dx} = \frac{\varepsilon_2}{x_2} \qquad (3.16)$$

as shown in Fig. (3.3a). Equations (3.15) and (3.16) furnish different results unless the state of stress is uniform; i.e. if

$$\frac{d\varepsilon}{dx} = \frac{\varepsilon_1}{x_1}$$

3.3 HOMOGENEOUS AND CRACKED SECTIONS

The discussion of the previous section suggests that strain rate theory should always be used in analysis and that total strain theory is theoretically invalid except in the case of uniform stress state where both theories furnish similar results. This conclusion is correct as far as the analysis of homogeneous ductile materials is concerned but in materials with cracked sections such as reinforced concrete the situation will be shown to be different.

In Chapter 2, it was mentioned that some investigators like Wood (3) and Kemp (4) use the concept of total strain in the study of membrane action in concrete slabs, while others like Janas (22,26) and Morley (10) have used strain rate. None of these investigators has provided an explanation as to why a specific approach was adopted, nor has a study or discussion yet been presented to prove which theory is physically correct. The differences between total strain and strain rate theories in analysis and their effect on the behaviour of concrete slabs will be studied in detail in later chapters but here physical arguments will be given to establish the correct approach to be used in the analysis of cracked sections.

When a section is cracked (see Fig. 3.3b) the fibres of the section covering most (or all) of the tension zone will be split

apart leaving a physical gap or discontinuity between the adjacent faces of the section. It is important to note that the physical gap at the crack is essentially a zone of 'total tensile strains' since, for any fibre, it represents a tensile extension at a point, i.e. the integral of infinite total strains over an infinitely small length. This zone of total tensile strains will extend from the position of the neutral axis for total strain to the outer fibre representing the maximum total tensile strain. Therefore, in Fig. (3.3b) the triangular area Oaa' represents the zone of total tensile strains with point O defining the location of the neutral axis for total strain.

If due to a change of plastic stress state the neutral axis for strain rate moves into the compressive zone for total strain (i.e. to any point inside the shaded area above point O in Fig. 3.3b) the section is similar to a homogeneous one. In this case the strain rate theory should be applicable for predicting the new neutral axis position and the new strain increments (see Fig. 3.3c) and, therefore, equation (3.8) is valid.

If, however, due to a change of plastic stress state the neutral axis for strain rate moves into the crack or zone of total tensile strains (i.e. to any point below point O in Fig. 3.3b) then compressive stresses and strain increments will be required for all fibres above the new neutral axis position. This will only be possible if the physical gap above the new neutral axis position (from point O to O_t in Fig. 3.3d) is closed. This implies that the new neutral axis position is defined by total strain theory since the <u>total</u> tensile strains (or extensions) must be zero at the new neutral axis position for compressive stresses to exist on all fibres above it. Thus, whenever due to a change of plastic stress state, the neutral axis for strain rate moves into the cracked zone, the new neutral axis position and the new strain increments will be defined by equation (3.13).

A similar situation arises when there is a physical gap between the end of a slab or beam member and an axially restraining

body (see Fig. 3.3e). Accordingly, the discussion presented above about the applicability of the total strain and strain rate theories in cracked sections will be equally valid here. When due to a stress state change the neutral axis for strain rate moves into the compressive zone for total strain, the neutral axis position and strain increments will be defined by strain rate theory but when it moves into the physical gap or zone of total tensile strains, they will be defined by total strain theory as indicated in Figs. (3.3f) and (3.3g) respectively.

To summarize these conclusions, strain rate theory is valid for the analysis of all cases of homogeneous ductile materials but in cases of 'cracked sections' including gaps at axially restrained ends the theory is applicable only when the neutral axis for strain rate moves into the compressive zone for total strain.

The total strain theory is valid in cases of uniform stress state (uniform in time) since similar results to those of strain rate theory are then predicted and notably in 'cracked sections' when the neutral axis for strain rate moves into the zone of total tensile strains.

These important conclusions appear to be new and will play a significant part in the analysis of compressive membrane action which will be presented in later chapters of this thesis.

CHAPTER 4

AXIALLY RESTRAINED REINFORCED CONCRETE SLAB STRIPS (RIGID - PLASTIC THEORY)

4.1 INTRODUCTION AND ASSUMPTIONS

This chapter presents a rigid-plastic theory for the load carrying capacity and behaviour of reinforced concrete slab strips that are restrained axially against longitudinal expansion. Restraint is provided to the edges of the slab by the in-plane stiffness of the surrounding panels, generating compressive membrane action with a consequent rise in the yield moment. This increases the load-carrying capacity considerably beyond that predicted according to limit analysis based on failure by bending only. The rigid-plastic theory presented here helps to explain this kind of structural action, with reference initially to the simplest cases of one-way-spanning slabs, where all strips in such slabs behave alike. It is necessary to understand strip action before attempting to explain the compressive membrane behaviour of slabs.

The theoretical analysis presented in this chapter involves studying the load-deflection characteristics as well as determining the ultimate loads for rigid-plastic reinforced concrete slab strips that have their ends fixed against rotation and horizontal extension. The special case of slab strips with simple supports and lateral restraints will be treated as straightforward deductions from the general case of fixed-ended strips.

Throughout the discussion of this chapter, it will be shown that the movements of the neutral axis for strain rate at sections of yield in these rigid-plastic slabs occur only into the compressive zone for total strain; the case for which strain rate theory must be applied. However, for the sake of comparison, the analysis here will be presented following both total strain and strain rate concepts to show the influence of these two approaches (each of which has been used by other authors) on the prediction

of the plastic behaviour of such slabs.

The loading on the slab strips considered is two point but certain other loadings could be analysed in a similar way. The system of two point loading is suggested to avoid having biaxial stresses at sections of yield under the load.

The assumptions made in the analysis of the fixed-ended slab strips under study are as follows :

i. Plane sections before bending remain plane after bending, i.e. the strain distribution across the depth of a section is linear.

ii. The strength of concrete in tension is neglected.

iii. The materials of the slab behave in a rigid - perfectly plastic manner.

iv. The outward movement of the surround due to axial forces is neglected.

v. The incipient yield-line collapse mode is applied to the deformed slab strip (i.e. the strip yields at the fixed ends and at the weakest section of the central region between the two applied loads).

vi. The collapse mechanism remains unchanged with deformation.

vii. The slab strip is assumed to be reinforced in the bottom face only at mid-span and in the top face only at the ends. The reinforcement is assumed to extend far enough in the slab to ensure plastic hinges form at the central region of the slab and at the ends.

Furthermore, the yield criterion represented by equation (3.5) of Chapter 3 will be adopted and assumed valid for all analyses. The equations for the collapse loads and the membrane forces will be given in dimensionless forms as ratios of the simple yield line theory load and the yield force in the tensile reinforcement respectively. The effect of some important factors will also be discussed.

4.2 GENERAL ANALYSIS

4.2.1 THE SLAB STRIP AND THE MECHANISM OF COLLAPSE

Fig. (4.1b) shows a fixed-ended reinforced concrete slab strip AB of unit width, depth d and length L subjected to two point loading each of magnitude P/2 located at a distance 'a' from the nearest fixed end A or B . The slab strip is reinforced with steel bars of yield stress f_y , cover $(d-d_1)$ and having a total cross sectional area of A_s in the bottom face only at mid-span and area A_s' in the top face only at supports as shown.

Strictly, the central plastic hinge C (Fig. 4.1a) does not necessarily form at mid-span but may form at any section (whichever is the weakest) in the portion extending between the two concentrated loads since this part of the slab is the region of maximum bending moment. In the analysis, this hinge will be assumed to form at a distance c from the centre of the slab as shown in Fig. (4.1a).

Since the materials of the slab behave in a rigid - perfectly plastic manner, as the assumption states, the slab will yield at a particular load P and the mechanism of collapse shown in Fig. (4.1c) is then assumed to form.

4.2.2 MEMBRANE ACTION - DEVELOPMENT OF MEMBRANE FORCE AND RELATIONS TO MOMENTS AND NEUTRAL AXIS POSITION AT THE PLASTIC HINGES

After formation of the collapse mechanism, the slab deflects and the ends rotate. The rotation of the ends produces horizontal movement but since the slab strip is restrained axially such movement is resisted and hence a compressive membrane force is generated. Let this force be denoted by N . The value of N at any section of yield is, as shown in Eq. (3.2) of Chapter 3; the difference between the compressive force in the concrete and the tensile force in the reinforcement. However, the horizontal equilibrium of the slab strip requires that the membrane force at both ends of the slab

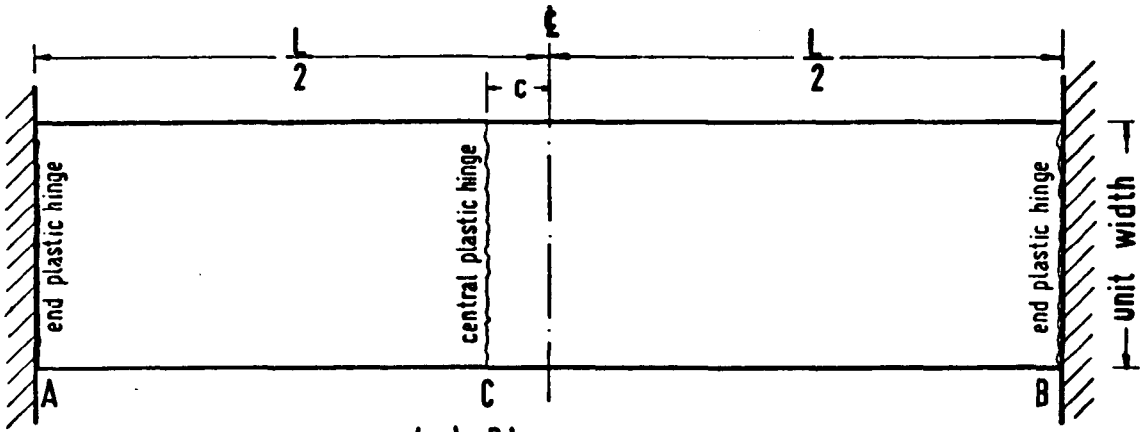

(a) Plan

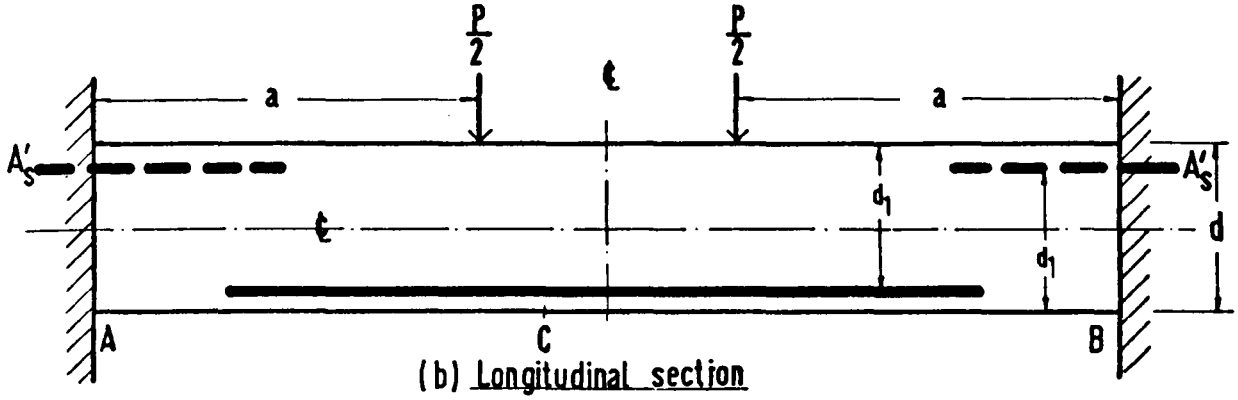

(b) Longitudinal section

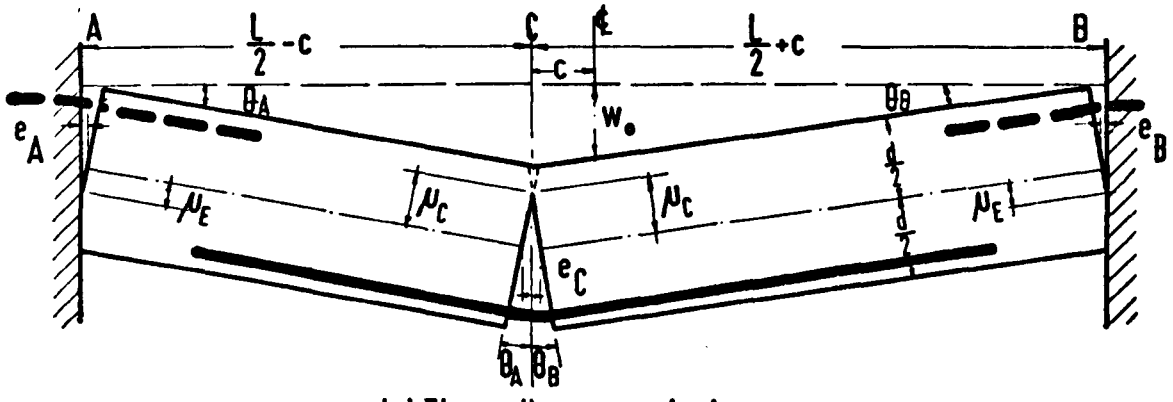

(c) The collapse mechanism

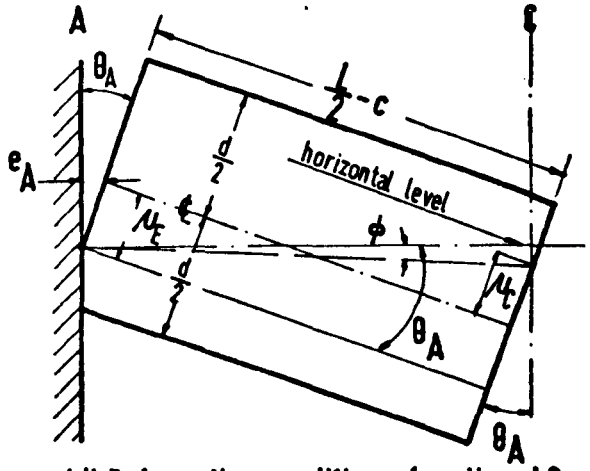

(d) Deformation condition of portion AC

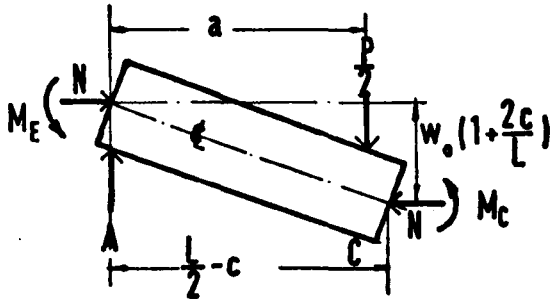

(e) Moment equilibrium of the rigid portion AC

FIG.(4.1) Axially Restrained Fixed Ended Reinforced Concrete Slab Strip with Two Point Loading At Yield

and at section C should be identical;

$$\text{i.e.} \qquad N_E^* = N_C = N \tag{4.1}$$

If the yield bending moment corresponding to zero axial force at the central hinge C is designated M_o and the yield force in the reinforcement T_o, the relationship between the moment M and the membrane force N at this particular section will be exactly the same as that given by Eq. (3.5);

$$\frac{M_C}{M_o} = 1 + \alpha \left(\frac{N}{T_o}\right) - \beta\left(\frac{N}{T_o}\right)^2 \tag{4.2}$$

At the fixed ends A and B, the cross sectional area of reinforcement is A_s' and, therefore, if

$$\gamma = \frac{A_s'}{A_s}$$

the relationship between M and N at these sections in a dimensionless form with reference to M_o and T_o will be

$$\frac{M_E}{M_o} = \gamma[1 + \beta(1 - \gamma)] + [\alpha + 2\beta\,(1 - \gamma)]\left(\frac{N}{T_o}\right) - \beta\left(\frac{N}{T_o}\right)^2 \tag{4.3}$$

It is of interest to note that $\gamma[1 + \beta(1 - \gamma)]$ is the ratio of the yield bending moment corresponding to zero axial force at the fixed ends to the corresponding moment at section C so that

$$\frac{M_{oE}}{M_o} = \gamma\,[1 + \beta(1 - \gamma)] \tag{4.4}$$

Generally, the plastic analysis of any concrete slab subjected to flexure as well as membrane action is based on finding the positions of the neutral axis at sections of yield at any stage of deformation. In the analysis of the slab strip AB the position

---

* The subscript E (for end) represents both of the ends A and B of the slab strip AB.

of the neutral axis at the central and end hinges may be related to the value of the membrane force N in accordance with Eq. (3.11). Thus;

$$\mu_C = \frac{d}{2} - \frac{2k_2}{k_1 k_3} \frac{(N + A_s f_y)}{u}$$

$$\mu_E = \frac{d}{2} - \frac{2k_2}{k_1 k_3} \frac{(N + \gamma A_s f_y)}{u}$$

These relations may be written in a different form by using the notations α and β defined by Eq. (3.5). Therefore,

$$\mu_C = \left[1 - \frac{2}{(\frac{\alpha}{\beta} + 2)} (1 + \frac{N}{T_o})\right] \frac{d}{2} \qquad (4.5a)$$

$$\mu_E = \left[1 - \frac{2}{(\frac{\alpha}{\beta} + 2)} (\gamma + \frac{N}{T_o})\right] \frac{d}{2} \qquad (4.5b)$$

In these equations, μ_C is positive if the neutral axis is located above the mid-depth of the yield section C and, similarly, μ_E is positive when this axis forms below the mid-depth of the fixed end sections A and B.

4.2.3 COMPATIBILITY EQUATION

When the vertical deflection at the centre of the slab strip is w_o the plastic rotation and horizontal extension of the mid-depth of the sections at yield A, B and C are, as shown in Fig. (4.1c), respectively, θ_A and e_A for section A, θ_B and e_B for section B and $(\theta_A + \theta_B)$ and e_C for section C. Then due to the assumed rigidity of the slab strip and the surround, these plastic rotations and extensions are related so that for horizontal compatibility,

$$e_A + (\frac{L}{2} - c) \cos \theta_A + e_C + (\frac{L}{2} + c) \cos \theta_B + e_B = L$$

When θ is small

$$\cos \theta \simeq 1 - \frac{\theta^2}{2}$$

and the compatibility equation becomes

$$e_A + e_B + e_C - (\tfrac{L}{2} - c)\frac{\theta_A^2}{2} - (\tfrac{L}{2} + c)\frac{\theta_B^2}{2} = 0 \qquad (4.6)$$

4.2.4 EVALUATION OF THE MEMBRANE FORCE ACCORDING TO 'TOTAL STRAIN' AND 'STRAIN RATE' THEORIES

(a) Total Strain Theory

If the total strain concept is adopted in this analysis, the relationships between the plastic rotations θ and the plastic extensions e at sections A, B and C will be according to Eq. (3.13) and consequently ;

$$e_A = \mu_E' \theta_A \qquad (4.7a)$$

$$e_B = \mu_E' \theta_B \qquad (4.7b)$$

$$e_C = \mu_C' (\theta_A + \theta_B) \qquad (4.7c)$$

Substituting equations (4.7) into equation (4.6) yields

$$\mu_E' (\theta_A + \theta_B) + \mu_C' (\theta_A + \theta_B) - (\tfrac{L}{2} - c)\frac{\theta_A^2}{2} - (\tfrac{L}{2} + c)\frac{\theta_B^2}{2} = 0$$

From the geometry of the collapse mechanism (Fig. 4.1c), the plastic rotations θ_A and θ_B can be related to the central deflection w_o ;

$$\theta_A = \frac{2w_o}{L}\frac{1 + \frac{2c}{L}}{1 - \frac{2c}{L}} \qquad (4.8a)$$

$$\theta_B = \frac{2w_o}{L} \tag{4.8b}$$

and therefore the compatibility equation becomes

$$\mu_E' + \mu_C' - \frac{w_o}{2}\left(1 + \frac{2c}{L}\right) = 0 \tag{4.9}$$

The values of μ_E' and μ_C' are given in equations (4.5) in terms of the membrane force N. Therefore, substituting these values into equation (4.9) and solving for N gives

$$\frac{N}{T_o} = \frac{1}{2}\left[\left(\frac{\alpha}{\beta} + 1 - \gamma\right) - \frac{1}{2}\left(\frac{\alpha}{\beta} + 2\right)\left(1 + \frac{2c}{L}\right)\frac{w_o}{d}\right] \tag{4.10}$$

(b) Strain Rate Theory

When the strain rate theory is applied, the analysis will be concerned with the incremental variation in the plastic rotations and extensions (as Eq. 3.9 states) and therefore in this case

$$de_A = \mu_E \cdot d\theta_A \tag{4.11a}$$

$$de_B = \mu_E \cdot d\theta_B \tag{4.11b}$$

$$de_C = \mu_C\,(d\theta_A + d\theta_B) \tag{4.11c}$$

Substituting equations (4.11) into the derivative of equation (4.6) gives

$$\mu_E\,(d\theta_A + d\theta_B) + \mu_C\,(d\theta_A + d\theta_B) - \left(\frac{L}{2} - c\right)\theta_A\,d\theta_A - \left(\frac{L}{2} + c\right)\theta_B\,d\theta_B = 0$$

and when the values of the plastic rotations θ_A and θ_B given by Eqs. (4.8) are introduced the equation becomes

$$\mu_E\,(d\theta_A + d\theta_B) + \mu_C(d\theta_A + d\theta_B) - w_o\left(1 + \frac{2c}{L}\right)(d\theta_A + d\theta_B) = 0$$

or

$$\mu_E + \mu_C - w_o \left(1 + \frac{2c}{L}\right) = 0 \qquad (4.12)$$

Equations (4.5) and (4.12) together produce

$$\frac{N}{T_o} = \frac{1}{2}\left[\left(\frac{\alpha}{\beta} + 1 - \gamma\right) - \left(\frac{\alpha}{\beta} + 2\right)\left(1 + \frac{2c}{L}\right)\frac{w_o}{d}\right] \qquad (4.13)$$

For any deflection w_o equations (4.10) and (4.13) furnish different values for the membrane force N. The difference between these two equations lies in the last term where a factor of 1/2 appears in the total strain equation (4.10) which increases the value of N above that predicted according to the strain rate theory. However, both equations represent a linear relationship between N and w_o with N being maximum at the start of collapse when $w_o = 0$. This is shown graphically in Fig. (4.2) for the case of a slab strip with the following properties ;

$\gamma = 1.5$, $A_s/d_1 = 0.285\%$, $f_y = 276$ N/mm^2 (40,000 lbf/in^2)

$u = 27.6$ N/mm^2 (4,000 lbf/in^2) , $d/d_1 = 1.2$ and $c = 0$.

The maximum compressive membrane force in this figure; being 13.2 T_o , puts the slab strip under direct stress of 8.65 N/mm^2 (1254 lbf/in^2) which is less than one third of the cube strength of the slab concrete.

4.2.5 DETERMINATION OF THE NEUTRAL AXIS POSITION

The value of the membrane force having been determined, the position of the neutral axis at the plastic hinges can be defined in terms of the deflection w_o in accordance to Eqs. (4.5). Therefore ;

$$\left.\begin{aligned} \mu_C &= \left[\frac{(\gamma - 1)}{\left(\frac{\alpha}{\beta} + 2\right)} + \left(1 + \frac{2c}{L}\right)\frac{w_o}{d}\right]\frac{d}{2} \\ \mu_E &= \left[\frac{(1 - \gamma)}{\left(\frac{\alpha}{\beta} + 2\right)} + \left(1 + \frac{2c}{L}\right)\frac{w_o}{d}\right]\frac{d}{2} \end{aligned}\right\} \text{(strain rate)} \qquad (4.14a)$$

or

$$\left.\begin{aligned} \mu_C &= \left[\frac{(\gamma - 1)}{(\frac{\alpha}{\beta} + 2)} + \frac{1}{2}\left(1 + \frac{2c}{L}\right)\frac{w_o}{d}\right]\frac{d}{2} \\ \mu_E &= \left[\frac{(1 - \gamma)}{(\frac{\alpha}{\beta} + 2)} + \frac{1}{2}\left(1 + \frac{2c}{L}\right)\frac{w_o}{d}\right]\frac{d}{2} \end{aligned}\right\} \text{(total strain)} \quad (4.14b)$$

Equations (4.14) show that the neutral axis according to the strain rate theory moves more rapidly towards the compressed face of the slab than that predicted by total strain theory. For the special case $\gamma = 1$ and $c = 0$ the depth of the neutral axis μ at the plastic hinges according to the strain rate theory is exactly half the value of the central deflection w_o while the total strain theory predicts half this amount; i.e. one quarter of the central deflection.

It is worth commenting here that according to the strain rate theory the neutral axis at the central and end hinges, for any value of deflection, is located at the same horizontal level but in total strain theory the position of this axis at the central hinge is always lower than that at the end hinges. From Fig. (4.1d); if Φ denotes the angle which the line joining the positions of the neutral axis at the central hinge C and at the end hinge A makes with the horizontal level, one can set

$$\theta_A - \Phi = \frac{\mu_E + \mu_C}{\frac{L}{2} - c}$$

Replacing θ_A by the value given in Eq. (4.8a) leads to

$$\Phi = \frac{1}{(\frac{L}{2} - c)}\left[w_o\left(1 + \frac{2c}{L}\right) - (\mu_E + \mu_C)\right]$$

The quantity $(\mu_E + \mu_C)$ is given in equations (4.12) of strain rate and (4.9) of total strain as a function of the central deflection w_o. when these relations are considered the value of the angle Φ becomes

$$\dot{\Phi} = 0 \qquad \text{(strain rate)}$$

$$\Phi = \frac{w_o}{L} \frac{(1 + \frac{2c}{L})}{(1 - \frac{2c}{L})} = \frac{\theta_A}{2} \qquad \text{(total strain)}$$

4.2.6 YIELD LOAD

At any given central deflection, the yield load can be found by considering the equilibrium of one of the two rigid portions of the slab strip. Referring to Fig. (4.1e), the equilibrium equation obtained by taking moments about the mid-depth of the fixed end A is

$$\frac{P}{2} a = M_C + M_E - N. w_o(1 + \frac{2c}{L})$$

Introducing the expressions for M_C and M_E given by equations (4.2) and (4.3) respectively leads to

$$\frac{P a}{2M_o} = [1 + \gamma\{1 + \beta(1 - \gamma)\}] + 2\beta [(\frac{\alpha}{\beta} + 1 - \gamma) - (\frac{\alpha}{\beta} + 2) (1 + \frac{2c}{L}) \frac{w_o}{d}] (\frac{N}{T_o}) - 2\beta (\frac{N}{T_o})^2$$

Noting that the yield load predicted by the simple yield line theory is

$$P_y = \frac{2M_o}{a} [1 + \gamma\{1 + \beta(1 - \gamma)\}] \qquad (4.15)$$

and, therefore, the equation of the load in a dimensionless form becomes

$$\frac{P}{P_y} = 1 + \frac{2\beta[\frac{\alpha}{\beta} + 1 - \gamma - (\frac{\alpha}{\beta} + 2)(1 + \frac{2c}{L}) \frac{w_o}{d}]}{[1 + \gamma\{1 + \beta(1 - \gamma)\}]} (\frac{N}{T_o}) - \frac{2\beta}{[1 + \gamma\{1 + \beta(1 - \gamma)\}]} (\frac{N}{T_o})^2$$

(4.16)

For any value of deflection at the centre of the slab the yield load P/P_y can be obtained by combining Eq. (4.16) with either Eq. (4.10) for 'total strain' or Eq. (4.13) for 'strain rate'. Hence

$$\frac{P}{P_y} = 1 + \frac{\beta}{2\,[1 + \gamma\{1 + \beta(1 - \gamma)\}]}\,[(\tfrac{\alpha}{\beta} + 1 - \gamma)^2 - 2(\tfrac{\alpha}{\beta} + 2)(\tfrac{\alpha}{\beta} + 1 - \gamma)$$
$$(1 + \tfrac{2c}{L})\,(\tfrac{w_o}{d}) + (\tfrac{\alpha}{\beta} + 2)^2\,(1 + \tfrac{2c}{L})^2\,(\tfrac{w_o}{d})^2\,] \qquad \text{(strain rate)} \qquad (4.17a)$$

or

$$\frac{P}{P_y} = 1 + \frac{\beta}{2[1 + \gamma\{1 + \beta(1 - \gamma)\}]}\,[(\tfrac{\alpha}{\beta} + 1 - \gamma)^2 - 2(\tfrac{\alpha}{\beta} + 2)(\tfrac{\alpha}{\beta} + 1 - \gamma)$$
$$(1 + \tfrac{2c}{L})\,(\tfrac{w_o}{d}) + \tfrac{3}{4}\,(\tfrac{\alpha}{\beta} + 2)^2\,(1 + \tfrac{2c}{L})^2\,(\tfrac{w_o}{d})^2\,] \qquad \text{(total strain)} \qquad (4.17b)$$

These equations represent a falling parabola (Fig. 4.2) with the maximum load P/P_y occurring at the start of collapse ($w_o = 0$). Both theories (total strain and strain rate) predict the same value for the peak load but as the deflection w_o increases the load according to the total strain theory (Eq. 4.17b) falls off more rapidly than that of the strain rate concept (Eq. 4.17a).

4.3 THE PLASTIC BEHAVIOUR OF THE SLAB STRIP FOR DIFFERENT VALUES OF THE RATIO OF REINFORCEMENT γ

The plastic behaviour of the slab strip during the stages of deformation is now discussed with reference to three ranging values of γ.

4.3.1 THE CASE $\gamma > 1$

This is the case when more reinforcement is provided at the fixed ends than at the central region of the slab strip. The

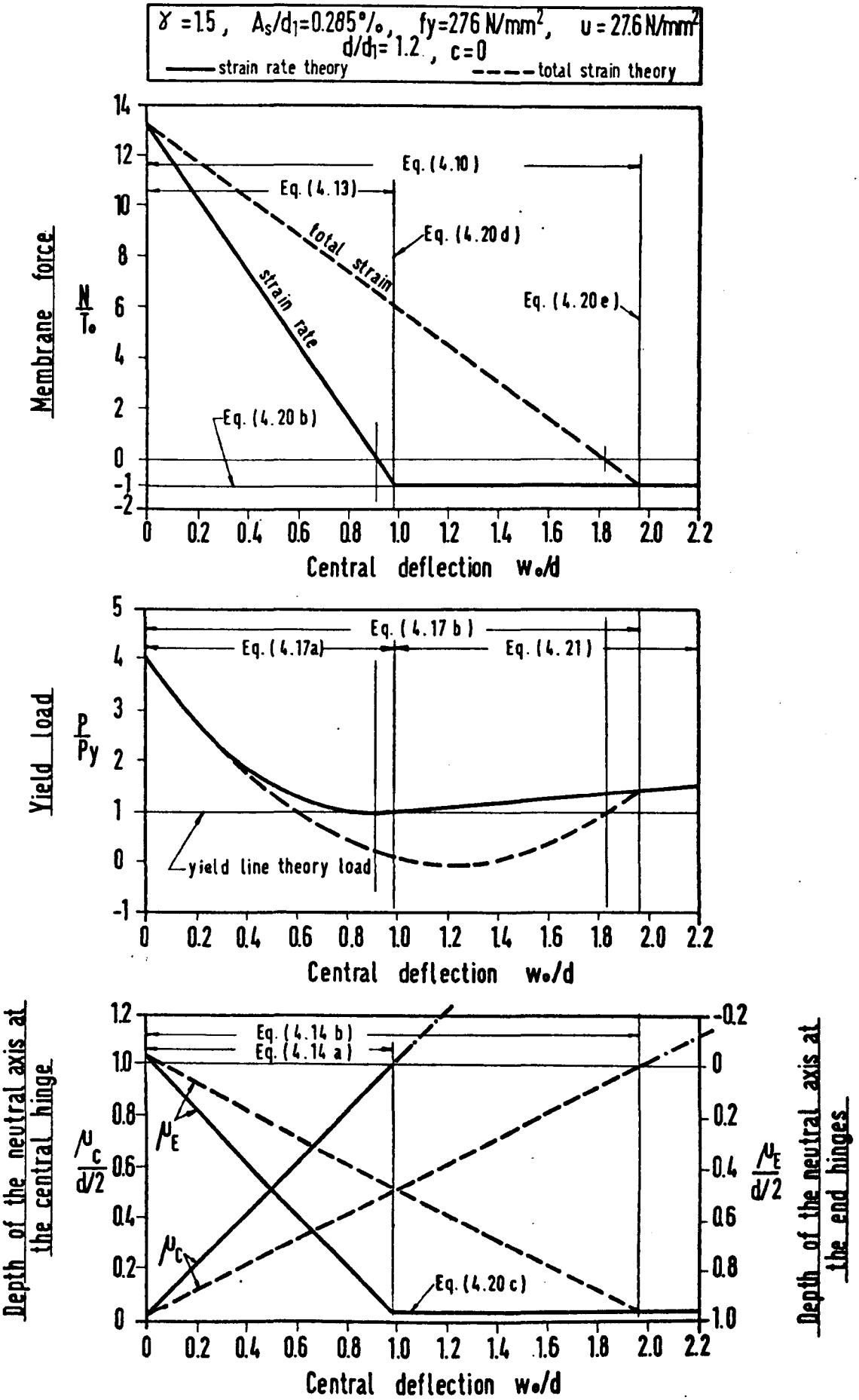

FIG (4.2) Behaviour of a Rigid-Plastic Reinforced Concrete Slab Strip with Fixed Ends and Axial Restraints (The Case $\gamma > 1$)

plastic behaviour of the slab strip for this case is shown in Fig. (4.2). When the collapse mechanism forms at zero deflection, the values of the compressive membrane force as well as the yield load are at their maxima. These values are equally predicted by both 'total strain' and 'strain rate' theories ;

from Eq. (4.13) for strain rate or Eq. (4.10) for total strain

$$\frac{N_{max}}{T_o} = \frac{1}{2}\left(\frac{\alpha}{\beta} + 1 - \gamma\right) \tag{4.18a}$$

and from Eqs. (4.17)

$$\frac{P_{max}}{P_y} = 1 + \frac{\beta\left(\frac{\alpha}{\beta} + 1 - \gamma\right)^2}{2[1 + \gamma\{1 + \beta(1 - \gamma)\}]} \tag{4.18b}$$

The position of the neutral axis at the central and end hinges for $w_o = 0$ is from Eqs. (4.14) ;

$$\mu_C = \frac{(\gamma - 1)}{\left(\frac{\alpha}{\beta} + 2\right)} \frac{d}{2} \tag{4.18c}$$

$$\mu_E = -\frac{(\gamma - 1)}{\left(\frac{\alpha}{\beta} + 2\right)} \frac{d}{2} \tag{4.18d}$$

indicating that the neutral axis at the three plastic hinges lies above the mid-depth of the slab (by the distance given in these equations) and on the same horizontal level.

If a diagram relating the moment M_C at the central hinge and the membrane force N is constructed similar to that shown in Fig. (3.2), the point representing the start of collapse ($w_o = 0$, $N = N_{max}$) will be located on the yield locus to the right of the peak point representing M_{Cmax} since the mid-depth of this hinge at this stage is undergoing tensile axial strain (i.e. the neutral axis is above the mid-depth). How far this starting point is from M_{Cmax} depends entirely on the value of γ . The larger the value of γ ,

the farther the point will be from the peak M_C .

If a similar diagram is made which relates the moment M_E at the fixed ends with the membrane force N , the point representing the start of collapse will be located to the left of the peak point representing M_{Emax} since in this case the mid-depth of the slab ends is undergoing compressive axial strain rather than tensile. Again the larger the value of γ , the greater the distance on the yield locus between the initial stress state and M_{Emax} will be. For practical values of γ , the shifting of the starting collapse point on the M - N curves from M_{max} is in fact very small.

As the central deflection w_o increases the magnitude of the membrane force N/T_o and also the yield load P/P_y decrease. The reduction in N/T_o is linear (Eqs. 4.10 and 4.13) but P/P_y follows a parabolic path (Eqs. 4.17, see also Fig. 4.2). The moment M_C decreases too when w_o increases but the moment M_E will increase slightly until the neutral axis at the ends of the slab strip forms exactly at the mid-depth of the section (in which case M_E becomes maximum) and then decreases. Nevertheless, the point representing the state of stress on the yield locus for both M_C - N and M_E - N diagrams will always move, as w_o increases, in the negative direction of N . Physically, this implies that the neutral axis for strain rate at the three plastic hinges of the slab moves into the compressive zone for total strain in which case the strain rate theory must be adopted. Despite this fact the analysis and discussion are attempted taking into account both the total strain and strain rate theories to show the differences between these two theories and their influence on the general plastic behaviour of the slab strip but it must be emphasized that the correct analysis for this particular example is the one based on the strain rate theory. The movement of the neutral axis into the 'compressive zone for total strain' indicates increases in the values of μ_C and μ_E at the central and end hinges respectively with the neutral axis forming closer to the compressed face of the slab as the deflection becomes larger.

At one stage while w_o is increasing the membrane force N/T_o becomes zero and consequently the yield load P/P_y, as from Eq. (4.16), is unity. The value of the central deflection w_o corresponding to zero membrane force is obtained from Eq. (4.13) for strain rate or Eq. (4.10) for total strain,

$$\frac{w_o}{d} = \frac{(\frac{\alpha}{\beta} + 1 - \gamma)}{(\frac{\alpha}{\beta} + 2)\ (1 + \frac{2c}{L})} \qquad \text{(strain rate)} \qquad (4.19a)$$

or

$$\frac{w_o}{d} = 2\frac{(\frac{\alpha}{\beta} + 1 - \gamma)}{(\frac{\alpha}{\beta} + 2)\ (1 + \frac{2c}{L})} \qquad \text{(total strain)} \qquad (4.19b)$$

which shows that the total strain theory would predict a zero membrane force in the slab at a central deflection exactly double that predicted by the strain rate theory. From Eqs. (4.5), the neutral axis at the central and end hinges when $N/T_o = 0$ will be located close to the compressed face of the slab ;

$$\mu_C = \frac{\frac{\alpha}{\beta}}{(\frac{\alpha}{\beta} + 2)}\ \frac{d}{2} \qquad (4.19c)$$

and

$$\mu_E = \frac{[\frac{\alpha}{\beta} - 2\ (\gamma - 1)]}{(\frac{\alpha}{\beta} + 2)}\ \frac{d}{2} \qquad (4.19d)$$

These equations indicate that μ_C is always greater than μ_E for this particular case $(\gamma > 1)$ which means that the neutral axis moves more rapidly towards the compressed face of the slab in the central hinge than that at the end hinges.

With further increments in deflection the membrane force N becomes tensile rather than compressive and the limiting stage is reached when the compressive stress block of the concrete at the central hinge vanishes (the slab is cracked throughout the depth) and the neutral axis forms at the top face of the slab where the concrete

is just touching. This implies

$$\mu_C = \frac{d}{2} \tag{4.20a}$$

and

$$\frac{N}{T_o} = -1 \tag{4.20b}$$

At this particular stage the fixed ends A and B are not cracked throughout the depth yet and there is still some compressive stress in the concrete. From Eq. (4.5b) the value of μ_E corresponding to $N/T_o = -1$ is

$$\mu_E = \frac{[\frac{\alpha}{\beta} - 2(\gamma - 2)]}{(\frac{\alpha}{\beta} + 2)} \frac{d}{2} \tag{4.20c}$$

The deflection at the centre of the slab w_o for $N/T_o = -1$ can be obtained from Eq. (4.13) for strain rate or Eq. (4.10) for total strain. Thus

$$\frac{w_o}{d} = \frac{(\frac{\alpha}{\beta} + 3 - \gamma)}{(\frac{\alpha}{\beta} + 2)(1 + \frac{2c}{L})} \qquad \text{(strain rate)} \tag{4.20d}$$

or

$$\frac{w_o}{d} = 2\,\frac{(\frac{\alpha}{\beta} + 3 - \gamma)}{(\frac{\alpha}{\beta} + 2)(1 + \frac{2c}{L})} \qquad \text{(total strain)} \tag{4.20e}$$

Again the total strain theory implies that the slab strip will be cracked throughout the depth at the central hinge at a value of central deflection twice that predicted by the strain rate theory. The yield load ratios corresponding to these deflections when $N/T_o = -1$ are from Eqs. (4.17),

$$\frac{P}{P_y} = 1 + \frac{2\beta}{[1 + \gamma\{1 + \beta(1 - \gamma)\}]} \qquad \text{(strain rate)} \tag{4.20f}$$

or

$$\frac{P}{P_y} = 1 + \frac{2\beta(\frac{\alpha}{\beta} + 4 - \gamma)}{[1 + \gamma\{1 + \beta(1 - \gamma)\}]} \quad \text{(total strain)} \qquad (4.20g)$$

If the central deflection is increased further the position of the neutral axis at the central hinge will lie outside the slab section ($\mu_C > \frac{d}{2}$) and the value of the membrane force will remain unchanged; i.e. tensile and equal to the yield force of the reinforcement at the central hinge. The condition of horizontal equilibrium requires that the position of the neutral axis at the end hinges μ_E should remain constant and as given by Eq. (4.20c). However, the slab can carry some extra load with further increment in deflection until all the bars at the central hinge commence to fracture leading to failure. The yield load corresponding to deflections greather than that specified by Eq. (4.20d,e) can be obtained by substituting $N/T_o = -1$ into Eq. (4.16). The result is the following linear equation:

$$\frac{P}{P_y} = 1 + \frac{2\beta}{[1 + \gamma\{1 + \beta(1 - \gamma)\}]} [(\frac{\alpha}{\beta} + 2)(1 + \frac{2c}{L}) \frac{w_o}{d} - (\frac{\alpha}{\beta} + 2 - \gamma)] \qquad (4.21)$$

It is of interest to note that according to the strain rate theory the yield load $P/P_y = 1$ represents the minimum yield load the slab strip will carry during all stages of deformation. The value of the membrane force corresponding to $P/P_y = 1$ is zero and the central deflection is given by Eq. (4.19a). However, the total strain theory predicts a different value for P_{min}/P_y and from Eq. (4.17b) the minimum value occurs when,

$$\frac{w_o}{d} = \frac{4}{3} \frac{(\frac{\alpha}{\beta} + 1 - \gamma)}{(\frac{\alpha}{\beta} + 2)(1 + \frac{2c}{L})} \qquad (4.22a)$$

This value of deflection, which is 2/3 of that corresponding to $N/T_o = 0$ (Eq. 4.19b), gives

$$\frac{P_{min}}{P_y} = 1 + \frac{\beta}{6\,[1 + \gamma\{1 + \beta(1 - \gamma)\}]}\,[(\frac{2\alpha}{\beta} + 3) - 2(\frac{\alpha}{\beta} + 2)^2 + 2\gamma\,(\frac{\alpha}{\beta} + 1)$$

$$+ \gamma^2\{\frac{1}{6}\,(\frac{\alpha}{\beta} + 2)^2 - 1\}] \qquad (4.22b)$$

and

$$\frac{N}{T_o} = \frac{1}{6}\,(\frac{\alpha}{\beta} + 1 - \gamma) \qquad (4.22c)$$

(which is 1/3 the maximum value of N at zero deflection; Eq. 4.18a).

4.3.2 THE CASE $\gamma < 1$

This is the case when the reinforcement at the fixed ends of the slab is less than that at the central region. The plastic behaviour of the slab strip for this case is shown in Fig. (4.3) which is constructed for the same typical slab strip described in section 4.2.4 (or Fig. 4.2) with the only exception that γ in this case is taken to be 0.5. All of the equations derived for the case $\gamma > 1$ are also valid here except those corresponding to tensile membrane force (Eqs. 4.20 and 4.21).

When the deflection is zero the membrane force as well as the yield load are maxima and given by equations (4.18a) and (4.18b) respectively. The neutral axis position at the central hinge is defined by Eq. (4.18c) and that at the end hinges is given by Eq. (4.18d). Since γ in this case is less than 1; these equations imply that the neutral axis at the three plastic hinges form below the mid-depth of the slab by the distance stated. Therefore in this case the starting stress state is located on the yield locus of the M_C - N diagram to the left of M_{Cmax}. Similarly, the initial stress state lies to the right of M_{Emax} on the yield locus representing the relationship between M_E and N. As w_o increases the point representing the stress state on these curves moves to the right, and the compressive force becomes smaller. Again the reduction in N/T_o is linear (Eqs. 4.10 and 4.13) and in P/P_y is parabolic (Eqs. 4.17). The neutral axis at the end hinges in this case will

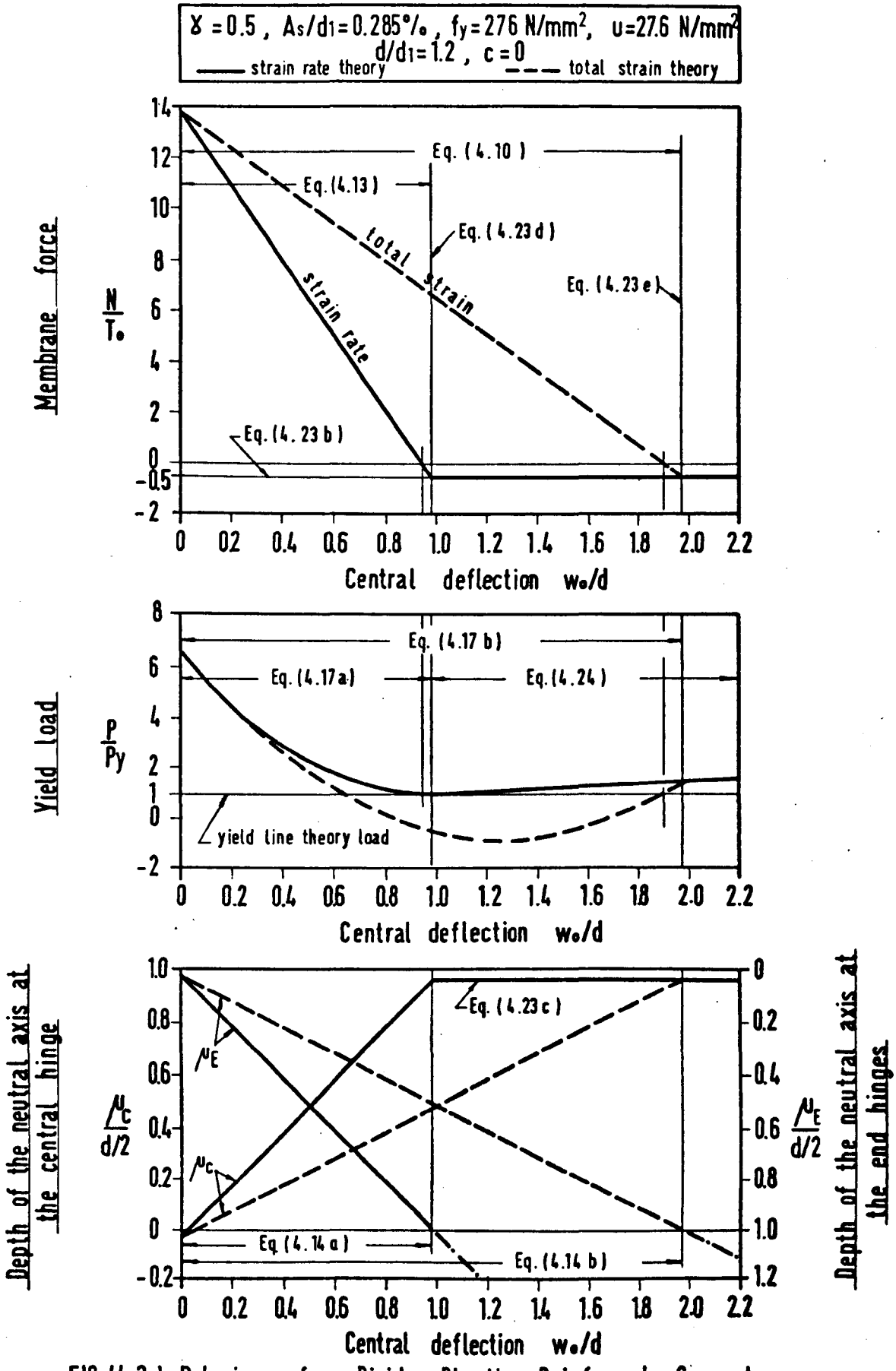

FIG. (4.3) Behaviour of a Rigid - Plastic Reinforced Concrete Slab Strip with Fixed Ends and Axial Restraints (The Case $\chi < 1$)

move more rapidly towards the compressed face of the slab than that at the central hinge; the movement being into the compressive zone for total strain.

When the central deflection reaches the value given by Eq. (4.19a, b) the membrane force becomes zero and, therefore, the yield load will be the simple yield line theory load and μ_C and μ_E will be as given by Eqs. (4.19c) and (4.19d) respectively.

With further increments in deflection the membrane force N becomes tensile and the limiting stage is reached when the compressive stress blocks of the concrete at the end hinges A and B vanish at the same time indicating that the neutral axis at these hinges forms at the bottom face of the slab where the concrete is just in contact with the surround. In this case, the equations which replace Eqs. (4.20) are

$$\mu_E = \frac{d}{2} \tag{4.23a}$$

and

$$\frac{N}{T_o} = -\gamma \tag{4.23b}$$

but at the central hinge there is still some compressive stress in the concrete. From Eq. (4.5a) the value of μ_C corresponding to $N/T_o = -\gamma$ is

$$\mu_C = \frac{(\frac{\alpha}{\beta} + 2\gamma)}{(\frac{\alpha}{\beta} + 2)} \cdot \frac{d}{2} \tag{4.23c}$$

This stage is reached at a value of central deflection obtained from Eq. (4.13) for strain rate or Eq. (4.10) for total strain for $N/T_o = -\gamma$;

$$\frac{w_o}{d} = \frac{(\frac{\alpha}{\beta} + 1 + \gamma)}{(\frac{\alpha}{\beta} + 2)(1 + \frac{2c}{L})} \qquad \text{(strain rate)} \tag{4.23d}$$

or

$$\frac{w_o}{d} = 2\,\frac{(\frac{\alpha}{\beta} + 1 + \gamma)}{(\frac{\alpha}{\beta} + 2)(1 + \frac{2c}{L})} \qquad \text{(total strain)} \tag{4.23e}$$

The yield load ratios corresponding to these deflections when $N/T_o = -\gamma$ are from Eqs. (4.17),

$$\frac{P}{P_y} = 1 + \frac{2\beta\gamma^2}{[1 + \gamma\{1 + \beta(1 - \gamma)\}]} \quad \text{(strain rate)} \qquad (4.23f)$$

or

$$\frac{P}{P_y} = 1 + \frac{2\beta\gamma\,(\frac{\alpha}{\beta} + 1 + 2\gamma)}{[1 + \gamma\{1 + \beta(1 - \gamma)\}]} \quad \text{(total strain)} \qquad (4.23g)$$

The value of the membrane force $(N/T_o = -\gamma)$ and the position of the neutral axis μ_C given by Eq. (4.23c) will remain unchanged for increases in w_o whereas the neutral axis at the end hinges will lie outside the slab section $(\mu_E > \frac{d}{2})$. This is due to the fact that once the slab strip is cracked throughout the depth at one section the value of the membrane force will be determined by the yield force of the reinforcement provided at that section (i.e. sections A and B in this case). The yield load may, however, be increased further until all the steel bars at the end hinges start to fracture when the slab strip collapses. The yield load corresponding to deflections greater than that specified by Eq. (4.23d, e) can be obtained from Eq. (4.16) by substituting $N/T = -\gamma$. Hence, the equation which replaces Eq. (4.21) is

$$\frac{P}{P_y} = 1 + \frac{2\beta\gamma}{[1 + \gamma\{1 + \beta(1 - \gamma)\}]}\left[(\frac{\alpha}{\beta} + 2)(1 + \frac{2c}{L})\frac{w_o}{d} - (\frac{\alpha}{\beta} + 1)\right] \qquad (4.24)$$

4.3.3 THE SPECIAL CASE $\gamma = 1$

This is the case when equal reinforcement is provided at the ends and at the central region of the slab strip. The plastic behaviour of the slab strip for this special case is shown in Fig. (4.4) which is constructed for the same typical slab strip described in section 4.2.4 with γ in this case is unity. The moments M_C and M_E as well as the depths of the neutral axis μ_C and μ_E in this case are identical at all stages of deformation.

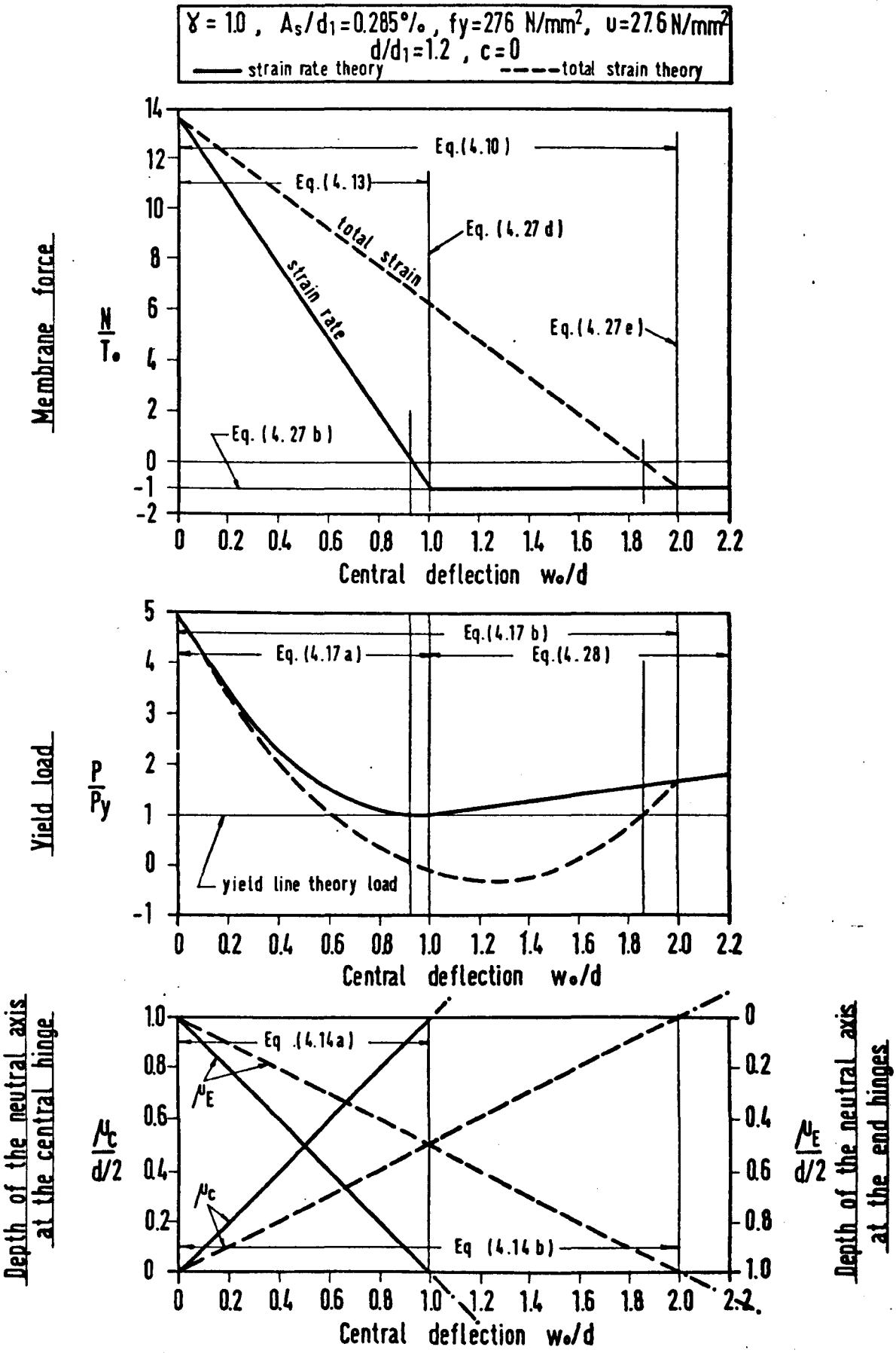

FIG.(4.4) Behaviour of a Rigid - Plastic Reinforced Concrete Slab Strip with Fixed-Ends and Axial Restraints (The Case γ = 1)

When the central deflection is zero the membrane force and the yield load are maxima. From Eqs. (4.18a) and (4.18b) for $\gamma = 1$

$$\frac{N_{max}}{T_o} = \frac{\alpha}{2\beta} \tag{4.25a}$$

$$\frac{P_{max}}{P_y} = 1 + \frac{\alpha^2}{4\beta} \tag{4.25b}$$

At this stage the neutral axis at all the three plastic hinges is located at the mid-depth of the section. Equations (4.18c) and (4.18d), considering $\gamma = 1$, give

$$\mu_C = \mu_E = 0 \tag{4.25c}$$

The start of collapse in this case is indicated by the peak point ($M = M_{max}$) of the yield locus representing the M - N diagram. The value of this moment can be obtained by combining Eq. (4.25a) with each of Eqs. (4.2) and (4.3) for $\gamma = 1$. Hence

$$\frac{M_{Cmax}}{M_o} = \frac{M_{Emax}}{M_o} = 1 + \frac{\alpha^2}{4\beta} \tag{4.25d}$$

As w_o increases the state of stress changes and the membrane force N, the bending moment at the plastic hinges M and the yield load P all decline. When the membrane force becomes zero the ratios P/P_y and M/M_o will be unity and the neutral axis at all the three hinges forms close to the compressed face of the slab so that from Eqs. (4.19c) and (4.19d) for $\gamma = 1$

$$\mu_C = \mu_E = \frac{\frac{\alpha}{\beta}}{\frac{\alpha}{\beta} + 2} \frac{d}{2} \tag{4.26a}$$

The corresponding value of the central deflection is from Eq. (4.19a, b) with $\gamma = 1$;

$$\frac{w_o}{d} = \frac{\frac{\alpha}{\beta}}{(\frac{\alpha}{\beta} + 2)(1 + \frac{2c}{L})} \qquad \text{(strain rate)} \qquad (4.26b)$$

or

$$\frac{w_o}{d} = \frac{2\frac{\alpha}{\beta}}{(\frac{\alpha}{\beta} + 2)(1 + \frac{2c}{L})} \qquad \text{(total strain)} \qquad (4.26c)$$

When w_o exceeds this value the membrane force will be tensile and the compressive stress block of the concrete reduces by an equal amount at all hinges until the limiting stage is reached when the slab is cracked throughout the depth at the central and end hinges simultaneously. In this case and for $\gamma = 1$;

from Eqs. (4.20a) and (4.20c) or Eqs. (4.23a) and (4.23c)

$$\mu_C = \mu_E = \frac{d}{2} \qquad (4.27a)$$

from Eq. (4.20b) or Eq. (4.23b)

$$\frac{N}{T_o} = -1 \qquad (4.27b)$$

and by combining Eq. (4.27b) with each of Eqs. (4.2) and (4.3)

$$\frac{M_C}{M_o} = \frac{M_E}{M_o} = 1 - \alpha - \beta \qquad (4.27c)$$

This will occur at a value of central deflection obtained from Eq. (4.20d, e) or Eq. (4.23d, e) for $\gamma = 1$;

$$\frac{w_o}{d} = \frac{1}{(1 + \frac{2c}{L})} \qquad \text{(strain rate)} \qquad (4.27d)$$

or

$$\frac{w_o}{d} = \frac{2}{(1 + \frac{2c}{L})} \qquad \text{(total strain)} \qquad (4.27e)$$

and the corresponding yield load ratios are from Eq. (4.20f, g) or Eq. (4.23f, g) for $\gamma = 1$;

$$\frac{P}{P_y} = 1 + \beta \qquad \text{(strain rate)} \qquad (4.27f)$$

or

$$\frac{P}{P_y} = 1 + \alpha + 3\beta \qquad \text{(total strain)} \qquad (4.27g)$$

With further increments in the central deflection the position of the neutral axis at the three sections of yield will lie outside the slab section [i.e. $\mu_c (= \mu_E) > d/2$]. The increase in w_o will have no effect on the values given by Eqs. (4.27b and c) for the membrane force and the yield moment but the load will increase linearly until all the bars commence to fracture leading to failure. Thus for all values of central deflection greater than that specified by Eq. (4.27d, e) the ratio P/P_y can be obtained from Eq. (4.21) or Eq. (4.24) by substituting $\gamma = 1$. Therefore;

$$\frac{P}{P_y} = (1 - \alpha - \beta) + (\alpha + 2\beta)(1 + \frac{2c}{L}) \frac{w_o}{d} \qquad (4.28)$$

4.4 THE SPECIAL CASE OF SIMPLE SUPPORTS

One of the main assumptions in the technology of concrete structures is that concrete, as a material, has no resistance to tension. Based on this assumption, a simply supported reinforced concrete slab strip may theoretically be considered as identical to a similar fixed end slab strip with no reinforcement at the ends ($\gamma = 0$) . The analysis of this case can, therefore, be derived from the general case of fixed-ended strips. The equations representing

the plastic behaviour of an axially restrained reinforced concrete slab strip with simple supports may be summarized as follows (see also Fig. 4.5).

i. When $w_o = 0$

$$\frac{N_{max}}{T_o} = \frac{1}{2}\left(\frac{\alpha}{\beta} + 1\right) \tag{4.29a}$$

$$\frac{P_{max}}{P_y} = 1 + \frac{1}{2}\beta\left(\frac{\alpha}{\beta} + 1\right)^2 \tag{4.29b}$$

$$\mu_C = -\frac{1}{\left(\frac{\alpha}{\beta} + 2\right)}\frac{d}{2} \tag{4.29c}$$

$$\mu_E = \frac{1}{\left(\frac{\alpha}{\beta} + 2\right)}\frac{d}{2} \tag{4.29d}$$

ii. When $0 \leq \frac{w_o}{d} \leq$

$$\begin{cases} \dfrac{\left(\frac{\alpha}{\beta} + 1\right)}{\left(\frac{\alpha}{\beta} + 2\right)\left(1 + \frac{2c}{L}\right)} & \text{(strain rate)} \\ \text{or} & \\ 2\dfrac{\left(\frac{\alpha}{\beta} + 1\right)}{\left(\frac{\alpha}{\beta} + 2\right)\left(1 + \frac{2c}{L}\right)} & \text{(total strain)} \end{cases}$$

$$\frac{N}{T_o} = \begin{cases} \frac{1}{2}\left[\left(\frac{\alpha}{\beta} + 1\right) - \left(\frac{\alpha}{\beta} + 2\right)\left(1 + \frac{2c}{L}\right)\frac{w_o}{d}\right] & \text{(strain rate)} \\ \text{or} & \\ \frac{1}{2}\left[\left(\frac{\alpha}{\beta} + 1\right) - \frac{1}{2}\left(\frac{\alpha}{\beta} + 2\right)\left(1 + \frac{2c}{L}\right)\frac{w_o}{d}\right] & \text{(total strain)} \end{cases} \tag{4.29e}$$

$$\frac{P}{P_y} = \begin{cases} 1 + \frac{\beta}{2}\cdot\left[\left(\frac{\alpha}{\beta} + 1\right)^2 - 2\left(\frac{\alpha}{\beta} + 2\right)\left(\frac{\alpha}{\beta} + 1\right)\left(1 + \frac{2c}{L}\right)\left(\frac{w_o}{d}\right) + \left(\frac{\alpha}{\beta} + 2\right)^2\left(1 + \frac{2c}{L}\right)^2\left(\frac{w_o}{d}\right)^2\right] & \\ \text{or} \quad \text{(strain rate)} & \\ 1 + \frac{\beta}{2}\cdot\left[\left(\frac{\alpha}{\beta} + 1\right)^2 - 2\left(\frac{\alpha}{\beta} + 2\right)\left(\frac{\alpha}{\beta} + 1\right)\left(1 + \frac{2c}{L}\right)\left(\frac{w_o}{d}\right) + \frac{3}{4}\left(\frac{\alpha}{\beta} + 2\right)^2\left(1 + \frac{2c}{L}\right)^2\left(\frac{w_o}{d}\right)^2\right] & \\ \text{(total strain)} & \end{cases} \tag{4.29f}$$

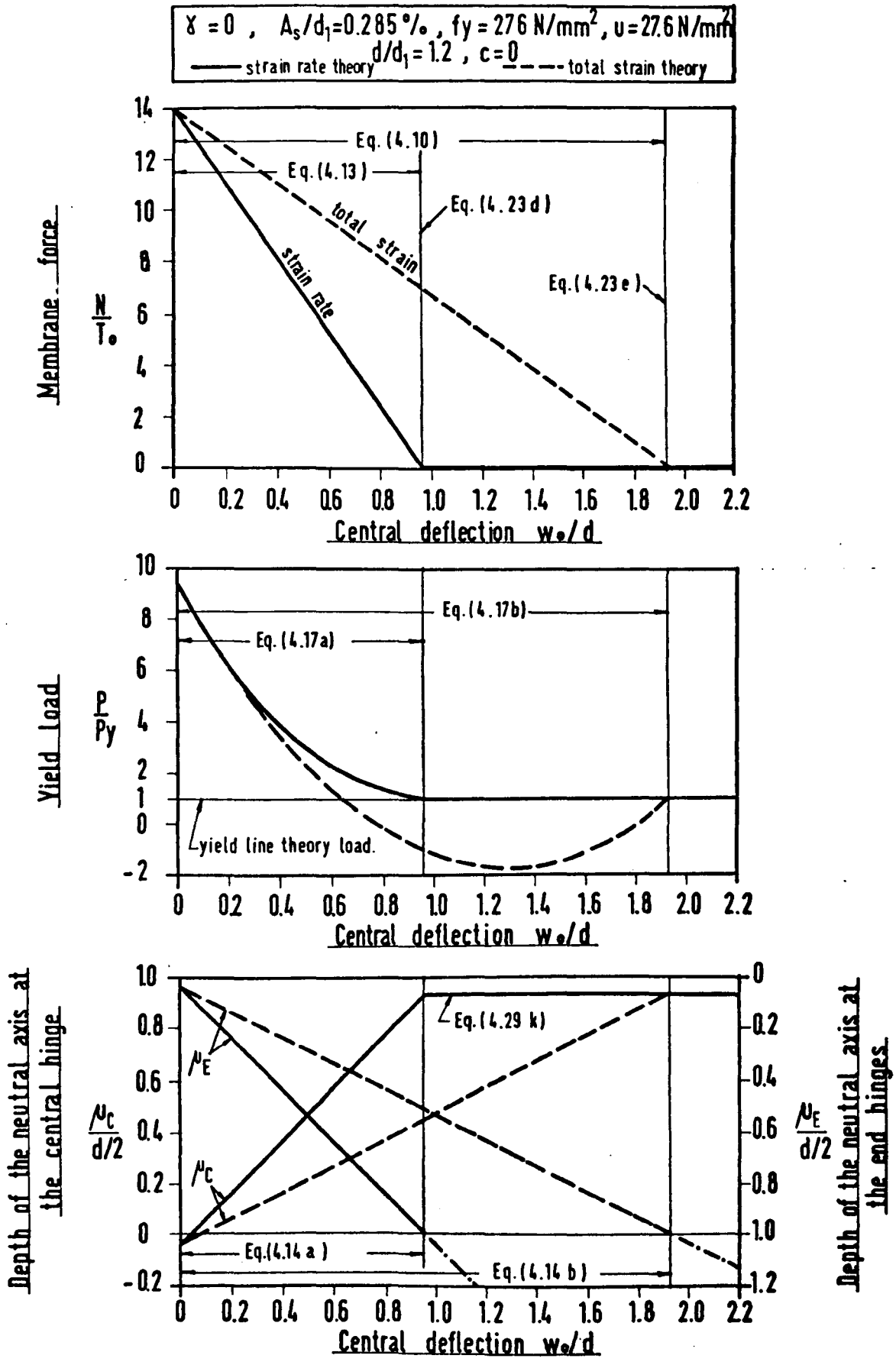

FIG. (4.5) Behaviour of a Rigid-Plastic Reinforced Concrete Slab Strip with Simple Supports ($\gamma = 0$) and Axial Restraints

$$\mu_C = \begin{cases} \left[-\frac{1}{(\frac{\alpha}{\beta}+2)} + (1+\frac{2c}{L})\frac{w_o}{d}\right]\cdot\frac{d}{2} & \text{(strain rate)} \\ \text{or} & \\ \left[-\frac{1}{(\frac{\alpha}{\beta}+2)} + \frac{1}{2}(1+\frac{2c}{L})\frac{w_o}{d}\right]\cdot\frac{d}{2} & \text{(total strain)} \end{cases} \quad (4.29g)$$

$$\mu_E = \begin{cases} \left[\frac{1}{(\frac{\alpha}{\beta}+2)} + (1+\frac{2c}{L})\frac{w_o}{d}\right]\cdot\frac{d}{2} & \text{(strain rate)} \\ \text{or} & \\ \left[\frac{1}{(\frac{\alpha}{\beta}+2)} + \frac{1}{2}(1+\frac{2c}{L})\frac{w_o}{d}\right]\cdot\frac{d}{2} & \text{(total strain)} \end{cases} \quad (4.29h)$$

iii. When $\frac{w_o}{d} \geq$ $\begin{cases} \frac{(\frac{\alpha}{\beta}+1)}{(\frac{\alpha}{\beta}+2)(1+\frac{2c}{L})} & \text{(strain rate)} \\ \text{or} & \\ 2\frac{(\frac{\alpha}{\beta}+1)}{(\frac{\alpha}{\beta}+2)(1+\frac{2c}{L})} & \text{(total strain)} \end{cases}$

$$\frac{N}{T_o} = 0 \quad (4.29i)$$

$$\frac{P}{P_y} = 1 \quad (4.29j)$$

$$\mu_C = \frac{\frac{\alpha}{\beta}}{(\frac{\alpha}{\beta}+2)}\cdot\frac{d}{2} \quad (4.29k)$$

$$\mu_E \geq \frac{d}{2} \quad (4.29l)$$

Similar to all the previously discussed cases; when the membrane force N becomes zero the yield load P is equal to the yield line theory load P_y. However, in this case the load will

remain unchanged with further increments in deflection due to the vanishing of the compressive stress block between the edge of the simply supported slab strip and the restraining body and consequently the disappearance of the membrane force.* Hence, as shown in Fig. (4.5), the load-deflection relationship for all values of deflection greater than that corresponding to $N = 0$ will show a horizontal line $(P = P_y)$ until the limit of usefulness of the slab is reached when all the bars at the central region begin to fracture leading to collapse.

Equations (4.29) may be compared with the theoretical analysis presented by Roberts (24) on a similar simply supported - axially restrained reinforced concrete slab strip with uniformly distributed load. Roberts' analysis was based on a total strain approach and assumed that the central plastic hinge forms at mid-span. For $\bar{S} = \infty$, $\Delta = 0$ and $c = 0$, Roberts' equations (2.37 and 2.39) will be identical with the 'total strain' equations (4.29). This implies that the dimensionless values of the membrane force N/T_o and the yield load P/P_y are not affected by the type of loading but they do depend on the shape of the collapse mechanism. The 'total strain' approach of Roberts for the special case of rigid-plastic strips is not physically correct, however.

4.5 SUMMARY OF ANALYSIS

The equations for determining the values of the membrane force, the yield load and the neutral axis depth at the central and end hinges at any value of deflection for rigid-plastic and axially-restrained fixed-ended reinforced concrete slab strips with any ratio of reinforcement γ are summarized following the correct approach of strain rate theory as follows :

i. For $w_o = 0$

$$\frac{N_{max}}{T_o} = \frac{1}{2}\left(\frac{\alpha}{\beta} + 1 - \gamma\right) \qquad (4.30a)$$

$$\frac{P_{max}}{P_y} = 1 + \frac{\beta\left(\frac{\alpha}{\beta} + 1 - \gamma\right)^2}{2\left[1 + \gamma\{1 + \beta(1 - \gamma)\}\right]} \qquad (4.30b)$$

* The membrane force developing at the edge of an axially restrained simply supported concrete slab strip is solely represented by the compressive stress block of the concrete.

$$\mu_C = \frac{(\gamma - 1)}{(\frac{\alpha}{\beta} + 2)} \frac{d}{2} \tag{4.30c}$$

$$\mu_E = \frac{(1 - \gamma)}{(\frac{\alpha}{\beta} + 2)} \frac{d}{2} \tag{4.30d}$$

ii. For $0 \leqq \frac{W_o}{d} \leqq$ $\begin{cases} \text{or} & \frac{(\frac{\alpha}{\beta} + 3 - \gamma)}{(\frac{\alpha}{\beta} + 2)(1 + \frac{2c}{L})} \quad (\text{if } \gamma \geqq 1) \\ & \frac{(\frac{\alpha}{\beta} + 1 + \gamma)}{(\frac{\alpha}{\beta} + 2)(1 + \frac{2c}{L})} \quad (\text{if } \gamma \leqq 1) \end{cases}$

$$\frac{N}{T_o} = \frac{1}{2} \left[(\frac{\alpha}{\beta} + 1 - \gamma) - (\frac{\alpha}{\beta} + 2)(1 + \frac{2c}{L}) \frac{W_o}{d} \right] \tag{4.30e}$$

$$\frac{P}{P_y} = 1 + \frac{\beta}{2 \left[1 + \gamma\{1 + \beta(1 - \gamma)\} \right]} \left[(\frac{\alpha}{\beta} + 1 - \gamma)^2 - 2(\frac{\alpha}{\beta} + 2)(\frac{\alpha}{\beta} + 1 - \gamma) \right.$$

$$\left. (1 + \frac{2c}{L})(\frac{W_o}{d}) + (\frac{\alpha}{\beta} + 2)^2 (1 + \frac{2c}{L})^2 (\frac{W_o}{d})^2 \right] \tag{4.30f}$$

$$\mu_C = \left[\frac{(\gamma - 1)}{(\frac{\alpha}{\beta} + 2)} + (1 + \frac{2c}{L}) \frac{W_o}{d} \right] \frac{d}{2}. \tag{4.30g}$$

$$\mu_E = \left[\frac{(1 - \gamma)}{(\frac{\alpha}{\beta} + 2)} + (1 + \frac{2c}{L}) \frac{W_o}{d} \right] \frac{d}{2} \tag{4.30h}$$

iii. For $\frac{W_o}{d} \geqq$ $\begin{cases} \text{or} & \frac{(\frac{\alpha}{\beta} + 3 - \gamma)}{(\frac{\alpha}{\beta} + 2)(1 + \frac{2c}{L})} \quad (\text{if } \gamma \geqq 1) \\ & \frac{(\frac{\alpha}{\beta} + 1 + \gamma)}{(\frac{\alpha}{\beta} + 2)(1 + \frac{2c}{L})} \quad (\text{if } \gamma \leqq 1) \end{cases}$

$$\frac{N}{T_o} = \left\{ \begin{array}{ll} -1 & (\text{if } \gamma \geqq 1) \\ \text{or} & \\ -\gamma & (\text{if } \gamma \leqq 1) \end{array} \right\} \tag{4.30i}$$

$$\frac{P}{P_y} = \begin{cases} 1 + \dfrac{2\beta}{[1 + \gamma\{1 + \beta(1-\gamma)\}]}\left[\left(\frac{\alpha}{\beta} + 2\right)\left(1 + \frac{2c}{L}\right)\frac{w_o}{d}\right. \\ \qquad \left. - \left(\frac{\alpha}{\beta} + 2 - \gamma\right)\right] \qquad (\text{if } \gamma \geqq 1) \\ \text{or} \\ 1 + \dfrac{2\beta\gamma}{[1 + \gamma\{1 + \beta(1-\gamma)\}]}\left[\left(\frac{\alpha}{\beta} + 2\right)\left(1 + \frac{2c}{L}\right)\frac{w_o}{d}\right. \\ \qquad \left. - \left(\frac{\alpha}{\beta} + 1\right)\right] \qquad (\text{if } \gamma \leqq 1) \end{cases} \qquad (4.30j)$$

$$\mu_C \begin{cases} \geqq \dfrac{d}{2} & (\text{if } \gamma \geqq 1) \\ \text{or} \\ = \dfrac{\left(\frac{\alpha}{\beta} + 2\gamma\right)}{\left(\frac{\alpha}{\beta} + 2\right)} & (\text{if } \gamma \leqq 1) \end{cases} \qquad (4.30k)$$

$$\mu_E \begin{cases} = \dfrac{\left[\frac{\alpha}{\beta} - 2(\gamma - 2)\right]}{\left(\frac{\alpha}{\beta} + 2\right)}\dfrac{d}{2} & (\text{if } \gamma \geqq 1) \\ \text{or} \\ \leqq \dfrac{d}{2} & (\text{if } \gamma \leqq 1) \end{cases} \qquad (4.30l)$$

4.6 STUDY OF THE EFFECT OF SOME IMPORTANT PARAMETERS

Equations (4.30) which describe the plastic behaviour of the slab strip AB of Fig. (4.1) are based on three main factors. These are, namely, the properties of the slab at the central hinge represented by the notations α and β, the ratio of reinforcement γ and the mechanism parameter c/L. The values of α and β as defined by Eq. (3.5) in turn depend on the amount of reinforcement A_s/d_1, the cube strength of the concrete u, the yield stress of the reinforcement f_y, the ratio of the depth of the slab to the effective depth d/d_1 and finally the concrete stress block parameters k_1k_3 and k_2 which may be considered as either a function of u (Eqs. 3.1) or fixed quantities like the values used by Wood (3) in which $k_1k_3 = 2/3$ and $k_2 = 1/2$.

To enable a close study of the effect of each parameter to be made, the same typical slab strip described in section 4.2.4 of

this chapter is considered with the only exception that γ in this case is taken to be unity.

The study of the effect of each parameter is made possible by keeping the rest of the parameters constant.

4.6.1 RATIO OF REINFORCEMENT γ

Fig. (4.6) shows the relationships of the membrane force, the yield load and the depths of the neutral axis at the central and end hinges with the central deflection for different values of γ ranging from 0 (the case of the slab with simple supports) to 2 .

It can be seen from this figure that at any value of deflection the non-dimensional values of the compressive membrane force (N/T_o) and the yield load (P/P_y) are greater for smaller values of γ . The differences in the values of N/T_o are small but in P/P_y they are large. Especially in the simply supported case the maximum yield load obtained at the start of collapse $(w_o = 0)$ is 9.5 times the simple yield line theory load whereas the enhancement factor of the load for the case $\gamma = 2$ is only 3.5 .

The neutral axis position at the plastic hinges is slightly affected by the steel ratio parameter. At any central deflection less than that corresponding to $N/T_o = -1$, the depth of the neutral axis at the central hinge is bigger for higher values of γ but it is smaller at the end hinges. However, when $\gamma = 1$ the neutral axis depths at all hinges are the same and equal to half the value of the deflection w_o .

4.6.2 AMOUNT OF REINFORCEMENT A_s/d_1

Fig. (4.7) shows the changes in the plastic behaviour of the same typical slab strip when the percentage of reinforcement at the central hinge is varied from 0.1% to 1% .

The relations of the non-dimensional membrane force N/T_o and the non-dimensional yield load P/P_y with the central deflection w_o/d are found to be greatly influenced by the parameter A_s/d_1 . At any value of central deflection the ratios N/T_o and P/P_y are larger in lightly reinforced slabs. For example a typical slab strip with

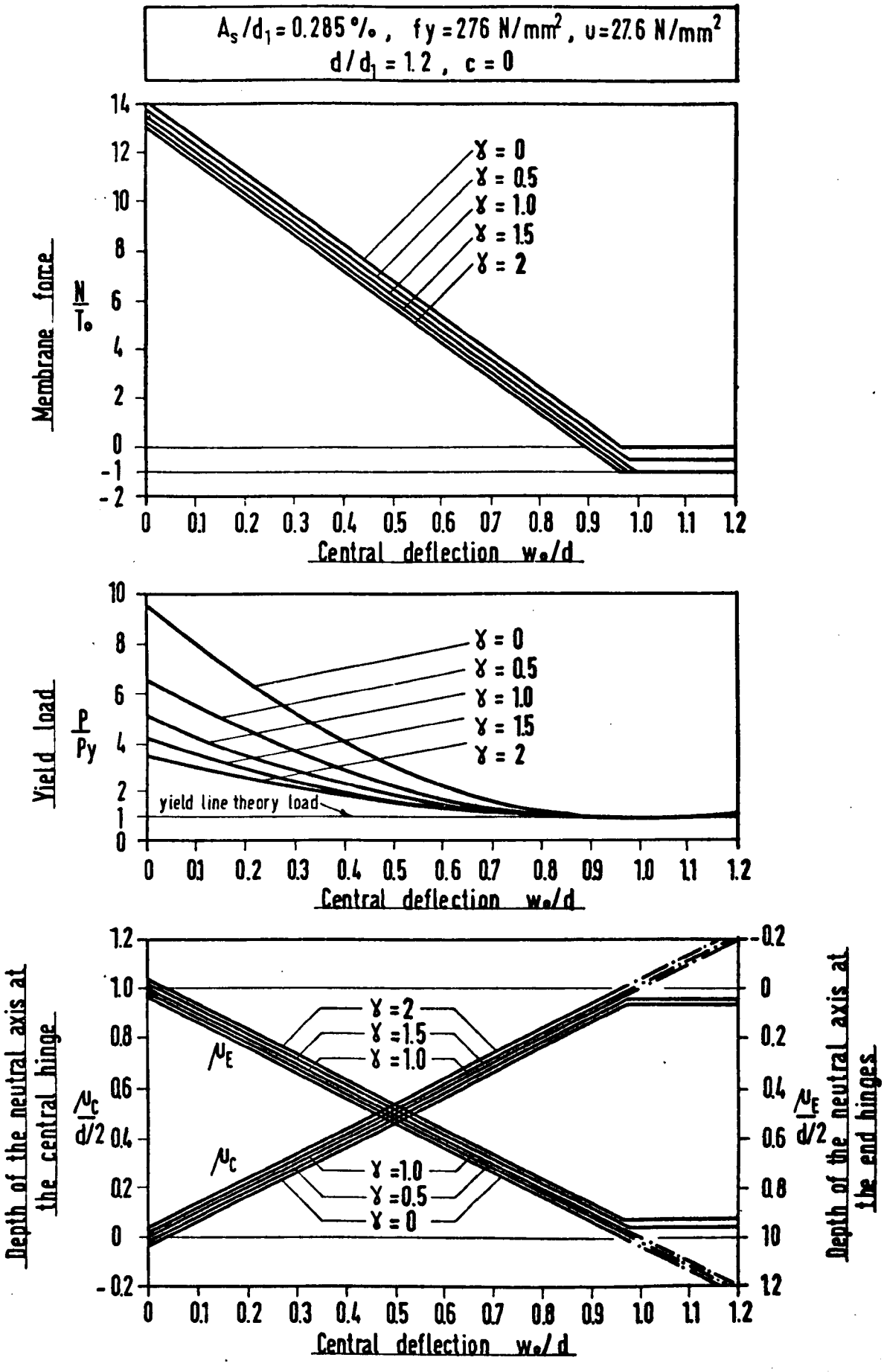

FIG. (4.6) Effect of the Ratio of Reinforcement γ on the Behaviour of a Rigid-Plastic Reinforced Concrete Slab Strip with Fixed-Ends and Lateral Restraints

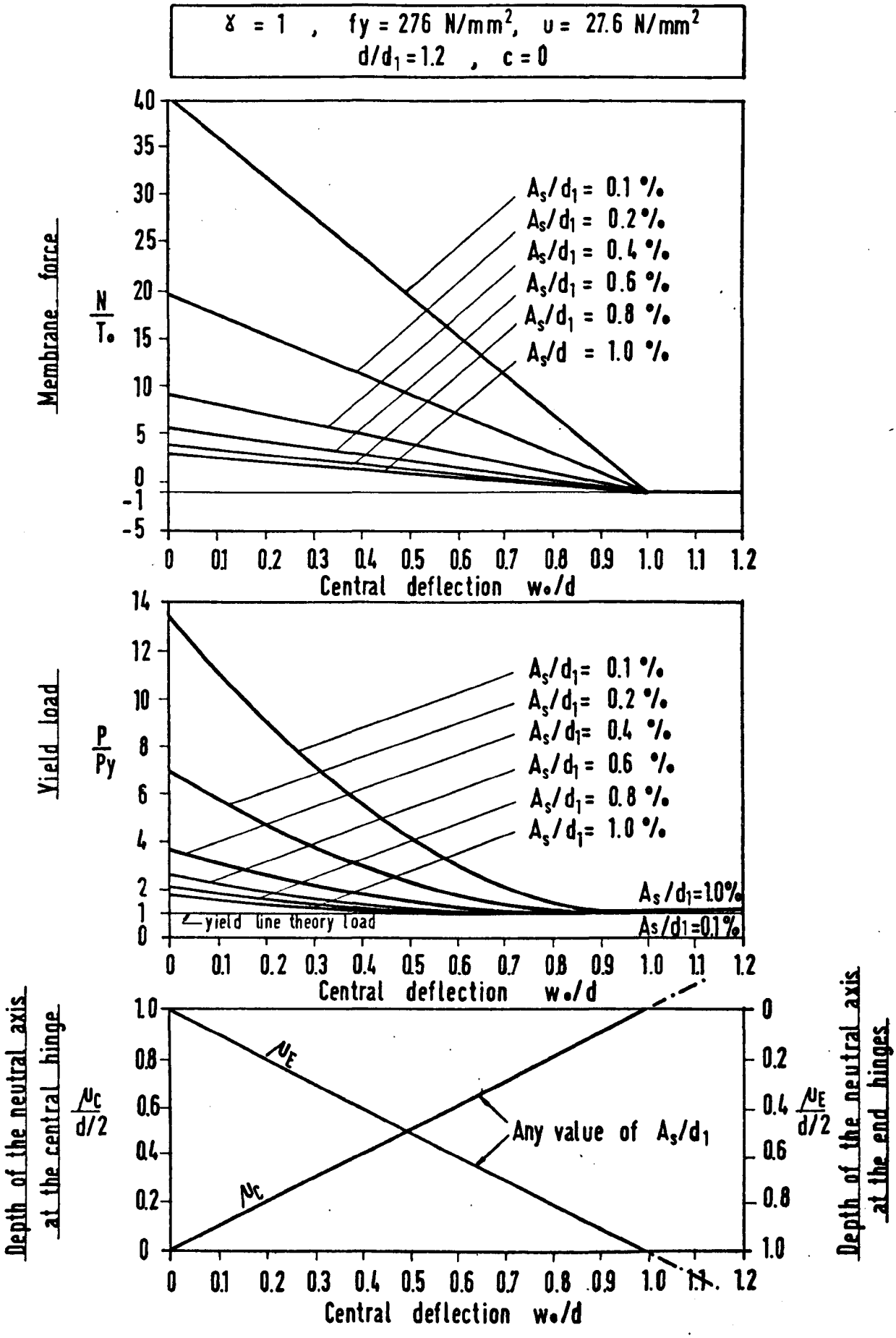

FIG. (4.7) Effect of the Amount of Reinforcement A_s/d_1 on the Behaviour of a Rigid-Plastic Reinforced Concrete Slab Strip with Fixed-Ends and Lateral Restraints

percentage of reinforcement as little as 0.1% when restrained axially and loaded will be subjected to a maximum membrane force of 40.5 T_o and the ultimate load carrying capacity of this slab will be 13.3 times the yield line theory load whereas if the same slab is heavily reinforced with percentage of reinforcement of 1% the corresponding values of N_{max}/T_o and P_{max}/P_y will be as low as 3.0 and 1.8 respectively. However, the recovery in the load for values of w_o/d greater than 1 (i.e. for all values of deflection corresponding to $N/T_o = -1$) is greater in heavily reinforced slabs.

The neutral axis position at the plastic hinges will not be affected by the amount of reinforcement in this particular example. It happens that in Eqs. (4.14) when $\gamma = 1$ and $c = 0$ are substituted the effect of the rest of the parameters are cancelled and the neutral axis depths μ_C and μ_E are then equal to half the value of the central deflection w_o.

4.6.3 CUBE STRENGTH OF CONCRETE u

The effect of this parameter is shown in Fig. (4.8). Values of u ranging between 13.8 N/mm^2 (2000 lbf/in^2) and 69.0 N/mm^2 (10,000 lbf/in^2) are considered and the results show that high values of the cube strength of concrete increase the capacity of the slab at any value of deflection less than that corresponding to $N/T_o = -1$. For larger values of deflection; the slab will show a better recovery in the yield load P/P_y if concrete with a lower cube strength is used.

The membrane force is also affected by using concrete with different cube strengths and the effect shows greater membrane force for higher value of u.

The neutral axis depth at the plastic hinges for this particular example ($\gamma = 1$, $c = 0$) is not affected by the cube strength.

4.6.4 MECHANISM PARAMETER c/L

Fig. (4.9) demonstrates the effect of the location of the central plastic hinge on the general plastic behaviour of the slab

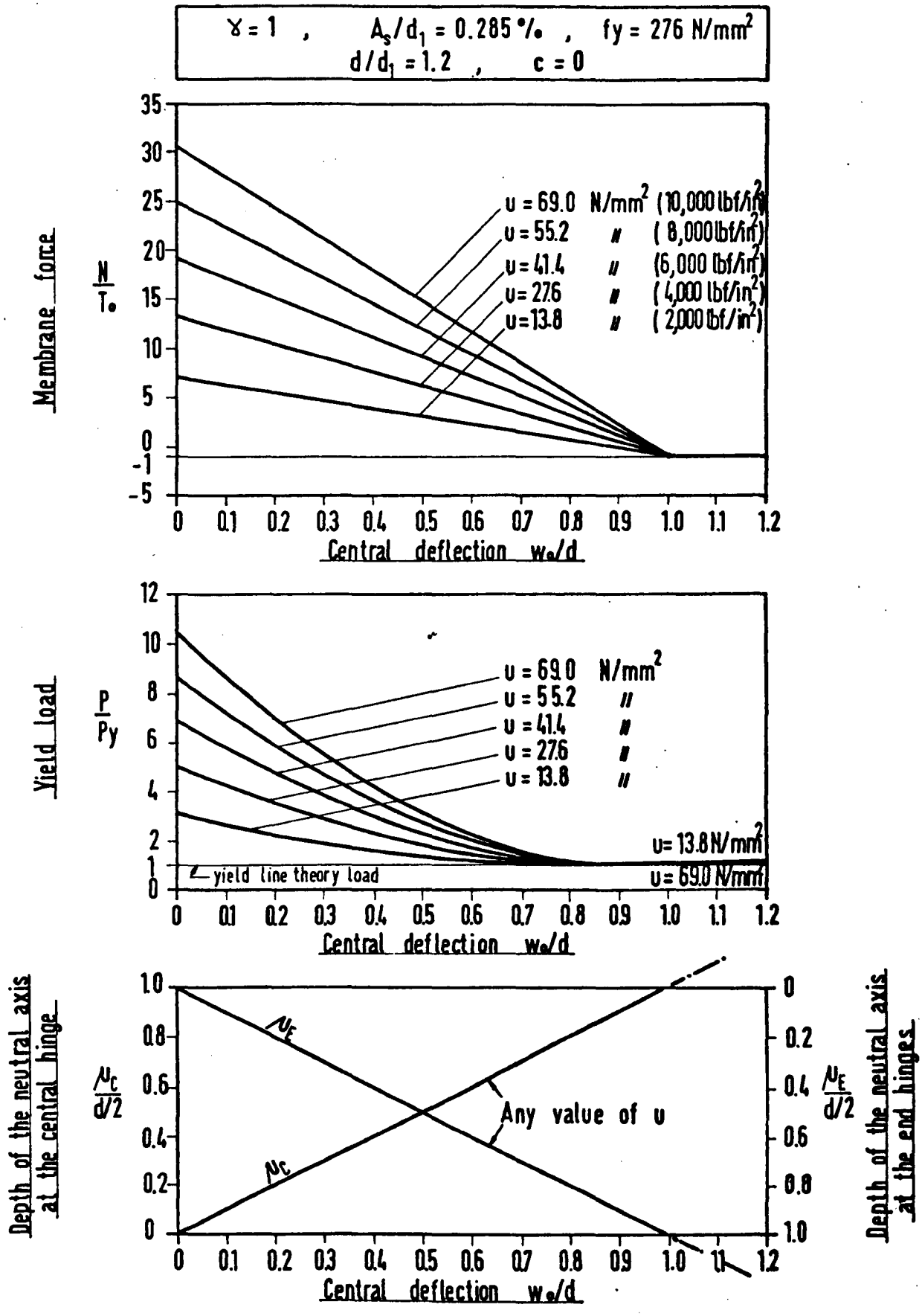

FIG.(4.8) Effect of the Cube Strength of Concrete u on the Behaviour of a Rigid-Plastic Reinforced Concrete Slab Strip with Fixed-Ends and Lateral Restraints

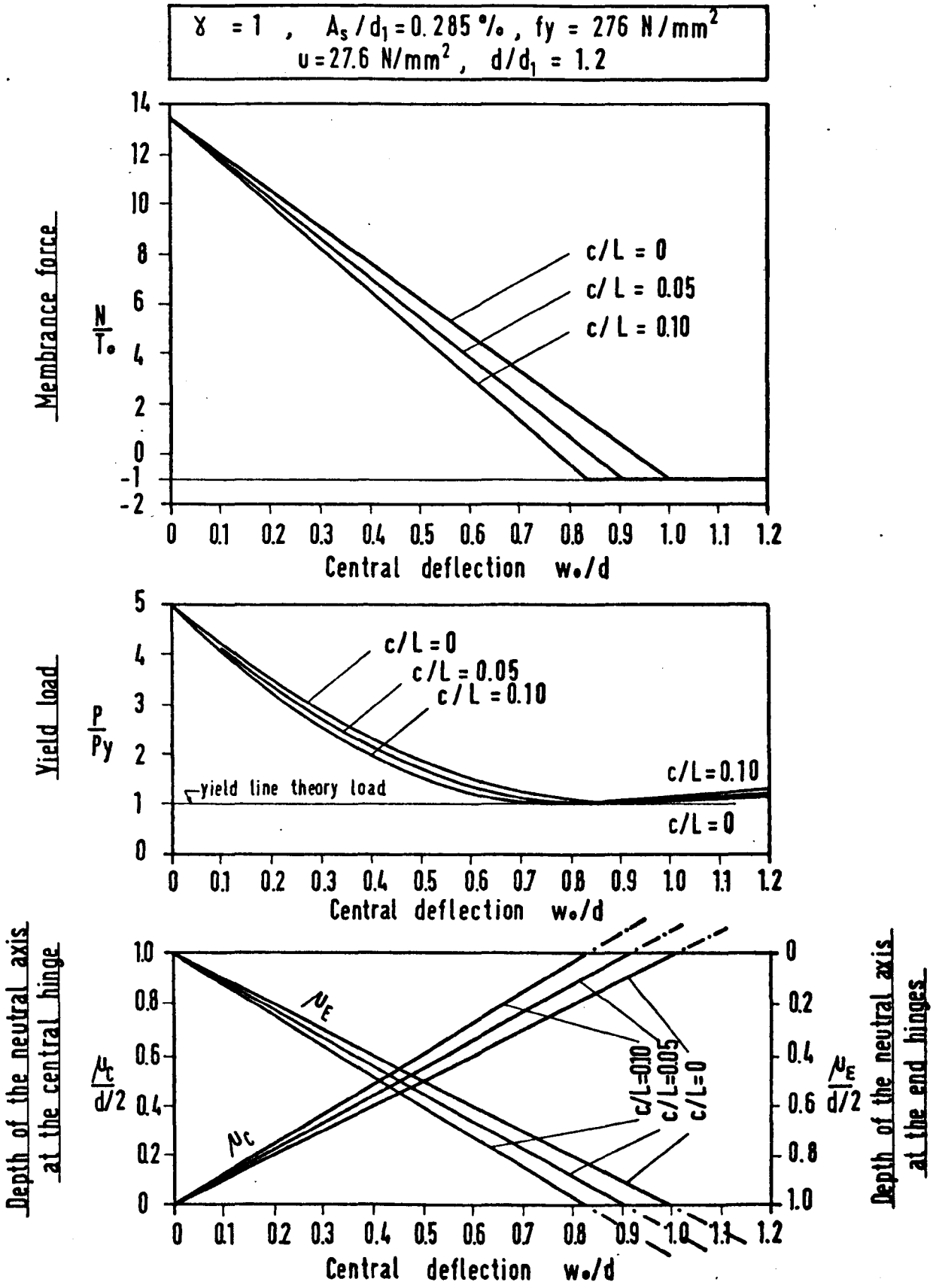

FIG.(4.9) Effect of the Mechanism Parameter c/L on the Behaviour of a Rigid-Plastic Reinforced Concrete Slab Strip with Fixed-Ends and Lateral Restraints

strip under study. The loads on the slab are considered to be exerted at distance $a = 0.4\ L$ from the fixed ends; thus the possible values of c/L range from 0 to 0.1 .

It can be seen from Fig. (4.9) that neither the maximum values of the membrane force and the yield load nor the depths of the neutral axis μ_C and μ_E at zero deflection are influenced by this parameter. However, with increasing deflection the behaviour of the slab changes slightly for different values of c/L . Although the discrepancy is small, it is found that for deflections less than that corresponding to $N/T_o = -1$ the ratios N/T_o and P/P_y are greater for smaller values of c/L . For large deflections the recovery in the load is better in slabs with high values of c/L .

The neutral axis position at the sections of yield is also slightly affected by the parameter c/L as the deflection increases. In slabs having the central plastic hinge formed close to the mid-span section, i.e. c/L small, the movement of the neutral axis towards the compressed face of the slab at the plastic hinges is slow. This implies that the slab will be cracked throughout the depth at these hinges at an earlier stage of deformation when the value of c/L is higher.

4.6.5 CONCRETE STRESS BLOCK PARAMETERS k_1k_3 AND k_2

It has been shown in section 3.2 of Chapter 3 that unless $k_2 = 0.5$ equations (3.11) and (3.12), which determine the neutral axis depth according to the plastic potential theory and the equilibrium method respectively, are inconsistent. The value $k_2 = 0.5$ could be chosen to have consistency between the two predictions but the analysis would not be representative, simply because experimental tests on reinforced concrete beams usually indicate values of k_2 rather less than 0.5 ; the tests carried out by Hognestad, Hanson and McHenry (25) reveal a linear relationship between k_2 and the cube strength of the concrete u (Eq. 3.1b). In the study of the problem of membrane action in slabs different authors have considered different values of the concrete stress block parameters. For instance, Wood (3), Powell (8) and Roberts (24) use $k_1k_3 = 2/3$ and $k_2 = 1/2$; Kemp (4) has presented his analysis

using these parameters in their general form of k_1k_3 and k_2 but when numerical examples are worked out he also followed Wood; Park (12-16) has used Hognestad's k_1k_3 and k_2 (Eqs. 3.1) while some other investigators like Morley (10), Janas (22,26) and Sawczuk (17) prefer to present their analysis using σ_c (the compressive strength of the concrete) in general to indicate $k_1k_3.u$ but k_2 was taken to be 1/2. However, none of the mentioned authors has commented on the effect of these parameters on the plastic behaviour of slabs except Morley who mentioned, while comparing some peak loads of square and rectangular slabs, that the relationship between the compressive strength of the concrete σ_c and the cube strength u is important.

Figure (4.10) illustrates the effect of these stress block parameters on the plastic behaviour of the typical slab strip under study. For any given cube strength of concrete u three pairs of values of the concrete stress block parameters are considered. These are ; Hognestad's k_1k_3 and k_2 represented by Eqs. (3.1), Hognestad's k_1k_3 but $k_2 = 1/2$ and Wood's design coefficients $k_1k_3 = 2/3$ and $k_2 = 1/2$. The figure shows variations in the values of the membrane force N/T_o and the yield load P/P_y at any central deflection; the differences being more pronounced at high values of u and small deflections. However, at low cube strengths of concrete; the approximate coefficients of Wood are found to predict lower values of N/T_o and P/P_y (for any deflection w_o) than those of Hognestad but as higher values of u are used the effects change and Wood's parameters begin to overestimate the membrane force N/T_o and the yield load P/P_y . If concrete of cube strength $u = 30$ N/mm^2 (4348 lbf/in^2) is used in this particular slab strip, the behaviour of the slab will be equally predicted by both Wood's approximate coefficients and the more representative coefficients of Hognestad.

In the case of k_1k_3 given by Eq. (3.1a) and $k_2 = 0.5$ (to satisfy equilibrium but not to represent reality) the values of the membrane force and the yield load are found to be lower than the corresponding values obtained by using Hognestad's parameters for all but very low values of u . Again the discrepancy is greater at higher values of u .

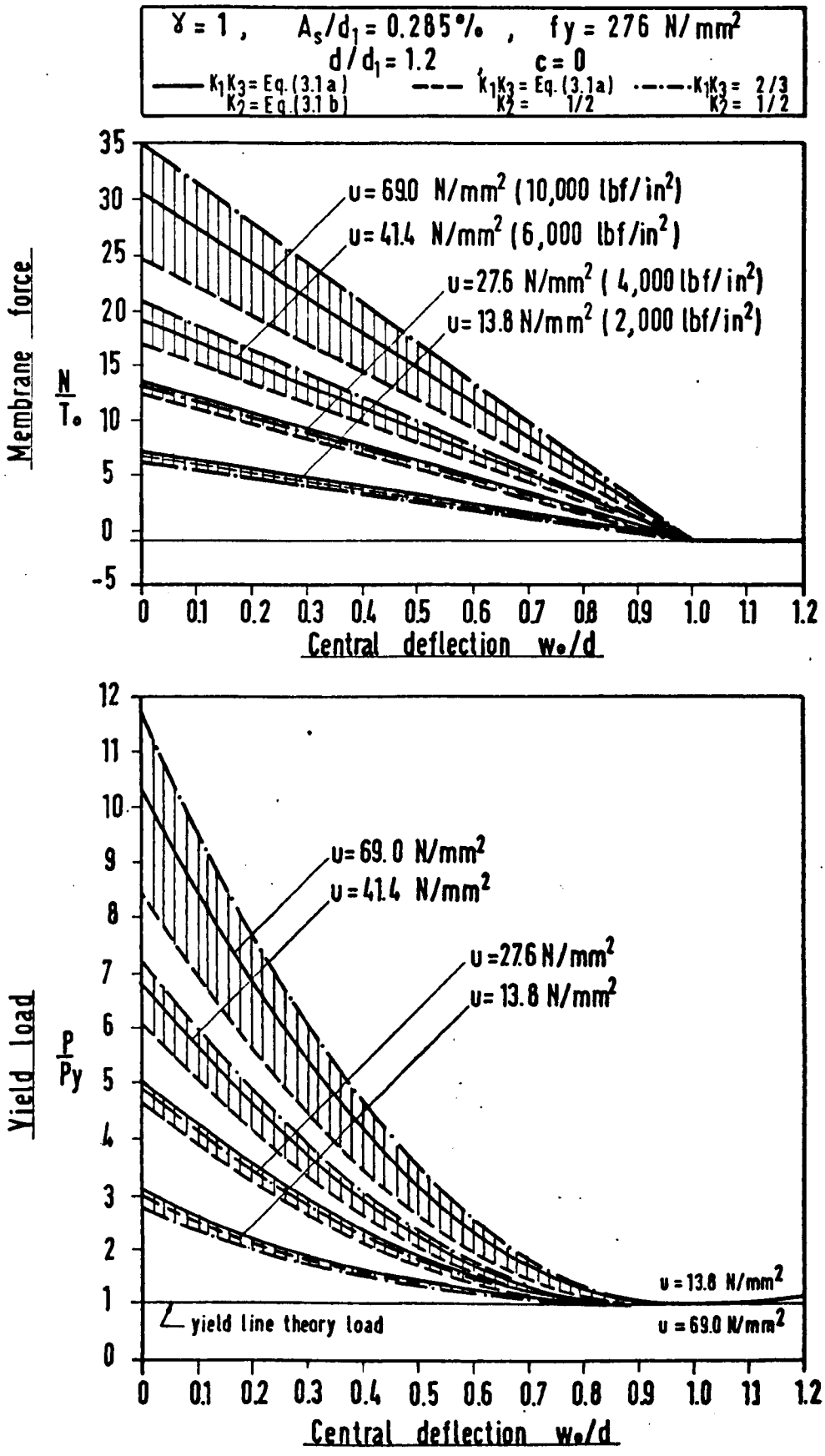

FIG. (4.10) Effect of Using Different Concrete Stress Block Parameters on the Behaviour of a Rigid-Plastic Reinforced Concrete Slab Strip with Fixed-Ends and Lateral Restraints

A measure of the effect of using the three different pairs of concrete stress block parameters may be obtained by comparing the maximum values of N/T_o and P/P_y obtained at the start of collapse of the slab strip under study using $u = 69\ N/mm^2$ (the highest value shown in the figure where the differences are expected to be largest).

	$\frac{N_{max}}{T_o}$	$\frac{P_{max}}{P_y}$
Wood's approximate coefficients $k_1k_3 = 2/3$ and $k_2 = 1/2$	35.0	11.7
Hognestad's k_1k_3 (Eq. 3.1a) and k_2 (Eq. 3.1b)	30.6	10.3
Hognestad's k_1k_3 (Eq. 3.1a) and $k_2 = 1/2$	24.6	8.4

4.7 STUDY OF THE MAXIMUM YIELD LOAD

The previous analysis and discussion shows that the simple yield line theory underestimates the capacity of axially restrained slabs by a considerable margin. The enhancements in the loads have been found to be more pronounced in lightly reinforced concrete slabs made of concrete with high cube strengths.

For any given fixed-ended slab strip, the maximum yield load is represented by Eq. (4.30b). This equation written in a dimensional form ,

$$P_{max} = P_y + \frac{M_o}{a} \cdot \beta \cdot \left(\frac{\alpha}{\beta} + 1 - \gamma\right)^2$$

By considering equations (4.15) and (3.4) and the definitions of the notations α and β as given by Eq. (3.5), the value of P_{max}

can be expressed as ,

$$P_{max} = 2 \frac{(\frac{d}{L})}{(\frac{a}{L})} \cdot \frac{A_s}{d_1} \cdot f_y \cdot d \cdot \frac{(1 - \frac{k_2}{k_1 k_3} t)}{(\frac{d}{d_1})^2} [1 + \gamma \{ 1 + \frac{\frac{k_2}{k_1 k_3} t}{(1 - \frac{k_2}{k_1 k_3} t)} (1 - \gamma) \}]$$

$$+ \frac{k_1 k_3}{k_2} \cdot u \cdot d \cdot \frac{(\frac{d}{L})}{(\frac{a}{L})} \cdot [\frac{1}{2} - \frac{k_2}{k_1 k_3} t \frac{(1 - \gamma)}{(\frac{d}{d_1})}]^2 \qquad (4.31)$$

where $t = \frac{A_s}{d_1} \cdot \frac{f_y}{u}$

Equation (4.31) is the sum of two terms. For specified geometry of a slab strip, the first term depends mainly on the percentage of reinforcement and is slightly affected by the cube strength of the concrete u (see Fig. 4.11). This term expresses the effect of pure bending (yield line theory solution) whereas the second term shows the effect of membrane action. However, the second term depends mainly on the value of the cube strength of the concrete u. It is to be noted here that for the practical values of the percentage of reinforcement and the cube strength of the concrete the second term dominates the value of the maximum yield load P_{max}. In other words, for a given value of u, the percentage of reinforcement will have only a slight effect on P_{max} especially for slabs with high concrete cube strengths. This is readily seen in Fig. (4.11) which is constructed for the same typical slab strip assuming that $d/L = 1/20$ and $a/L = 0.4$. This figure clearly shows that the maximum yield load is influenced by the quality of the concrete and not the amount of reinforcement. For example, the same maximum yield load, say 1.5 N/mm^2 (216 lbf/in^2) can be obtained by using a slab with u = 27.6 N/mm^2 (4000 lbf/in^2) and percentage of reinforcement $A_s/d_1 = 1\%$ or the same slab with no reinforcement at all but u = 38N/mm^2 (5500 lbf/in^2). This illustrates that the amount of reinforcement can be reduced by using a richer mix of concrete to obtain equal initial collapse loads.

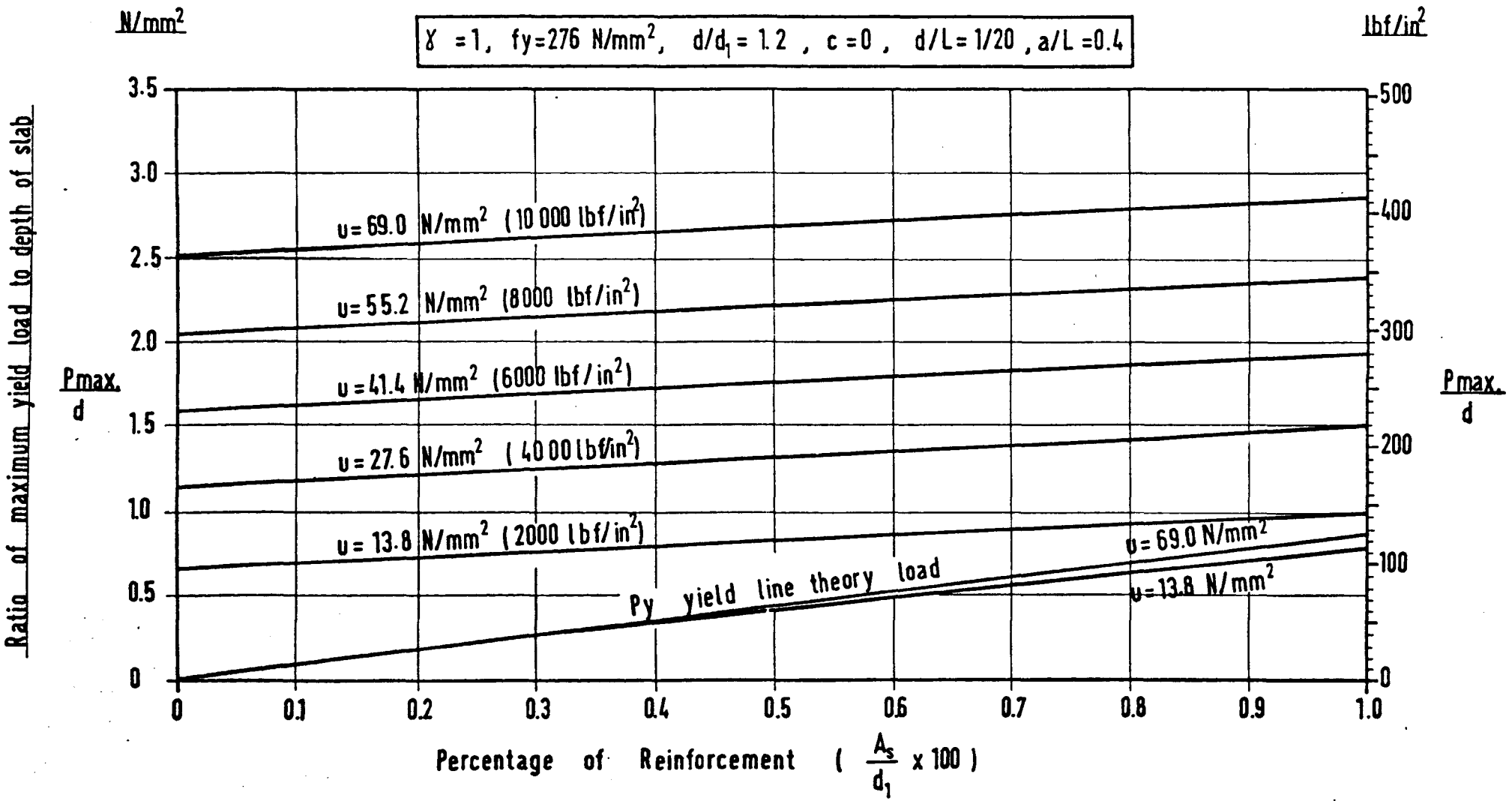
N/mm²
lbf/in²
γ = 1, fy=276 N/mm², d/d1 = 1.2 , c = 0 , d/L = 1/20 , a/L = 0.4
Ratio of maximum yield load to depth of slab
Pmax./d
3.5
3.0
2.5
2.0
1.5
1.0
0.5
0
500
400
300
200
100
0
u = 69.0 N/mm² (10 000 lbf/in²)
u = 55.2 N/mm² (8000 lbf/in²)
u = 41.4 N/mm² (6000 lbf/in²)
u = 27.6 N/mm² (4000 lbf/in²)
u = 13.8 N/mm² (2000 lbf/in²)
Py yield line theory load
u = 69.0 N/mm²
u = 13.8 N/mm²
0
0.1
0.2
0.3
0.4
0.5
0.6
0.7
0.8
0.9
1.0
Percentage of Reinforcement (As/d1 x 100)

FIG. (4.11)

4.8 SUMMARY

The analysis and discussion of this chapter showed that strain rate theory is always applicable to rigid-plastic and axially restrained concrete slabs; the movement of the neutral axis for strain rate at the yield sections in these slabs was found to be always into the compressive zone for total strain.

The variation in the stress state due to deflection of such slabs was shown to cover an extensive part of the yield locus. It ranges from $M \triangleq M_{max}$ (the start of collapse at zero deflection where the membrane force as well as the yield load are maxima and at which the neutral axis forms close to the mid-depth of the slab at all yielding hinges) to $M \triangleq M_{min}$ (the stage of large values of deflection where the membrane force becomes tensile and the cracks penetrate the whole thickness of the slab at some yield sections). This large movement of the stress state point on the yield locus causes highly significant discrepancies between the predictions of total strain and strain rate theories.

The start of collapse of a rigid-plastic concrete slab shows consistency between total strain and strain rate theories due to the maximum values of the membrane force and the yield load as well as the position of the neutral axis at the yield sections being the same for both theories. As the deflection of the slab increases the total strain theory overestimates the membrane force and underestimates the yield load for any specific value of deflection when compared to strain rate theory. Total strain theory shows a slower movement of the neutral axis at yield sections towards the compressed face of the slab than that predicted by strain rate theory. The values of deflection corresponding to zero membrane force and when the cracks penetrate the whole thickness of the slab were found to be double those obtained by strain rate theory. The errors caused by using total strain theory in the analysis of rigid-plastic and axially restrained reinforced concrete slabs instead of strain rate theory, therefore, result in a steeper load-deflection curve, a smaller decline in the value of the membrane force and a slower increase in the depth of the neutral axis at the yield sections with increasing deflection.

In general, a rigid-plastic and axially restrained slab strip analysed by the strain rate theory produces a load-deflection curve with the following features :

i. The start of collapse (zero deflection) is a load (maximum) many times greater than the simple yield line theory load (or Johansen load). The value of the compressive membrane force corresponding to this load is also maximum.

ii. With increasing deflection, the load falls off rapidly due to the value of the compressive membrane force becoming smaller. The reduction in the load follows a parabolic path. At one stage of deflection the membrane force becomes zero and the value of the load is minimum and equal to the yield line theory load. The equilibrium of the slab during this stage of deformation is 'unstable'.

iii. When the deflection increases further, the slab will show some recovery in the load with the membrane force becoming tensile. Although the slab, at a certain stage of deformation, will be cracked throughout the depth at some sections of yield, it will continue to carry increasing load until all the reinforcing bars fracture and collapse occurs. The equilibrium of the slab during this stage of recovery in load is 'stable'.

CHAPTER 5

PARTIALLY RESTRAINED REINFORCED CONCRETE SLAB STRIPS (ELASTIC - PLASTIC THEORY)

5.1 INTRODUCTION AND ASSUMPTIONS

The ultimate strength and behaviour of axially restrained reinforced concrete slab strips were studied in Chapter 4 assuming that the materials of the slab were rigid - perfectly plastic and that the slab ends were fully restrained against lateral displacements. In this chapter, the theory for the load carrying capacity and behaviour of these slabs will be generalized to include the effects of the elastic shortening of the slab and the outward movement of the surround, both due to membrane forces. The ends of the slab strip will be considered as 'simply supported' and to be separated from the surrounding body by a physical gap. It is well known that compressive membrane action in axially restrained slabs, in general, depends upon the restriction of small outward displacements at the boundaries and, therefore, the elastic shortening of the slab, the partial restraint against lateral displacement at the ends and the existence of a physical gap between the ends of the slab and the surrounding body may all cause a significant reduction in the ultimate strengths and may give a completely different picture for the relationship between the load and the deflection as yield proceeds.

The analysis and discussion of this chapter will show that the movements of the neutral axis for strain rate at the yield sections, in these partially restrained reinforced concrete slab strips, occur initially into the zone of total tensile strains, the case for which total strain theory must be applied, but for large deflections the neutral axis (for strain rate) starts to move into the compressive zone for total strain and, hence, the strain rate theory should be used. However, for the sake of comparison, the analysis will be first attempted following separately 'total strain' and 'strain rate' concepts to show the influence of these two approaches on the prediction of the plastic behaviour of these slabs

and then the correct approach which involves the use of both total strain and strain rate theories will be presented in detail. Some important conclusions about the validity and applicability of these theories in the plastic analysis of concrete slabs, in general, will be reached in this chapter.

The assumptions made in this investigation are the same as those adopted in Chapter 4 except that in this case the effects of the elastic shortening of the slab strip and the outward movement of the surround due to membrane forces are taken into account. The loading on the slab strips considered is, again, two point loading so that in comparing with experiments, the effect of biaxial compression on the concrete can be neglected. The analysis is confined to simply supported reinforced concrete slab strips with bottom reinforcement only. The reinforcement is assumed to extend far enough in the slab to ensure a plastic hinge can form at any section in the central region of the slab between the two applied loads. Although the slab strip is reinforced in the bottom face only, the elastic strains of the slab due to membrane forces are assumed uniform which is consistent with the assumption of ignoring the elastic curvature of the slab member.

Wherever possible, the procedure of analysis presented in Chapter 4 will be followed. The yield criterion represented by equation (3.5) of Chapter 3 will be adopted and assumed valid for all analyses. The equations of the collapse loads and the membrane forces will be given in dimensionless forms as ratios of the simple yield line theory load and the yield force in the reinforcement respectively. In addition, some typical slab strips will be analysed to show the differences between the approximate rigid-plastic theory presented in Chapter 4 and the more representative elastic-plastic theory of this Chapter.

5.2 GENERAL ANALYSIS

5.2.1 THE SLAB STRIP AND THE MECHANISM OF COLLAPSE

A simply supported reinforced concrete slab strip AB of unit width, depth d and length L is shown in Fig. (5.1a). The slab strip is subjected to two point loading each of magnitude $P/2$

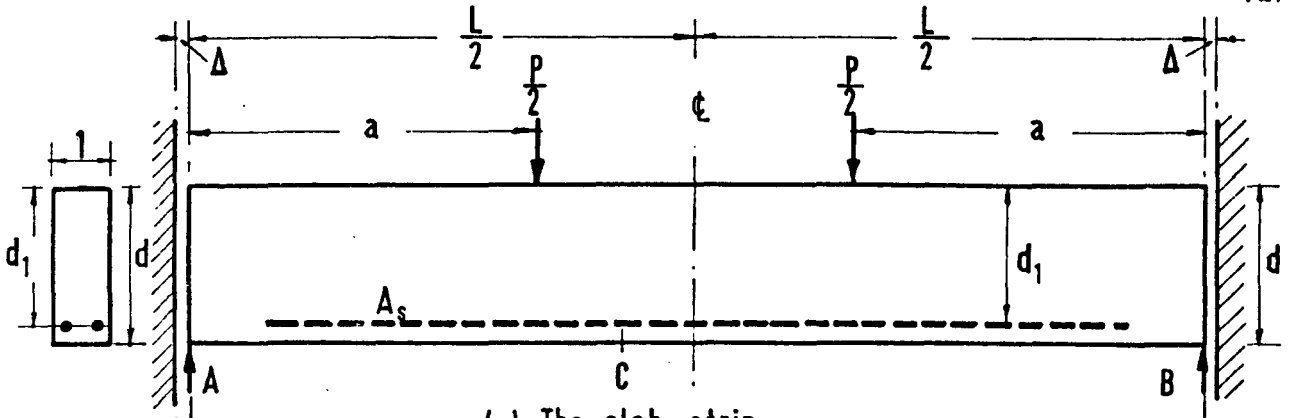

(a) The slab strip

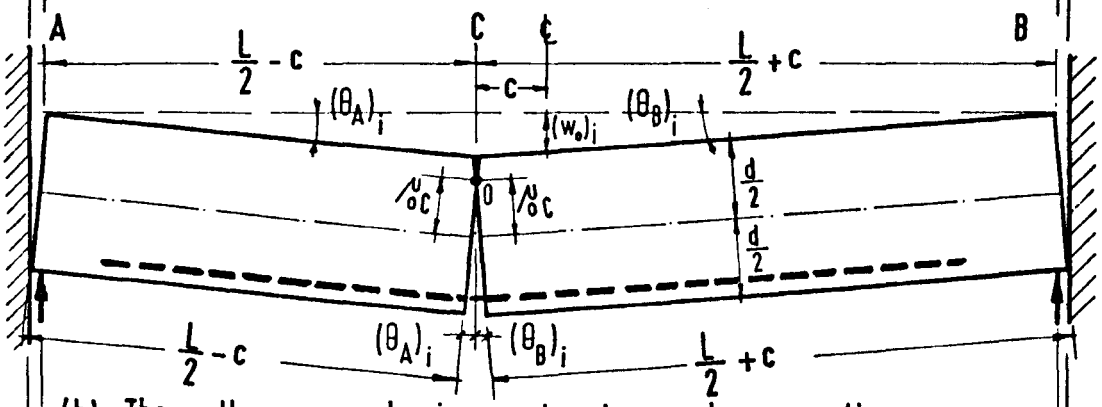

(b) The collapse mechanism prior to membrane action

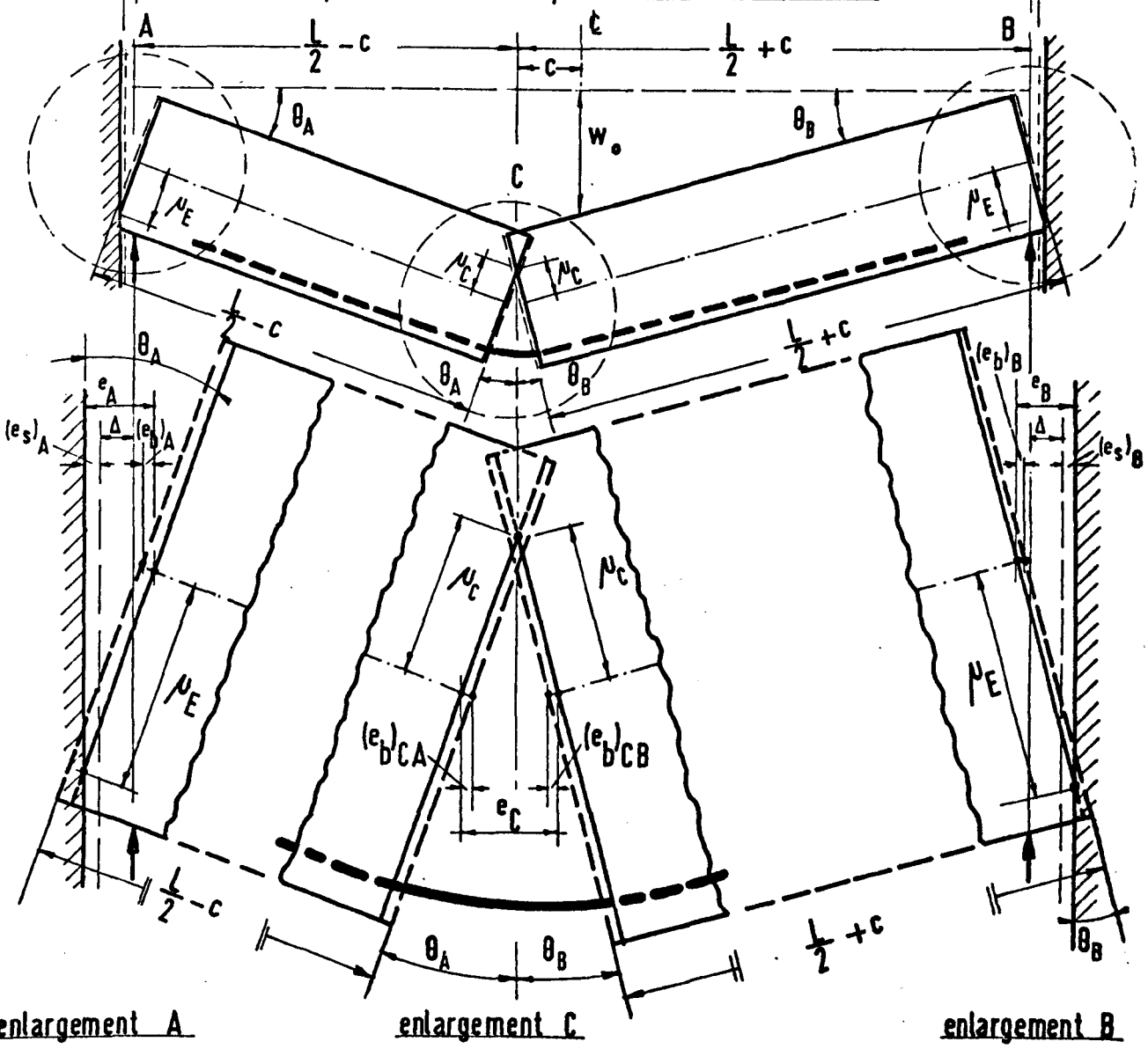

enlargement A enlargement C enlargement B

(c) The collapse mechanism after membrane action is developed

FIG.(5.1) Partially Restrained Simply Supported Reinforced Concrete Slab Strip With Two Point Loading At Yield

located at distance 'a' from the nearest simply supported end A or B as shown. Reinforcement of area A_s, yield stress f_y and cover $(d-d_1)$ is placed at the bottom face only of the given slab strip.

As discussed in Chapter 4, the central plastic hinge C does not necessarily form at mid-span but will form at the weakest section of the portion extending between the two applied loads; at distance c from the centre of the slab.

If the partially-stiff surrounding body is separated from each of the two simply supported ends of the slab strip by a physical gap Δ (see Fig. 5.1a), the slab will initially yield under the simple yield line theory load P_y and a mechanism of collapse will form as shown in Fig. (5.1b).

5.2.2 BEHAVIOUR OF THE SLAB STRIP PRIOR TO MEMBRANE ACTION

The analysis presented in the previous chapter showed that compressive membrane action in an axially restrained slab is formed because of the restraint to the outward movement of the bottom edges of the slab. Due to compressive membrane action very high loads, many times greater than the yield line theory load, were found to be sustained for very small deflections. However, when the edges of the slab are separated from the restraining body by a physical gap, the initial collapse of the slab will be due to pure flexure. The yield load as well as the neutral axis position at the yield sections will be defined according to the yield line theory. Therefore, the initial stress state of the deformed slab strip AB of Fig. (5.1b) is defined by

$$P = P_y \tag{5.1a}$$

$$\mu_{oC} = \frac{\frac{\alpha}{\beta}}{(\frac{\alpha}{\beta} + 2)} \frac{d}{2} \tag{5.1b}$$

Where μ_{oC} denotes the neutral axis depth at the plastic hinge C corresponding to zero axial force; and α and β are as defined

by Eq. (3.5) of Chapter 3. Equation (5.1b) is obtained from either Eq. (4.5a) of Chapter 4 assuming $N = 0$ or directly according to Eq. (4.29k) of the same chapter.

With increasing deflection the two portions AC and BC of the slab strip rotate about point o defining the neutral axis position at the central plastic hinge according to the yield line theory. The load-deflection relationship during this stage of pure flexure will show a horizontal line ($P = P_y$) until the limit is reached when the bottom edges of the two simply supported ends A and B of the slab just come into contact with the surrounding body and the membrane force begins to be generated. The value of the central deflection $(w_o)_i$ corresponding to this stage can be obtained as follows :

Assume that when this stage is reached the two portions AC and BC of the slab strip have rotated through angles $(\theta_A)_i$ and $(\theta_B)_i$ respectively. The maximum total tensile strain at the bottom face of the plastic hinge C corresponding to these rotations is $(\mu_{oC} + \frac{d}{2})\,[\sin(\theta_A)_i + \sin(\theta_B)_i]$. From Fig. (5.1b) when the elastic curvature of the slab strip is ignored the following geometrical equation can be obtained;

$$\left(\frac{L}{2} - c\right)\cos(\theta_A)_i + \left(\mu_{oC} + \frac{d}{2}\right)\left[\sin(\theta_A)_i + \sin(\theta_B)_i\right] + \left(\frac{L}{2} + c\right)\cos(\theta_B)_i = L + 2\Delta$$

Since θ is small

$$\cos\theta \simeq 1 - \frac{\theta^2}{2}$$

and $$\sin\theta \simeq \theta$$

and when the value of μ_{oC} as given by Eq. (5.1b) is introduced the geometrical equation becomes

$$\frac{\left(\frac{\alpha}{\beta} + 1\right)}{\left(\frac{\alpha}{\beta} + 2\right)}\left[(\theta_A)_i + (\theta_B)_i\right]\frac{L}{d} - \left(1 - \frac{2c}{L}\right)\frac{(\theta_A)_i^2}{4}\frac{L^2}{d^2} - \left(1 + \frac{2c}{L}\right)\frac{(\theta_B)_i^2}{4}\frac{L^2}{d^2} = 2\frac{\Delta}{d}\frac{L}{d}$$

Replacing the values of the rotations $(\theta_A)_i$ and $(\theta_B)_i$ by the central deflection $(w_o)_i$ according to Eqs. (4.8) and solving the resulting equation gives

$$\left(\frac{w_o}{d}\right)_i = \frac{1}{\left(1 + \frac{2c}{L}\right)}\left[\frac{\left(\frac{\alpha}{\beta} + 1\right)}{\left(\frac{\alpha}{\beta} + 2\right)} - \sqrt{\frac{\left(\frac{\alpha}{\beta} + 1\right)^2}{\left(\frac{\alpha}{\beta} + 2\right)^2} - \frac{\Delta}{d} \cdot \frac{L}{d}\left(1 - \frac{2c}{L}\right)\left(1 + \frac{2c}{L}\right)}\right] \tag{5.2}$$

Equation (5.2) gives the value of the central deflection of the slab strip when the bottom edges of the two simply supported ends of the slab are just in contact with the surround. For the special case of zero gap at the slab boundaries (i.e. $\Delta = 0$) the value of the central deflection $(w_o)_i$ will be zero indicating that the membrane action takes place at the start of collapse.

5.2.3 MEMBRANE ACTION - DEVELOPMENT OF MEMBRANE FORCE AND DEFINITION OF STIFFNESS FACTOR

When the central deflection of the slab exceeds the value given by Eq. (5.2) the horizontal outward movement of the bottom edges of the slab will be resisted by the partially stiff surrounding body and therefore a compressive membrane force N will be generated. This membrane force will compress the slab strip and spread the surrounding body by amounts that depend on their stiffnesses.

If the elastic stiffness of the whole slab strip is denoted by S_b and the elastic stiffness of the two surrounds by S_s the total effective deformation of the mid-plane of the slab strip under the force N will be ;

$$\left\{\begin{matrix}\text{Total Effective}\\ \text{Deformation Due}\\ \text{to } N\end{matrix}\right\} = \left\{\begin{matrix}\text{Elastic Shortening}\\ \text{of the Whole Slab}\\ \text{Strip}\end{matrix}\right\} + \left\{\begin{matrix}\text{Outward Movement}\\ \text{of the Two Surrounds}\end{matrix}\right\}$$

$$= \frac{N}{S_b} + \frac{N}{S_s} = \frac{N}{S}$$

in which S is a stiffness factor ;

$$\frac{1}{S} = \frac{1}{S_b} + \frac{1}{S_s}$$

$$S = \frac{S_b\, S_s}{S_b + S_s} = \lambda\, S_b$$

where $$\lambda = \frac{\frac{S_s}{S_b}}{1 + \frac{S_s}{S_b}}$$

Note that if $S_s = \infty$ then $\lambda = 1.0$ and $S = S_b$; and if $S_s = 0$ then $\lambda = 0$ and $S = 0$, so the stiffness factor S can vary between 0 and S_b. Thus, when both stiffnesses S_s and S_b are assumed infinite (which represents the case of a rigid plastic slab strip with fully lateral restraint) the stiffness factor S becomes infinity.

Value of S_b :

$$S_b = \frac{\text{Force } N}{\left\{\begin{array}{c}\text{Elastic Shortening}\\ \text{of the Slab Strip}\\ \text{Due to } N\end{array}\right\}} = \frac{N}{\frac{N.L}{A.E_c}} = \frac{A.E_c}{L}$$

where A is the cross sectional area of the slab strip (A = unit width x d) and E_c is the modulus of elasticity of the concrete which can be related to the cube strength of the concrete u according to the following approximate relationship [as adopted by Roberts (24), Eq. (2.38d) of Chapter 2] ;

$$E_c = \frac{\sqrt{u}}{180.6} \times 10^6 \text{ N/mm}^2 \quad \left(\text{or } \frac{\sqrt{u}}{15} \times 10^6 \text{ lbf/in}^2\right)$$

Therefore

$$S_b = \frac{d}{L}\,\frac{\sqrt{u}}{180.6} \times 10^6 \text{ N/mm}^2 \quad \left(\text{or } \frac{d}{L}\,\frac{\sqrt{u}}{15} \times 10^6 \text{ lbf/in}^2\right) \quad (5.3)$$

Value of S_s :

No general expression can be given for S_s since it depends on the particular structural form of the surround. When comparisons

are made between theory and experiments, S_s will be determined by tests.

5.2.4 COMPATIBILITY EQUATION

For the slab strip shown in Fig. (5.1c) ; when the vertical deflection at the centre of the slab strip is w_o where $[\, w_o \cong (w_o)_i \,]$ the horizontal displacement compatibility equation becomes ;

$$e_A - (e_s)_A - (e_b)_A + (\tfrac{L}{2} - c)\cos\theta_A + e_C - (e_b)_{CA} - (e_b)_{CB} + (\tfrac{L}{2} + c)\cos\theta_B + e_B - (e_s)_B - (e_b)_B = L + 2\Delta$$

Noting that

$$(e_s)_A + (e_s)_B = e_s = \frac{N}{S_s}$$

$$(e_b)_A + (e_b)_{CA} + (e_b)_{CB} + (e_b)_B = e_b = \frac{N}{S_b}$$

and $$\frac{N}{S_s} + \frac{N}{S_b} = \frac{N}{S}$$

Therefore

$$e_A + (\tfrac{L}{2} - c)\cos\theta_A + e_C + (\tfrac{L}{2} + c)\cos\theta_B + e_B = L + \frac{N}{S} + 2\Delta$$

When θ is small

$$\cos\theta \simeq 1 - \frac{\theta^2}{2}$$

and the compatibility equation becomes

$$e_A + e_B + e_C - (\tfrac{L}{2} - c)\frac{\theta_A^2}{2} - (\tfrac{L}{2} + c)\frac{\theta_B^2}{2} = \frac{N}{S} + 2\Delta \qquad (5.4)$$

5.2.5 EVALUATION OF THE MEMBRANE FORCE, THE YIELD LOAD AND THE NEUTRAL AXIS POSITION AT THE YIELD SECTIONS ACCORDING TO ' TOTAL STRAIN' AND 'STRAIN RATE' THEORIES

(a) Total Strain Theory:

If the total strain concept (Eq. 3.13) is followed in this analysis, the relationships between the rotations θ and the extensions e at the yield sections A , B and C will be the same as those given by Eqs. (4.7) of Chapter 4. Therefore, substituting these equations into Eq. (5.4) yields

$$\mu'_E\,(\theta_A + \theta_B) + \mu'_C\,(\theta_A + \theta_B) - (\tfrac{L}{2} - c)\,\frac{\theta_A^2}{2} - (\tfrac{L}{2} + c)\,\frac{\theta_B^2}{2} = \frac{N}{S} + 2\Delta$$

The geometry of the collapse mechanism of Fig. (5.1c) implies that the rotations θ_A and θ_B are related to the central deflection w_o according to Eqs. (4.8). When these relations are introduced the compatibility equation becomes

$$\mu'_E + \mu'_C - \frac{w_o}{2}\,(1 + \frac{2c}{L}) = \frac{1}{4}\,\frac{N}{S}\,\frac{(1 - \frac{2c}{L})}{(\frac{w_o}{L})} + \frac{1}{2}\,\Delta\,\frac{(1 - \frac{2c}{L})}{(\frac{w_o}{L})} \qquad (5.5)$$

Noting that the values of μ'_E and μ'_C are given in equations (4.5) in terms of the membrane force N and substituting these values (with γ being 0 in this case) into equation (5.5) and solving for N gives

$$\frac{N}{T_o} = \frac{\frac{1}{2}\,[(\frac{\alpha}{\beta} + 1) - \frac{1}{2}\,(\frac{\alpha}{\beta} + 2)(1 + \frac{2c}{L})\,\frac{w_o}{d} - \frac{1}{2}\,(\frac{\alpha}{\beta} + 2)(1 - \frac{2c}{L})\,\frac{\frac{\Delta}{d}\,\frac{L}{d}}{\frac{w_o}{d}}]}{[1 + \frac{(1 - \frac{2c}{L})}{\bar{S}\,\frac{w_o}{d}}]} \qquad (5.6)$$

where $\bar{S} = \dfrac{16\,k_2}{k_1 k_3}\,\dfrac{S}{\frac{L}{d}\,u}$

Equation (5.6) may be compared with the corresponding rigid-plastic solution given by Eq. (4.10) of Chapter 4. For $\Delta = 0$, $\bar{S} = \infty$ and $\gamma = 0$, the two equations are identical.

(b) Strain Rate Theory

The analysis according to the strain rate theory is based on the incremental variation in the rotations and extensions (Eq. 3.9). When this concept is applied the relationships between the increments of rotation and extension at the yield sections A , B and C will be the same as those given by Eqs. (4.11). For an infinitely small variation in w_o equation (5.4) gives

$$\mu_E\,(d\theta_A + d\theta_B) + \mu_C\,(d\theta_A + d\theta_B) - (\tfrac{L}{2} - c)\,\theta_A\,d\theta_A$$

$$- (\tfrac{L}{2} + c)\,\theta_B\,d\theta_B = d(\tfrac{N}{S}) \qquad (5.7)$$

It should be noted that the gap parameter Δ does not appear in this differential equation since Δ is not a function of w_o .

The values of the rotations θ_A and θ_B are related to the central deflection w_o according to Eqs. (4.8). The incremental values of these rotations ($d\theta_A$ and $d\theta_B$) are related to the incremental value of the central deflection dw_o in the same proportion. Differentiating Eqs. (4.8) gives

$$d\theta_A = \frac{2}{L}\,\frac{1 + \frac{2c}{L}}{1 - \frac{2c}{L}} \cdot dw_o$$

$$d\theta_B = \frac{2}{L} \cdot dw_o$$

When these values are considered the compatibility equation (5.7) becomes

$$\mu_E + \mu_C - w_o\,(1 + \tfrac{2c}{L}) = \frac{1}{4}\,\frac{LT_o}{Sd} \cdot (1 - \tfrac{2c}{L})\,\frac{d(\frac{N}{T_o})}{d(\frac{w_o}{d})}$$

Introducing the values of μ_E and μ_C as given by Eqs. (4.5) gives

$$\frac{d(\frac{N}{T_o})}{d(\frac{w_o}{d})} + \frac{\bar{S}}{(1 - \frac{2c}{L})} (\frac{N}{T_o}) + \frac{\bar{S}}{2} (\frac{\alpha}{\beta} + 2) \frac{(1 + \frac{2c}{L})}{(1 - \frac{2c}{L})} (\frac{w_o}{d}) - \frac{\bar{S}}{2} \frac{(\frac{\alpha}{\beta} + 1)}{(1 - \frac{2c}{L})} = 0$$

where $\bar{S}$ is as defined by Eq. (5.6). The solution of this first order differential equation is

$$\frac{N}{T_o} = F \cdot e^{- \frac{\bar{S}}{(1 - \frac{2c}{L})} (\frac{w_o}{d})} - \frac{1}{2} (\frac{\alpha}{\beta} + 2)(1 + \frac{2c}{L}) (\frac{w_o}{d}) + \frac{1}{2\bar{S}} (\frac{\alpha}{\beta} + 2)(1 + \frac{2c}{L})(1 - \frac{2c}{L}) + \frac{1}{2} (\frac{\alpha}{\beta} + 1) \qquad (5.8)$$

where F is a constant which can be evaluated by satisfying the following boundary condition,

$$\frac{N}{T_o} = 0 \quad \text{when} \quad \frac{w_o}{d} = (\frac{w_o}{d})_i \quad \text{given by Eq. (5.2)} .$$

Thus

$$F = [\frac{1}{2} (\frac{\alpha}{\beta} + 2)(1 + \frac{2c}{L})(\frac{w_o}{d})_i - \frac{1}{2\bar{S}} (\frac{\alpha}{\beta} + 2)(1 + \frac{2c}{L})(1 - \frac{2c}{L}) - \frac{1}{2} (\frac{\alpha}{\beta} + 1)] \cdot e^{\frac{\bar{S}}{(1 - \frac{2c}{L})} (\frac{w_o}{d})_i}$$

and the equation of the membrane force becomes

$$\frac{N}{T_o} = [\frac{1}{2} (\frac{\alpha}{\beta} + 2)(1 + \frac{2c}{L})(\frac{w_o}{d})_i - \frac{1}{2\bar{S}} (\frac{\alpha}{\beta} + 2)(1 + \frac{2c}{L})(1 - \frac{2c}{L}) - \frac{1}{2} (\frac{\alpha}{\beta} + 1)] \cdot e^{- \frac{\bar{S}}{(1 - \frac{2c}{L})} [(\frac{w_o}{d}) - (\frac{w_o}{d})_i]} - \frac{1}{2} (\frac{\alpha}{\beta} + 2)(1 + \frac{2c}{L})(\frac{w_o}{d}) + \frac{1}{2\bar{S}} (\frac{\alpha}{\beta} + 2)(1 + \frac{2c}{L})(1 - \frac{2c}{L}) + \frac{1}{2} (\frac{\alpha}{\beta} + 1) \qquad (5.9)$$

For the case $\bar{S} = \infty$, Eq. (5.9) reduces to the corresponding rigid-plastic solution given by the special case $\gamma = 0$ of Eq. (4.13).

The relationship between the membrane force and the central deflection having been established, the position of the neutral axis at the central plastic hinge and at the simply supported ends of the slab can be defined in terms of the deflection w_o from Eqs.(4.5) with $\gamma = 0$.

The general expression of the yield load with the membrane force derived in Chapter 4 (namely Eq. 4.16) for fully restrained rigid-plastic slab strip with any steel ratio γ can be equally applied here. Substituting $\gamma = 0$ into Eq. (4.16) to represent the case of slab strips with simple supports, the yield load - membrane force relationship becomes ;

$$\frac{P}{P_y} = 1 + 2\beta \left[\left(\frac{\alpha}{\beta} + 1\right) - \left(\frac{\alpha}{\beta} + 2\right)\left(1 + \frac{2c}{L}\right) \frac{w_o}{d} \right] \frac{N}{T_o} - 2\beta \left(\frac{N}{T_o}\right)^2 \qquad (5.10)$$

To obtain the yield load ratio P/P_y for any given central deflection w_o , either Eq. (5.6) for total strain or Eq. (5.9) for strain rate should be combined with Eq. (5.10).

5.2.6 APPLICATION OF 'TOTAL STRAIN' AND 'STRAIN RATE' TO TWO EXAMPLES

Comparison of the values of the membrane force, the yield load and the position of the neutral axis at sections of yield given by total strain and strain rate theories is shown in Figs. (5.2) and (5.3) for a simply supported slab strip with the following properties (as adopted in the typical slab strip of Chapter 4) ; $A_s/d_1 = 0.285\%$; $f_y = 276\ N/mm^2$ ($40{,}000\ lbf/in^2$) ; $u = 27.6\ N/mm^2$ ($4000\ lbf/in^2$) ; $d/d_1 = 1.2$; $c = 0$ and $L/d = 20$.

In constructing Fig. (5.2) two more properties are considered. These are :

(a) Stiffnesses of both the slab strip and the surround are assumed infinite (i.e. $\bar{S} = \infty$) .

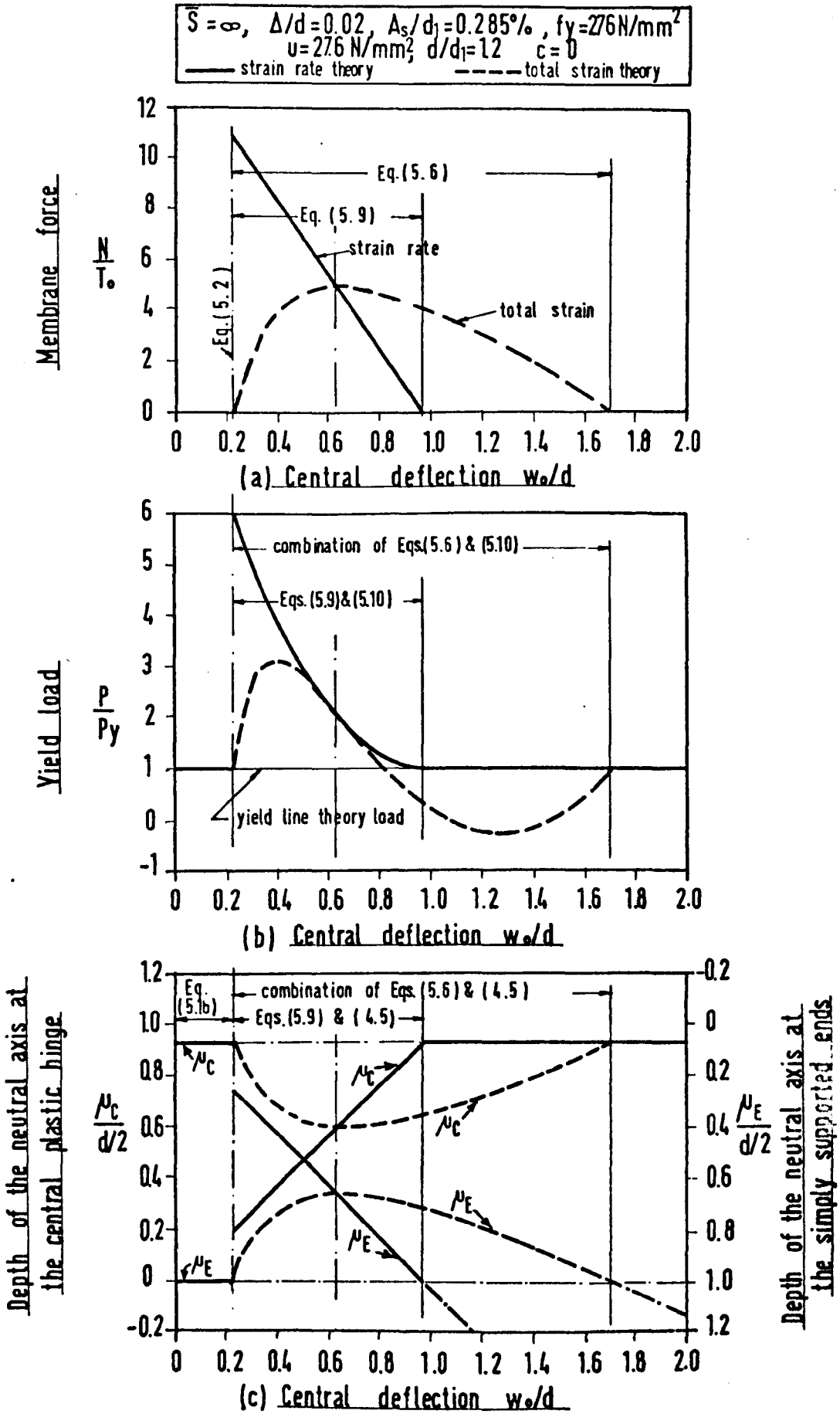

FIG. (5.2) Behaviour of a Simply-Supported Rigid-Plastic Reinforced Concrete Slab Strip With Physical Gap at the Infinitely Stiff Boundaries

(b) At each end of the slab strip there exists a gap of width equivalent to 0.02 times the slab depth (i.e. $\Delta/d = 0.02$).

For Fig. (5.3), the two additional features are :

(a) $\Delta = 0$

(b) The elastic stiffness of the surround S_s is 550 N/mm^2 (79,700 lbf/in^2).* From Eq. (5.3), the elastic stiffness of the slab strip S_b is 1456 N/mm^2 (211,000 lbf/in^2) and hence the dimensionless terms λ and $\bar{S}$ for this example are 0.274 and 8.65 respectively.

Fig. (5.2), therefore, shows the behaviour of a rigid-plastic, simply-supported reinforced concrete slab strip with a physical gap at the infinitely stiff boundaries. It can be seen from this figure that the membrane action starts after the slab has deflected a distance (w_o) equal to 0.23 d (Eq. 5.2). The total strain theory predicts an increase in the value of the membrane force with increasing deflection (Fig. 5.2a) until the membrane force becomes a maximum at a value of central deflection equal to 0.63 d and then decreases. The strain rate theory shows a linear fall in the value of the membrane force with the deflection from a maximum at $w_o = (w_o)_i = 0.23\ d$. This cannot be valid since it contradicts the fact that at $w_o = (w_o)_i$ the membrane force should be zero and the reason for this is that, in this special case ($\bar{S} = \infty$), Δ did not appear in the governing equations. It will be shown later that for values of deflection corresponding to increasing membrane force the analysis of the slab must be associated with total strain theory and, that, the strain rate theory is only applicable for the part of membrane action that corresponds to decreasing membrane force.

It is of interest to note here that for this slab strip with $\bar{S} = \infty$ the total strain and strain rate theories predict the same value of the membrane force at the 'total strain' maximum (i.e. at $w_o = 0.63d$). This point will be discussed in detail in Section 5.3.3.

---

* This figure represents the average elastic stiffness of the model rig used by the author in experimental tests.

The relationship between the yield load and the central deflection is shown in Fig. (5.2b). For values of central deflection ranging between zero and 0.23d the relationship is a horizontal line ($P = P_y$). As the deflection continues compressive membrane action develops which, according to total strain theory, enables the slab to carry an increasing yield load. The stage of increasing yield load ceases at $w_o = 0.39d$. With further increments in deflection the yield load falls off rapidly indicating that the equilibrium of the slab is unstable and the maximum membrane force occurs in this deflection range. For large values of deflection the total strain theory predicts negative values for the yield load but then shows recovery of load at a later stage.

The load - deflection relationship according to strain rate is in two parts with a discontinuity between them. The first part is the horizontal line $P = P_y$ of pure flexure and the second is a falling curve from a maximum at the start of membrane action (i.e. at $w_o = 0.23d$) to a minimum, equal to the yield line theory load, when the membrane force vanishes at $w_o = 0.97d$. The discontinuity at $w_o = 0.23d$ is a further indication of the invalidity of the strain rate theory during the initial stages of membrane action. The load - deflection curve according to total strain theory is lower than that of strain rate except at the point representing maximum membrane force (according to total strain) where the two curves coincide and a mathematical explanation of the point of tangency will be presented later.

Fig. (5.2c) shows the different predictions of the total strain and strain rate theories for the position of the neutral axis at sections of yield. It can be seen from this figure that the depths of the neutral axis μ_C at the central plastic hinge and μ_E at the simply supported ends for values of central deflection such that $0 \leq \frac{w_o}{d} \leq 0.23$ are respectively $0.93\,\frac{d}{2}$ (Eq. 5.1b) and $\frac{d}{2}$. When the central deflection exceeds the value $(w_o)_i$ the neutral axis at all yield sections according to total strain theory starts to move towards the mid-depth of the slab into the zone of total tensile strains with reducing values of μ_C and μ_E. When $\frac{w_o}{d} = 0.63$ the neutral axis will be at its closest position to the mid-depth of

the slab. For greater deflections the neutral axis moves back towards the compressed face of the slab into the compressive zone for total strain until the membrane force becomes zero.

The strain rate theory, however, predicts linear variation for the position of the neutral axis with deflection. Moreover, it shows that the movement of the neutral axis at the yield sections is always into the compressive zone for total strain. This is not valid since it implies a discontinuity in the relationship between the position of the neutral axis and the central deflection at $\frac{w_o}{d} = 0.23$. As demonstrated by Fig. (5.2c), the predictions of the total strain and strain rate theories for the position of the neutral axis at the yield sections of this special slab strip with $\bar{S} = \infty$ are different except at $w_o = 0.63\ d$ (i.e. when the membrane force is maximum) and this will be explained later.

Fig. (5.3) shows the effect of the elastic shortening of the slab and the elastic spread of the surround on the behaviour of the typical slab strip under study. The membrane action in this example starts at zero deflection since $\Delta = 0$. Both total strain and strain rate theories show similar shapes for the membrane force - central deflection curve (Fig. 5.3a). The membrane force increases with deflection to a maximum value at a certain value of central deflection and then decreases for larger deflections. During the stage of increasing membrane force the strain rate theory predicts slightly higher values for the membrane force than those of total strain but for large values of deflection the strain rate curve falls more rapidly than that of total strain. The two curves intersect at a value of central deflection $(\frac{w_o}{d} = 0.45)$ slightly beyond that corresponding to the maximum membrane force according to total strain $(\frac{w_o}{d} = 0.36)$.

The membrane force at the point of intersection is very close to the 'total-strain' maximum (8.01 T_o and 8.12 T_o respectively), but the maximum membrane force predicted by strain rate theory is 19% higher (9.64 T_o).

The yield load - central deflection diagram of this example is shown in Fig. (5.3b). Both total strain and strain rate theories predict that at the start of collapse $(w_o = 0)$ the yield load is the yield line theory load and that as the slab deflects the load

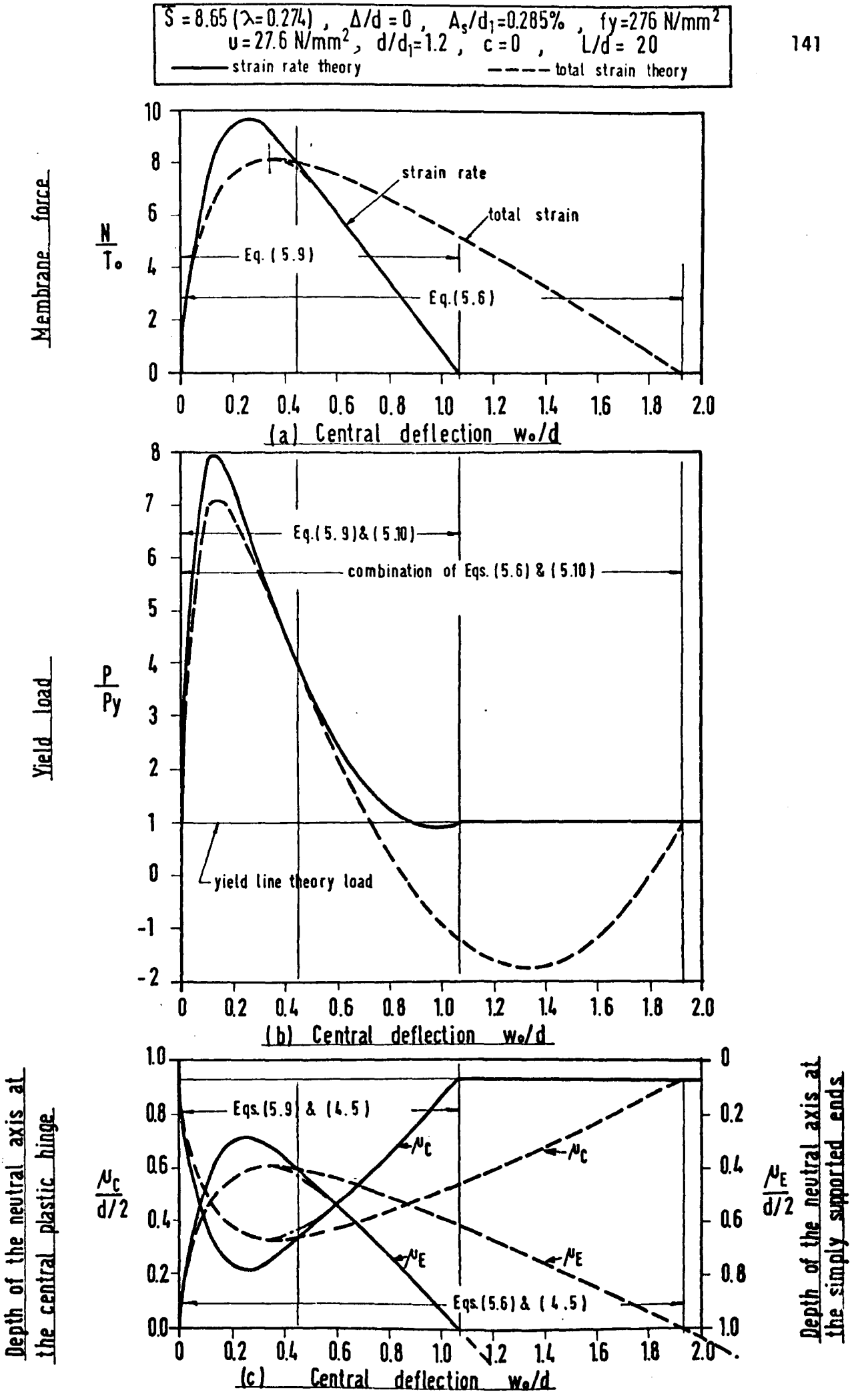

FIG. (5.3) Behaviour of a Non-Rigid Reinforced Concrete Slab Strip With Simple Supports and Partial Lateral Restraints

will be increased until at a certain value of central deflection (less than that corresponding to maximum membrane force) the yield load becomes a maximum and thereafter it falls off rapidly as the deflection increases. For any value of central deflection the yield load estimated by strain rate theory is greater than that of total strain except at $w_o = 0.45\ d$ where they are equal which is also the stage when the membrane force is identical for both theories. The discrepancy in the maximum yield load predicted by strain rate theory compared to that of total strain is, for this example, 12%. As in the example of Fig. (5.2), the total strain theory for large deflections predicts negative values for the yield load but then shows recovery of load at larger deflections.

From Fig. (5.3c) it can be seen that at $w_o = 0$ the depth of the neutral axis at the central plastic hinge is $0.93\ d/2$ and at the simply supported ends is $d/2$. These values are equally predicted by both total strain and strain rate theories. As the slab deflects the neutral axis at all yield sections, according to the two theories, moves towards the mid-depth of the slab into the zone of total tensile strains until at a certain value of central deflection (normally corresponding to the maximum membrane force) the neutral axis is close to the mid-depth of the slab and thereafter it moves back towards the compressed face of the slab. During this deformation process the strain rate theory predicts a more rapid movement for the neutral axis at sections of yield than does the total strain theory. The 'strain-rate' and 'total-strain' curves of course intersect at the same value of central deflection at which the membrane force curves and/or the yield load curves intersect (i.e. at $\frac{w_o}{d} = 0.45$). The position of the neutral axis at this stress state is in fact very close to that corresponding to the maximum membrane force according to total-strain.

5.2.7 LIMITS OF APPLICATION OF 'TOTAL STRAIN' AND 'STRAIN RATE' IN THE PLASTIC ANALYSIS OF SLAB STRIPS

It has been argued in Chapter 3 that the analysis of cracked sections must be associated with total strain theory if, due to a change of plastic stress state, the neutral axis for strain rate moves

into the 'crack' or 'zone of total tensile strains'; but when the neutral axis (for strain rate) moves into the compressive zone for total strain the strain rate theory must be adopted.

The general analysis and discussion of the previous sections have shown that the initial behaviour of slab strips with physical gaps at the boundaries is that of pure flexure until the bottom surfaces of the slabs, with continuing deflection, come into contact with the surround and compressive membrane action develops. When this happens the neutral axis at all yield sections, being close to the compressed face, starts to move towards the mid-depth of the slab into the zone of total tensile strains. This indicates a stage of increasing membrane force which terminates when the neutral axis is close to the mid-depth of the slab at which stage the membrane force is a maximum.

For a simply-supported rigid-plastic slab strip with a physical gap at an infinitely stiff surround the position of the neutral axis at the central plastic hinge according to strain rate (for this stage of increasing membrane force) is, as shown in Fig. (5.4a), closer to the mid-depth of the slab than that of total strain (see also Fig. 5.2c). When the membrane force becomes a maximum the position of the neutral axis for both theories will be identical (Fig. 5.4b). This indicates that during the stage of increasing membrane force the neutral axis for strain rate moves into the zone of total tensile strains in which case the total strain theory is applicable. When the deflection of the rigid-plastic slab strip exceeds that corresponding to N_{max} the neutral axis for strain rate at the central plastic hinge moves upward into the compressive zone for total strain (N decreasing) and therefore the strain rate theory applies. In this case, the position of the neutral axis for strain rate is higher than that of total strain (Fig. 5.4c). The curves relating the membrane force and the position of the neutral axis with the central deflection are discontinuous in slope at the transition point.

When the elastic shortening of the slab strip and/or the outward movement of the surround is considered the position of the neutral axis at the central plastic hinge according to strain rate, during the stage of increasing membrane force, is lower than that of total strain

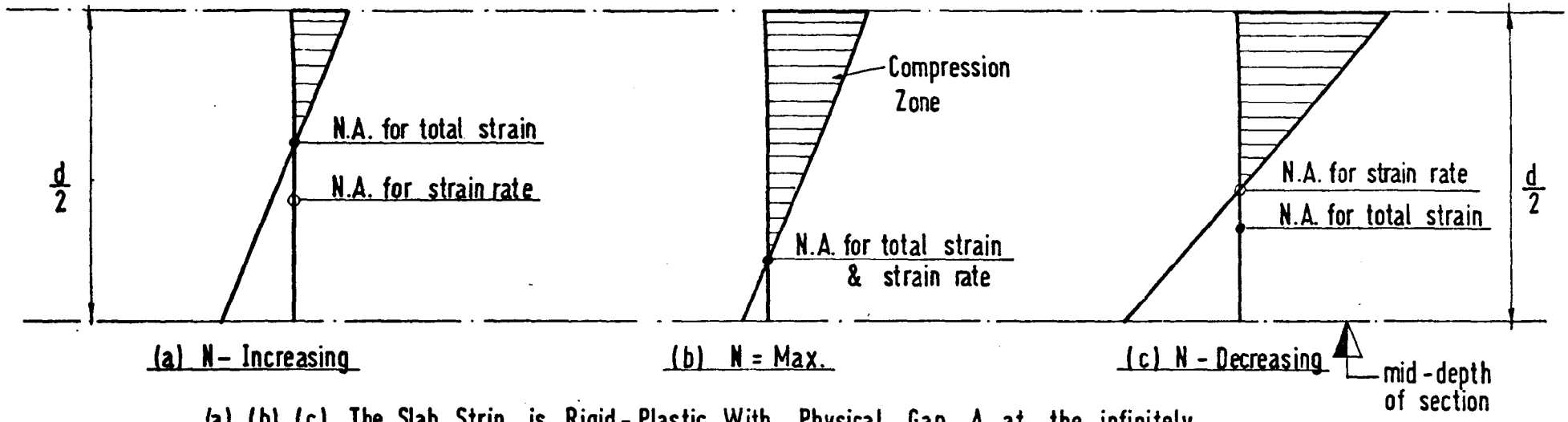

(a), (b), (c). The Slab Strip is Rigid-Plastic With Physical Gap Δ at the infinitely Stiff Boundaries

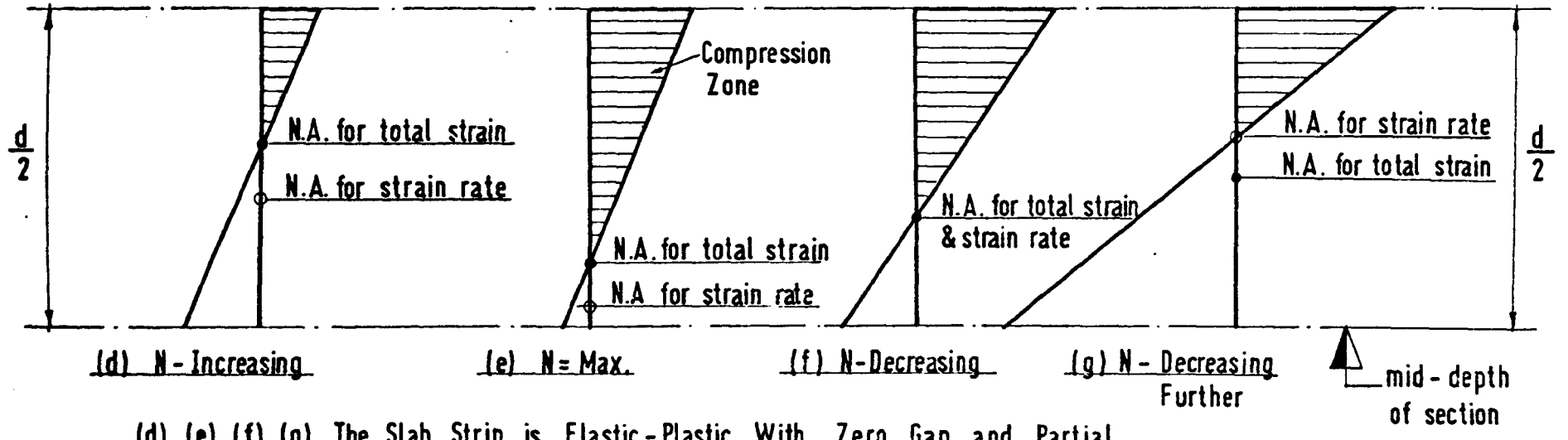

(d), (e), (f), (g), The Slab Strip is Elastic-Plastic With Zero Gap and Partial Lateral Restraints

FIG.(5.4) The Position of the Neutral Axis at the Central Plastic Hinge for Different Stages of Deformation (According to Total Strain and Strain Rate Theories)

(Fig. 5.4d) and will continue to be lower even when the stress state of maximum membrane force is reached (Figs. 5.4e and 5.3c). Similar to the previous case of a rigid-plastic slab strip with physical gaps, the total strain theory is valid for the stage of increasing membrane force since an increment in the membrane force implies a reduction in the depth of the neutral axis. As the membrane force decreases the neutral axis at the central plastic hinge according to both theories moves upward but since the neutral axis for strain rate is still within the crack the strain rate theory cannot be applied. Although the movement of the neutral axis for strain rate is more rapid than that of total strain the total strain theory continues to govern until the state of stress is reached when the position of the neutral axis for both theories coincides (Fig. 5.4f). As N decreases further the neutral axis for strain rate does move into the compressive zone for total strain (Fig. 5.4g) and therefore the strain rate theory becomes applicable. The curves relating the membrane force and the position of the neutral axis with the central deflection are discontinuous in slope at the transition point.

Whatever the type of slab strip, the stage of decreasing membrane force terminates when the membrane force vanishes at large deflection. Strictly, the membrane force vanishes when the bottom surfaces of the slab strip are just in contact with the surround. Unreinforced concrete slab strips will collapse at this stage but for reinforced slab strips the behaviour will be purely flexural and $P = P_y$ up to the fracture of the steel.

The limits of application of total strain and strain rate theories in the plastic analysis of slab strips are summarized in the following table ;

Type of slab strip	Stage of deformation	Theory to be used in analysis
Rigid-plastic with physical gaps at infinitely stiff boundaries, $\bar{S} = \infty$	Increasing N	Total strain
	Decreasing N	Strain rate
Elastic-plastic with partial lateral restraints	Increasing N and early part of decreasing N up to the stress state where N, P and μ are equally predicted by both total strain and strain rate theories	Total strain
	Remainder of decreasing N	Strain rate

5.3 THE PLASTIC BEHAVIOUR OF PARTIALLY RESTRAINED SLAB STRIPS

The analysis and discussion of Section 5.2 has shown that the plastic behaviour of slab strips with physical gaps at the boundaries consists of four successive stages. First, an early stage of pure flexure which is associated with the yield line theory, second, a stage of increasing membrane force where the total strain theory is valid, third, a stage of decreasing membrane force where the strain rate theory is 'mainly' applicable and, fourth, the final stage of pure flexure where the behaviour of the slab strip follows, once again, the yield line theory. These four stages are shown clearly in Fig. (5.5) in connection with the behaviour of the same typical slab strip of Section 5.2.6 with $\Delta/d = 0.02$ and $\bar{S} = 8.65$ ($\lambda = 0.274$).

A detailed study of each stage will now be discussed.

5.3.1 EARLY STAGE OF PURE FLEXURE (YIELD LINE THEORY)

This is the initial stage of deformation which covers values of central deflection between zero (start of collapse) to $(w_o)_i$ given by Eq. (5.2). The slab strip during this stage yields under pure flexure and rotates freely about the point defining the neutral axis position at the central plastic hinge. The yield load in this case is the yield line theory load and the depth of the neutral axis at the central plastic hinge μ_{oC} is according to Eq. (5.1b). In a moment - membrane force diagram this stage is represented by the point $(M = M_o , N = 0)$.

The early stage of pure flexure, however, forms only if a gap exists at the boundaries of the slab.

5.3.2 STAGE OF INCREASING MEMBRANE FORCE (TOTAL STRAIN THEORY)

When the central deflection is $(w_o)_i$ the bottom surfaces of the slab strip are just in contact with the surround. With increasing deflection the value of the compressive membrane force

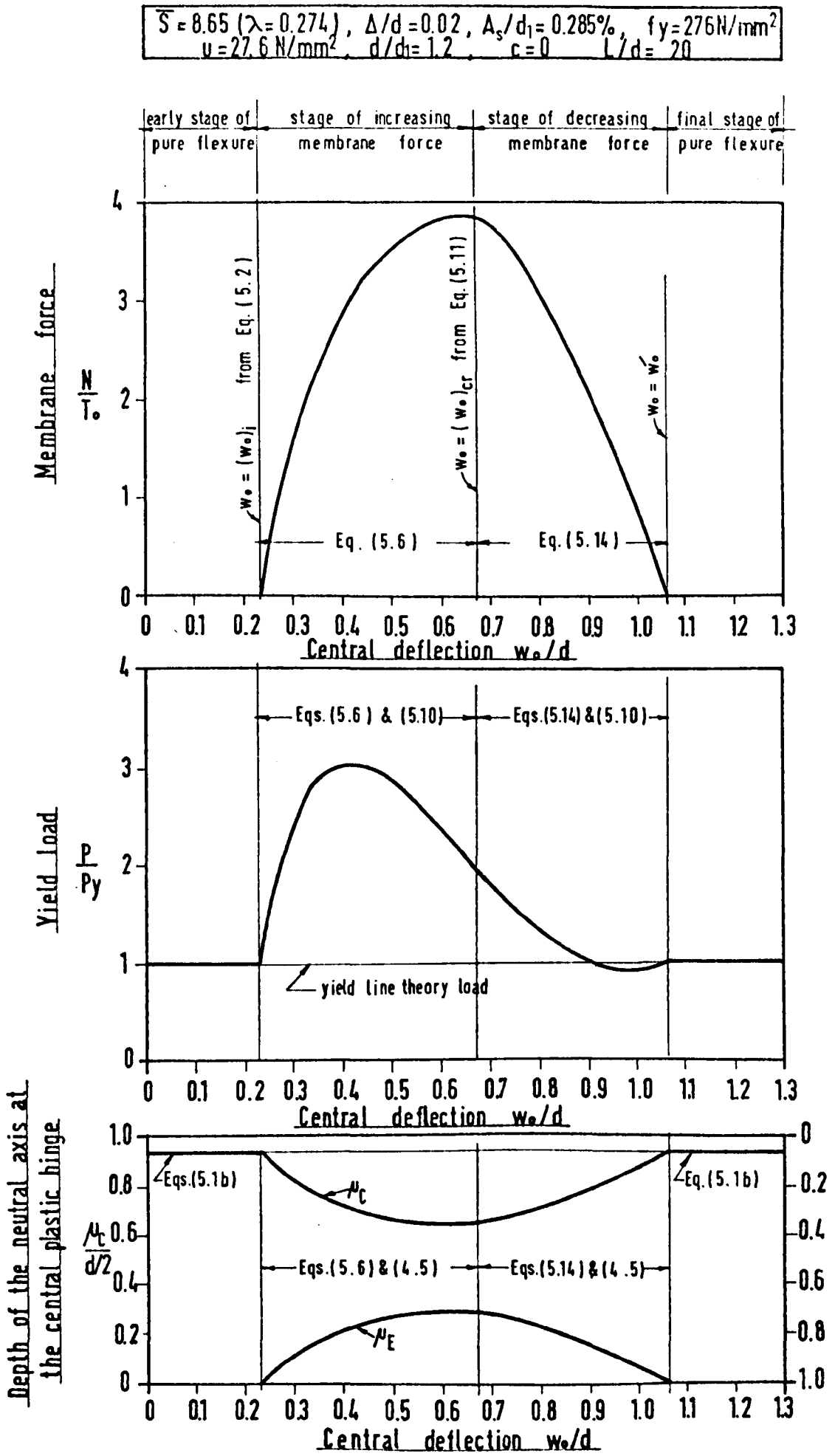

FIG. (5.5) Behaviour of a Non-Rigid Reinforced Concrete Slab Strip With Physical Gap at the Simply Supported ends and Partial Lateral Restraints

increases and the neutral axis, at plastic sections, moves towards the mid-depth of the slab into the zone of total tensile strain. On the yield surface (Fig. 3.2) the point representing the state of stress moves to the left of the diagram. The analysis of the slab during this stage, therefore, requires the use of total strain theory which provides a membrane force - central deflection relationship given by Eq. (5.6). In this equation the maximum membrane force is obtained when the central deflection reaches a 'critical' value $(w_o)_{cr}$ such that ;

$$\left(\frac{w_o}{d}\right)_{cr} = -\frac{1}{\bar{S}}\left(1-\frac{2c}{L}\right) + \sqrt{\frac{\left(1-\frac{2c}{L}\right)}{\left(1+\frac{2c}{L}\right)}\left[\frac{1}{\bar{S}^2}\left(1-\frac{2c}{L}\right)\left(1+\frac{2c}{L}\right) + \frac{2}{\bar{S}}\frac{\left(\frac{\alpha}{\beta}+1\right)}{\left(\frac{\alpha}{\beta}+2\right)} + \frac{\Delta}{d}\cdot\frac{L}{d}\right]} \qquad (5.11)$$

The stage of increasing membrane force covers all values of central deflection between $(w_o)_i$ and $(w_o)_{cr}$. For any deflection w_o within this range, the yield load will be given by Eqs. (5.10) and (5.6) and the neutral axis positions by Eqs. (4.5) and (5.6).

The yield load initially increases with deflection until a maximum value is reached and thereafter falls rapidly. The falling part of the load - deflection curve indicates a state where the equilibrium of the slab is unstable. The maximum yield load occurs at a value of central deflection given by the following equation ;

$$A\left(\frac{w_o}{d}\right)^5 + B\left(\frac{w_o}{d}\right)^4 + C\left(\frac{w_o}{d}\right)^3 + D\left(\frac{w_o}{d}\right)^2 + E\left(\frac{w_o}{d}\right) + F = 0 \qquad (5.12)$$

where

$$A = \frac{3}{4}\left(\frac{\alpha}{\beta}+2\right)^2\left(1+\frac{2c}{L}\right)^2$$

$$B = \frac{11}{4}\frac{1}{\bar{S}}\left(\frac{\alpha}{\beta}+2\right)^2\left(1+\frac{2c}{L}\right)^2\left(1-\frac{2c}{L}\right) - \left(\frac{\alpha}{\beta}+1\right)\left(\frac{\alpha}{\beta}+2\right)\left(1+\frac{2c}{L}\right)$$

$$C = \frac{7}{2}\frac{1}{\bar{S}^2}\left(\frac{\alpha}{\beta}+2\right)^2\left(1+\frac{2c}{L}\right)^2\left(1-\frac{2c}{L}\right)^2 - \frac{4}{\bar{S}}\left(\frac{\alpha}{\beta}+1\right)\left(\frac{\alpha}{\beta}+2\right)\left(1+\frac{2c}{L}\right)\left(1-\frac{2c}{L}\right)$$

$$D = \frac{3}{2}\frac{1}{\bar{S}^3}\left(\frac{\alpha}{\beta}+2\right)^2\left(1+\frac{2c}{L}\right)^2\left(1-\frac{2c}{L}\right)^3 - \frac{6}{\bar{S}^2}\left(\frac{\alpha}{\beta}+1\right)\left(\frac{\alpha}{\beta}+2\right)\left(1+\frac{2c}{L}\right)\left(1-\frac{2c}{L}\right)^2$$

$$E = -\frac{1}{4}\frac{1}{\bar{S}^4}\left(\frac{\alpha}{\beta}+2\right)^2\left(1+\frac{2c}{L}\right)^2\left(1-\frac{2c}{L}\right)^4 - \frac{4}{\bar{S}^3}\left(\frac{\alpha}{\beta}+1\right)\left(\frac{\alpha}{\beta}+2\right)\left(1+\frac{2c}{L}\right)\left(1-\frac{2c}{L}\right)^3$$
$$+\frac{1}{4}\left(\frac{\alpha}{\beta}+2\right)^2\left(1-\frac{2c}{L}\right)^2\left[\frac{1}{\bar{S}^2}\left(1-\frac{2c}{L}\right)\left(1+\frac{2c}{L}\right)+\frac{2}{\bar{S}}\frac{\left(\frac{\alpha}{\beta}+1\right)}{\left(\frac{\alpha}{\beta}+2\right)}+\frac{\Delta}{d}\frac{L}{d}\right]^2$$

$$F = -\frac{1}{4}\frac{1}{\bar{S}^5}\left(\frac{\alpha}{\beta}+2\right)^2\left(1+\frac{2c}{L}\right)^2\left(1-\frac{2c}{L}\right)^5 - \frac{1}{\bar{S}^4}\left(\frac{\alpha}{\beta}+1\right)\left(\frac{\alpha}{\beta}+2\right)\left(1+\frac{2c}{L}\right)\left(1-\frac{2c}{L}\right)^4$$
$$+\frac{1}{4}\frac{1}{\bar{S}}\left(\frac{\alpha}{\beta}+2\right)^2\left(1-\frac{2c}{L}\right)^3\left[\frac{1}{\bar{S}^2}\left(1-\frac{2c}{L}\right)\left(1+\frac{2c}{L}\right)+\frac{2}{\bar{S}}\frac{\left(\frac{\alpha}{\beta}+1\right)}{\left(\frac{\alpha}{\beta}+2\right)}+\frac{\Delta}{d}\frac{L}{d}\right]^2$$

The solution of this equation shows that the central deflection at maximum yield load is significantly less than the corresponding $(w_o)_{cr}$. This is clearly shown in Figs. (5.7) to (5.12). It is therefore of critical importance to note here that the maximum yield load, being attained within this stage of increasing membrane force, is always associated with total strain theory. However, some authors [Morley (10) and Janas (22,26)] incorrectly specify maximum yield loads according to strain rate theory.

5.3.3. STAGE OF DECREASING MEMBRANE FORCE (STRAIN RATE THEORY)

When the central deflection exceeds $(w_o)_{cr}$ the value of the membrane force decreases and, consequently, the neutral axis at the yield sections moves back towards the compressed face of the slab. For the special theoretical case of a rigid-plastic slab strip restrained by an infinitely stiff surround (i.e. $\bar{S} = \infty$) the strain rate theory is then applicable. Where the elastic shortening of the slab strip and/or the outward movement of the surround are considered the total strain theory continues to govern until the state of stress is reached when the values of the membrane force, the yield load and the positions of the neutral axis are equally predicted by both total strain and strain rate theories, and thereafter the strain rate theory becomes applicable.

It has been shown by the example given in Fig. (5.3) that the stress state at which the total strain and strain rate theories become identical corresponds to a central deflection reasonably close to $(w_o)_{cr}$.

The difference in the values of these two deflections reduces as slab strips and surrounds are used with higher stiffnesses and when these stiffnesses become infinite ($\bar{S} = \infty$) the two deflections will be identical. This implies that for the special case $\bar{S} \neq \infty$ the values of the membrane force, the yield load and the positions of the neutral axis, at the critical value of central deflection $(w_o)_{cr}$, are equally predicted by both total strain and strain rate theories. This can be proved mathematically by referring to Eq. (5.11). If $\bar{S}$ in this equation is replaced by infinity, the critical value of central deflection will become

$$\left(\frac{w_o}{d}\right)_{cr} = \sqrt{\frac{(1 - \frac{2c}{L})}{(1 + \frac{2c}{L})} \cdot \frac{\Delta}{d} \cdot \frac{L}{d}}$$

When this value of deflection is introduced into the special case $\bar{S} = \infty$ of Eq. (5.6) of total strain theory the value of the membrane force (maximum) becomes ;

$$\frac{N}{T_o} = \frac{1}{2}\left[\left(\frac{\alpha}{\beta} + 1\right) - \left(\frac{\alpha}{\beta} + 2\right)\sqrt{\left(1 + \frac{2c}{L}\right)\left(1 - \frac{2c}{L}\right) \cdot \frac{\Delta}{d} \cdot \frac{L}{d}}\right]$$

The same result can also be obtained from the special case $\bar{S} = \infty$ of Eq. (5.9) of strain rate theory by substituting the same value of $(w_o)_{cr}$ in that equation. Referring to Eqs. (5.10) and (4.5); the yield load as well as the positions of the neutral axis are given as functions of the membrane force N and, therefore, they will be equally predicted by both theories at $(w_o)_{cr}$.

With respect to the general case of a specified value of $\bar{S}$, the substitution of Eq. (5.11) into Eq. (5.6) furnishes the following value for the maximum membrane force ;

$$\left(\frac{N}{T_o}\right)_{max} = \frac{1}{2}\left(\frac{\alpha}{\beta} + 1\right) - \frac{1}{2}\left(\frac{\alpha}{\beta} + 2\right)\left(1 + \frac{2c}{L}\right)\left[-\frac{1}{\bar{S}}\left(1 - \frac{2c}{L}\right) + \sqrt{\frac{(1 - \frac{2c}{L})}{(1 + \frac{2c}{L})}\left\{\frac{1}{\bar{S}^2}\left(1 - \frac{2c}{L}\right)\left(1 + \frac{2c}{L}\right) + \frac{2}{\bar{S}}\,\frac{(\frac{\alpha}{\beta} + 1)}{(\frac{\alpha}{\beta} + 2)} + \frac{\Delta}{d} \cdot \frac{L}{d}\right\}}\right]$$

In this expression the quantity between the brackets [ ] is indeed

$(w_o/d)_{cr}$ and the value of the maximum membrane force may, therefore, be rewritten as :

$$(\frac{N}{T_o})_{max} = \frac{1}{2}(\frac{\alpha}{\beta} + 1) - \frac{1}{2}(\frac{\alpha}{\beta} + 2)(1 + \frac{2c}{L})(\frac{w_o}{d})_{cr} \qquad (5.13)$$

It has been stated in Chapter 3, Eq. (3.6a), that when a reinforced concrete section is subjected to a bending moment M and a direct compressive force N applied at its mid-depth, the maximum moment will be obtained when $N/T_o = \alpha/(2\beta)$. The form of Eq. (5.13) gives an idea about the location of the point representing the state of stress at the critical deflection $(w_o)_{cr}$ on the yield surface relative to M_{max} . For a known value of $(w_o)_{cr}$ equation (5.13) usually provides a lower value for the maximum membrane force than that specified by Eq. (3.6a) and, accordingly, the point representing the stress state at the critical value of central deflection will be shifted along the yield locus to the right of the peak point representing M_{max} . The shift depends on several parameters, the principal ones being the gap parameter Δ , the stiffness of the slab strip S_b and the stiffness of the surround S_s . However, it is only when the gap Δ is zero and both stiffnesses of the slab strip and the surround are assumed infinite that the critical deflection $(w_o)_{cr}$ becomes zero and, consequently, the point representing the stress state at maximum membrane force lies just to the left of the peak point M_{max} . This special case has already been discussed in detail in Chapter 4. Furthermore, it must be noted that as the deformation of the slab goes through the stage of decreasing membrane force the movement of the stress state point on the yield locus will be in the negative direction of N .

It is worth emphasizing here that when the point representing the state of stress is located on the yield locus to the right of the peak point M_{max} , the position of the neutral axis at the yield section* at this particular stress state will be above the mid-depth of the slab (see Fig. 3.2). Therefore, for the slab strip AB of Fig. (5.1), having established that for almost any value of deflection the point representing the stress state lies on the yield locus to the

---

* The yield section considered in this discussion is the central plastic hinge.

right of the peak point M_{max} ; it is correct to state that the neutral axis at the plastic hinges, throughout the whole deformation process of the slab, will never reach the mid-depth of the slab. Strictly, when the stiffnesses of both the slab strip and the surround are low and the gap at the boundaries of the slab is wide the movement of the neutral axis towards the mid-depth of the slab at sections of yield, with continuing deflection, will be small [the closest position to the mid-depth of the slab the neutral axis reaches at sections of yield being at $(w_o)_{cr}$].

It has been stated earlier and shown by the example given in Fig. (5.3) that the difference between the value of the central deflection corresponding to the state of stress where both of the total strain and strain rate theories are equally valid and $(w_o)_{cr}$ is small. It has also been shown that the membrane forces corresponding to these two deflections are apparently close (a discrepancy of just over 1% in the example given by Fig. (5.3) in which the value 8.65 used for $\bar{S}$ is considered to be very small). Therefore, if a slight approximation in analysis is made here by applying the strain rate theory through the whole stage of decreasing membrane force, it will neither affect the value of the maximum membrane force nor the value of the peak load but the shape of the curves representing the relationships with the central deflection of the membrane force and the depth of the neutral axis at sections of yield will be slightly affected (compare the dotted line —·—·— with the solid line ——— in the stage of decreasing membrane force of Fig. (5.3); also notice that the effect on the yield load - central deflection curve is negligible). This approximation, therefore, simplifies the analysis but ensures that the predicted behaviour of the slab strip does not depart too far from the exact behaviour.

According to the preceding discussion, if Eq. (5.13) is equated to Eq. (5.8) the value of the integration constant F in this case will be ;

$$F = -\frac{1}{2\bar{S}}\left(\frac{\alpha}{\beta}+2\right)\left(1+\frac{2c}{L}\right)\left(1-\frac{2c}{L}\right) e^{\frac{\bar{S}}{\left(1-\frac{2c}{L}\right)}\cdot\left(\frac{w_o}{d}\right)_{cr}}$$

and when this value is introduced into Eq. (5.8) the relationship of

the membrane force with the central deflection for this stage becomes

$$\frac{N}{T_o} = \frac{1}{2}\left[\left(\frac{\alpha}{\beta}+1\right)-\left(\frac{\alpha}{\beta}+2\right)\left(1+\frac{2c}{L}\right)\left(\frac{w_o}{d}\right)+\frac{1}{\bar{S}}\left(\frac{\alpha}{\beta}+2\right)\left(1+\frac{2c}{L}\right)\left(1-\frac{2c}{L}\right)\left\{1-e^{-\frac{\bar{S}}{\left(1-\frac{2c}{L}\right)}\left[\left(\frac{w_o}{d}\right)-\left(\frac{w_o}{d}\right)_{cr}\right]}\right\}\right] \qquad (5.14)$$

Equation (5.14) is valid for values of central deflection greater than $(w_o)_{cr}$ and expresses a falling membrane force - central deflection curve. The combination of this equation with Eqs. (5.10) and (4.5) defines, respectively, the relationships of the yield load and the position of the neutral axis at the yield sections with the central deflection.

The stage of decreasing membrane force terminates when the membrane force vanishes at large deflection. Let the value of this deflection be denoted by w_o'. Systematically, w_o' would be obtained by equating Eq. (5.14) to zero and solving the resulting equation. Unfortunately, the form of Eq.(5.14) makes an exact explicit solution for w_o' impossible, but a numerical solution can be obtained. A computer programme was written which gave for each incremental value of central deflection beyond $(w_o)_{cr}$ the value of the membrane force according to Eq. (5.14). The value of the central deflection which changed the value of the membrane force from positive to negative was thus considered as w_o'.

5.3.4 FINAL STAGE OF PURE FLEXURE (YIELD LINE THEORY)

When the central deflection is w_o' the bottom edges of the slab ends are just in contact with the surround. The value of the membrane force at this stage is zero, the yield load is the yield line theory load and the depth of the neutral axis at the central plastic hinge is as defined by Eq. (5.1b).

When the deflection increases, the two portions of the slab strip move inwards away from the surrounding body while rotating

about the point representing the position of the neutral axis at the central plastic hinge. This expresses yielding of the slab strip according to pure flexure and the yield line theory is applicable. The load-deflection relationship of this stage, therefore, shows a horizontal line $P = P_y$ until the limit is reached when the reinforcement starts to fracture leading to collapse.

On a moment - membrane force diagram, the final stage of pure flexure is defined by the point $(M = M_o\ ,\ N = 0)$.

5.4 SUMMARY OF ANALYSIS

The equations for determining the values of the membrane force, the yield load and the neutral axis depth at the cracked and end sections at any value of deflection for partially-restrained simply-supported reinforced concrete slab strips with physical gaps Δ at the boundaries are summarized as follows :

i. For $0 \leq \frac{w_o}{d} \leq \frac{1}{(1 + \frac{2c}{L})} \left[\frac{(\frac{\alpha}{\beta} + 1)}{(\frac{\alpha}{\beta} + 2)} - \sqrt{\frac{(\frac{\alpha}{\beta} + 1)^2}{(\frac{\alpha}{\beta} + 2)^2} - \frac{\Delta}{d}\frac{L}{d}(1 - \frac{2c}{L})(1 + \frac{2c}{L})}\right]$

$$\frac{N}{T_o} = 0 \qquad (5.15a)$$

$$\frac{P}{P_y} = 1 \qquad (5.15b)$$

$$\frac{\mu_C}{\frac{d}{2}} = \frac{\frac{\alpha}{\beta}}{(\frac{\alpha}{\beta} + 2)} \qquad (5.15c)$$

$$\frac{\mu_E}{\frac{d}{2}} \geq 1 \qquad (5.15d)$$

ii. For $\frac{1}{(1+\frac{2c}{L})}\left[\frac{(\frac{\alpha}{\beta}+1)}{(\frac{\alpha}{\beta}+2)} - \sqrt{\frac{(\frac{\alpha}{\beta}+1)^2}{(\frac{\alpha}{\beta}+2)^2} - \frac{\Delta}{d}\frac{L}{d}(1-\frac{2c}{L})(1+\frac{2c}{L})}\right] \leq \frac{w_o}{d} \leq$

$$- \frac{1}{\bar{S}}(1-\frac{2c}{L}) + \sqrt{\frac{(1-\frac{2c}{L})}{(1+\frac{2c}{L})}\left\{\frac{1}{\bar{S}^2}(1-\frac{2c}{L})(1+\frac{2c}{L}) + \frac{2}{\bar{S}}\frac{(\frac{\alpha}{\beta}+1)}{(\frac{\alpha}{\beta}+2)} + \frac{\Delta}{d}\frac{L}{d}\right\}}$$

$$\frac{N}{T_o} = \frac{\frac{1}{2}\left[(\frac{\alpha}{\beta}+1) - \frac{1}{2}(\frac{\alpha}{\beta}+2)(1+\frac{2c}{L})\frac{w_o}{d} - \frac{1}{2}(\frac{\alpha}{\beta}+2)(1-\frac{2c}{L})\frac{\frac{\Delta}{d}\frac{L}{d}}{\frac{w_o}{d}}\right]}{\left[1 + \frac{(1-\frac{2c}{L})}{\bar{S}\frac{w_o}{d}}\right]} \qquad (5.15e)$$

$$\frac{P}{P_y} = 1 + 2\beta\left[(\frac{\alpha}{\beta}+1) - (\frac{\alpha}{\beta}+2)(1+\frac{2c}{L})\frac{w_o}{d}\right](\frac{N}{T_o}) - 2(\frac{N}{T_o})^2 \qquad (5.15f)^*$$

$$\frac{\mu_C}{\frac{d}{2}} = 1 - \frac{2}{(\frac{\alpha}{\beta}+2)}(1+\frac{N}{T_o}) \qquad (5.15g)^*$$

$$\frac{\mu_E}{\frac{d}{2}} = 1 - \frac{2}{(\frac{\alpha}{\beta}+2)}(\frac{N}{T_o}) \qquad (5.15h)^*$$

iii. For $-\frac{1}{\bar{S}}(1-\frac{2c}{L}) + \sqrt{\frac{(1-\frac{2c}{L})}{(1+\frac{2c}{L})}\left\{\frac{1}{\bar{S}^2}(1-\frac{2c}{L})(1+\frac{2c}{L}) + \frac{2}{\bar{S}}\frac{(\frac{\alpha}{\beta}+1)}{(\frac{\alpha}{\beta}+2)} + \frac{\Delta}{d}\frac{L}{d}\right\}} \leq \frac{w_o}{d} \leq \frac{w_o'}{d}$ **

$$\frac{N}{T_o} = \frac{1}{2}\left[(\frac{\alpha}{\beta}+1) - (\frac{\alpha}{\beta}+2)(1+\frac{2c}{L})\frac{w_o}{d} + \frac{1}{\bar{S}}(\frac{\alpha}{\beta}+2)(1+\frac{2c}{L})(1-\frac{2c}{L})\cdot\right.$$

$$\left.\left\{1 - e^{-\frac{\bar{S}}{(1-\frac{2c}{L})}\left[(\frac{w_o}{d}) - (\frac{w_o}{d})_{cr}\right]}\right\}\right] \qquad (5.15i)$$

---

* The dimensionless value of the membrane force N/T_o in Equations (5.15f, g and h) is given by Eq. (5.15e).

** w_o' is the value of the central deflection when the membrane force decreases to zero and can be obtained by equating Eq. (5.15i) to zero.

where

$$\left(\frac{w_o}{d}\right)_{cr} = -\frac{1}{\bar{S}}\left(1 - \frac{2c}{L}\right) + \sqrt{\frac{\left(1 - \frac{2c}{L}\right)}{\left(1 + \frac{2c}{L}\right)}\left\{\frac{1}{\bar{S}^2}\left(1 - \frac{2c}{L}\right)\left(1 + \frac{2c}{L}\right) + \frac{2}{\bar{S}}\frac{\left(\frac{\alpha}{\beta} + 1\right)}{\left(\frac{\alpha}{\beta} + 2\right)} + \frac{\Delta}{d}\frac{L}{d}\right\}}$$

$$\frac{P}{P_y} = 1 + 2\beta\left[\left(\frac{\alpha}{\beta} + 1\right) - \left(\frac{\alpha}{\beta} + 2\right)\left(1 - \frac{2c}{L}\right)\frac{w_o}{d}\right]\left(\frac{N}{T_o}\right) - 2\beta\left(\frac{N}{T_o}\right)^2 \qquad (5.15j)\ \dagger$$

$$\frac{\mu_C}{\frac{d}{2}} = 1 - \frac{2}{\left(\frac{\alpha}{\beta} + 2\right)}\left(1 + \frac{N}{T_o}\right) \qquad (5.15k)\ \dagger$$

$$\frac{\mu_E}{\frac{d}{2}} = 1 - \frac{2}{\left(\frac{\alpha}{\beta} + 2\right)}\left(\frac{N}{T_o}\right) \qquad (5.15l)\ \dagger$$

iv. For $\frac{w_o}{d} \geq \left(\frac{w_o}{d}\right)'$

$$\frac{N}{T_o} = 0 \qquad (5.15m)$$

$$\frac{P}{P_y} = 1 \qquad (5.15n)$$

$$\frac{\mu_C}{\frac{d}{2}} = \frac{\frac{\alpha}{\beta}}{\left(\frac{\alpha}{\beta} + 2\right)} \qquad (5.15o)$$

$$\frac{\mu_E}{\frac{d}{2}} \geq 1 \qquad (5.15p)$$

Equations (5.15) may be compared with the theoretical solutions obtained by Roberts (24) and Janas (26) on similar slab strips. The analysis presented by the former was based on total strain theory. Simply supported reinforced concrete slab strips with physical gaps at the supports and partial lateral restraints were considered under uniformly distributed load. The dimensionless values of the membrane

---

† The dimensionless value of the membrane force N/T_o in equations (5.15j, k and l) is given by Eq. (5.15i)

force N/T_o and the yield load P/P_y obtained (Eqs. 2.37 and 2.39) are identical to those of Eqs. (5.15e and f) for the case $c = 0$ (the value of the mechanism parameter c in slab strips with uniformly distributed load is zero). This indicates that the type of loading does not affect the dimensionless values of the membrane force and the yield load if the mechanism of collapse is unchanged. The similarity between Roberts' solution and Eq. (5.20) holds for the stage of increasing membrane force only, i.e. for values of central deflection falling within the range given by step ii where the total strain theory is valid, but as the value of the central deflection is outside this range Roberts' solution starts to predict higher membrane forces and lower yield loads than those specified by Eqs. (5.15i and j). The early and final stages of pure flexure (steps i and iv) were not considered by Roberts at all. Although Roberts presented his solution considering a physical gap at the supports of the slab strip, he made no attempt to study, theoretically or experimentally, the crucial effect of this parameter on the plastic behaviour of the slab.

In contrast to Roberts' analysis, Janas presented his solution for the problem of elastic fully restrained clamped slab strip based on strain rate theory. The slab strip was assumed to be subjected to a concentrated load at mid-span ($c = 0$) and to be reinforced in the bottom face only at middle sections and in the top face only at supports. The dimensionless values of the membrane force and the yield load obtained (Eqs. 2.40 and 2.42) are, for the stage of increasing membrane force, higher than the corresponding ones given by Eqs. (5.15e and f) in which case their maxima are higher but for the stage of decreasing membrane force they are of a similar order (Eqs. 5.15i and j). Janas's purely strain rate approach, however, gives erroneous results, especially when slab strips are analysed with physical gaps existing at their boundaries the discrepancies in the maximum values of the yield load and the membrane force become large, as has been shown in the example of Fig. (5.2).

5.5 THE SPECIAL CASE OF PARTIALLY RESTRAINED UNREINFORCED CONCRETE SLAB STRIPS

The summary of analysis presented in the previous section

will now be modified to account for the behaviour of unreinforced concrete slab strips. The values of the membrane force and the yield load will be presented in dimensional form (for a unit width of slab) since T_o and P_y are zero in this case.

Ignoring the tensile strength of concrete, a simply supported unreinforced concrete slab strip with physical gaps at the supports and partial lateral restraints, theoretically, collapses at zero yield load until the gap at the slab supports is closed. The zero collapse state defines the stage of pure flexure for the unreinforced slab strips. With further increments in deflection, compressive membrane action develops which enables the slab to carry some load. The development of membrane action is represented by two successive stages. These are the stage of increasing membrane force within which the maximum yield load is achieved and the stage of decreasing membrane force which terminates when the yield load becomes zero. The behaviour of these slabs, therefore, includes steps i, ii and iii of the summary of analysis given in the previous section.

The values of the membrane force and the yield load for any central deflection of these partially restrained plain concrete slab strips are obtained by multiplying both sides of Eqs. (5.15a, e and i) by T_o (i.e. $A_s f_y$) and Eqs. (5.15b, f and j) by P_y [i.e. $\frac{2}{a} A_s f_y \left(1 - \frac{k_2}{k_1 k_3} \cdot \frac{A_s}{d_1} \frac{f_y}{u}\right)$] and then equating A_s in all the resulting equations to zero. By noting also that the values of the dimensionless notations α and β for plain concrete sections are respectively $\frac{d}{2d_1}$ and zero the behaviour of partially restrained unreinforced concrete slab strips (of unit width) with any physical gap Δ at the simply supported ends can be expressed as follows :

i. For $0 \leqq \frac{w_o}{d} \leqq \frac{1}{(1 + \frac{2c}{L})} \left[1 - \sqrt{1 - \frac{\Delta}{d} \frac{L}{d} (1 - \frac{2c}{L})(1 + \frac{2c}{L})}\right]$

$$N = 0 \tag{5.16a}$$

$$P = 0 \tag{5.16b}$$

$$\mu_C = \frac{d}{2} \tag{5.16c}$$

$$\mu_E \geqq \frac{d}{2} \tag{5.16d}$$

ii. For $\frac{1}{(1+\frac{2c}{L})}\left[1-\sqrt{1-\frac{\Delta}{d}\frac{L}{d}(1-\frac{2c}{L})(1+\frac{2c}{L})}\right] \leqq \frac{w_o}{d} \leqq$

$$-\frac{1}{\bar{S}}(1-\frac{2c}{L})+\sqrt{\frac{(1-\frac{2c}{L})}{(1+\frac{2c}{L})}\left\{\frac{1}{\bar{S}^2}(1-\frac{2c}{L})(1+\frac{2c}{L})+\frac{2}{\bar{S}}+\frac{\Delta}{d}\frac{L}{d}\right\}}$$

$$N=\frac{1}{4}\frac{k_1k_3}{k_2}\,ud\,\frac{\left[1-\frac{1}{2}(1+\frac{2c}{L})\frac{w_o}{d}-\frac{1}{2}(1-\frac{2c}{L})\frac{\frac{\Delta}{d}\frac{L}{d}}{\frac{w_o}{d}}\right]}{\left[1+\frac{(1-\frac{2c}{L})}{\bar{S}\,\frac{w_o}{d}}\right]} \qquad (5.16e)$$

$$P=\frac{2d}{a}\left[1-(1+\frac{2c}{L})\frac{w_o}{d}\right]N-4\frac{k_2}{k_1k_3}\frac{N^2}{ua} \qquad (5.16f)\ *$$

$$\mu_C=\mu_E=(1-4\frac{k_2}{k_1k_3}\frac{N}{ud})\frac{d}{2} \qquad (5.16g)\ *$$

iii. For $\frac{w_o}{d} \geqq -\frac{1}{\bar{S}}(1-\frac{2c}{L})+\sqrt{\frac{(1-\frac{2c}{L})}{(1+\frac{2c}{L})}\left\{\frac{1}{\bar{S}^2}(1-\frac{2c}{L})(1+\frac{2c}{L})+\frac{2}{\bar{S}}+\frac{\Delta}{d}\frac{L}{d}\right\}}$

$$N=\frac{1}{4}\frac{k_1k_3}{k_2}\,u\,d\left[1-(1+\frac{2c}{L})\frac{w_o}{d}+\frac{1}{\bar{S}}(1+\frac{2c}{L})(1-\frac{2c}{L})\left\{1-e^{-\frac{\bar{S}}{(1-\frac{2c}{L})}\left[(\frac{w_o}{d})-(\frac{w_o}{d})_{cr}\right]}\right\}\right] \qquad (5.16h)$$

where $(\frac{w_o}{d})_{cr}=-\frac{1}{\bar{S}}(1-\frac{2c}{L})+\sqrt{\frac{(1-\frac{2c}{L})}{(1+\frac{2c}{L})}\left\{\frac{1}{\bar{S}^2}(1-\frac{2c}{L})(1+\frac{2c}{L})+\frac{2}{\bar{S}}+\frac{\Delta}{d}\frac{L}{d}\right\}}$

$$P=\frac{2d}{a}\left[1-(1+\frac{2c}{L})\frac{w_o}{d}\right]N-4\frac{k_2}{k_1k_3}\frac{N^2}{ua} \qquad (5.16i)\ **$$

$$\mu_C=\mu_E=(1-4\frac{k_2}{k_1k_3}\frac{N}{ud})\frac{d}{2} \qquad (5.16j)\ **$$

---

* The value of the membrane force N in Eqs. (5.16f and g) is given by Eq. (5.16e).

** The value of the membrane force N in Eqs. (5.16i and j) is given by Eq. (5.16h).

Equations (5.16) are plotted in Fig. (5.6) for the case of a simply supported unreinforced concrete slab strip (of unit width) with the following properties :

$$\bar{S} = 8.65\ (\lambda = 0.274)\ ; \quad \Delta = 0\ ; \quad u = 27.6\ N/mm^2\ (4000\ lbf/in^2)\ ;$$

$$c = 0\ ; \quad d/L = 1/20\ ; \quad a/L = 0.4$$

From figure (5.6), it can be seen that the behaviour of the plain concrete slab includes the two stages of increasing and decreasing membrane force only since $\Delta = 0$. The value of the maximum membrane force, occurring at $\frac{w_o}{d} = 0.32$, is 5.5d N/mm (780d lbf/in) and the maximum yield load, obtained at $\frac{w_o}{d} = 0.14$, is 0.65d N/mm (100 d lbf/in). It is of interest to compare this value of maximum yield load with that obtained by the yield line theory for a reinforced slab strip. If a percentage of reinforcement as high as 1% is considered in this comparison then the yield line theory will predict an ultimate load P_y of 0.402 d N/mm (58.3 d lbf/in), only 60% of the mentioned maximum yield load of the partially restrained plain concrete slab strip.

Another point of interest in Fig. (5.6) concerns the behaviour of the slab strip at large deflections. The figure shows that the yield load becomes zero at $\frac{w_o}{d} = 0.77$. Therefore if the deformation of the slab was to be continued, the applied load would need to be negative (upward) for all values of central deflection ranging between 0.77d and 1.02 d (where the membrane force would become zero) but obviously such a deformation state cannot be encountered in practice.

5.6 STUDY OF THE EFFECT OF NEW AND IMPORTANT PARAMETERS

The plastic behaviour of partially restrained simply supported reinforced concrete slab strips depends, as demonstrated by Eqs. (5.15), on five variables. These are, namely, the properties of the slab at the central hinge represented by the notations α and β , the stiffness factor $\bar{S}$, the gap parameter Δ/d , the span-depth ratio L/d and the mechanism parameter c/L . The stiffness factor $\bar{S}$ is the compound effect of the elastic stiffness of the slab S_b and the elastic stiffness of the surrounds S_s . For a specified slab strip

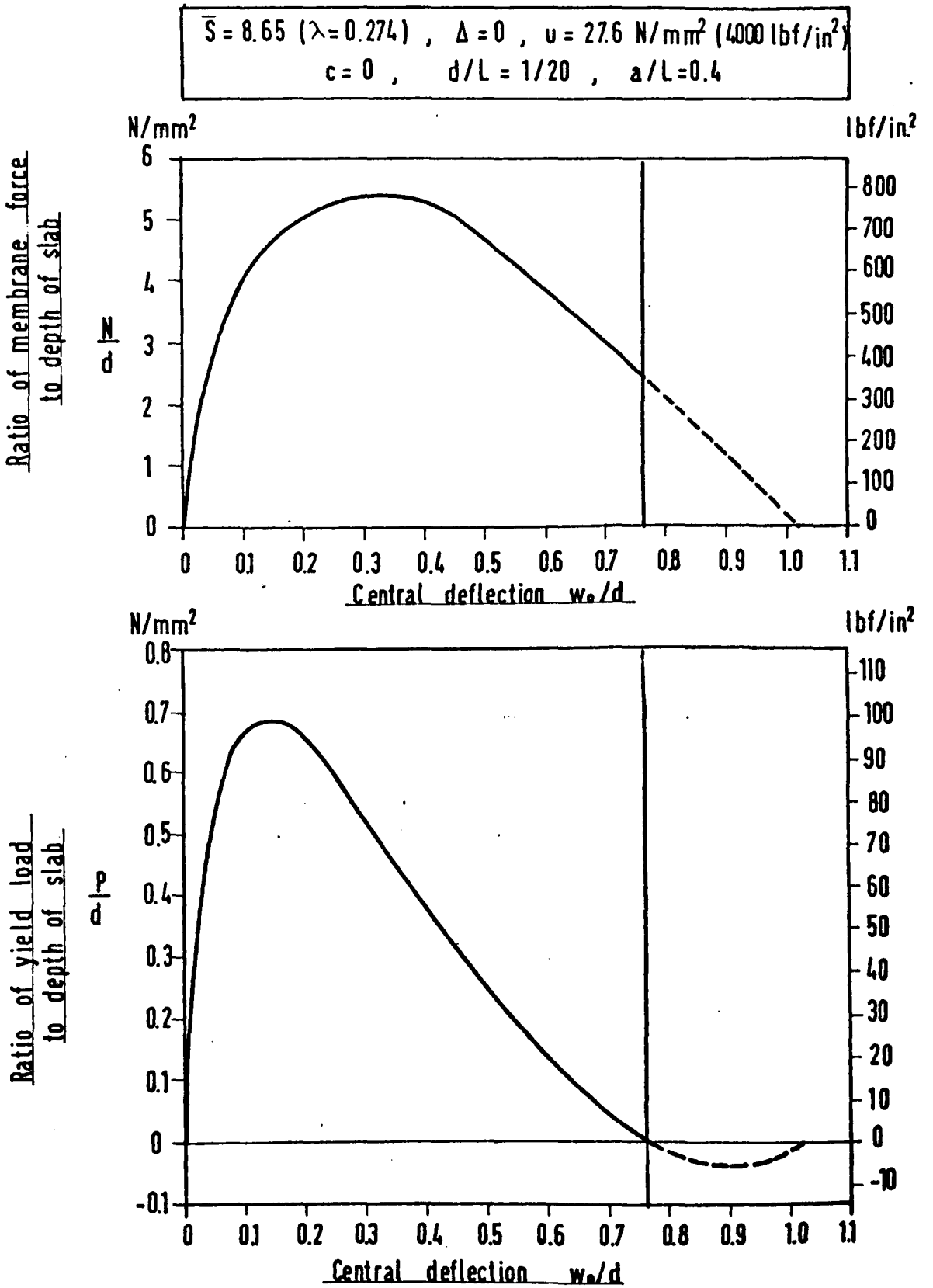

FIG.(5.6) Behaviour of a Non-Rigid Plain Concrete Slab Strip with Simple Supports and Partial Lateral Restraints

the elastic stiffness of the slab S_b, as given by Eq. (5.3), is a fixed quantity whereas the elastic stiffness of the surrounds S_s can vary from zero (the case of no restraint) to infinity (the case of rigid surrounds). Therefore, the effect of the stiffness factor $\bar{S}$ will be more usefully studied in terms of the degree of the stiffness of the surround λ. Also noting that the dimensionless parameters α and β, as given by Eq.(3.5), are functions of the amount of reinforcement A_s/d_1, the cube strength of the concrete u, the yield stress of the reinforcement f_y, the ratio of the depth of the slab to the effective depth d/d_1, and the concrete stress block parameters k_1k_3 and k_2.

The effect of some of these parameters have already been outlined in Chapter 4 in connection with the behaviour of fully-restrained rigid-plastic slab strips. In this section the effect of the same parameters as well as the effect of some new and important parameters will be studied regarding the behaviour of partially restrained non-rigid simply supported reinforced concrete slab strips.

To enable a close study of the effect of each parameter to be made, the same typical slab strip described in Section 5.2.5 and Fig. (5.3) is considered. The study of the effect of each parameter is made possible by keeping the rest of the parameters constant.

5.6.1 GAP PARAMETER Δ/d

Fig. (5.7) shows the relationships of the membrane force and the yield load with the central deflection for different values of Δ/d ranging from 0 to 15/300.

It can be seen from this figure that the membrane action in a slab with wider physical gaps at the boundaries starts at a later stage of deformation. The relationships of the membrane force and the yield load with the central deflection are greatly influenced by the gap parameter Δ/d. At any value of central deflection within the two stages of membrane action, the values of the membrane force and the yield load are smaller for higher values of Δ/d. If the width of the gap at the slab supports is larger than 15/300 of the slab depth, the behaviour of the slab will be purely flexural and $P = P_y$. For the case of a slab strip with zero gap at the slab

$\bar{S}$ = 8.65 (λ = 0.274), A_s/d_1 = 0.285%, f_y = 276 N/mm^2
u = 27.6 N/mm^2, d/d_1 = 1.2, c = 0, L/d = 20

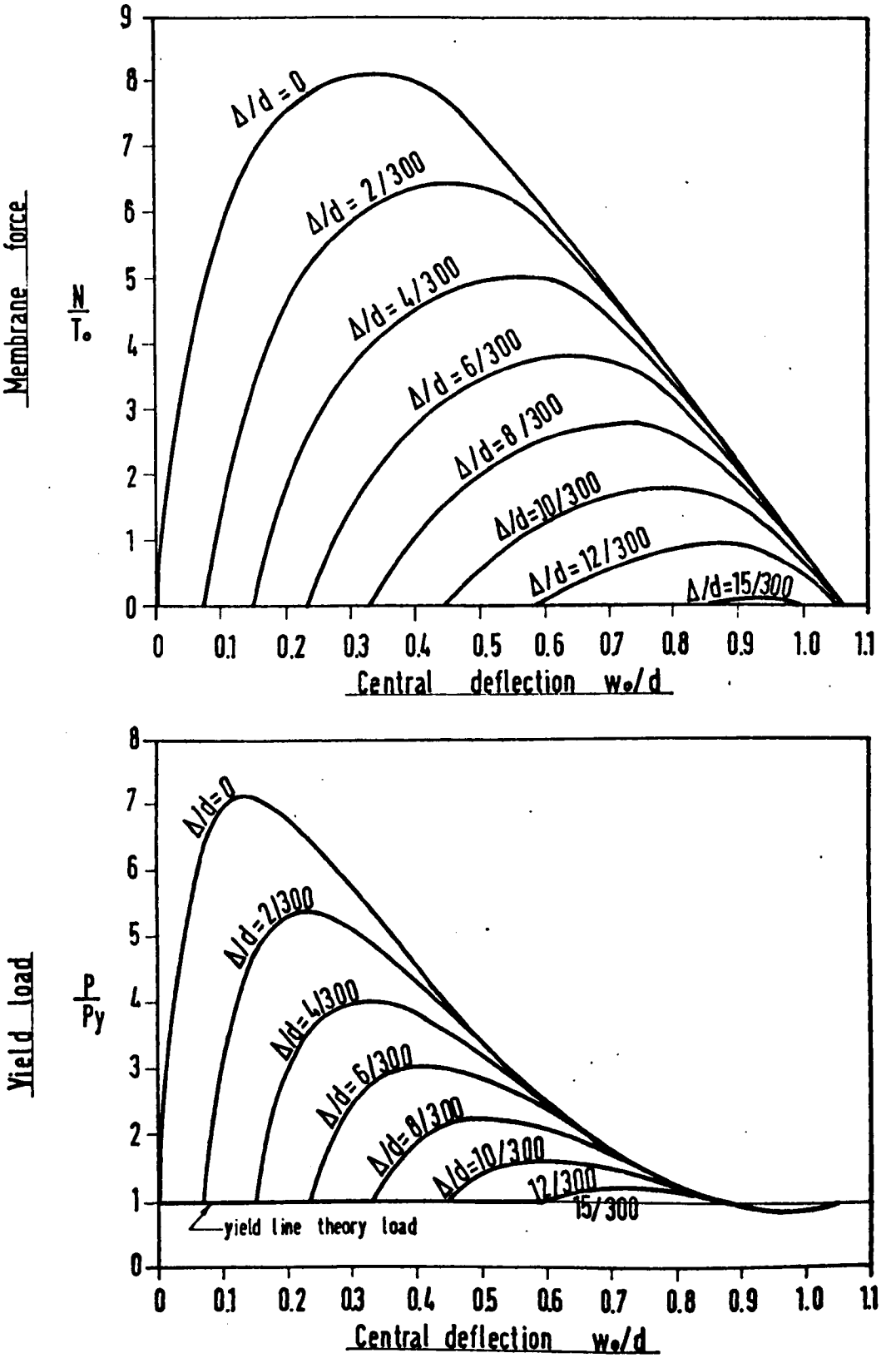

FIG. (5.7) Effect of the Gap Parameter Δ/d on the Behaviour of a Non-Rigid Reinforced Concrete Slab Strip With Simple Supports and Partial Lateral Restraints

boundaries the maximum value of the membrane force is 8.1 T_o and that of the yield load is 7.1 P_y . The state of stress at which the membrane force vanishes (i.e. the start of the final stage of pure flexure) is, however, very slightly influenced by the Δ/d parameter.

5.6.2 DEGREE OF THE STIFFNESS OF THE SURROUND λ

Fig. (5.8) demonstrates the effect of the degree of the stiffness of the surround λ on the general plastic behaviour of the slab strip under study. Values of λ ranging between 0 (the case of a slab with no lateral restraint) and 1.0 (the case of a rigidly restrained slab) are used to illustrate the behaviour.

Due to the absence of a gap in this example, all the curves representing the relationship between the membrane force and the central deflection show that the membrane force starts to increase from a zero value once the slab deflects until it becomes a maximum and thereafter decreases rapidly. The membrane force rises more steeply to a higher value in slabs restrained by stiffer surrounds. The deflection range of the membrane action is, however, greater with low stiffness surrounds and the value of the central deflection corresponding to the maximum membrane force increases as the stiffness decreases.

The relationship between the yield load and the central deflection is also greatly influenced by the degree of stiffness of the surround λ . For any value of central deflection the yield load is larger in slabs with higher λ . At large values of central deflection the yield load falls below the yield line theory load, but this is more pronounced in slabs with less stiff surrounds. The value of the maximum yield load is higher in slabs restrained by stiffer surrounds and is attained at smaller values of central deflection.

When $\lambda = 1.0$ the value of the maximum membrane force is 10.2 T_o and that of the yield load is 8.9 P_y and when $\lambda = 0$ no compressive membrane action occurs.

5.6.3 AMOUNT OF REINFORCEMENT A_s/d_1

The effect of this parameter is shown in Fig. (5.9). Values

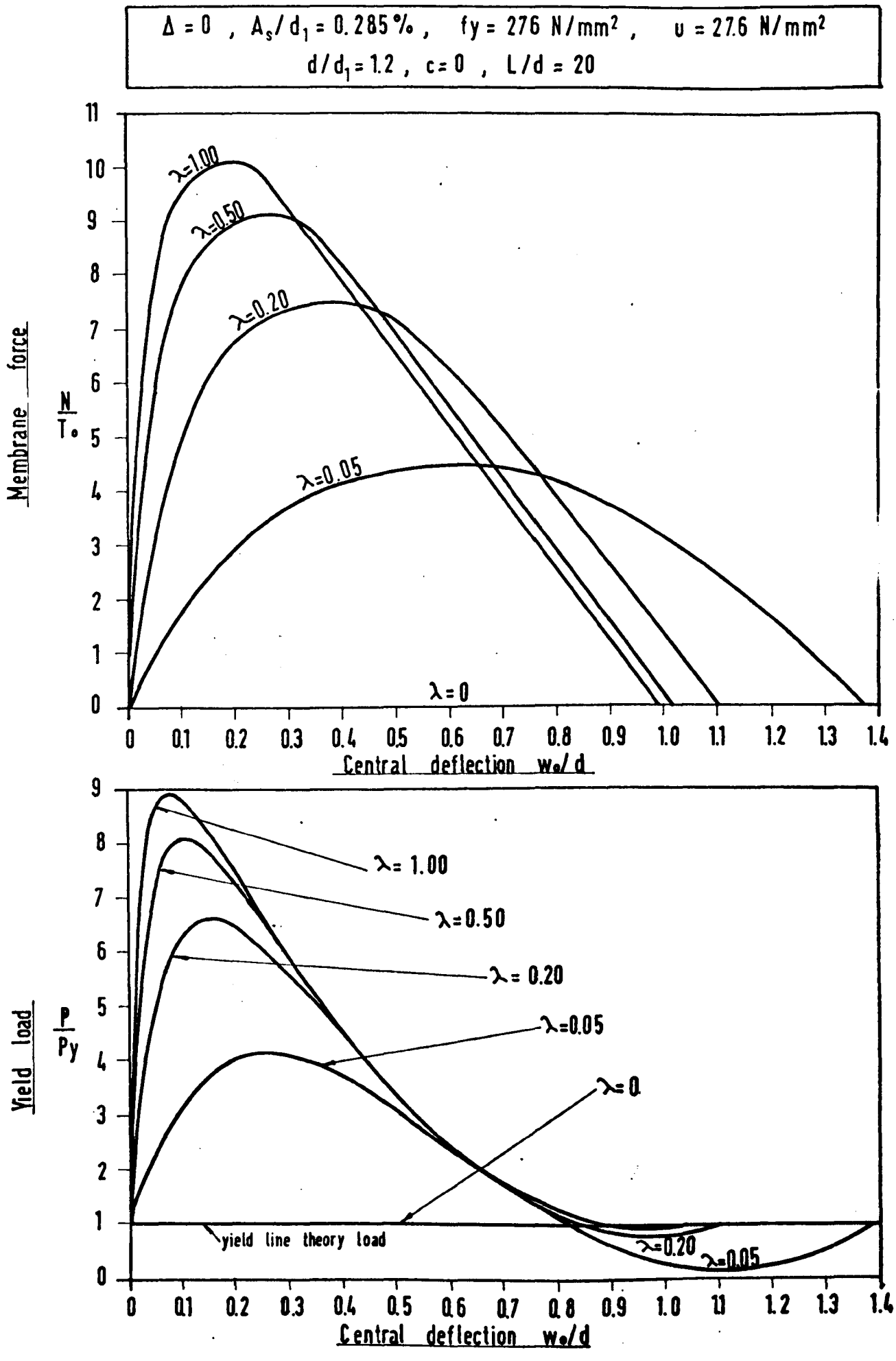

FIG.(5.8) Effect of the Degree of the Stiffness of the Surround λ on the Behaviour of a Non-Rigid Reinforced Concrete Slab Strip With Simple Supports and Partial Lateral Restraints

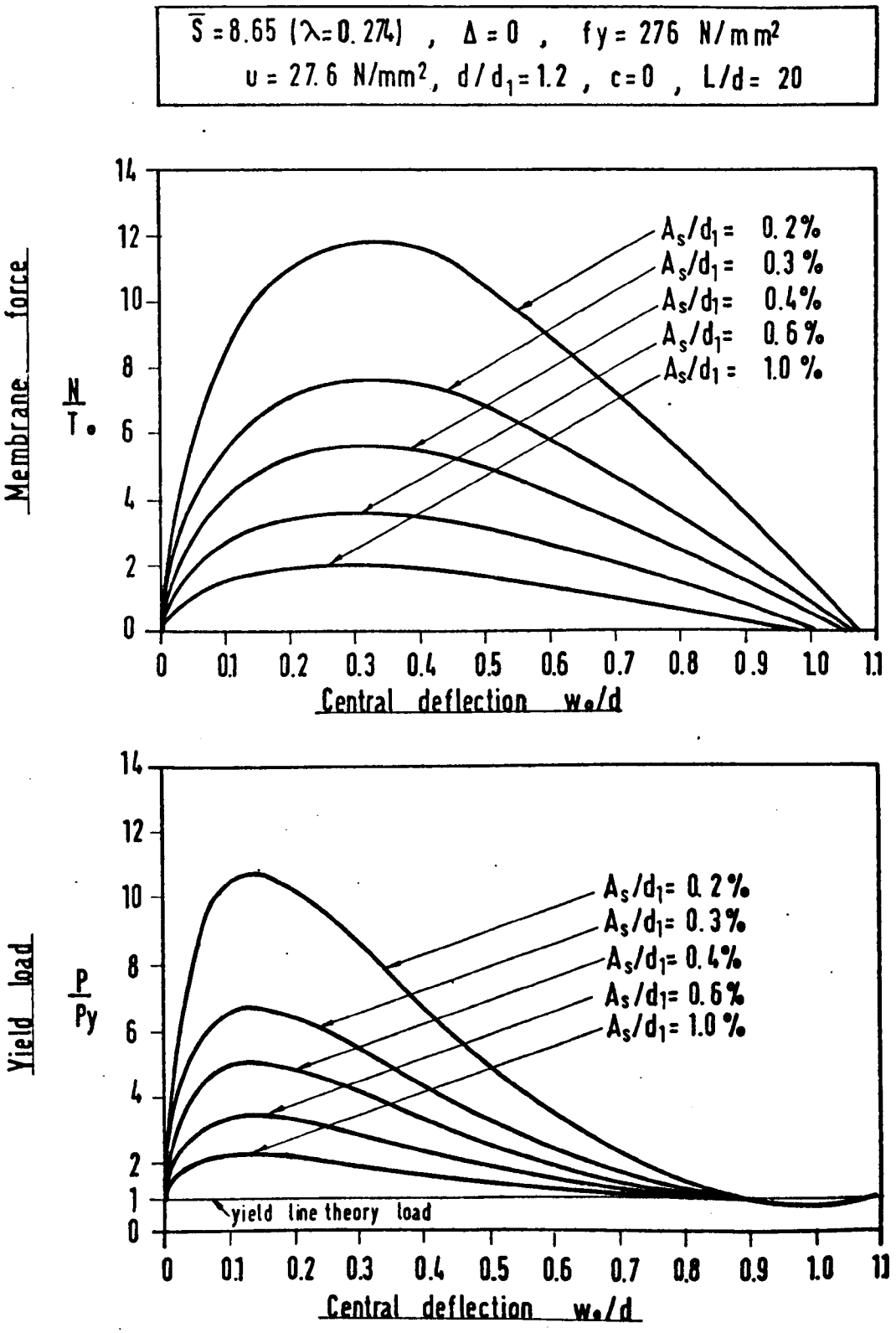

FIG. (5.9) Effect of the Amount of Reinforcement A_s/d_1 on the Behaviour of a Non-Rigid Reinforced Concrete Slab Strip With Simple Supports and Partial Lateral Restraints

of A_s/d_1 ranging between 0.2% and 1% are considered and the results show that for any value of central deflection (within the two stages of membrane action) the non-dimensional values of the membrane force N/T_o and the yield load P/P_y are larger in lightly reinforced slabs. A measure of the differences may be obtained by comparing the maximum values of N/T_o and P/P_y for the two extreme cases shown in the figure. When a typical simply supported slab strip with percentage of reinforcement as little as 0.2% is restrained partially along its longitudinal axis and loaded will be subjected to a maximum membrane force of 11.75 T_o and the ultimate yield load will be 10.72 P_y, whereas if the same slab is heavily reinforced with percentage of reinforcement of 1% the corresponding values of N_{max}/T_o and P_{max}/P_y will be as low as 2.04 and 2.30 respectively. However, the duration of the membrane action in heavily reinforced slabs is shorter.

5.6.4 CUBE STRENGTH OF CONCRETE u

Fig. (5.10) shows the changes in the plastic behaviour of the typical slab strip when the cube strength of the concrete u is varied from 13.8 N/mm^2 (2000 lbf/in^2) to 69.0 N/mm^2 (10,000 lbf/in^2).

For any value of central deflection the value of the membrane force is larger in concrete slabs with higher cube strengths and the deflection range of the membrane action in such slabs is longer. The enhancement in the yield load will be more pronounced when concrete is used with higher values of cube strengths but such enhancements reduce when the deformation of the slab goes through the stage of decreasing membrane force and when $\frac{w_o}{d} = 0.88$ the yield load for the typical slab strip with any concrete cube strength will be the yield line theory load. For values of the central deflection above 0.88 d the yield load declines and becomes less than P_y but then recovers at larger deflections. The drop in the value of the yield load at large deflections will be more pronounced for concrete of higher cube strength.

5.6.5 MECHANISM PARAMETER c/L

The effect of the location of the central plastic hinge is demonstrated by Fig. (5.11). The loads on the slab strip are applied

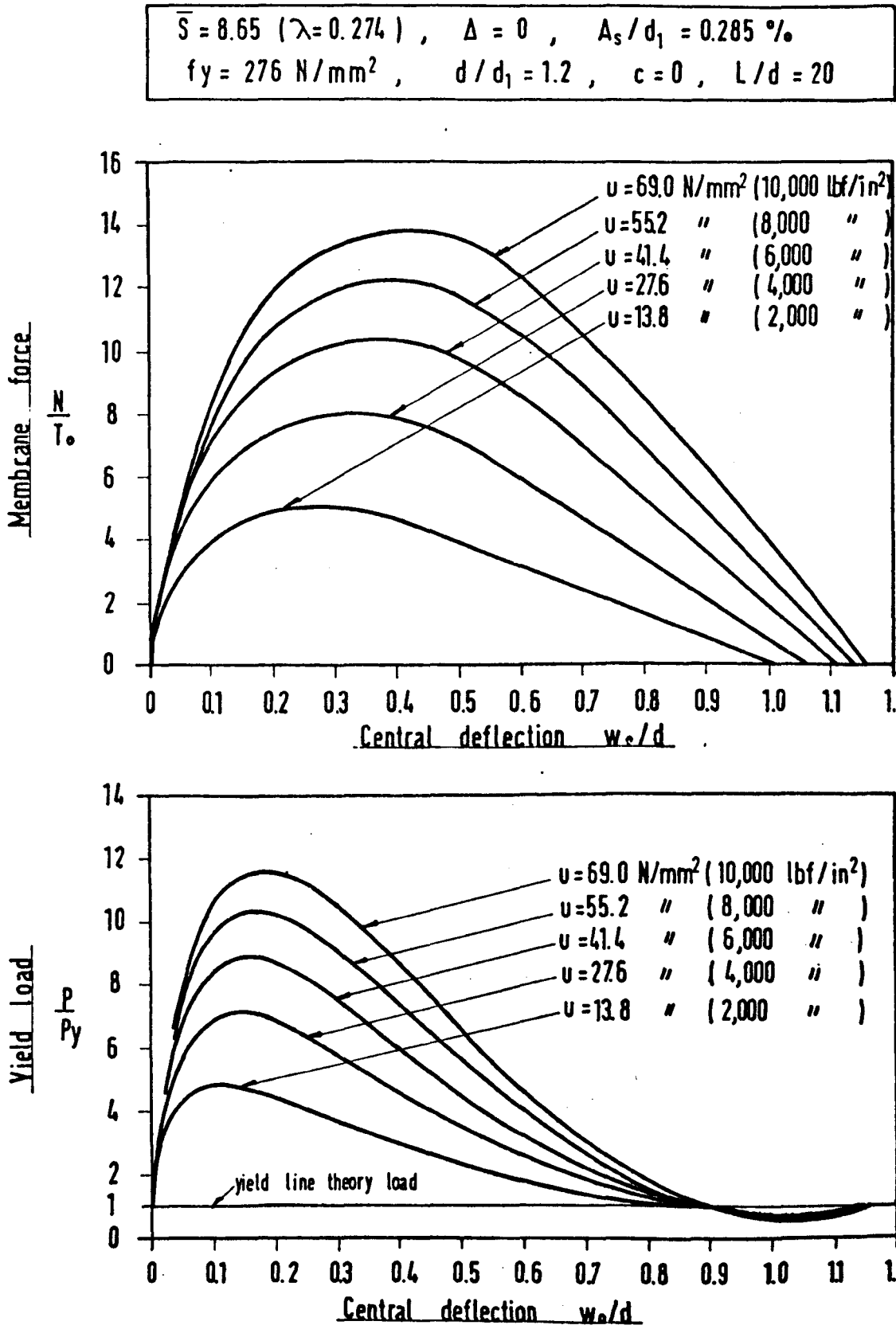

FIG. (5.10) Effect of the Cube Strength of Concrete u on the Behaviour of a Non-Rigid Reinforced Concrete Slab Strip With Simple Supports and Partial Lateral Restraints

$\bar{S} = 8.65$ ($\lambda = 0.274$) , $\Delta = 0$, $A_s / d_1 = 0.285$ %
$f_y = 276$ N/mm^2, $u = 27.6$ N/mm^2, $d/d_1 = 1.2$, $L/d = 20$

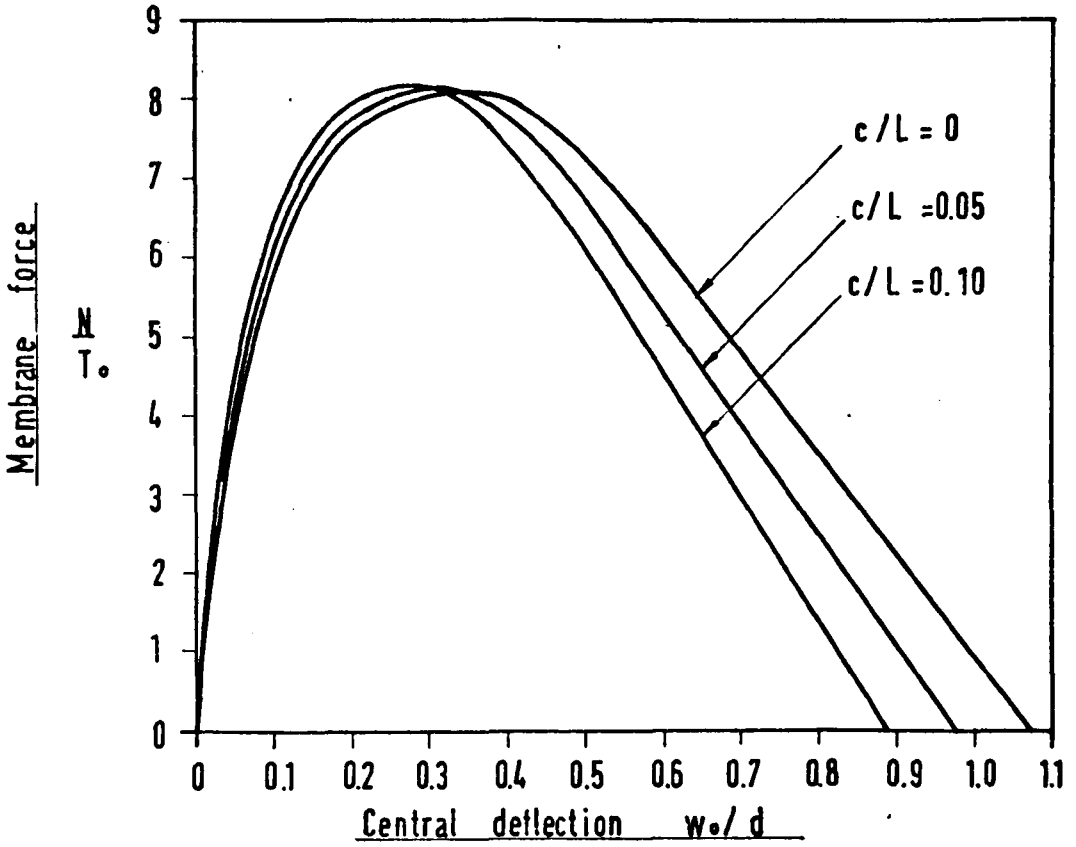

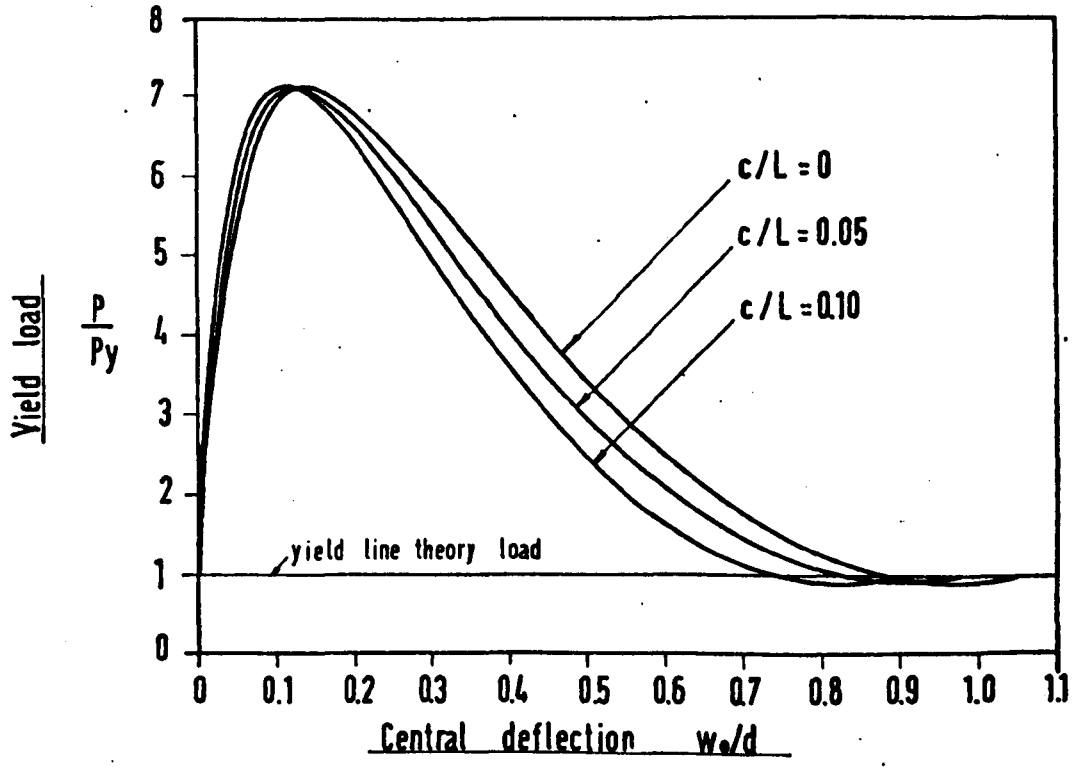

FIG.(5.11) Effect of the Mechanism Parameter c/L on the Behaviour of a Non-Rigid Reinforced Concrete Slab Strip With Simple Supports and Partial Lateral Restraints

at $a = 0.4\ L$ from the simply supported ends and, therefore, the possible values of c/L range from 0 to 0.1 .

It can be seen from Fig. (5.11) that the formation of the central plastic hinge at different positions has a negligible effect on the maximum values of the membrane force and the yield load, though the curves are changed slightly for different values of c/L . The difference in the value of the membrane force is small for deflections $w_o \leqq 0.33\ d$, but at larger deflections the ratio N/T_o is greater for smaller values of c/L . Similarly, the value of the yield load at deflections $\frac{w_o}{d} \leqq 0.13$ is not remarkably influenced by the location of the central plastic hinge, but for larger deflections the yield load will be higher in slabs having the central hinge formed closer to the mid-span section, i.e. c/L smaller.

5.6.6 CONCRETE STRESS BLOCK PARAMETERS k_1k_3 AND k_2

It has been mentioned in previous sections that in the study of the problem of membrane action in slabs, different authors have considered different values of the concrete stress block parameters. The values of these parameters commonly used by investigators are Hognestad's k_1k_3 and k_2 represented by Eqs. (3.1) and Wood's design coefficients where $k_1k_3 = 2/3$ and $k_2 = 1/2$.

The effect of using either pair of these values on the plastic behaviour of the typical slab strip under study is shown in Fig. (5.12). Values of u ranging between 13.8 N/mm^2 (2000 lbf/in^2) and 69.0 N/mm^2 (10,000 lbf/in^2) are used to illustrate the effect. The figure shows variations in the values of the membrane force N/T_o and the yield load P/P_y for any central deflection; the differences are significant and are more pronounced at high values of u and at deflections corresponding to maximum membrane force and maximum yield load. For high cube strengths of concrete, the approximate coefficients of Wood predict higher value of N/T_o than Hognestad's parameters for any central deflection. The relationship between the yield load and the central deflection indicates that during the whole stage of increasing membrane force and part of the stage of decreasing membrane force the yield load P/P_y using Wood's parameters is greater than that

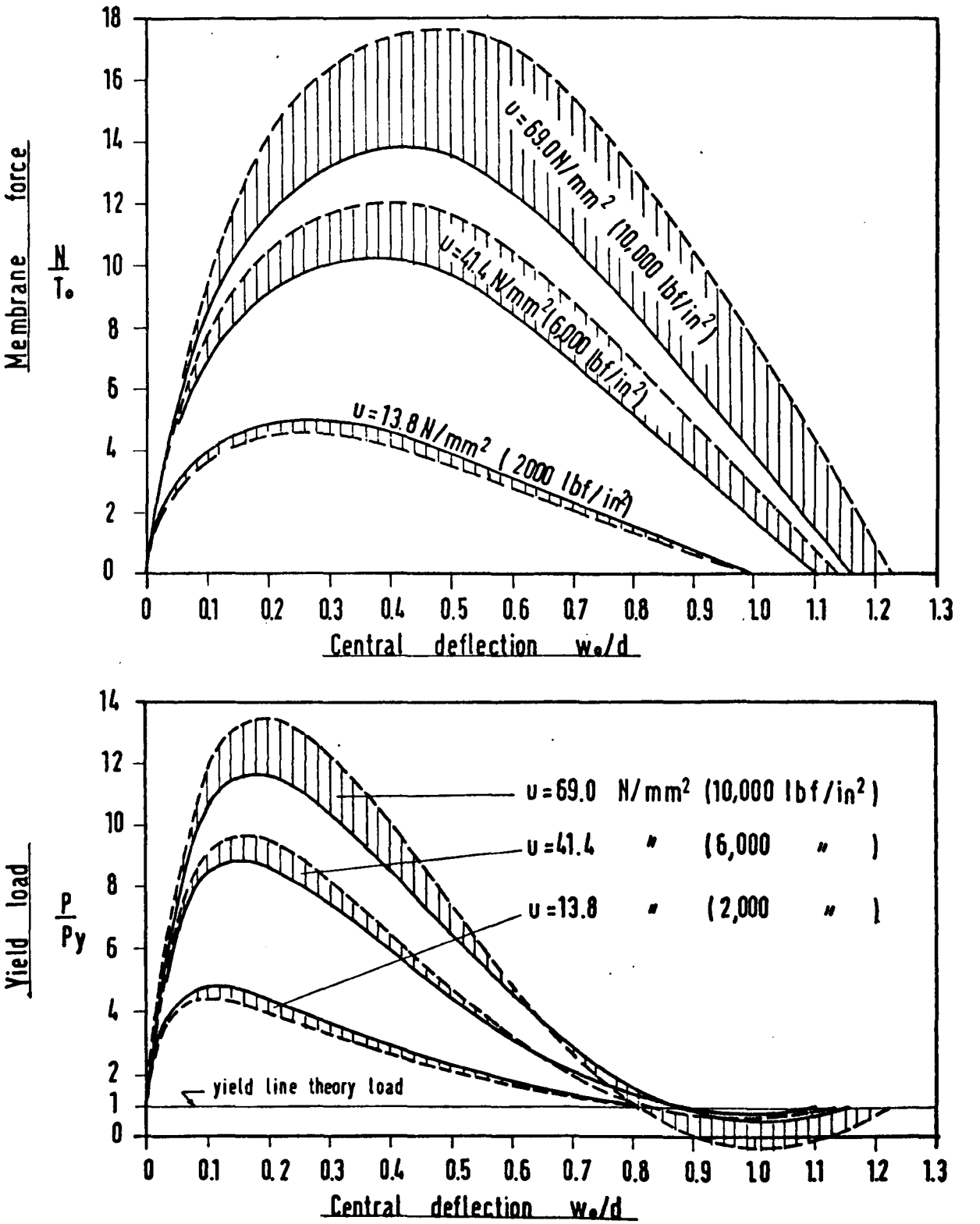

FIG. (5.12) Effect of Using Different Concrete Stress Block Parameters on the Behaviour of a Non-Rigid Reinforced Concrete Slab Strip With Simple Supports and Partial Lateral Restraints

using Hognestad's parameters for higher values of u but for large values of central deflection the effect reverses and Wood's parameters start to underestimate P/P_y.

A measure of the effect of using either Wood's or Hognestad's concrete stress block parameters in analysis may be obtained by comparing the maximum values of N/T_o and P/P_y for a typical slab strip with $u = 69\ N/mm^2$ (the highest value shown in the figure where the differences are expected to be largest).

	N_{max}/T_o	P_{max}/P_y
Wood's approximate coefficients $k_1k_3 = \frac{2}{3}$ and $k_2 = \frac{1}{2}$	17.68	13.51
Hognestad's k_1k_3 (Eq. 3.1a) and k_2 (Eq. 3.1b)	13.80	11.66

5.7 STUDY OF THE MAXIMUM YIELD LOAD

The analysis and discussion of this chapter have shown that due to compressive membrane action, partially restrained reinforced concrete slab strips can carry loads far beyond those of Johansen's simple yield line theory. The reserves in strengths have been found to be more pronounced in lightly reinforced slabs made of concrete with high cube strengths.

The maximum yield load is obtained at a value of central deflection given by Eq. (5.12). Substitution of this value into Eqs.(5.15e and f) provides the maximum yield load but unfortunately, the form of Eq. (5.12) makes an exact explicit solution of the dimensional yield load P_{max} impossible. However, with the aid of a digital computer a graph was constructed (Fig. 5.13) which gave the relationship of P_{max} with both the percentage of reinforcement $\frac{A_s}{d_1} \times 100$ and the cube strength of the concrete u for the same typical slab strip of Section 5.3.6 and Fig. (5.3) assuming that $d/L = 1/20$ and $a/L = 0.4$.

Fig. (5.13) clearly shows that the maximum yield loads increase with the percentage of reinforcement and with the strength of the concrete, the latter being the more dominant effect. For example, the same maximum yield load, say $0.93\ N/mm^2$ ($135\ lbf/in^2$)

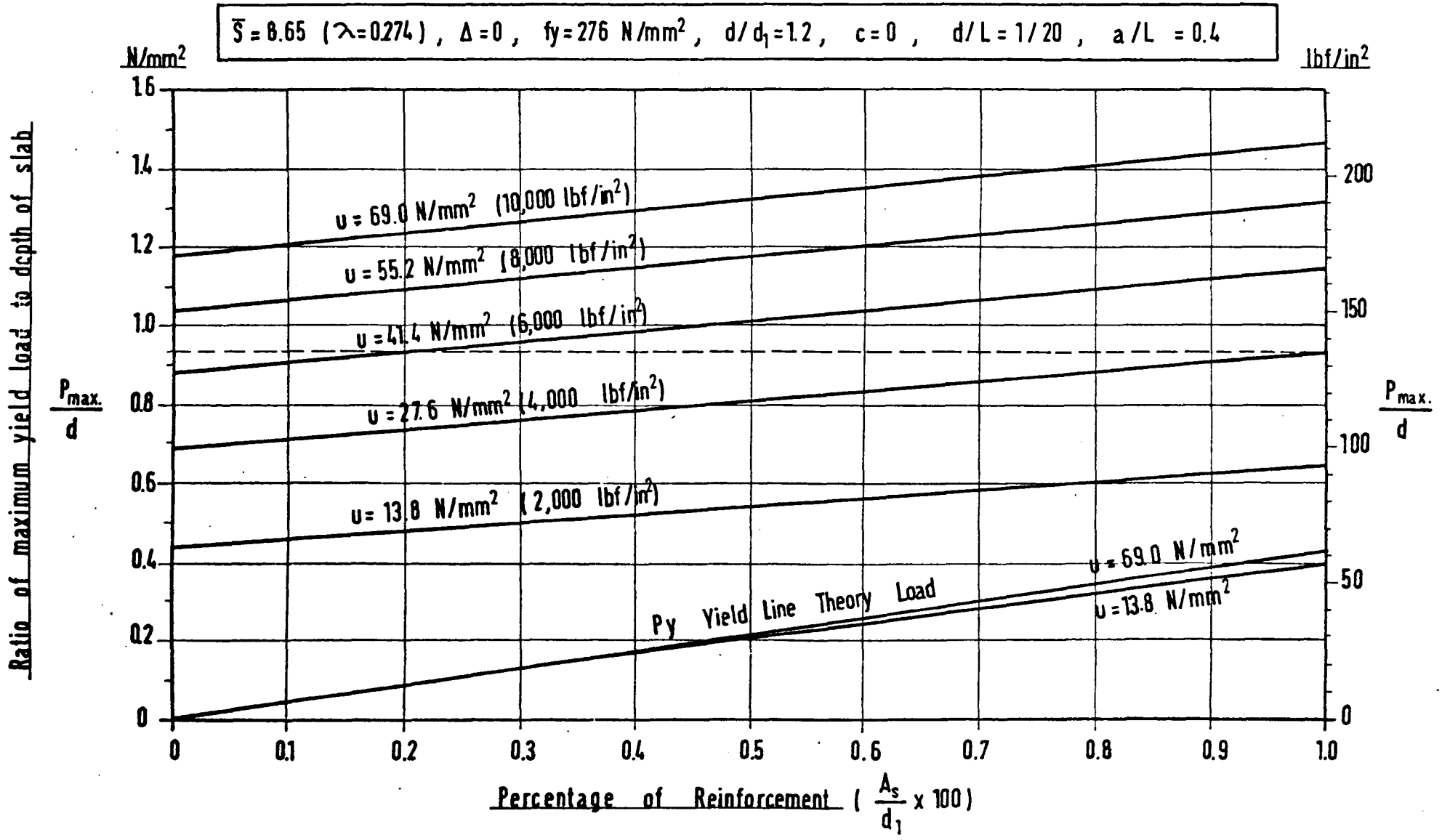
$\bar{S}$ = 8.65 (λ=0.274), Δ = 0, fy = 276 N/mm², d/d₁ = 1.2, c = 0, d/L = 1/20, a/L = 0.4
N/mm²
lbf/in²
Ratio of maximum yield load to depth of slab
Pmax./d
u = 69.0 N/mm² (10,000 lbf/in²)
u = 55.2 N/mm² (8,000 lbf/in²)
u = 41.4 N/mm² (6,000 lbf/in²)
u = 27.6 N/mm² (4,000 lbf/in²)
u = 13.8 N/mm² (2,000 lbf/in²)
Py Yield Line Theory Load
u = 69.0 N/mm²
u = 13.8 N/mm²
Percentage of Reinforcement (As/d1 x 100)

FIG. (5.13)

can be obtained by using a typical slab strip with $u = 27.6$ N/mm^2 (4000 lbf/in^2) and percentage of reinforcement $A_s/d_1 = 1\%$ or with no reinforcement at all but $u = 44.8$ N/mm^2 (6500 lbf/in^2). Thus, to obtain equal maximum yield loads the amount of reinforcement can be reduced by using a higher strength concrete.

5.8 COMPARISON BETWEEN ELASTIC-PLASTIC AND RIGID-PLASTIC SOLUTIONS

Eqs. (5.15) which describe the plastic behaviour of a simply supported reinforced concrete slab strip including the effects of the elastic shortening of the slab and the outward movement of the surround are compared in Fig. (5.14) with the corresponding rigid-plastic solution ($\bar{S} = \infty$) for the same typical slab strip of Section 5.2.6, considering two values of the gap parameter $\Delta/d = 0$ and 0.02 . The rigid-plastic solution for $\Delta = 0$ (governed by strain rate theory only) is given by Eqs. (4.29) of Chapter 4 and that for $\Delta/d = 0.02$ by the special case $\bar{S} = \infty$ in Eq. (5.15).

For either case of Δ , the rigid-plastic solution at the initial stages of deformation provides higher values for the membrane force and the yield load than does the elastic-plastic solution but as the deflection becomes large the plastic behaviour of the slab strip changes and the rigid-plastic theory starts to give lower values for the membrane force but the yield load remains slightly larger. The membrane force - central deflection curves for both solutions intersect at the critical value of central deflection for elastic-plastic behaviour. This implies that at this value of deflection the membrane force according to the rigid-plastic solution is equal to the 'maximum' membrane force according to the elastic-plastic solution. A mathematical explanation for the point of intersection may be given by comparing the value of the maximum membrane force found by elastic-plastic; i.e. Eq. (5.13), with the rigid-plastic solution (4.29e) for the case $\Delta = 0$ and the special case $\bar{S} = \infty$ of Eq. (5.15i) for $\Delta/d = 0.02$. All equations are identical at $w_o = (w_o)_{cr}$ for elastic-plastic behaviour.

The yield load - central deflection curve according to the rigid-plastic theory for any value of Δ is higher than the

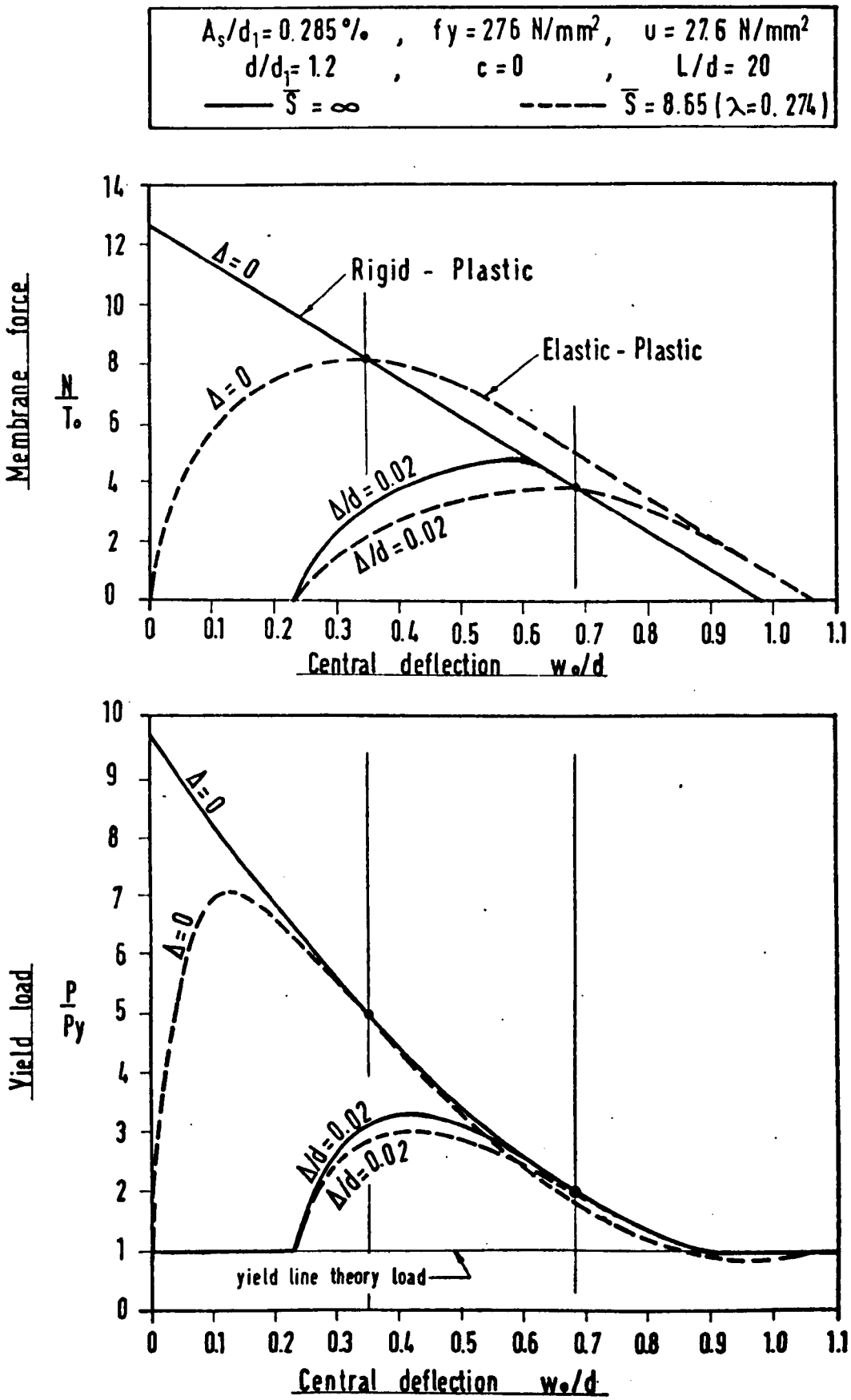

FIG. (5.14) Comparison Between Elastic - Plastic And Rigid - Plastic Solutions

corresponding elastic-plastic curve except at the critical (elastic-plastic) deflection where the two curves coincide. From Eq. (5.10), it follows that when the membrane forces for two identical slab strips become equal (at a certain value of central deflection) the yield loads will automatically be equal.

5.9 SUMMARY

The consideration of the elastic shortening of the slab member and the outward movement of the surround in the plastic analysis of axially restrained concrete slabs has not only shown the validity of the total strain theory during the early stages of membrane action, but has also demonstrated that this theory applies to the prediction of the maximum yield loads. Total strain theory has also been shown to be applicable during the stage of increasing membrane force in fully restrained rigid-plastic slab strips with physical gaps at the simply supported ends. The applicability of the total strain theory in these cases is due to the movement of the neutral axis at sections of yield into the zone of the crack.

The behaviour of an elastic-plastic simply-supported slab strip with physical gaps at partially stiff surrounds was found to consist of four successive stages. First, an early stage of pure flexure where the yield line theory is valid. Second, a stage of increasing membrane force where the neutral axis at the yield sections moves towards the mid-depth of the slab into the 'crack' or 'zone of total tensile strains' and thus the total strain theory is valid. The yield load during this stage increases rapidly (the equilibrium of the slab is 'stable') until it becomes a maximum at a certain value of central deflection and thereafter falls. The falling part of the load-deflection curve represents a state where the equilibrium of the slab is 'unstable'. The maximum yield load is always attained within the stage of increasing membrane force. The third stage is a stage of decreasing membrane force where the neutral axis at the yield sections moves back towards the compressed face of the slab. For slabs with $\bar{S} = \infty$ the movement of the neutral

axis for strain rate during the whole stage of decreasing membrane force is into the compressive zone for total strain in which case the strain rate theory applies (i.e. immediately after N becomes maximum) but for elastic plastic slabs with partial lateral restraints the neutral axis for strain rate during the early part of decreasing membrane force will continue to be into the crack, which requires the continuing use of total strain theory. When the state of stress is reached when both the total strain and strain rate theories predict equal values for the membrane force, yield load and position of the neutral axis at the yield sections, the strain rate theory becomes applicable since the neutral axis for strain rate then moves into the compressive zone for total strain with continuing deflection. For elastic plastic slabs, the strain rate theory applies over the major part of the decreasing membrane force stage. The fourth and final stage is pure flexure which starts when the membrane force vanishes at large deflection and yield line theory applies up to the fracture of the steel.

On the yield surface (Fig. 3.2), the stress state moves from the point $M = M_o$, $N = 0$ at the start of compressive membrane action to a point of largest membrane force just to the right of $M = M_{max}$ and then returns to its original position. This large movement of the stress state causes highly significant discrepancies between the predictions of total strain and strain rate theories.

The errors caused by using the wrong theory in the analysis of either of the two stages of membrane action can be summarized as follows :

i. The errors caused by using the strain rate theory in the analysis of the slab during the stage of increasing membrane force instead of total strain theory will result in predicting higher values of membrane force and yield load and smaller depth of the neutral axis at the yield sections.

ii. The errors caused by using the total strain theory in

the analysis of the slab during the stage of decreasing membrane force instead of strain rate theory include overestimates of membrane force and underestimates of yield load and depth of the neutral axis at sections of yield.

CHAPTER 6

EXPERIMENTAL TESTS

6.1 INTRODUCTION

The theoretical analysis presented in the previous chapter has been examined by a series of experiments. 36 simply supported concrete slab strips (28 reinforced and 8 unreinforced), restrained axially by a surround of low stiffness, were tested under two point loading. The main object of these experiments was to check the validity of the proposed hypothesis regarding the relevance of total strain and strain rate theories in cracked sections and their limits of application to slabs with membrane action. They were also intended to test the effect of certain significant parameters on the behaviour of axially restrained slab strips. The testing procedure and comparison of experimental results with the corresponding analytical predictions will be presented in this chapter.

During the loading of the slab, wherever possible, the following items were recorded :

i. The applied load and particularly the maximum value.
ii. Central deflection of the slab.
iii. Membrane force.
iv. The load corresponding to the first visible crack.
v. The shape of the collapse mechanism and the location of the positive plastic hinge from mid-span.

6.2 SPECIMEN SLABS AND SCOPE OF EXPERIMENTS

Because of factors such as casting, handling and the size of the testing rig, the dimensions of all the slab strips were 1.5621 m (61½ in) in length, 203.2 mm (8 in) in width and 76.2 mm (3 in) in depth. The span:depth ratio was 20.

The 36 slab strips tested were designed to cover as many important parameters as possible. Key parameters have been shown in Chapter 5 to be the following,

i. The gap parameter Δ/d
ii. The cube strength of concrete u
iii. The amount of reinforcement A_s/d_1 per unit width.
iv. The degree of stiffness of the surround λ
v. The span : depth ratio L/d
vi. The mechanism parameter c/L.

The effect of the latter (vi) has been shown theoretically to be of little significance. The effect of the span : depth ratio parameter can be predicted to be similar to that of the gap parameter (see Eqs. 5.15). Therefore, for a given stiffness of surround, the parameters that are most significant are the first three amongst those listed. The effects of the cube strength of concrete and the amount of reinforcement on the dimensionless values of the yield load and the membrane force in axially restrained slabs, are governed by the effect of one combined factor, that is $t = \frac{A_s}{d_1} \times \frac{f_y}{u}$ per unit width. This factor appears in the dimensionless notations α and β given by Eq. (3.5).

The programme consisted of five series of experiments I, II, III, IV and V. The first three series were for reinforced slab strips whereas the last two were for unreinforced strips. Series I, II and III had different t values and within each series the gap width Δ was varied as shown in table (6.1). The distribution of the reinforcing bars in the slab strips of each series is shown in Fig. (6.1). Series IV and V had different concrete cube strengths u and represented the cases of 'no gap' only. All the slab strips were tested in pairs and an average experimental value was used for comparison with corresponding theoretical predictions. The five series of tests provide an extensive experimental study of the effect of gap width on the ultimate loads and behaviour of slab strips with membrane action.

The sequence of testing was as follows ;

(a) The first pair of slab strips in each series were tested such that the surrounds were initially in contact with the surfaces of the slab ends (no gap) and by using a 1:1 ? mortar mix of high-alumina cement and sand (screened to pass a No. 25 sieve), having a water : cement ratio 0.35,

TABLE (6.1) Properties of the Test Slab Strips

Series No.	Type of Slab	Slab Mark	Depth of slab mm	Depth of slab in	Type of Mix *	Cube Strength (u) N/mm²	Cube Strength (u) lbf/in²	Average Cube Strength $(u)_{ave.}$ N/mm²	Average Cube Strength $(u)_{ave.}$ lbf/in²	Diameter of Reinforcing Bars mm	Diameter of Reinforcing Bars in	No. of Bars	Percentage of Reinforcement $\frac{A_s}{d_1} \times 100$ / unit width **	$t = \frac{A_s \times f_y}{d_1 \times u}$ / unit width †	Gap width mm	Gap width in
I	Reinforced	S1	76	3	A	48.3	7010	49.8	7215	5.5	0.216	2	0.378	0.0223	No Gap with Mortar	
		S2				51.2	7420									
		S3	76	3	A	48.8	7080	50.1	7265	5.5	0.216	2	0.378	0.0221	No Gap No Mortar	
		S4				51.4	7450									
		S5	76	3	A	54.5	7910	54.8	7940	5.5	0.216	2	0.378	0.0202	0.51	0.02
		S6				55.0	7970									
		S7	76	3	A	53.3	7730	53.0	7685	5.5	0.216	2	0.378	0.0209	1.27	0.05
		S8				52.7	7640									
		S9	76	3	A	51.3	7445	52.0	7545	5.5	0.216	2	0.378	0.0213	2.03	0.08
		S10				52.7	7645									
II	Reinforced	S17	76	3	B	27.6	4005	27.7	4010	5.5	0.216	2	0.378	0.0401	No Gap with Mortar	
		S18				27.7	4015									
		S19	76	3	B	30.6	4440	30.9	4480	5.5	0.216	2	0.378	0.0359	No Gap No Mortar	
		S20				31.2	4520									
		S21	76	3	B	30.1	4360	30.2	4370	5.5	0.216	2	0.378	0.0368	0.51	0.02
		S22				30.2	4380									
		S23	76	3	B	29.9	4330	30.3	4390	5.5	0.216	2	0.378	0.0366	1.02	0.04
		S24				30.7	4450									
		S25	76	3	B	29.8	4315	29.2	4235	5.5	0.216	2	0.378	0.0379	2.03	0.08
		S26				28.6	4155									
III	Reinforced	S29	76	3	C	38.8	5625	38.8	5625	5.5	0.216	5	0.945	0.0714	No Gap with Mortar	
		S30				38.8	5625									
		S31	76	3	C	40.9	5925	39.7	5755	5.5	0.216	5	0.945	0.0698	No Gap No Mortar	
		S32				38.5	5585									
		S33	76	3	C	37.7	5475	39.4	5720	5.5	0.216	5	0.945	0.0702	0.51	0.02
		S34				41.1	5965									
		S35	76	3	C	40.0	5795	38.1	5520	5.5	0.216	5	0.945	0.0728	1.02	0.04
		S36				36.2	5245									
IV	Unreinforced	S13	76	3	A	51.3	7435	50.5	7320	0	0	0	0	0	No Gap with Mortar	
		S14				49.7	7205									
		S15	76	3	A	54.0	7830	52.4	7590	0	0	0	0	0	No Gap No Mortar	
		S16				50.7	7350									
V	Unreinforced	S39	76	3	C	37.9	5500	37.9	5495	0	0	0	0	0	No Gap with Mortar	
		S40				37.8	5490									
		S41	76	3	C	36.6	5300	36.0	5210	0	0	0	0	0	No Gap No Mortar	
		S42				35.3	5120									

* The proportions of the different types of mixes are given in Tables (6.2) & (6.3)

** The cover used for reinforcement was 12mm (0.472 in)

† The yield stress of reinforcement f_y was 293 N/mm² (42,500 lbf/in²)

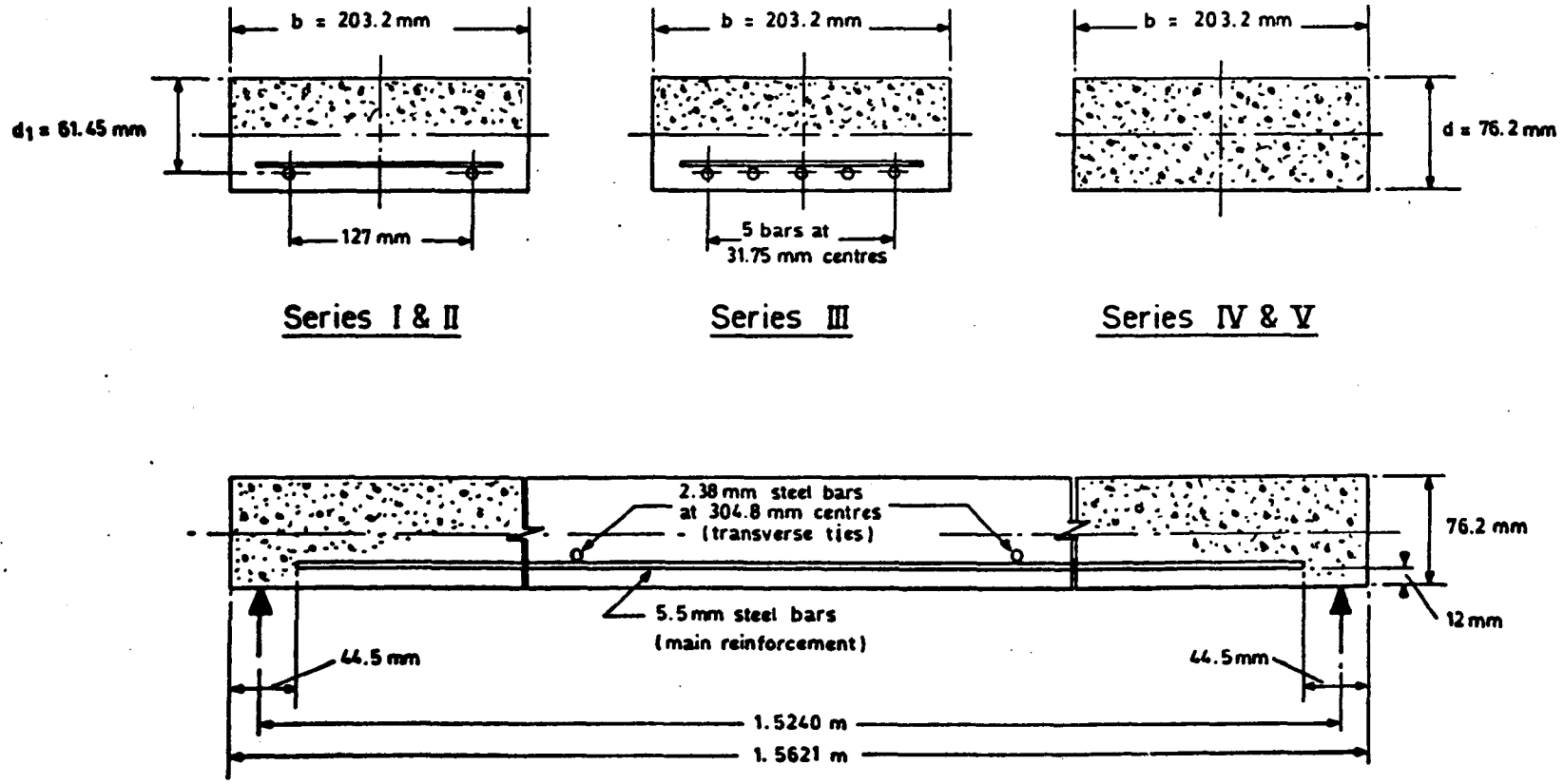

FIG. (6.1) The Slab Specimens

and a cube strength of at least 69 N/mm^2 (10,000 lbf/in^2) at 24 hours, the effective gaps existing due to irregularity of the concrete surfaces were filled.

(b) The second pair of slab strips in each series were also tested with 'no gap' but no cement mortar was used.

(c) In testing the third, fourth and fifth pair of slab strips in series I, II and III, gaps of different widths (see table 6.1) were provided at the slab boundaries prior to testing.

6.3 MATERIALS AND CONTROL SPECIMENS

(a) CONCRETE

Three concrete mixes were used for the slab strips designated as mixes A, B and C. In each mix, clean, washed and 24 hours oven dried aggregates of maximum size 19.05 mm (3/4 in) were used. The coarse aggregate [of sizes ranging between 19.05 mm (3/4 in) and 4.76 mm (3/16 in)] was irregular gravel whereas the fine aggregate [sizes 4.76 mm (3/16 in) and lower] was Thames Valley sand. The design of the concrete mixes was according to Grade 2 (see Fig. 6.2) specified by the Road Research Note No.4, London (31), for the 19.05 mm (3/4 in) maximum size of aggregate. The weight of the different sizes of aggregate, according to this grading, as a percentage of total weight of aggregate is given in table (6.3). Ordinary Portland Cement was used. The three mixes had the details listed in table (6.2).

Three 152.4 mm (6 in) cubes were cast with each slab strip as control specimens and these were vibrated and cured in the same manner (which will be described later) as the slab strips. At age 28 days, immediately after the corresponding slab strip was tested, the three concrete cubes were tested in uniaxial compression and their average crushing strength was considered as representative of the crushing strength of the slab concrete. The procedure of casting one slab at a time caused only small discrepancies in the values of the concrete cube strength in each series, the maximum differences being of the order $\pm 6.5\%$ for series I, $\pm 6.1\%$ for series II and $\pm 7.6\%$ for

TABLE (6.2) Details of Mixes

ITEM		Type of Mix		
		A	B	C
water : cement ratio		0.38	0.65	0.55
total aggregate : cement ratio		3.80	6.50	5.50
cement content	kg /m^3	462	288	335
	lb / yd^3	718	485	564
degree of workability		low	medium	medium

TABLE (6.3) Proportions of Aggregate

Size of aggregate (relative to B.S. sieve size)		Percentage of total aggregate
mm or μm	in or No.	
19.05mm – 9.52mm	3/4 in – 3/8 in	44
9.52mm – 4.76mm	3/8 in – 3/16 in	22
4.76mm – 2.40mm	3/16 in – No.7	7
2.40mm – 1.20mm	No.7 – No.14	7
1.20mm – 600 μm	No.14 – No.25	7
600μm – 300μm	No.25 – No.52	10
300μm – 150μm	No.52 – No.100	2½
below 150 μm	below No.100	½

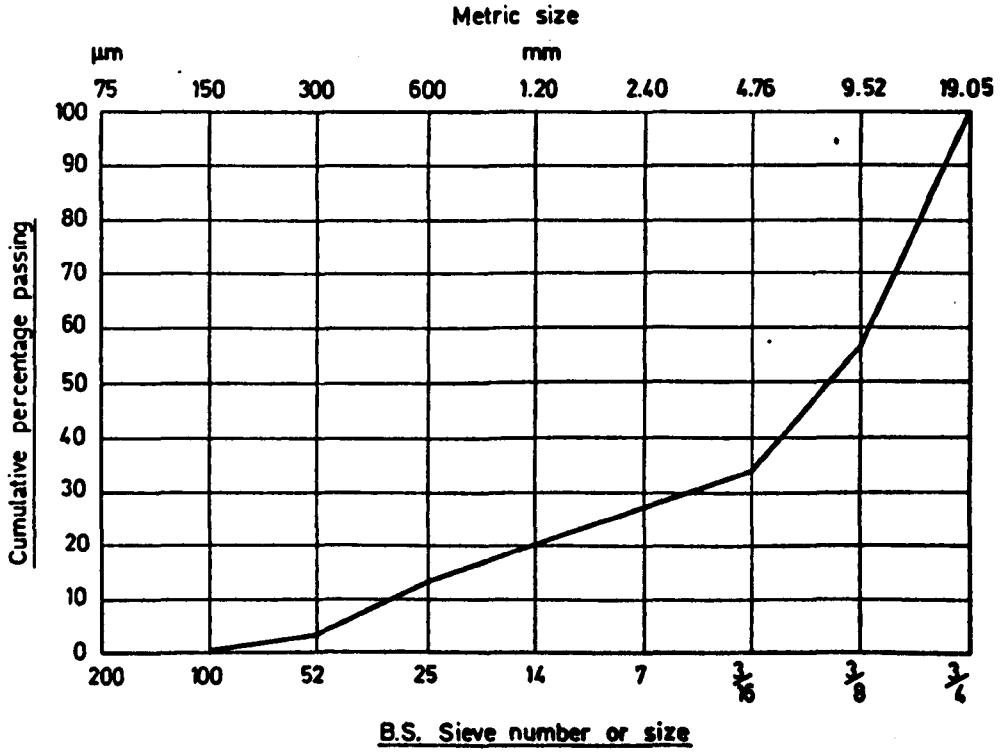

FIG. (6.2) Grading Curve for 19.05mm (3/4 in) Aggregate

series III. However, when theoretical predictions were compared with results of experiments an average value of the concrete cube strength obtained for the nominally identical pair of slabs was used.

(b) REINFORCEMENT

The theoretical analyses presented in the earlier chapters assumed that the reinforcement of the slab behaved in a rigid - perfectly plastic manner. Therefore, it was realised at the outset of this investigation that the type of reinforcing bars to use must have a definite yield point and a long yield plateau. These two properties were found in annealed black mild steel.

Surface rust was removed with wire wool and the average diameter of the steel bars, determined by micrometer measurements at three different locations on each bar, was 5.5 mm (0.216 in); the maximum differences in the diameters of the bars being of the order ±2%. This average size of bar with a cover of 12 mm (0.472 in) gave an effective depth d_1 of 61.5 mm (2.420 in) in the slab strips.

The stress-strain characteristics of the reinforcing steel was determined using a Hounsfield Tensometer. The extension of a 50.8 mm (2 in) length under test was measured using a mechanical extensometer. Fig. (6.3) shows the average of four stress-strain curves. The yield stress was well defined with an average value of 293 N/mm^2 (42,500 lbf/in^2) with a long yield plateau up to a value of strain 0.045. The ultimate stress was 386 N/mm^2 (56,000 lbf/in^2).

6.4 TESTING RIG

A steel testing rig (Fig. 6.4) was designed and constructed such that

i. It provided partial axial restraint against longitudinal expansion.

ii. It enabled controlled gaps to be provided at the simple supports.

iii. The slab was completely exposed to examination while the experiment was in progress and thus cracking was readily observed.

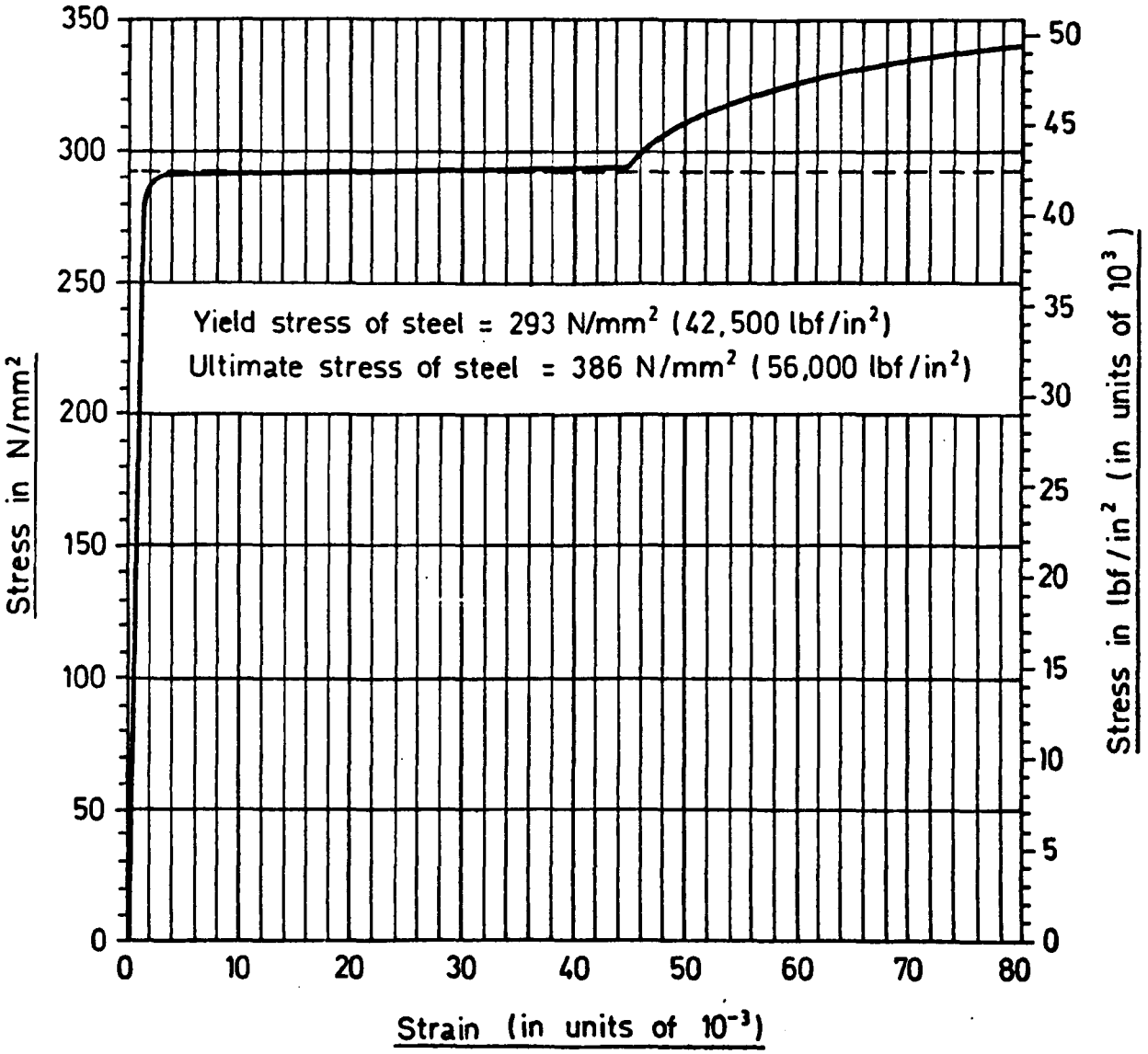

FIG. (6. 3) Stress - Strain Characteristics of 5.5mm (0.216 in) Diameter Annealed Black Mild Steel Reinforcement

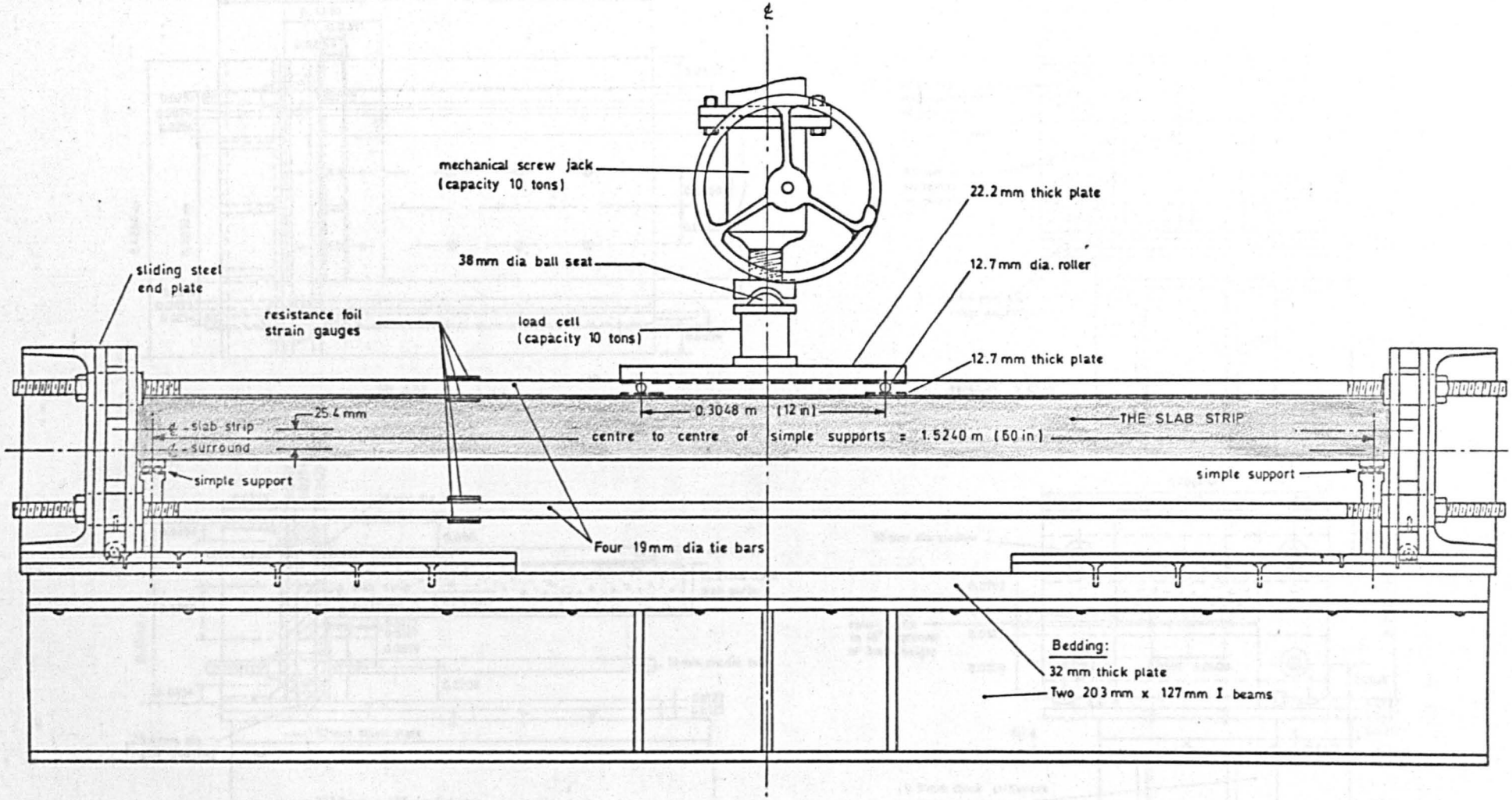

FIG. (6.4) The Testing Rig

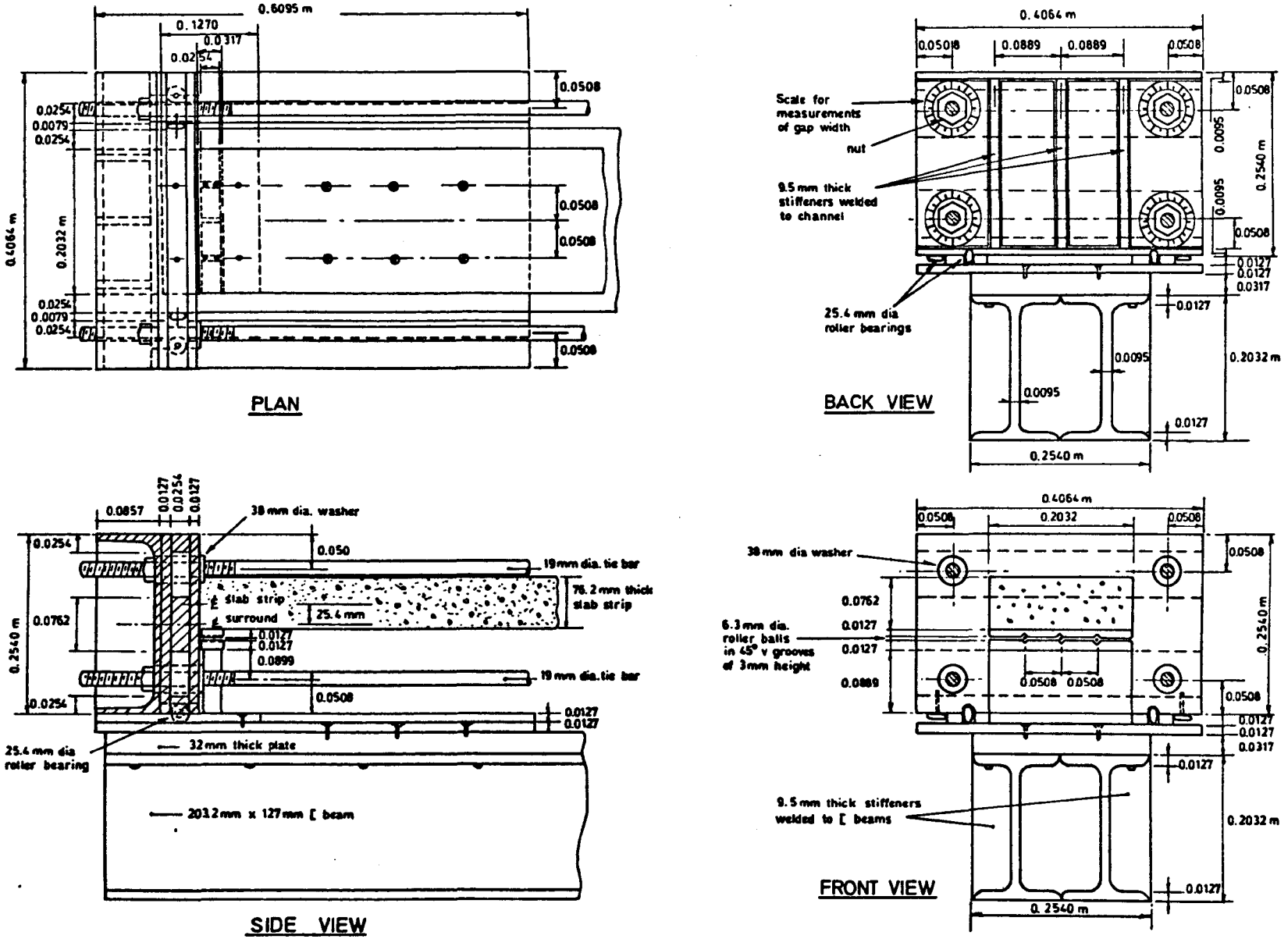

FIG. (6.5) Details of the Testing Rig

iv. The slab ends had the freedom of movement which eliminated any friction from developing at the interface between the slab and the supports.

v. The mid-depth of the slab was positioned so that the maximum compressive force resulting due to membrane action (as an average theoretical prediction of all slab strips tested) coincided with the centre line of the surround. This minimised the effect of rotation of the surround which was ignored in the theoretical model.

The rig consisted of two identical stiffened end plates with overall dimensions 0.4064 m (16 in) width and 0.2540 m (10 in) height (Fig. 6.5). The end plates were tied together by four 19 mm (3/4 in) diameter bright mild steel bars of yield stress 331 N/mm^2 (48,000 lbf/in^2) and Young's Modulus of Elasticity 207 x 10^3 N/mm^2 (30.1 x 10^6 lbf/in^2). The end plates were supported on a rigid base by roller bearings which provided longitudinal freedom of movement as shown in Fig. (6.5). The slab strip specimens were positioned between the end plates and supported by the end support system shown in Figs. (6.5) and (6.8) which provided rotational and longitudinal freedom. To minimize any rotation of the steel end plates and bending of the tie bars resulting from the compressive membrane action, the mid-depth of the slab strip was arranged to be 25.4 mm (1 in) above the centre of the four tie bars (i.e. the centre of the end plates) as shown in Figs. (6.4) and (6.5). This setting, based on a preliminary theoretical calculation, was to position the maximum compressive force resulting due to membrane action, as an average of all slab strips tested, at the centre of the four tie bars. The centre to centre distance between the two simple supports was constant at 1.5240 m (60 in) for all the slab strips.

The width of the gap between the slab end and the steel end plates was controlled by adjustment of the nuts at the anchorage of the tie bars. Each nut was provided with a circular scale having 20 divisions (Fig. 6.5), each division representing a longitudinal movement of 0.127 mm (0.005 in). A constant width gap was provided by turning each nut through an equal number of divisions.

6.5 LOADING SYSTEM

The conventional two point loading system was adopted and applied for all tests to avoid biaxial stresses in the concrete at sections of yield which was not considered in the theoretical model. To enable the falling branch of the load-deflection relationship of such partially restrained slab strips to be followed, a stiff loading system was used as shown in Fig. (6.6). The system consisted of a loading frame (capacity 50 tons), a mechanical screw jack (capacity 10 tons) and a load spreader system.

The load $\bar{P}$ was applied through the mechanical screw jack and was recorded by using a load cell and a digital voltmeter. With the loading arrangement as shown in Fig. (6.6), the load was distributed to two points at distance 304.8 mm (12 in) centre to centre, the bending moment across the central part between the two point loads being then constant at $\frac{1}{5}\bar{P}L$.

6.6 MEASUREMENTS OF MEMBRANE FORCE AND CENTRAL DEFLECTION

The membrane force exerted on the specimen when a slab was loaded was measured by resistance foil strain gauges (Fig. 6.7) mounted on the surface of each of the four tie bars. Two active gauges were used on each tie bar, one of which was mounted on the top surface of the bar and the other one on the bottom surface. These two gauges were wired in series in one arm of the strain gauge bridge and their resistance change was measured and compared with two similar dummy gauges wired in series in the other arm of the bridge. In this way, any effects of bending strains in the tie bars were eliminated. At each stage of loading, the readings from the strain gauge bridge were measured for each tie bar. The total value of these strain readings multiplied by 58.7×10^6 N or 13.3×10^6 lbf (i.e. Young's Modulus of Elasticity x cross sectional area of one tie bar) gave the measure of the membrane force. This measurement was checked by using a hydraulic jack system (see Photo 6.1) applied in the same position as the resultant membrane force in the slabs which confirmed that the measurements of the membrane force by the strain gauges were reliable with a maximum error of $\pm 1\%$.

The deflection at the centre of the slab was measured using a transducer of 101.6 mm (4 in) travel and a digital voltmeter.

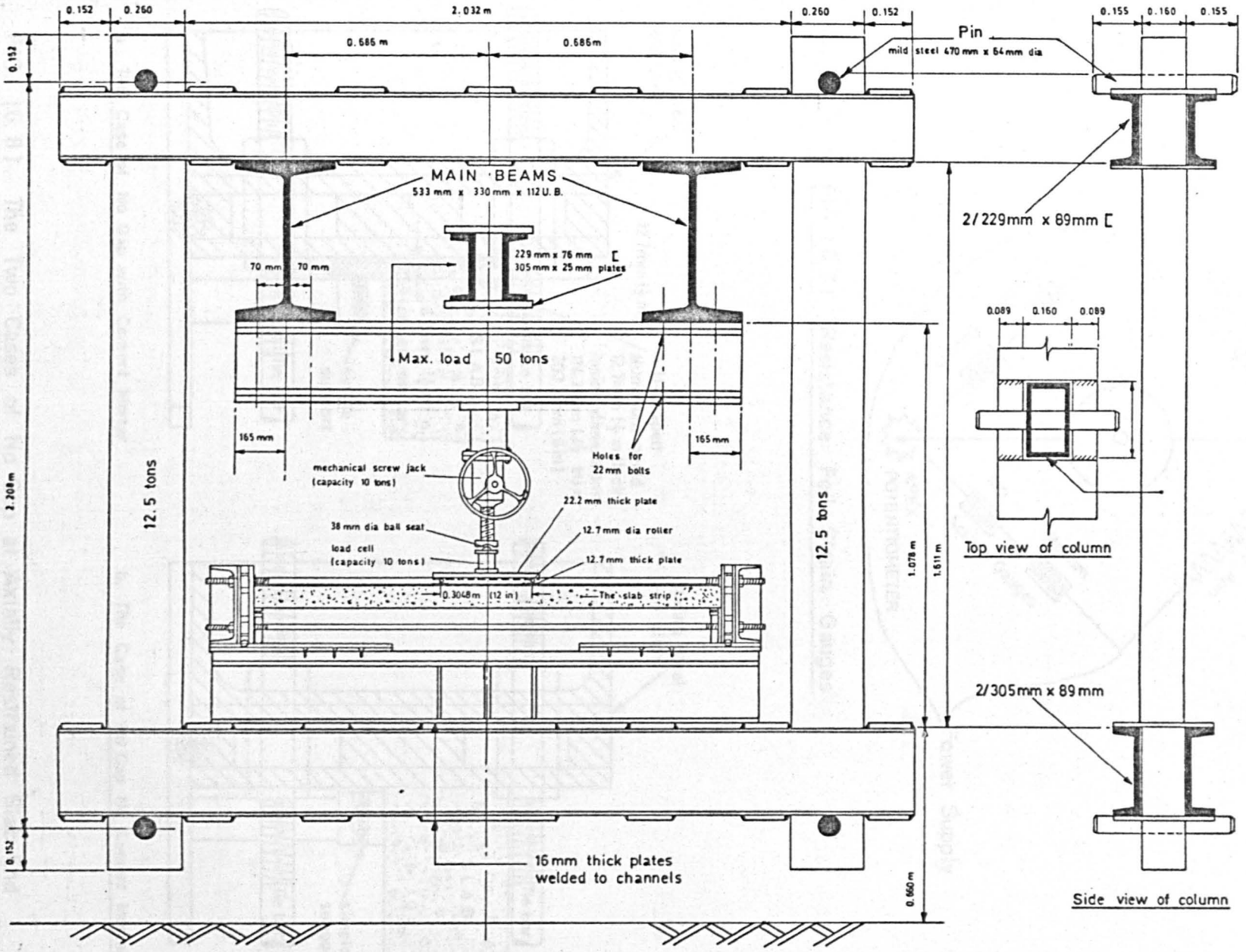

FIG. (6.6) The Loading System

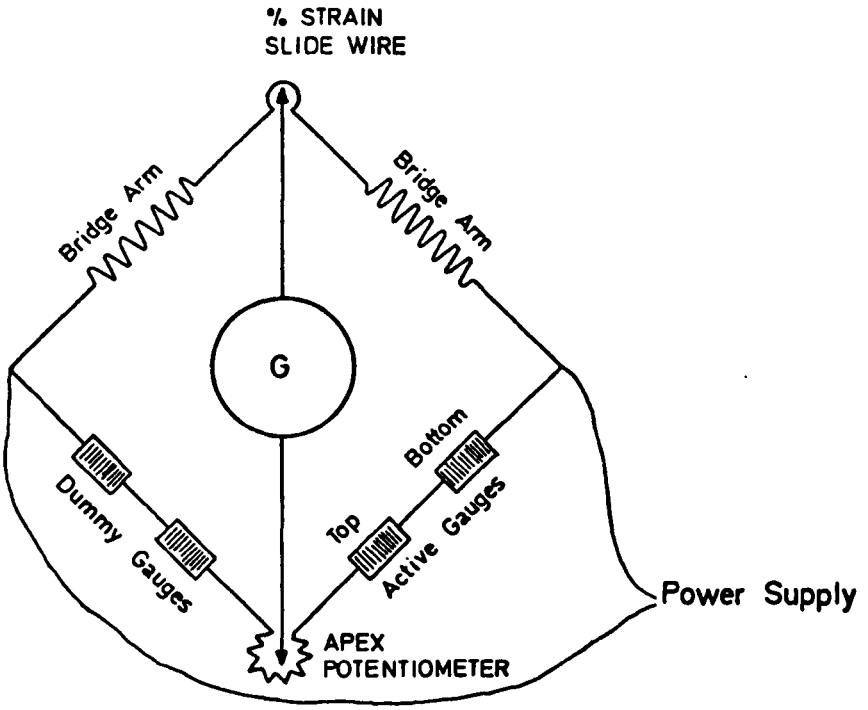

FIG. (6.7) Resistance Foil Strain Gauges

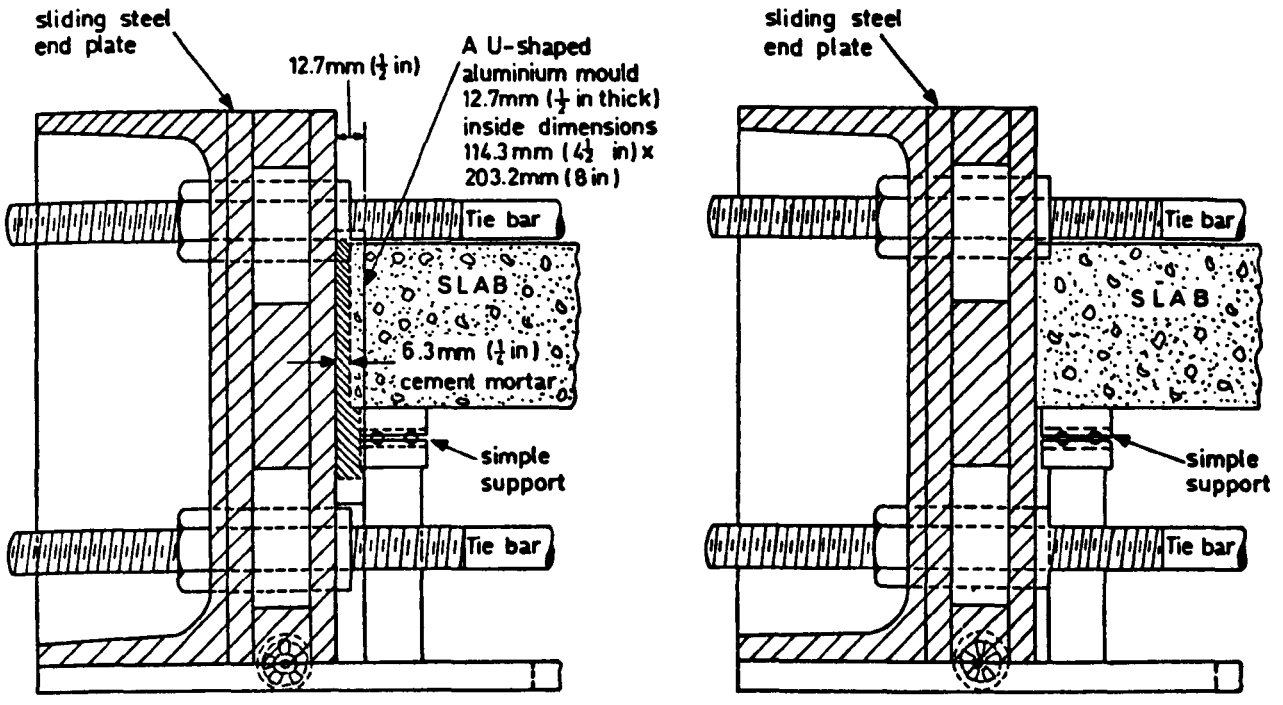

a. The Case of No Gap with Cement Mortar

b. The Case of No Gap No Cement Mortar

FIG. (6.8) The Two Cases of No Gap at Axially Restrained Slab End

6.7 MEASUREMENT OF THE ELASTIC STIFFNESS OF THE SURROUND S_s

The stiffness factor $\bar{S}$ has been introduced in Chapter 5 to represent the combined effect of the elastic stiffness of the whole slab strip S_b and the elastic stiffness of the two surrounds S_s. For a specific slab strip with known properties, S_b can be determined according to Eq. (5.3) and S_s (for the testing rig shown in Fig. 6.4) is the membrane force per unit movement of the two steel end plates at the point of application of the membrane force. If the two steel end plates had been infinitely stiff the elastic stiffness of the two surrounds would have been represented by the sum of the elastic stiffnesses of the four tie bars which is given by ;

$$\Sigma(S_s)_{\text{tie bar}} = 4\,\frac{(A_s)_{tb}\,(E_s)_{tb}}{L_{tb}} = 0.140 \times 10^6 \text{ N/mm } (0.802 \times 10^6 \text{ lbf/in})$$

where

$(A_s)_{tb}$: Cross sectional area of one tie bar
$= 285.0 \text{ mm}^2$ (0.4418 in^2)

$(E_s)_{tb}$: Young's Modulus of Elasticity of the steel
$= 0.207 \times 10^6 \text{ N/mm}^2$ $(30.1 \times 10^6 \text{ lbf/in}^2)$

L_{tb} : Length of the tie bar measured between the two nuts
$= 1.6795$ m (66.125 in) for the case of no gap.

Thus for unit width of the slab, $\Sigma(S_s)_{\text{tie bar}} = 689 \text{ N/mm}^2$ $(100{,}250 \text{ lbf/in}^2)$. However, when the membrane force is generated the two steel end plates deform and the elastic stiffness of the two surrounds varies slightly across the width of the slab.

The testing rig had been designed so that the compressive force acting on the end plates was at the centre of the four tie bars for the maximum membrane force. The elastic deformation of the end plates was measured for this case of maximum membrane force and assumed to apply linearly for other values of $\bar{N}$.

In preliminary tests on slab strips, dial gauges were used to measure the total horizontal movement of the two surrounds due to deformation of the end plates (see Photo 6.2). The measurements were taken immediately after maximum membrane forces had been reached. S_s was

then determined according to the following ;

$$S_s = \frac{\frac{\frac{\bar{N}_{max}}{e_{s1}} + \frac{\bar{N}_{max}}{e_{s2}}}{2} + \frac{\bar{N}_{max}}{e_{s3}}}{2}$$

where $\bar{N}_{max}$: Total maximum membrane force; obtained by multiplying the highest sum of the four strain gauge readings by 58.7×10^6 N or 13.3×10^6 lbf (i.e. Young's Modulus of Elasticity x cross sectional area of one tie bar).

e_{s1}, e_{s2} : Total horizontal movement of the two steel end plates corresponding to $\bar{N}_{max}$ measured at the centre of each of the two end plate side stiffeners.

e_{s3} : Total horizontal movement of the two steel end plates corresponding to $\bar{N}_{max}$ measured at the centre of the end plate middle stiffener.

From four slab tests it was found that the values of the elastic stiffness of the two end plates measured at the centre of the two end plate side stiffeners, i.e. $\bar{N}_{max}/e_{s1}$ and $\bar{N}_{max}/e_{s2}$, were very slightly different (average difference 0.5%) but at the centre of the end plate middle stiffener $\bar{N}_{max}/e_{s3}$ was, as an average, 5% lower than the average of $\bar{N}_{max}/e_{s1}$ and $\bar{N}_{max}/e_{s2}$. However, S_s was calculated as the mean of these values which was 0.112×10^6 N/mm (0.637×10^6 lbf/in), and per unit width of the slab 550 N/mm^2 (79,700 lbf/in^2). Comparing this value with the sum of the elastic stiffnesses of the four tie bars gives a measure of the deformation of the two end plates at maximum membrane force.

Another interesting comparison may be made between the values of S_s and S_b. The values of the latter varied from 1481 N/mm^2 (214,500 lbf/in^2) for S17 to 2087 N/mm^2 (302,600 lbf/in^2) for S6 giving a variation of $\bar{S}$ from 8.84 (λ = 0.271) to 5.40 (λ = 0.208) respectively. For an average value of S_b, the ratio of the elastic stiffness of the two surrounds to that of the slab was 0.31 which illustrates the low stiffness of the restraining frame.

6.8 CASTING AND TESTING OF SLABS

(a) CASTING

The base and the two longitudinal sides of the slab mould were made of steel channels bolted together whereas the two ends were equal steel angles which gave smooth and vertical ends to the slab strips. The base of the mould was covered with a teak wood finish to produce a smooth under surface for the slab strips and to give the required internal dimensions of the mould. All joints in the mould were filled with plastercene. The slab mould and the three 152.4 mm (6 in) cube moulds were thoroughly oiled before use.

The two reinforcing bars in the slab strips of series I and II were placed at distance 127 mm (5 in) centre to centre whereas in the slab strips of series III there were five steel bars at distance 31.8 mm (1¼ in) centre to centre. All the steel bars were 1.473 m (58 in) long without hooks. Transverse ties consisting of 2.38 mm (0.094 in) steel bars were used at 304.8 mm (12 in) centres to position the main steel. 12 mm (0.472 in) plastic blocks were used to provide the correct cover to the main reinforcement in the mould.

The concrete was mixed in a 0.0566 cu.m (2 cu.ft) horizontal paddle type pan mixer for 2 minutes. The casting of the slab strips and the control cubes was done on a vibrating table (frequency 3000 cycles per minute). The concrete was placed in 25.4 mm (1 in) layers and compacted well by varying the amplitude of vibration in a low-high-low cycle during the casting operation. The top surface was carefully levelled at the end. The time of placing and compaction was maintained uniform for all the slabs at approximately 15 minutes. After 24 hours the

slab and the three cubes were de-moulded and cured in thick polythene bags for 28 days.

(b) TESTING

The slab strip to be tested was placed symmetrically in the rig on the two simple supports. The slabs had a projection of 3.2 mm ($\frac{1}{8}$ in) at each support which prevented contact between the simple supports and the end plates.

To permit easy and accurate measurement of the central deflection of the slab, a thin plate of perspex 25.4 mm (1 in) wide was firmly glued onto the bottom face of the slab centre for the transducer contact. On the top surface of the slab the loading arrangement shown in Fig.(6.6) was set up. Before the test programme was performed, the voltage stabilizer was set and the load cell, the load and deflection digital voltmeters and the strain gauge galvanometer were all accurately zeroed.

The gap conditions at the slab ends were arranged as follows :

i. No gap with cement mortar :

The first pair of slab strips in each series was tested by using cement mortar to completely fill the gaps at the slab ends.

A U-shaped aluminium mould, see Fig. (6.8a) and Photo (6.4), was screwed onto the front surface (shown in Fig. 6.5) of each steel end plate. With the slab strip in position over the supports and the loading system on top of the slab the nuts of the four 19 mm ($\frac{3}{4}$ in) tie bars were turned until the bases of the aluminium moulds just came into contact with the webs of the supports and each strain gauge just started to indicate a reading. The contact of the aluminium moulds with the webs of the supports left a gap 6.35 mm ($\frac{1}{4}$ in) wide between each slab end and its corresponding end plate. This gap was then filled with cement mortar of the quality and proportions described in section 6.2. The cement mortar was fairly workable and placed in layers, each layer being compacted well by using a 2.38 mm (0.094 in) diameter steel rod. The top surface of the cement mortar was levelled with the top surface of the slab and left for 24 hours before loading was applied on the slab. The cube strength of the mortar fill was at least 69 N/mm^2 (10,000 lbf/in^2) compared with the maximum cube strength of the slab concrete 51.3 N/mm^2 (7435 lbf/in^2) so there was no possibility

of failure of the mortar instead of the slab concrete (Photo 6.4).

ii. No gap, No cement mortar :

This case applied to the second pair of slab strips in each series. The ends of the slab were arranged to be in contact with the end plates without using any cement mortar, as shown in Fig. (6.8b). With the slab strip in position over the supports and the loading system on top of the slab, the nuts of the four 19 mm ($\frac{3}{4}$ in) tie bars were turned until both end plates just came into contact with the vertical end surfaces of the slab strips and each strain gauge just started to indicate a reading. Under these conditions there was an effective gap at the slab ends and this will be shown in Section 6.9 to be equivalent to a uniform gap of width 0.18 mm (0.007 in). This figure represents an average value established theoretically by comparing the experimental results of this case with those found in case (i) using cement mortar filling.

iii. Specified gap width :

The remainder of the slab strips were tested after adjustment of the end plates to provide a specified gap width. The slab strip was first set according to case (ii) and thereafter each nut at each tie bar was turned the same number of scale divisions to produce a uniform gap of the specified width.

Increments of deflection of the order 0.25 mm (0.01 in) were used for early stages of deformation, 0.76 mm (0.03 in) for advanced stages of increasing membrane force (prior to maximum yield load) and the early part of decreasing membrane force, and 1.27 mm (0.05 in) for later stages of decreasing membrane force. Readings of the load, the central deflection and the strains in the four tie bars were recorded for each deflection increment. At each stage of loading the side faces of the slab between the two point loads were examined for cracks. Reinforced slabs were loaded until the final stage of pure flexure was well defined and the yield load became constant. Unreinforced slabs were loaded up to sudden failure. At the end of the test the shape of the collapse mechanism was sketched and the distance between the central plastic hinge and mid-span was measured. Photographs were taken of the collapse mode (Photo 6.3), the crushing on the top surface

of the slab at the central plastic hinge (Photo 6.5) and on the bottom surface at the ends (Photo 6.6). These photographs illustrate the large depth of the compression zone due to the membrane force in these slab strip tests.

6.9 RESULTS AND DISCUSSION

The following data is presented in tables (6.4) for each slab strip tested ;

i. The distance of the central plastic hinge from mid-span c .

ii. The experimental dimensionless* values of the maximum yield load $\frac{(P_{max})_E}{P_y}$, the maximum membrane force $\frac{(N_{max})_E}{T_o}$ and the corresponding central deflections $\frac{(w_o)_E}{d}$.

iii. The theoretical† dimensionless* values of the maximum yield load $\frac{(P_{max})_T}{P_y}$, the maximum membrane force $\frac{(N_{max})_T}{T_o}$ and the corresponding central deflections $\frac{(w_o)_T}{d}$, based on average values of the concrete cube strength $(u)_{ave}$ and the location of the central plastic hinge from mid-span $(c)_{ave}$ for the pair of similar slab strips.

iv. The ratios of the experimental 'average' values to the theoretical values of the maximum yield load $\frac{(P_{max})_{Eave}}{(P_{max})_T}$, the maximum membrane force $\frac{(N_{max})_{Eave}}{(N_{max})_T}$ and the corresponding central deflections $\frac{(w_o)_{Eave}}{(w_o)_T}$.

v. The dimensionless value of the yield load at the first visible crack $\frac{P_c}{P_y}$ for reinforced strips and P_c for unreinforced strips.

Figs. (6.9) show the experimental and theoretical variation of the yield load and the membrane force with the central deflection for all slab strips tested. To visualise the effect of gap on behaviour, separate figures are shown for each series.

---

* For unreinforced slabs, the values of the yield load and the membrane force are given in dimensional form since P_y and T_o are zero.

† The theoretical values given in tables (6.4) were obtained from Eqs. (5.15) for reinforced slab strips and from Eqs. (5.16) for unreinforced strips.

Series No.	Type of slab	Slab mark	Cube Strength (u) N/mm²	Cube Strength (u) lbf/in²	Average Cube Strength $(u)_{ave.}$ N/mm²	Average Cube Strength $(u)_{ave.}$ lbf/in²	$\frac{A_s}{d_1} \times \frac{f_y}{u}$ per unit width	Gap width (Δ) mm	Gap width (Δ) in	c mm	c in	c_{ave} mm	c_{ave} in	EXPERIMENTAL RESULTS $\frac{(P_{max})_E}{P_y}$	$\frac{(P_{max})_{Eave}}{P_y}$	$\frac{(w_o)_E}{d}$ @ P_{max}	$\frac{(w_o)_{Eave}}{d}$ @ P_{max}	$\frac{(N_{max})_E}{T_o}$	$\frac{(N_{max})_{Eave}}{T_o}$	$\frac{(w_o)_E}{d}$ @ N_{max}	$\frac{(w_o)_{Eave}}{d}$ @ N_{max}	THEORETICAL PREDICTIONS $\frac{(P_{max})_T}{P_y}$	$\frac{(w_o)_T}{d}$ @ P_{max}	$\frac{(N_{max})_T}{T_o}$	$\frac{(w_o)_T}{d}$ @ N_{max}	COMPARISON $\frac{(P_{max})_{Eave}}{(P_{max})_T}$	$\frac{(w_o)_{Eave}}{(w_o)_T}$ @ P_{max}	$\frac{(N_{max})_{Eave}}{(N_{max})_T}$	$\frac{(w_o)_{Eave}}{(w_o)_T}$ @ N_{max}	Load @ 1st visible crack $\frac{P_c}{P_y}$
I	REINFORCED	S1	48.3	7010	49.8	7215	0.0223	0	0	61	2.4	56	2.2	7.27	7.53	0.240	0.242	6.70	7.09	0.271	0.262	6.89	0.150	8.15	0.380	1.09	1.61	0.87	0.69	1.62
		S2	51.2	7420						51	2.0			7.79		0.244		7.48		0.253										1.69
		S3	48.8	7080	50.1	7265	0.0221	0.18	0.007	76	3.0	76	3.0	6.30	6.13	0.184	0.172	5.82	5.98	0.350	0.350	6.31	0.170	7.61	0.400	0.97	1.01	0.79	0.88	1.48
		S4	51.4	7450						76	3.0			5.96		0.160		6.14		0.350										1.35
		S5	54.5	7910	54.8	7940	0.0202	0.69	0.027	89	3.5	89	3.5	4.92	5.04	0.244	0.237	5.05	5.13	0.430	0.430	5.08	0.250	6.49	0.490	0.99	0.95	0.79	0.88	1.05
		S6	55.0	7970						89	3.5			5.16		0.230		5.21		0.430										1.12
		S7	53.3	7730	53.0	7685	0.0209	1.45	0.057	51	2.0	51	2.0	3.10	3.04	0.329	0.327	3.16	3.16	0.470	0.510	3.28	0.380	4.39	0.630	0.93	0.86	0.72	0.81	1.02
		S8	52.7	7640						51	2.0			2.98		0.325		3.16		0.550										0.98
		S9	51.3	7445	52.0	7545	0.0213	2.21	0.087	64	2.5	64	2.5	2.36	2.20	0.420	0.427	2.65	2.44	0.600	0.625	2.08	0.500	2.69	0.720	1.05	0.85	0.91	0.87	1.00
		S10	52.7	7645						64	2.5			2.04		0.434		2.23		0.650										0.97

TABLE (6.4a) Experimental Results and Comparison with Theoretical Predictions ((Series I, Reinforced))

Series No.	Type of Slab	Slab mark	Cube Strength (u)		Average Cube Strength $(u)_{ave.}$		$\frac{A_s}{d_1} \times \frac{f_y}{u}$ per unit width	Gap width (Δ)		c		c_{ave}		EXPERIMENTAL RESULTS								THEORETICAL PREDICTIONS				COMPARISON				Load @ 1st visible crack $\frac{P_t}{P_y}$
			N/mm²	lbf/in²	N/mm²	lbf/in²		mm	in	mm	in	mm	in	$\frac{(P_{max})_E}{P_y}$	$\frac{(P_{max})_{E_{ave}}}{P_y}$	$\frac{(w_o)_E}{d}$ @ P_{max}	$\frac{(w_o)_{E_{ave}}}{d}$ @ P_{max}	$\frac{(N_{max})_E}{T_o}$	$\frac{(N_{max})_{E_{ave}}}{T_o}$	$\frac{(w_o)_E}{d}$ @ N_{max}	$\frac{(w_o)_{E_{ave}}}{d}$ @ N_{max}	$\frac{(P_{max})_T}{P_y}$	$\frac{(w_o)_T}{d}$ @ P_{max}	$\frac{(N_{max})_T}{T_o}$	$\frac{(w_o)_T}{d}$ @ N_{max}	$\frac{(P_{max})_{E_{ave}}}{(P_{max})_T}$	$\frac{(w_o)_{E_{ave}}}{(w_o)_T}$ @ P_{max}	$\frac{(N_{max})_{E_{ave}}}{(N_{max})_T}$	$\frac{(w_o)_{E_{ave}}}{(w_o)_T}$ @ N_{max}	
II	REINFORCED	S17	27.6	4005	27.7	4010	0.0401	0	0	102	4.0	107	4.2	5.24	5.28	0.200	0.202	5.20	5.30	0.255	0.255	5.03	0.115	5.68	0.300	1.05	1.76	0.93	0.85	1.58
		S18	27.7	4015						112	4.4			5.32		0.204		5.40		0.255										1.63
		S19	30.6	4440	30.9	4480	0.0359	0.18	0.007	38	1.5	38	1.5	4.97	4.99	0.180	0.187	4.40	4.64	0.250	0.252	4.89	0.165	5.65	0.390	1.02	1.13	0.82	0.65	1.32
		S20	31.2	4520						38	1.5			5.01		0.194		4.88		0.254										1.34
		S21	30.1	4360	30.2	4370	0.0368	0.69	0.027	76	3.0	69	2.7	3.72	3.72	0.229	0.232	3.72	3.62	0.355	0.377	3.72	0.245	4.41	0.480	1.00	0.95	0.82	0.79	1.06
		S22	30.2	4380						61	2.4			3.72		0.235		3.52		0.399										1.09
		S23	29.9	4330	30.3	4390	0.0366	1.19	0.047	140	5.5	122	4.8	3.10	3.04	0.305	0.307	3.00	2.92	0.435	0.450	2.91	0.300	3.49	0.520	1.04	1.02	0.84	0.87	1.02
		S24	30.7	4450						104	4.1			2.98		0.309		2.84		0.465										0.98
		S25	29.8	4315	29.2	4235	0.0379	2.21	0.087	51	2.0	99	3.9	1.58	1.68	0.440	0.435	1.32	1.44	0.684	0.637	1.72	0.440	1.82	0.630	0.98	0.99	0.79	1.01	0.93
		S26	28.6	4155						147	5.8			1.78		0.430		1.56		0.590										1.02

TABLE (6.4b) Experimental Results and Comparison with Theoretical Predictions ((Series II, Reinforced))

Series No.	Type of slab	Slab mark	Cube Strength (u)		Average Cube Strength $(u)_{ave}$		$\frac{A_s}{d_1} \times \frac{f_y}{u}$ per unit width	Gap width (Δ)		c		c_{ave}		EXPERIMENTAL RESULTS								THEORETICAL PREDICTIONS				COMPARISON				Load @ 1st visible crack $\frac{P_c}{P_y}$
			N/mm^2	lbf/in^2	N/mm^2	lbf/in^2		mm	in	mm	in	mm	in	$\frac{(P_{max})_E}{P_y}$	$\frac{(P_{max})_{Eave}}{P_y}$	$\frac{(w_o)_E}{d}$ @ P_{max}	$\frac{(w_o)_{Eave}}{d}$ @ P_{max}	$\frac{(N_{max})_E}{T_o}$	$\frac{(N_{max})_{Eave}}{T_o}$	$\frac{(w_o)_E}{d}$ @ N_{max}	$\frac{(w_o)_{Eave}}{d}$ @ N_{max}	$\frac{(P_{max})_T}{P_y}$	$\frac{(w_o)_T}{d}$ @ P_{max}	$\frac{(N_{max})_T}{T_o}$	$\frac{(w_o)_T}{d}$ @ N_{max}	$\frac{(P_{max})_{Eave}}{(P_{max})_T}$	$\frac{(w_o)_{Eave}}{(w_o)_T}$ @ P_{max}	$\frac{(N_{max})_{Eave}}{(N_{max})_T}$	$\frac{(w_o)_{Eave}}{(w_o)_T}$ @ N_{max}	
III	REINFORCED	S29	38.8	5625	38.8	5625	0.0714	0	0	0	0	0	0	2.67	2.61	0.214	0.212	2.24	2.26	0.274	0.267	2.69	0.140	2.59	0.370	0.97	1.51	0.87	0.72	1.48
		S30	38.8	5625						0	0			2.55		0.210		2.28		0.260										1.41
		S31	40.9	5925	39.7	5755	0.0698	0.18	0.007	61	2.4	30	1.2	2.49	2.52	0.170	0.180	1.99	1.98	0.280	0.265	2.52	0.165	2.42	0.380	1.00	1.09	0.82	0.70	1.28
		S32	38.5	5585						0	0			2.55		0.190		1.97		0.250										1.38
		S33	37.7	5475	39.4	5720	0.0702	0.69	0.027	51	2.0	56	2.2	1.88	2.00	0.235	0.252	1.37	1.46	0.350	0.325	2.03	0.260	1.86	0.490	0.98	0.97	0.78	0.66	0.84
		S34	41.1	5965						61	2.4			2.12		0.269		1.55		0.300										0.89
		S35	40.0	5795	38.1	5520	0.0728	1.19	0.047	51	2.0	43	1.7	1.40	1.46	0.285	0.290	0.85	0.89	0.470	0.420	1.65	0.350	1.36	0.570	0.89	0.83	0.66	0.74	0.72
		S36	36.2	5245						36	1.4			1.52		0.295		0.93		0.370										0.80

TABLE (6.4c) Experimental Results and Comparison with Theoretical Predictions ((Series III, Reinforced))

Series No.	Type of slab	Slab mark	Cube Strength (u)		Average Cube Strength $(u)_{ave}$		Gap Width (Δ)		c		c_{ave}		EXPERIMENTAL RESULTS								THEORETICAL PREDICTIONS				COMPARISON				Load @ 1st visible crack $\bar{P}_c$ Newtons (Pounds)
			N/mm²	lbf/in²	N/mm²	lbf/in²	mm	in	mm	in	mm	in	$(\bar{P}_{max})_E$ Newtons (Pounds)	$(\bar{P}_{max})_{Eave}$ Newtons (Pounds)	$\frac{(w_o)_E}{d}$ @ P_{max}	$\frac{(w_o)_{Eave}}{d}$ @ P_{max}	$(\bar{N}_{max})_E$ Newtons (Pounds)	$(\bar{N}_{max})_{Eave}$ Newtons (Pounds)	$\frac{(w_o)_E}{d}$ @ N_{max}	$\frac{(w_o)_{Eave}}{d}$ @ N_{max}	$(\bar{P}_{max})_T$ Newtons (Pounds)	$\frac{(w_o)_T}{d}$ @ P_{max}	$(\bar{N}_{max})_T$ Newtons (Pounds)	$\frac{(w_o)_T}{d}$ @ N_{max}	$\frac{(\bar{P}_{max})_{Eave}}{(\bar{P}_{max})_T}$	$\frac{(w_o)_{Eave}}{(w_o)_T}$ @ P_{max}	$\frac{(\bar{N}_{max})_{Eave}}{(\bar{N}_{max})_T}$	$\frac{(w_o)_{Eave}}{(w_o)_T}$ @ N_{max}	
IV	UNREINFORCED	S13	51.3	7435	50.5	7320	0	0	51	2.0	51	2.0	14440N (3246lb)	15135N (3403lb)	0.195	0.210	86520N (19450lb)	91080N (20475lb)	0.274	0.262	15310N (3441lb)	0.155	117820N (26488lb)	0.390	0.99	1.35	0.77	0.67	2130N (480lb)
		S14	49.7	7205					51	2.0			15830N (3560lb)		0.225		95640N (21500lb)		0.250										2360N (530lb)
		S15	54.0	7830	52.4	7590	0.18	0.007	112	4.4	94	3.7	14550N (3270lb)	14060N (3160lb)	0.209	0.202	90970N (20450lb)	87300N (19625lb)	0.284	0.327	14060N (3160lb)	0.175	112500N (25290lb)	0.410	1.00	1.15	0.78	0.80	2000N (450lb)
		S16	50.7	7350					76	3.0			13570N (3050lb)		0.195		83630N (18800lb)		0.370										1730N (390lb)

TABLE (6.4d) Experimental Results and Comparison with Theoretical Predictions ((Series IV, Unreinforced))

													EXPERIMENTAL RESULTS								THEORETICAL PREDICTIONS				COMPARISON				
Series No.	Type of slab	Slab mark	Cube Strength (u)		Average Cube Strength $(u)_{ave}$		Gap Width (Δ)		c		c_{ave}		$(\bar{P}_{max})_E$	$(\bar{P}_{max})_{Eave}$	$\frac{(w_o)_E}{d}$ @	$\frac{(w_o)_{Eave}}{d}$ @	$(\bar{N}_{max})_E$	$(\bar{N}_{max})_{Eave}$	$\frac{(w_o)_E}{d}$ @	$\frac{(w_o)_{Eave}}{d}$ @	$(\bar{P}_{max})_T$	$\frac{(w_o)_T}{d}$ @	$(\bar{N}_{max})_T$	$\frac{(w_o)_T}{d}$ @	$\frac{(\bar{P}_{max})_{Eave}}{(\bar{P}_{max})_T}$	$\frac{(w_o)_{Eave}}{(w_o)_T}$ @	$\frac{(\bar{N}_{max})_{Eave}}{(\bar{N}_{max})_T}$	$\frac{(w_o)_{Eave}}{(w_o)_T}$ @	Load @ 1st visible crack $\bar{P}_c$ Newtons (Pounds)
			N/mm²	lbf/in²	N/mm²	lbf/in²	mm	in	mm	in	mm	in	Newtons (Pounds)	Newtons (Pounds)	P_{max}	P_{max}	Newtons (Pounds)	Newtons (Pounds)	N_{max}	N_{max}	Newtons (Pounds)	P_{max}	Newtons (Pounds)	N_{max}		P_{max}		N_{max}	
V	UNREINFORCED	S39	37.9	5500	37.9	5495	0	0	102	4.0	76	3.0	12520 N (2815lb)	12365 N (2780lb)	0.190	0.187	80510 N (18100lb)	77845 N (17500lb)	0.274	0.262	12970 N (2915lb)	0.140	100710 N (22640lb)	0.350	0.95	1.34	0.77	0.75	1600 N (360 lb)
		S40	37.8	5490					51	2.0			12210 N (2745lb)		0.184		75180 N (16900lb)		0.250										1510 N (340lb)
		S41	36.6	5300	36.0	5210	0.18	0.007	86	3.4	69	2.7	10630 N (2390lb)	10400 N (2338lb)	0.200	0.192	82740 N (18600lb)	78960 N (17750lb)	0.330	0.325	11270 N (2534lb)	0.165	90850 N (20423lb)	0.390	0.92	1.16	0.87	0.83	1380 N (310 lb)
		S42	35.3	5120					51	2.0			10170 N (2285lb)		0.184		75180 N (16900lb)		0.320										1200 N (270lb)

TABLE (6.4e) Experimental Results and Comparison with Theoretical Predictions ((Series V, Unreinforced))

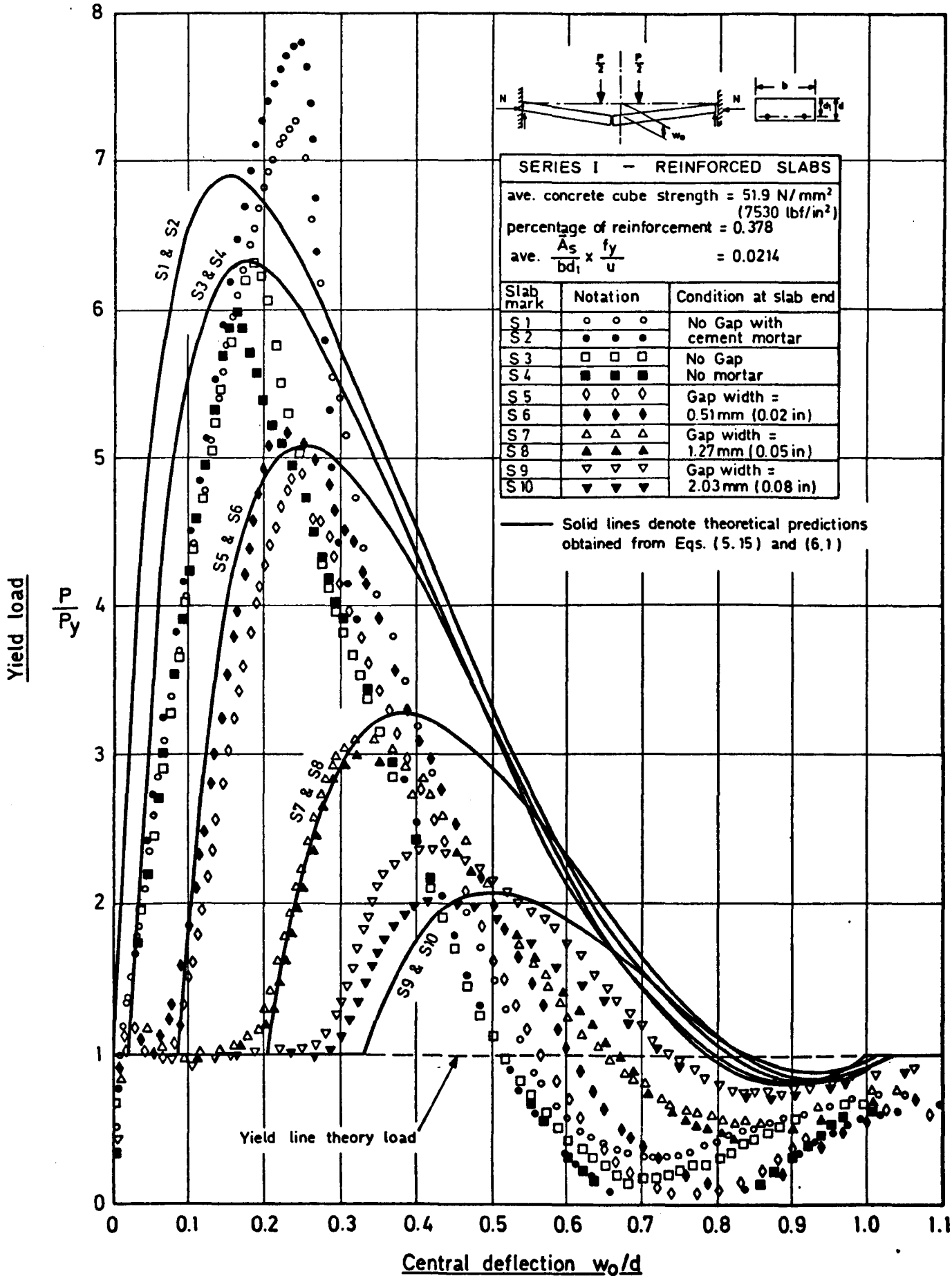

FIG. (6.9a) Experimental and Theoretical Relationship of the Yield Load with the Central Deflection ((Series I, Reinforced))

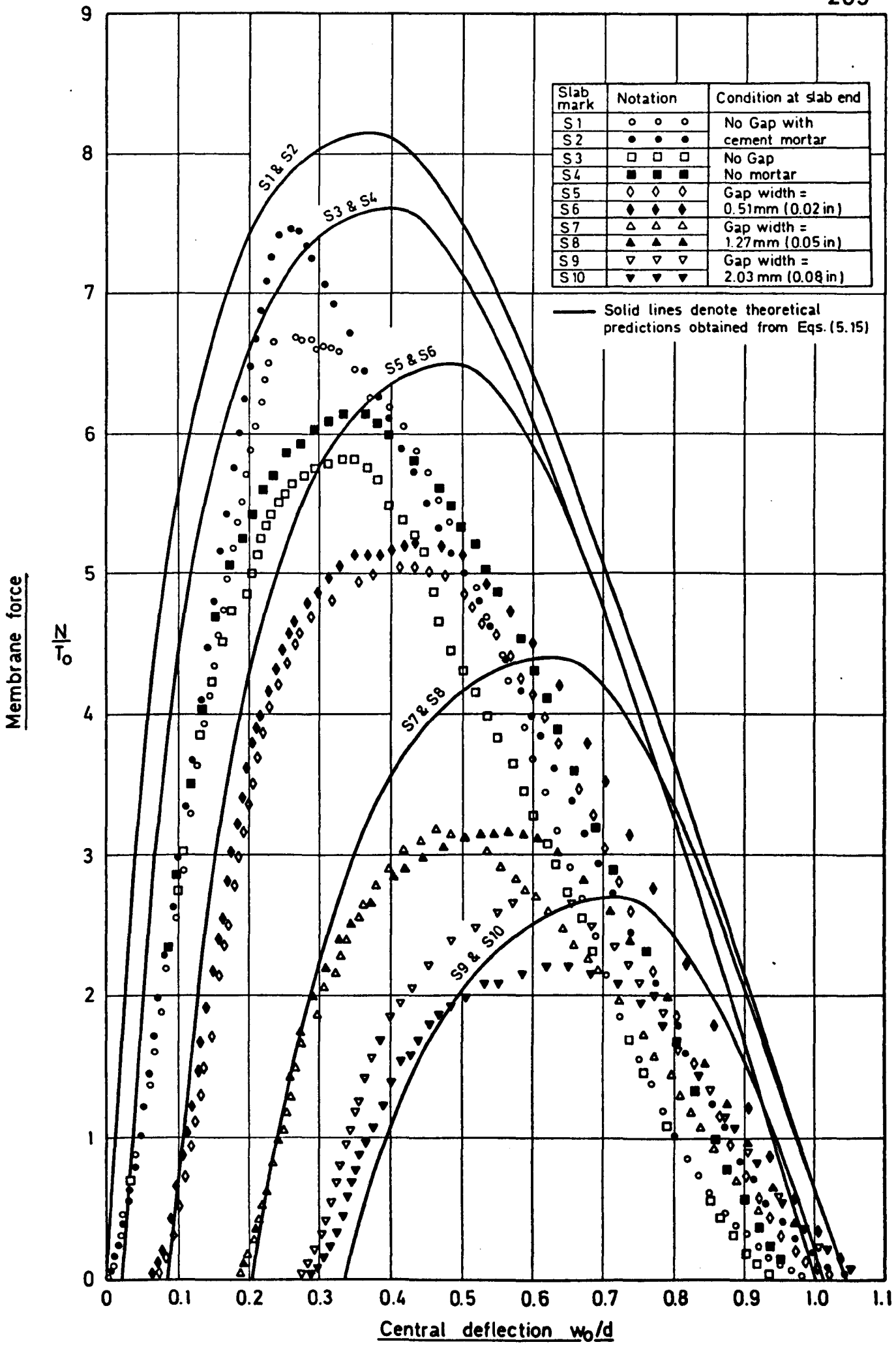

FIG. (6.9b) Experimental and Theoretical Relationship of the Membrane Force with the Central Deflection ((Series I, Reinforced))

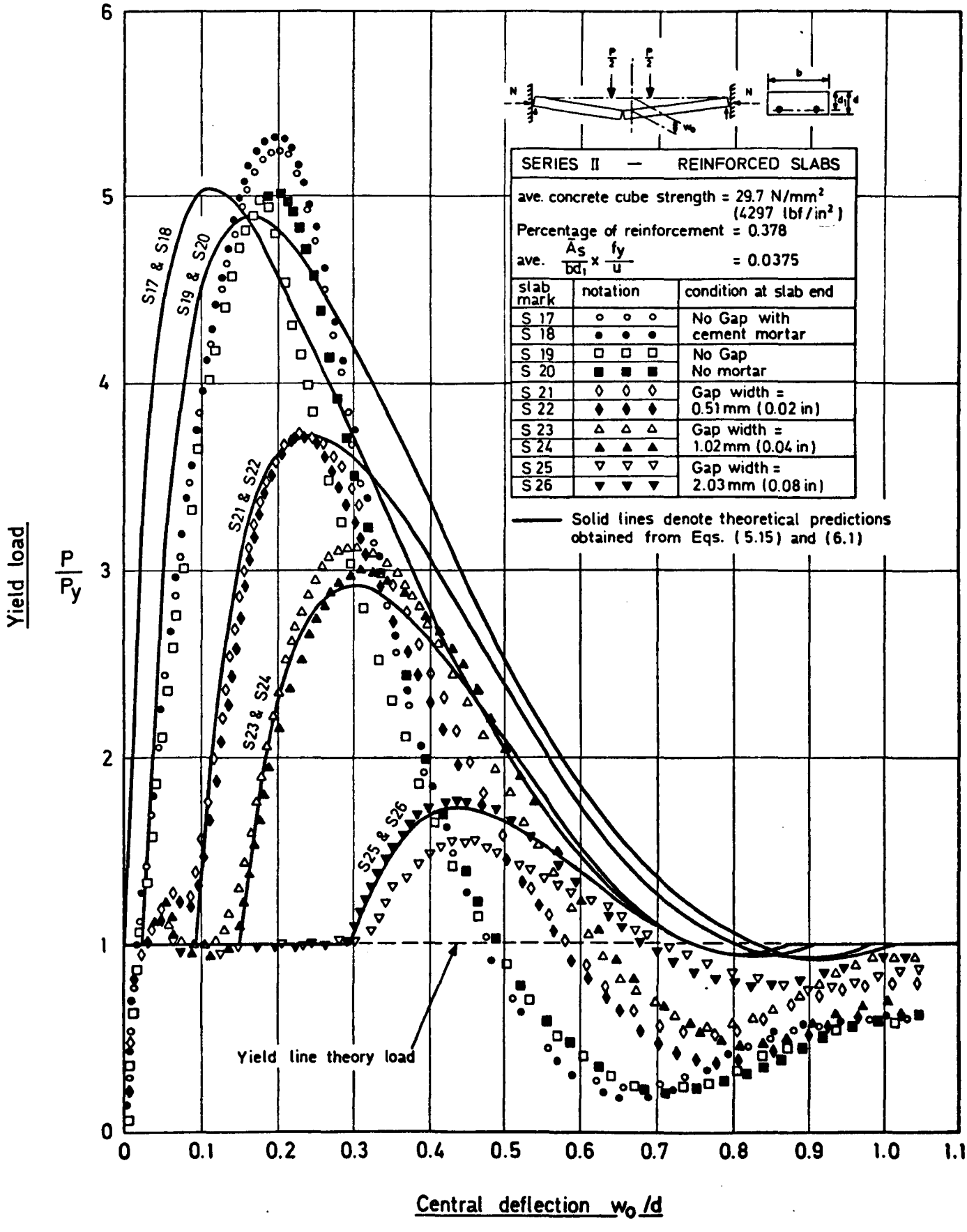

FIG. (6.9c) Experimental and Theoretical Relationship of the Yield Load with the Central Deflection ((Series II , Reinforced))

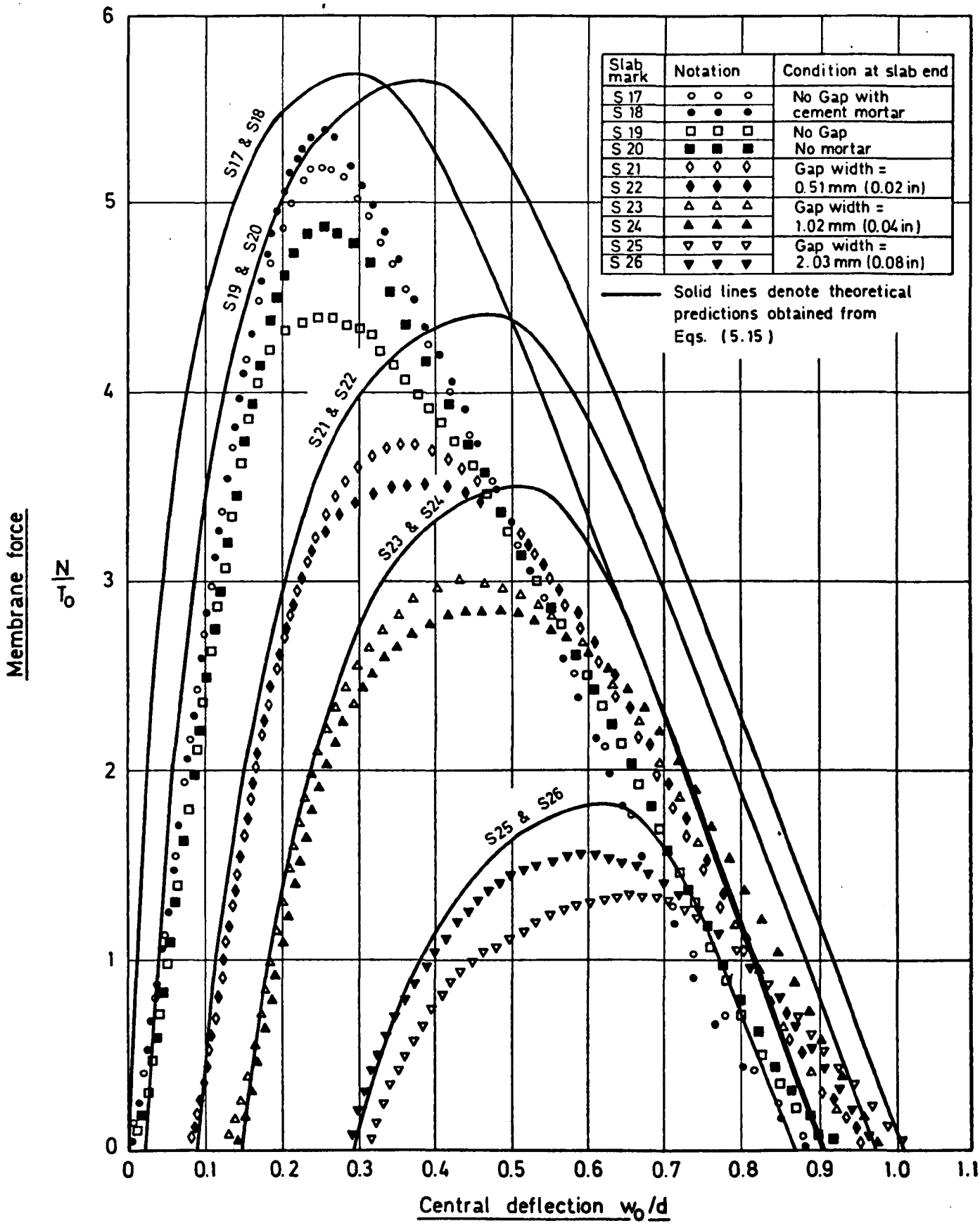

FIG. (6.9d) Experimental and Theoretical Relationship for the Membrane Force with the Central Deflection ((Series II, Reinforced))

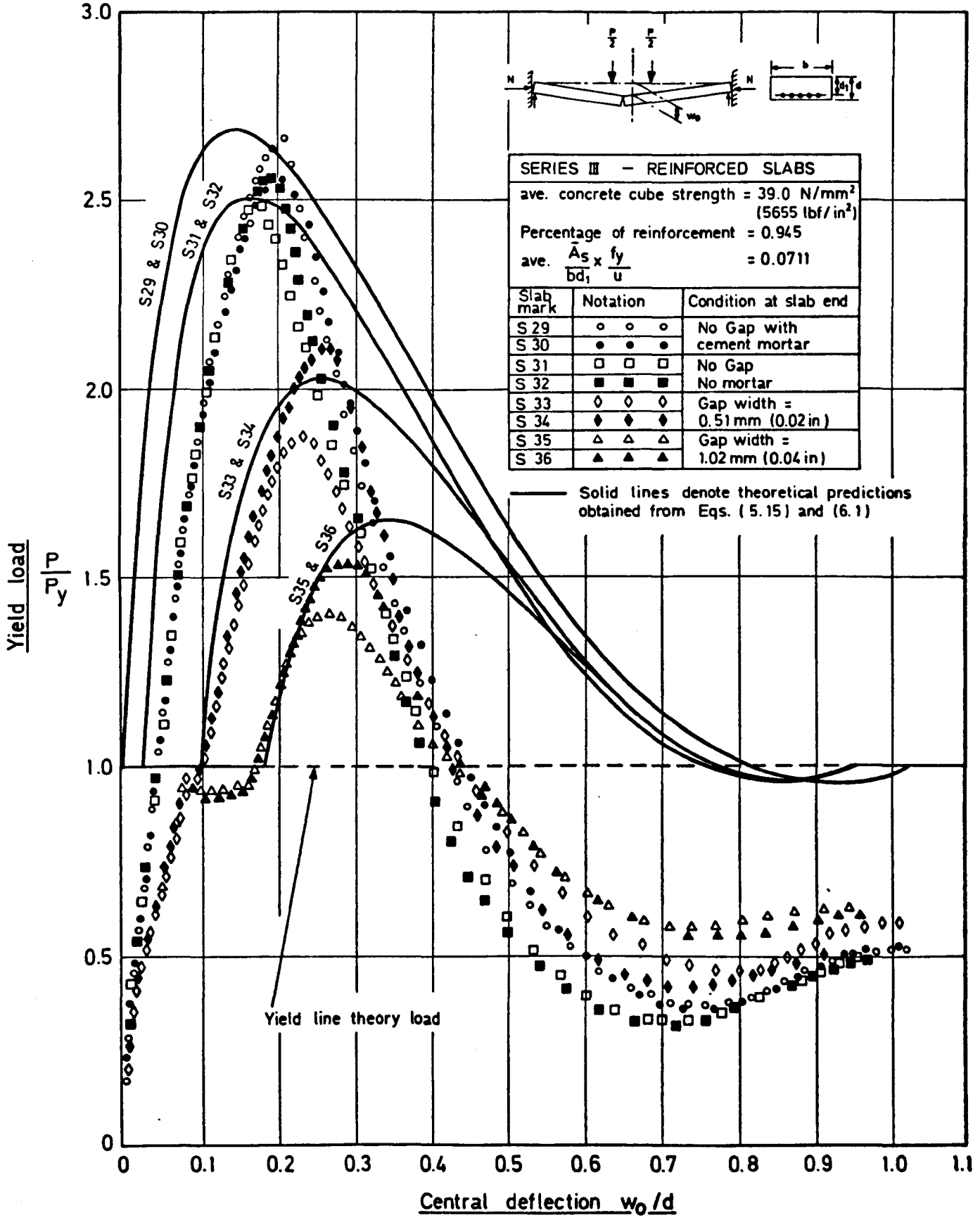

FIG. (6.9e) Experimental and Theoretical Relationship of the Yield Load with the Central Deflection ((Series III, Reinforced))

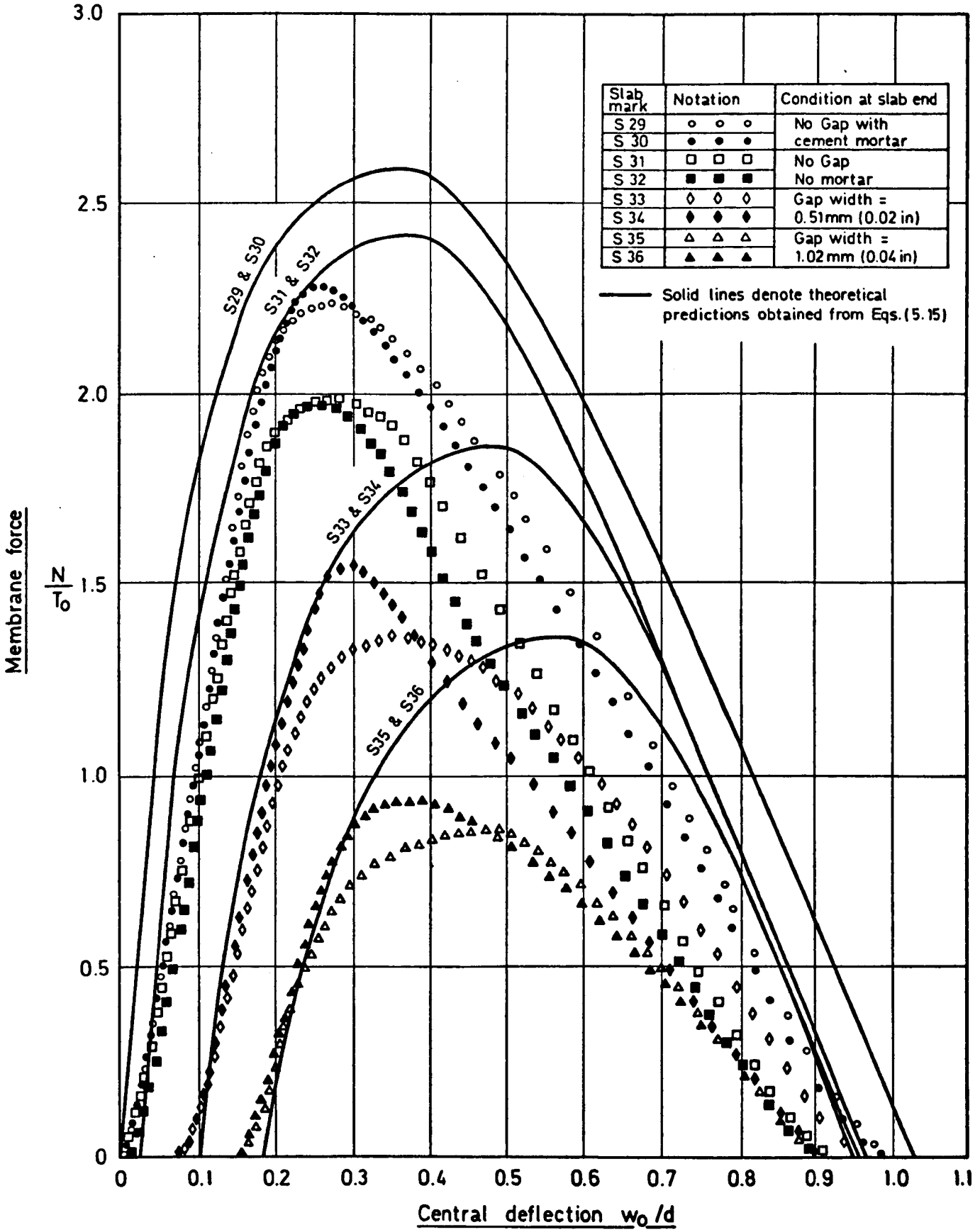

FIG. (6.9f) Experimental and Theoretical Relationship of the Membrane Force with the Central Deflection ((Series III, Reinforced))

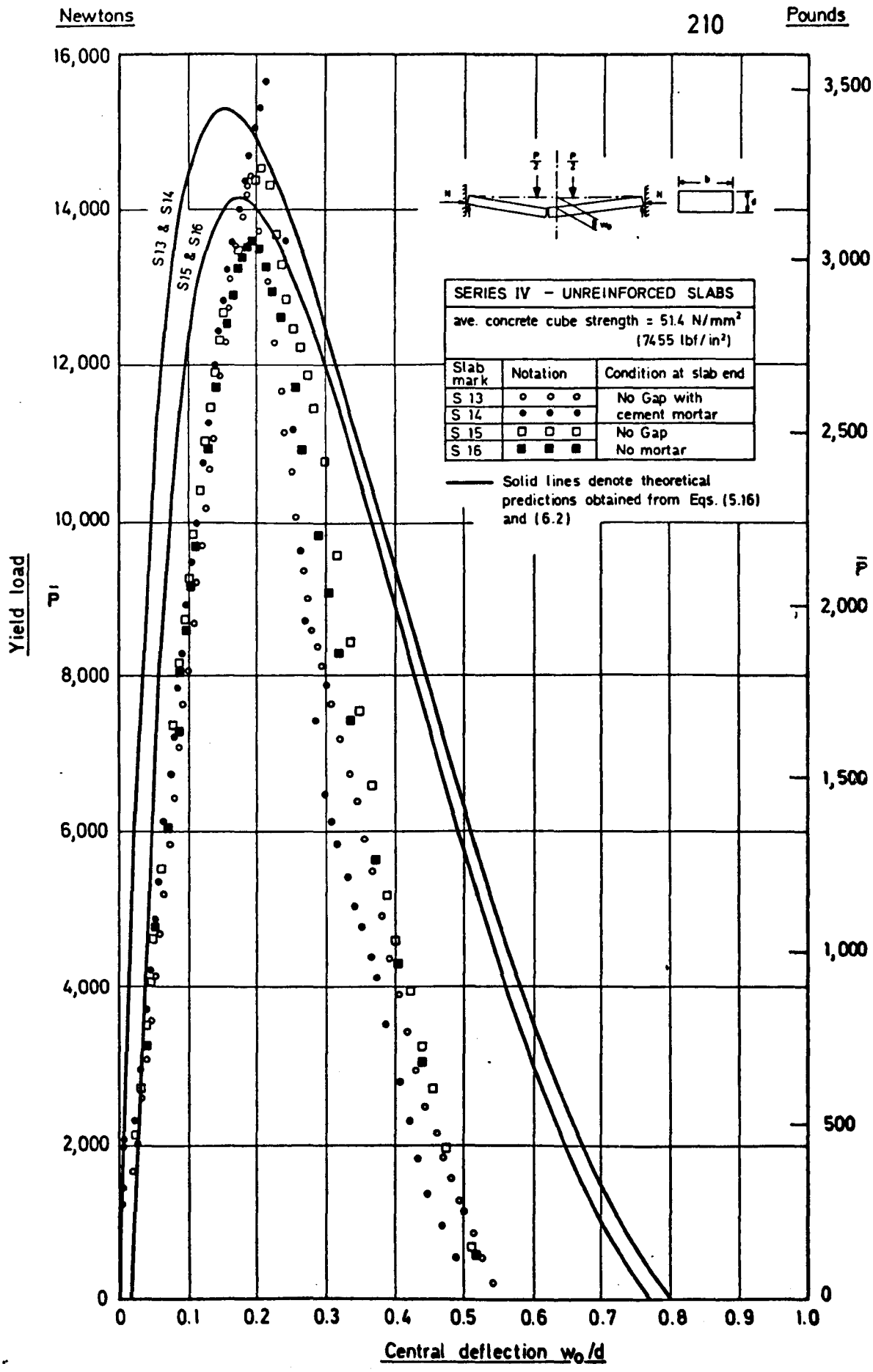

FIG. (6.9g) Experimental and Theoretical Relationship of the Yield Load with the Central Deflection ((Series IV, Unreinforced))

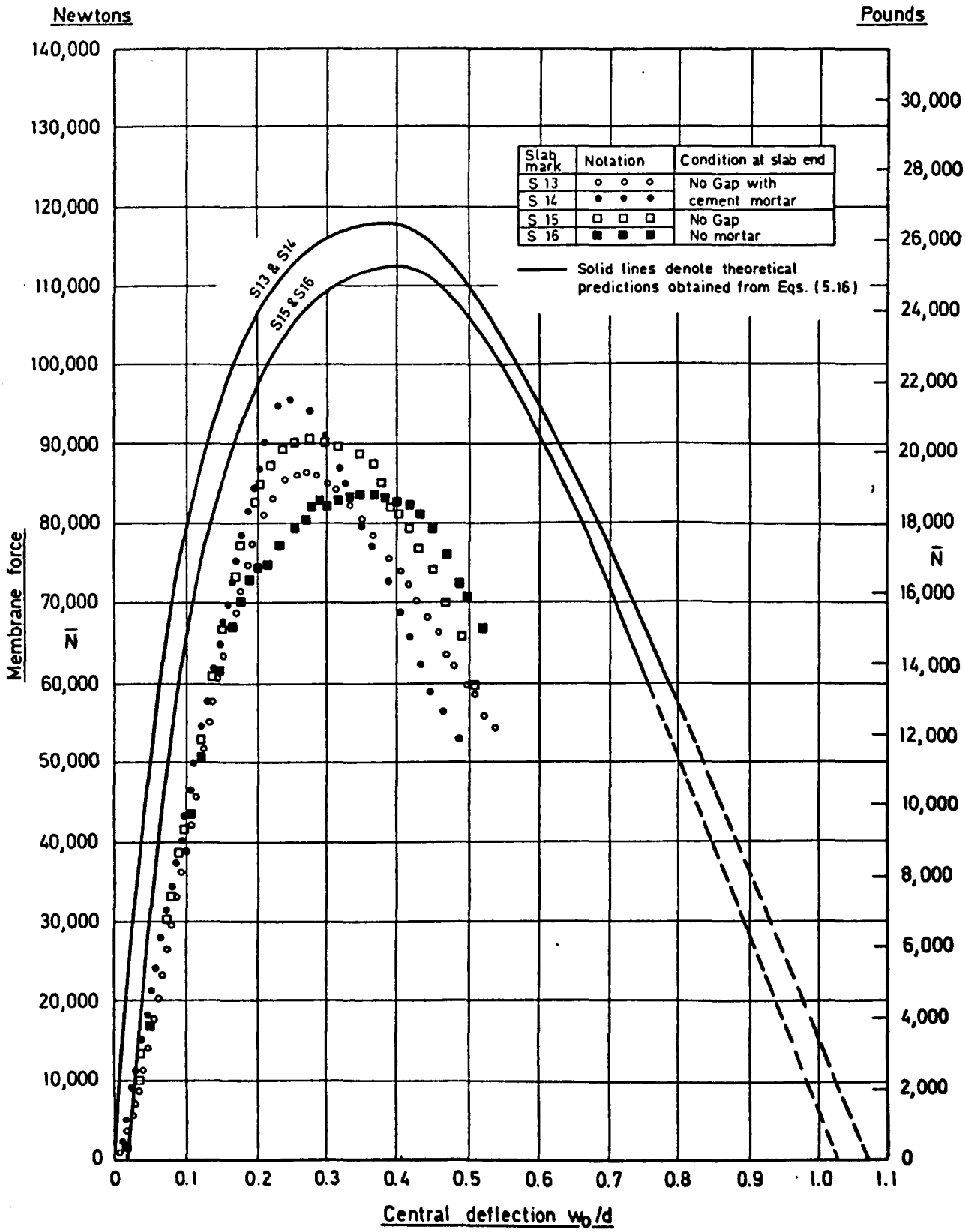

FIG. (6.9h) Experimental and Theoretical Relationship of the Membrane Force with the Central Deflection ((Series IV, Unreinforced))

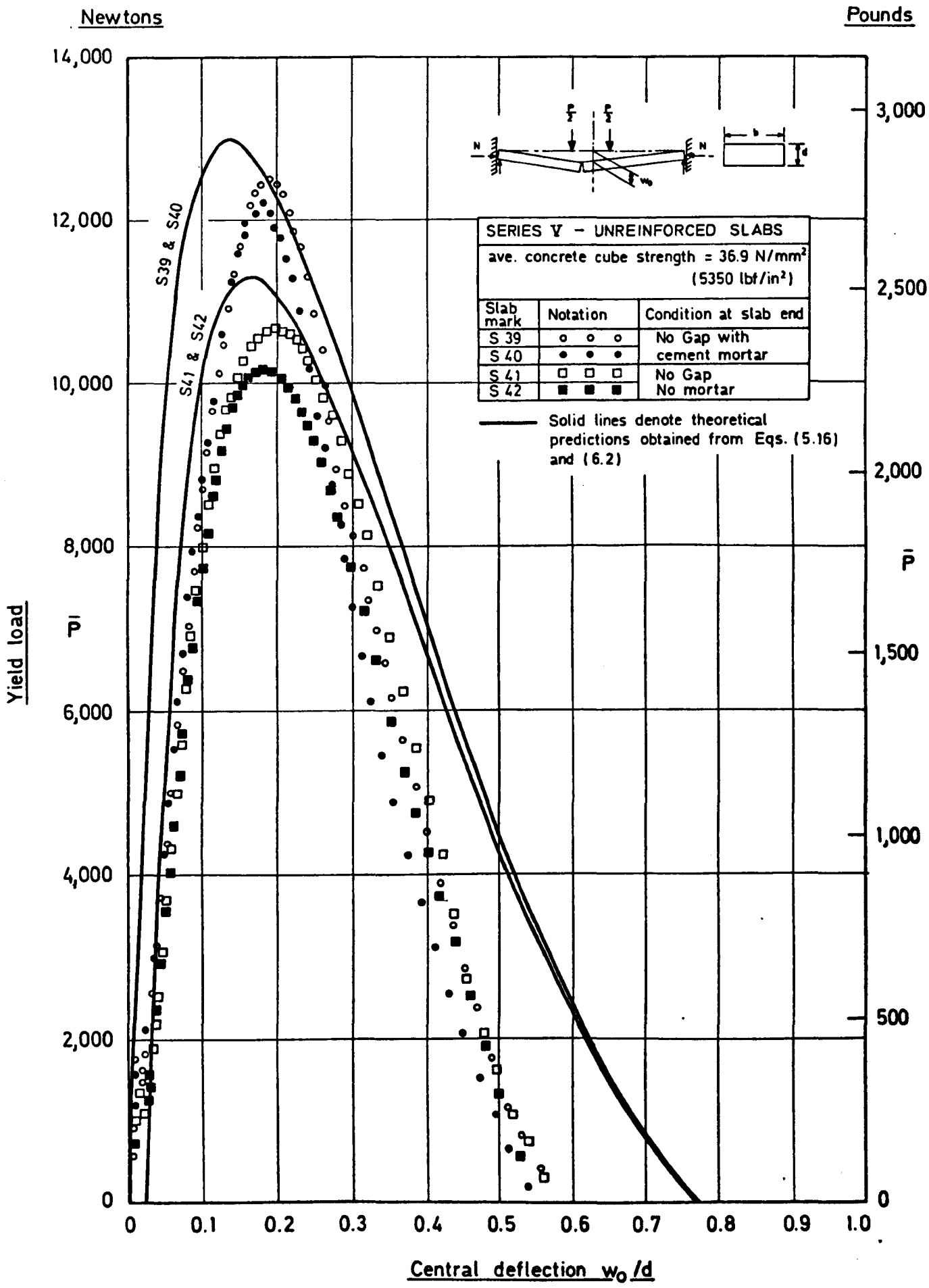

FIG. (6.9i) Experimental and Theoretical Relationship of the Yield Load with the Central Deflection ((Series V, Unreinforced))

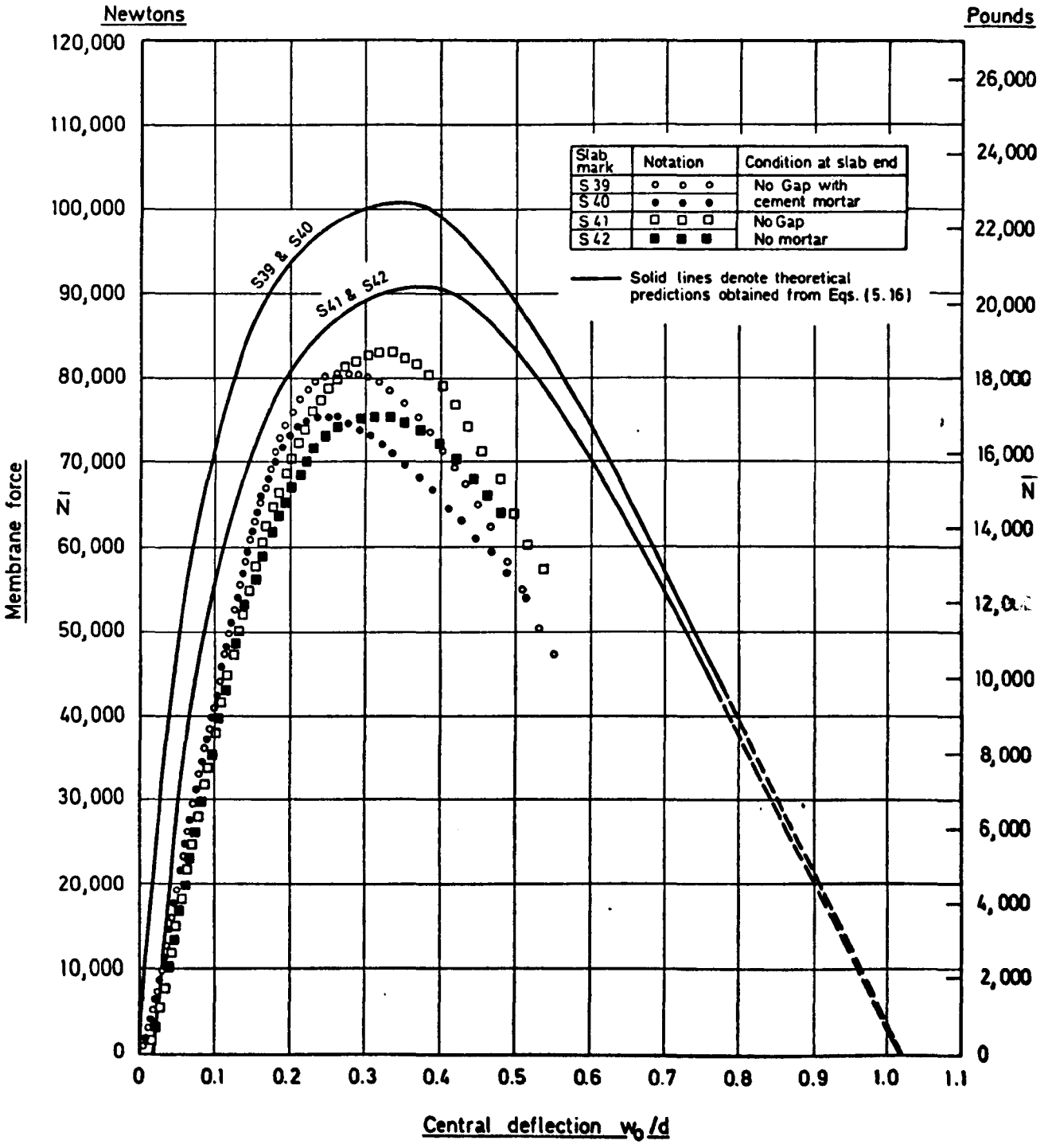

FIG. (6.9j) Experimental and Theoretical Relationship of the Membrane Force with the Central Deflection ((Series V, Unreinforced))

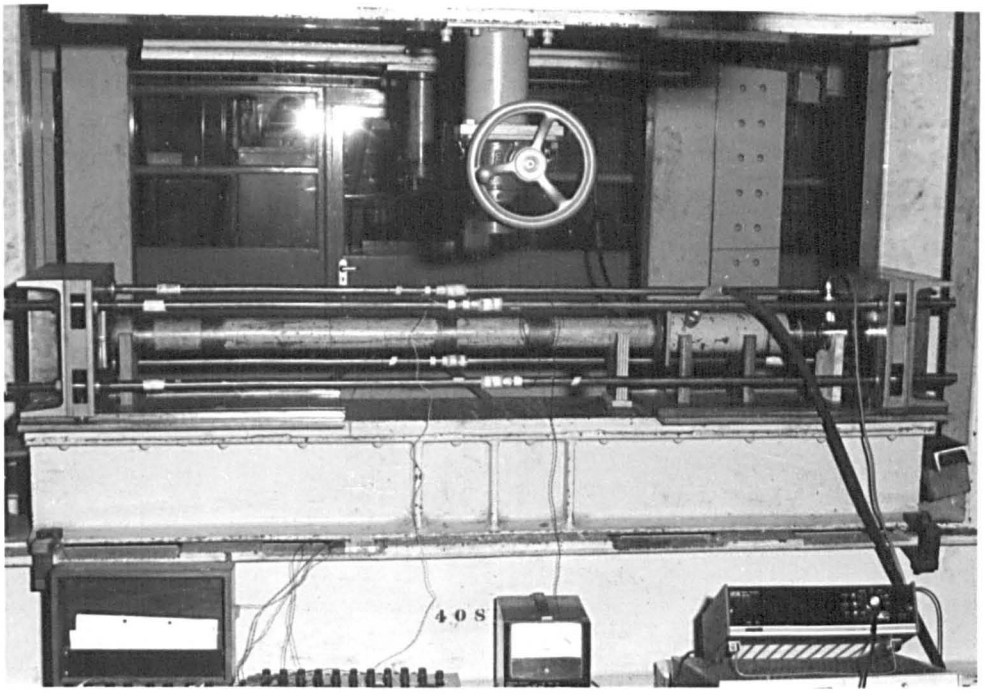

Photo (6.1) Checking the Measurement of the Membrane Force Using Hydraulic Jack System

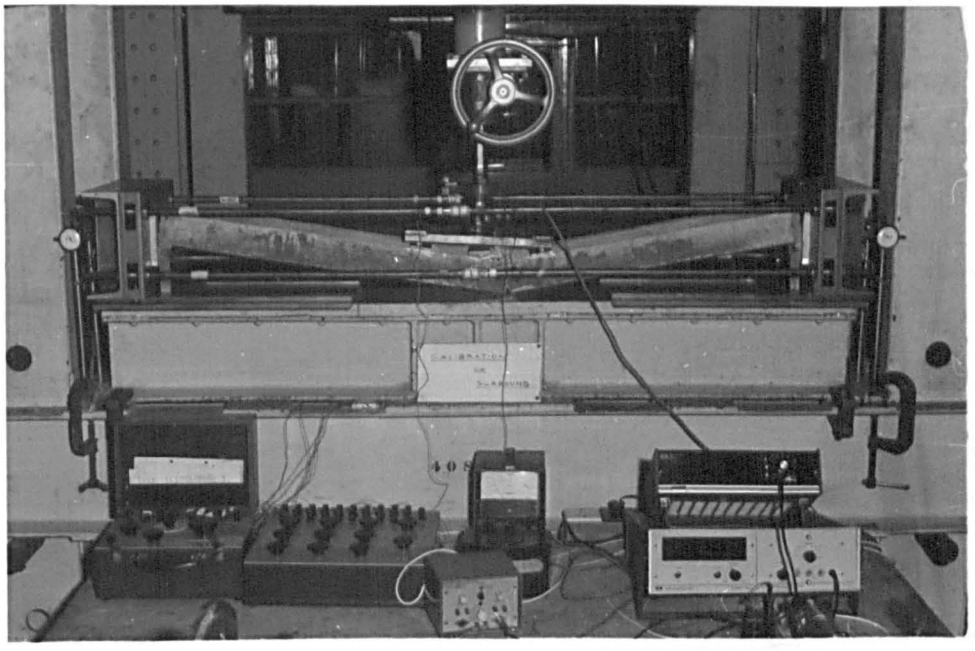

Photo (6.2) Measurement of the Stiffness of the Surround

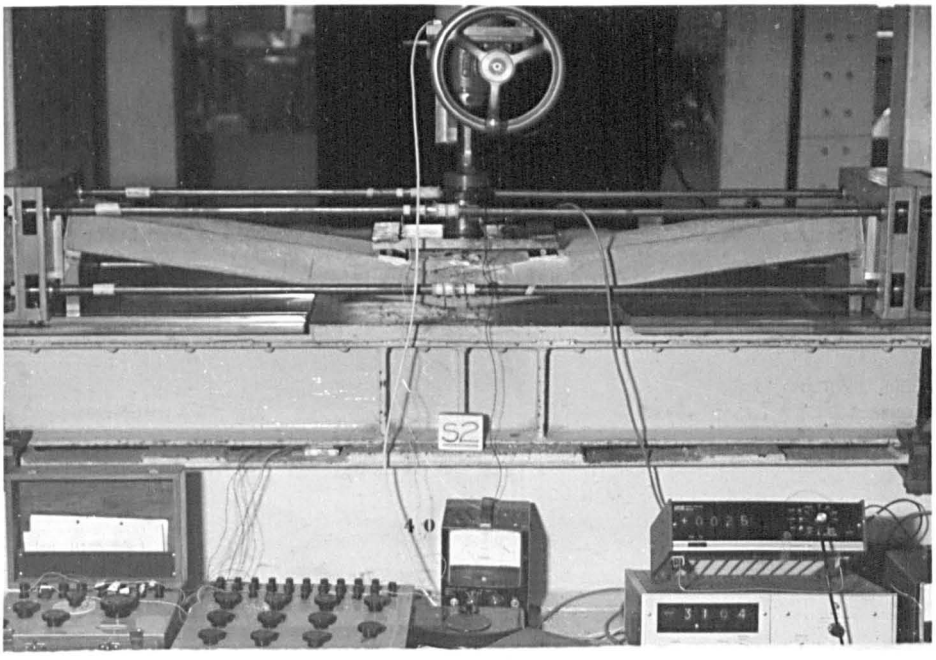

Photo (6.3) Reinforced Slab Strip S2 After Test

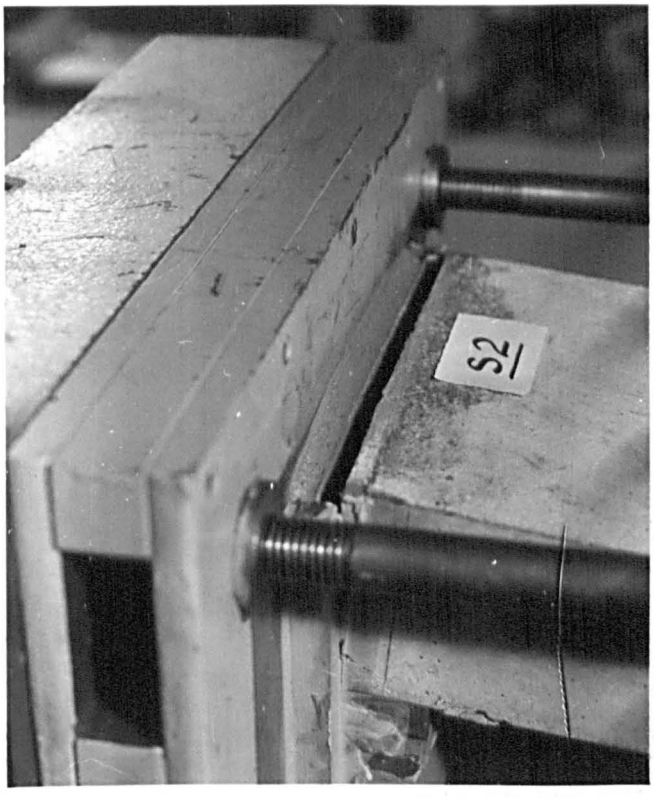

Photo (6.4) End of Slab Strip S2 Showing Failure of the Slab Concrete Without Failure of the Cement Mortar

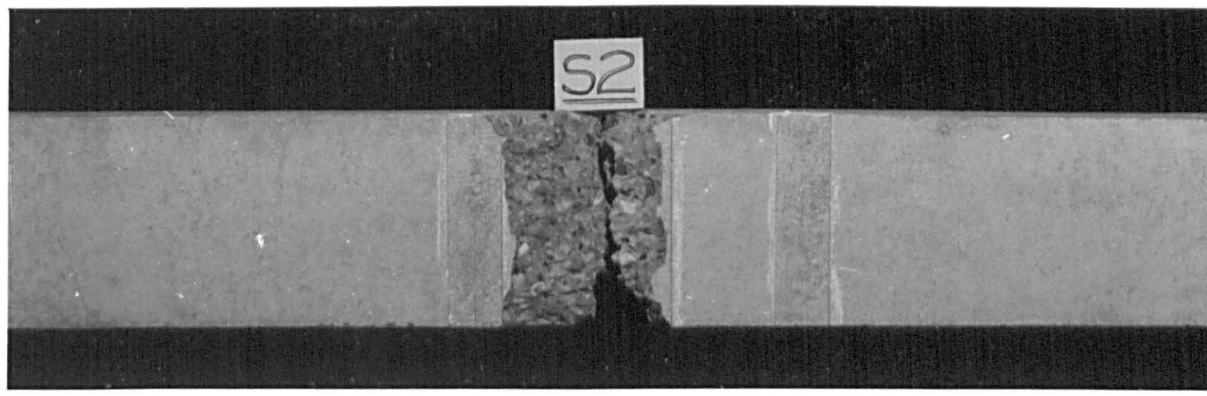

Photo (6.5) The Compressive Surface of Slab Strip S2 After Test

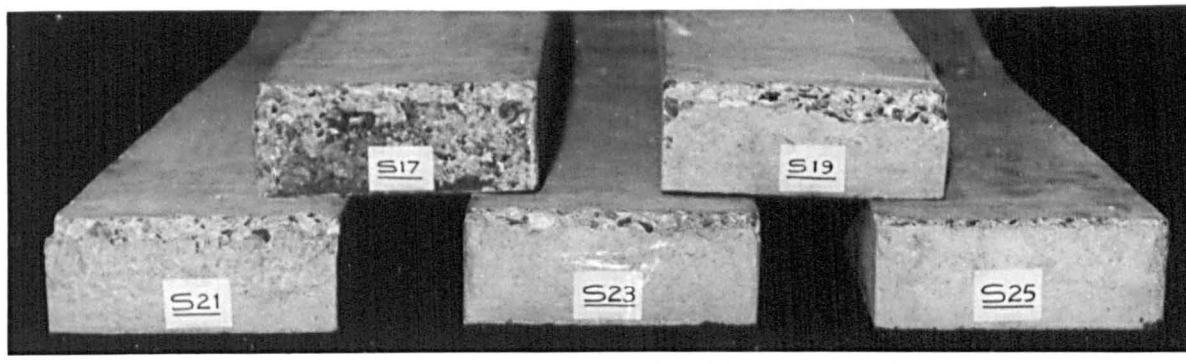

Photo (6.6) Compression Zones at the Ends of the Slab Strips of Series II After Test

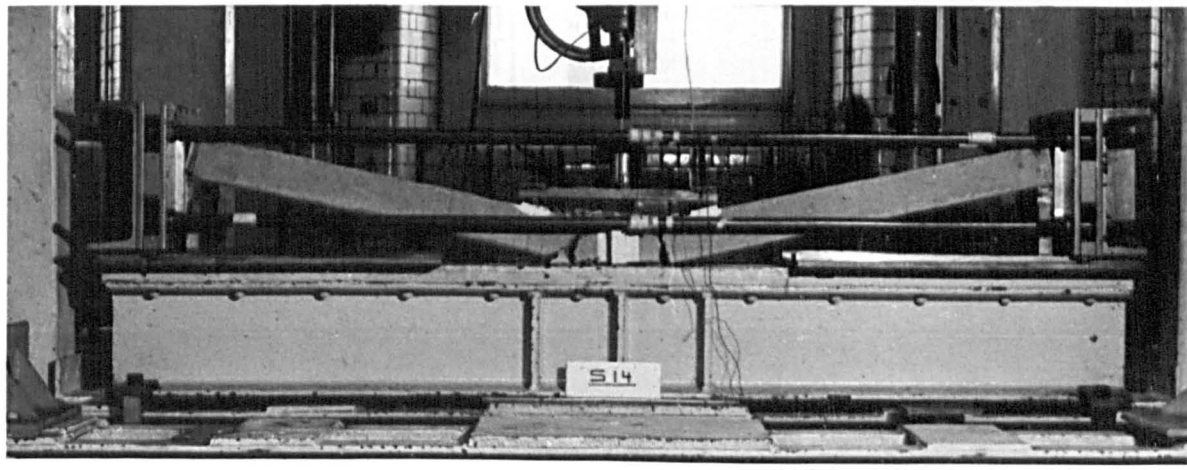

Photo (6.7) Unreinforced Slab Strip S14 After Test

The theoretical curves in Figs. (6.9) were obtained from a modified form of Eqs. (5.15) for reinforced slab strips and Eqs.(5.16) for unreinforced strips to allow for the self-weight of the slab. If the weight of the slab strip per unit length is p, the yield load - membrane force equation that replaces Eq. (5.15f, j) for reinforced strips is ;

$$\frac{P}{P_y} = 1 + \frac{2\beta}{f}\left[\left(\frac{\alpha}{\beta} + 1\right) - \left(\frac{\alpha}{\beta} + 2\right)\left(1 + \frac{2c}{L}\right)\frac{w_o}{d}\right]\left(\frac{N}{T_o}\right) - \frac{2\beta}{f}\left(\frac{N}{T_o}\right)^2 \qquad (6.1)$$

where

$$f = 1 - \frac{p\frac{L^2}{8}}{A_s f_y d_1\left(1 - \frac{k_2}{k_1 k_3}\frac{A_s}{d_1}\frac{f_y}{u}\right)}\left(1 - \frac{2c}{L}\right)\left(1 + \frac{2c}{L}\right)$$

and that which replaces Eq. (5.16f, i) for unreinforced slab strips is

$$P = \frac{2d}{a}\left[1 - \left(1 + \frac{2c}{L}\right)\frac{w_o}{d}\right]N - 4\frac{k_2}{k_1 k_3}\frac{N^2}{ua} - \frac{pL^2}{4a}\left(1 - \frac{2c}{L}\right)\left(1 + \frac{2c}{L}\right) \qquad (6.2)$$

As expected, the two cases of nominal zero gap width and mortar filled gap produced different results in the tests. The maximum values of the yield load and the membrane force were lower in the slabs tested with a nominal zero gap width than those with mortar filling. Excluding any effects due to the small differences in the value of the concrete cube strength, the differences illustrate the effective gap existing at the slab ends without mortar filling due to irregularity of the concrete surface. To enable a comparison to be made between theory and experiment these irregular gaps were considered to be equivalent to a uniform gap. The width of this uniform gap was determined as follows. First, the experimental dimensionless values of the maximum yield load $\frac{(P_{max})_E}{P_y}$ and the maximum membrane force $\frac{(N_{max})_E}{T_o}$ (or the dimensional values for the case of unreinforced slabs) for a slab strip tested with a nominal zero gap width were compared with the corresponding values obtained for a similar slab strip tested with mortar filling. Then a

trial gap width was introduced in the theoretical equations (5.15) and (6.1) (or 5.16 and 6.2 for the case of unreinforced slabs) to give the same relative change in maximum yield loads and membrane forces. When agreement was reached the introduced gap width was considered to be the width of the effective gap existing at the ends of the slab strip tested with nominal zero gap. This procedure was repeated for the five series of experiments and in each series a different effective gap width was obtained. The average value of these five effective gap widths was 0.18 mm (0.007 in), the maximum differences being of the order ±9%. This figure was then used in the theoretical predictions for the slab strips tested with specified gap widths, by adding 0.18 mm (0.007 in) to the specified width.

The experimental dimensionless value of the maximum yield load for the reinforced slabs $\frac{(P_{max})_E}{P_y}$, as shown in tables (6.4), varies from 7.79 to 1.40 and the maximum membrane force $\frac{(N_{max})_E}{T_o}$ ranges from 7.48 to 0.85. The highest values relate to a slab strip (S2) having a high cube strength [51.2 N/mm^2 (7420 lbf/in^2)], a low percentage of reinforcement (0.378%), i.e. t = 0.0217, and tested for the case of no gap with mortar filling; and the lowest values to a slab strip (S35) having a low cube strength [40.0 N/mm^2 (5795 lbf/in^2)], a high percentage of reinforcement (0.945%), i.e. t = 0.0693, and tested for the case of a specific gap width 1.02 mm (0.04 in).

The load $\frac{P_c}{P_y}$ at which first cracking occurred increased with the concrete cube strength, and with decreasing gap width and percentage of steel. Tables (6.4) show that the load at the first visible crack ranges from 1.69 P_y (slab S2) to 0.72 P_y (slab S35) which indicate that compressive membrane action not only increases the load carrying capacity of the slab but also delays the development of the first visible crack. It must be noted that in all the slabs tested the load at the first visible crack was well below the corresponding maximum yield load. In fact when the peak load was attained the central plastic hinge was well defined with a wide crack in the tension zone.

The degree of accuracy of the proposed theoretical model relative to total strain and strain rate approaches was examined for two pairs of slab strips with two different slab end conditions, the case of slab strips tested under end condition 'no gap with mortar filling' and the

case of a specified gap width. For the first case, the average experimental results of slab strips S17 and S18 (Δ = 0) are compared with the corresponding theoretical predictions in Fig. (6.10), and for the second case the average results of slab strips S25 and S26 [Δ = 2.21 mm (0.087 in)] are shown in Fig. (6.11). In both figures, the total strain curves were plotted according to Eqs. (5.6) and (6.1), the strain rate curves according to Eqs. (5.9) and (6.1) and the proposed theoretical curves according to Eqs. (5.15) and (6.1).

Comparing these theoretical curves with the experimental behaviour, it can be seen that the latter agreed reasonably well with the proposed theoretical model. The peak loads and maximum membrane forces are much better predicted by total strain theory than strain rate but for large values of deflection which correspond to decreasing membrane force the experimental results showed a closer agreement with strain rate theory than total strain. The lack of agreement between the experimental values and the strain rate predictions for the maximum yield load and the maximum membrane force is more apparent in slab strips tested with specific gap widths at their restraining ends (Fig. 6.11).

Based on the comparisons of Figs. (6.10) and (6.11), the experimental yield load - central deflection and membrane force - central deflection curves, plotted in Figs. (6.9) for all the slab strips, compared favourably with the corresponding proposed theoretical curves. The start of membrane action was well predicted. The slab strips showed ability to support increasing loads once the membrane forces developed. The maximum yield loads were many times greater than the simple yield line theory load and agreed reasonably well with the corresponding values obtained from proposed theoretical solution (see Fig.6.12). The deflection at maximum yield load, for slabs tested with no gaps at their boundaries, was only a small fraction of the thickness of the slab but was relatively larger in slabs tested with gaps. The deflection at maximum yield load did not agree with the one assumed by Park (12), half the thickness of the slab, but agreed fairly well with the theoretical model presented in the previous chapter. Large reductions in strength were apparent in slabs tested with small physical gaps existing at their restrained ends. The membrane forces in these slabs did not develop before the slabs had deflected certain distances. In all tests

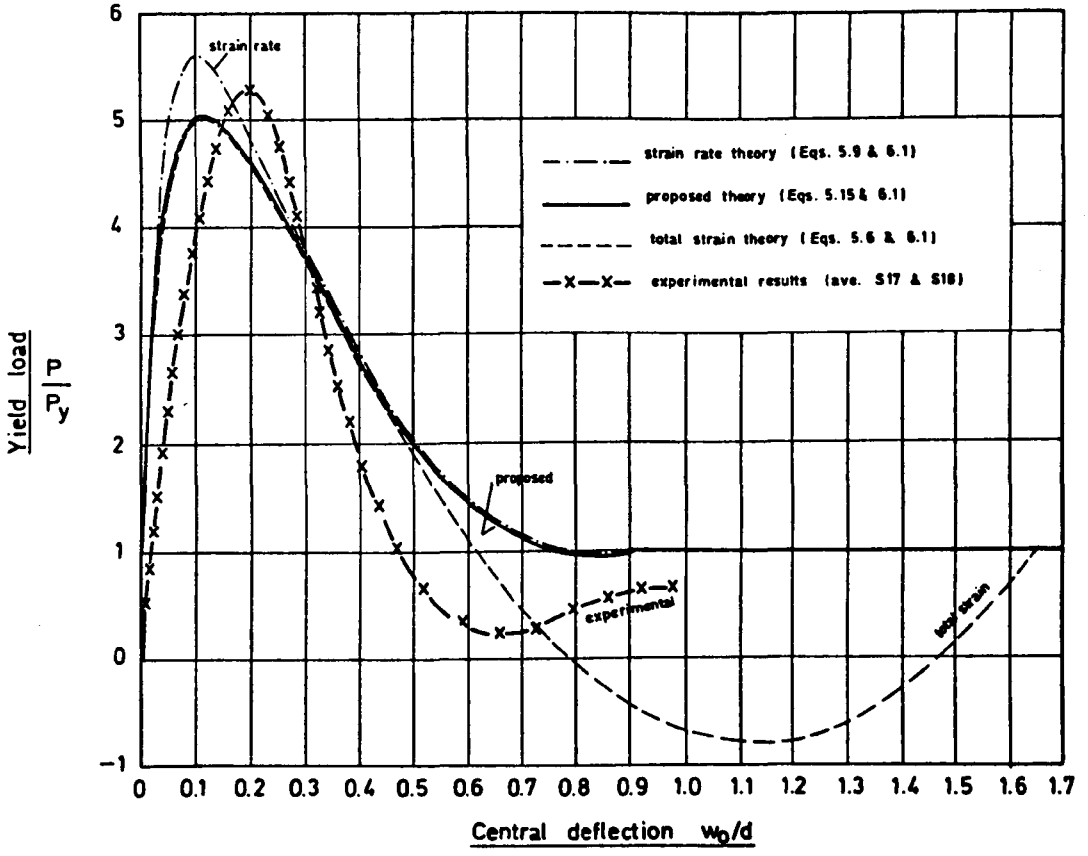

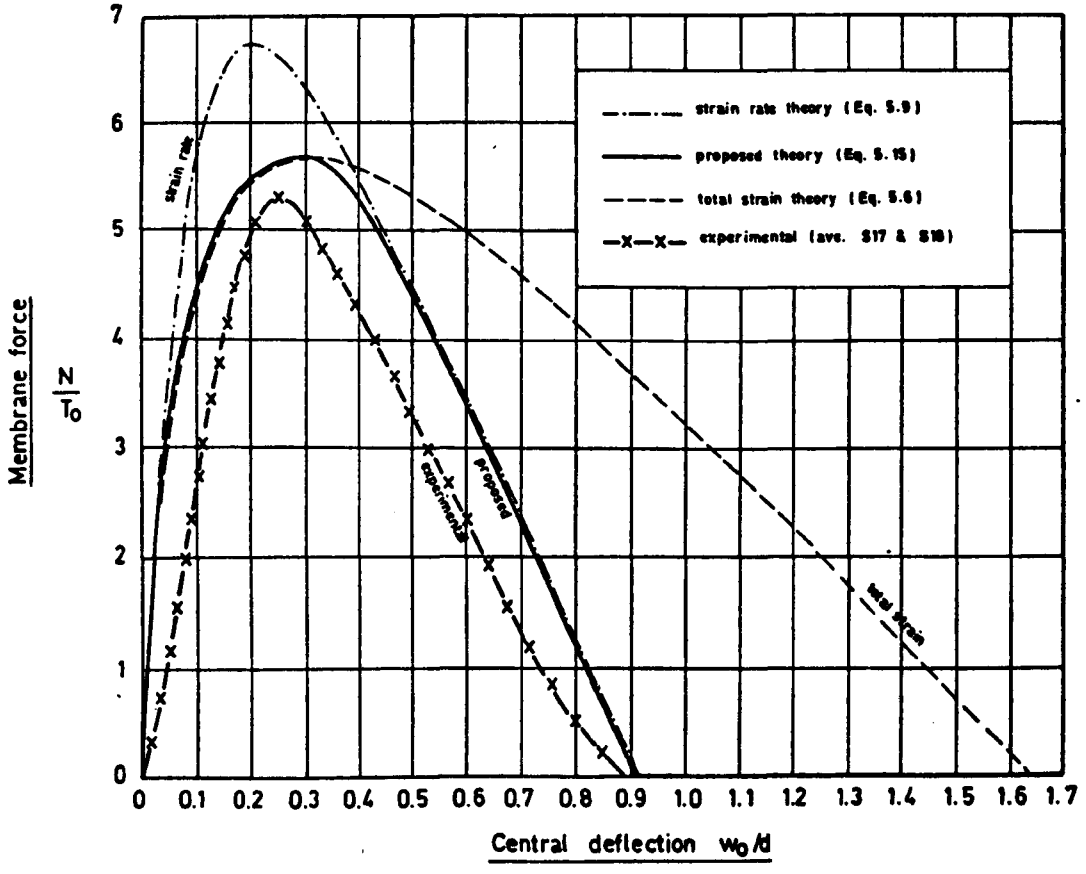

FIG. (6.10) Comparison Between Experimental Results and Theoretical Predictions ((S17 & S18 - Series II, Reinforced)).

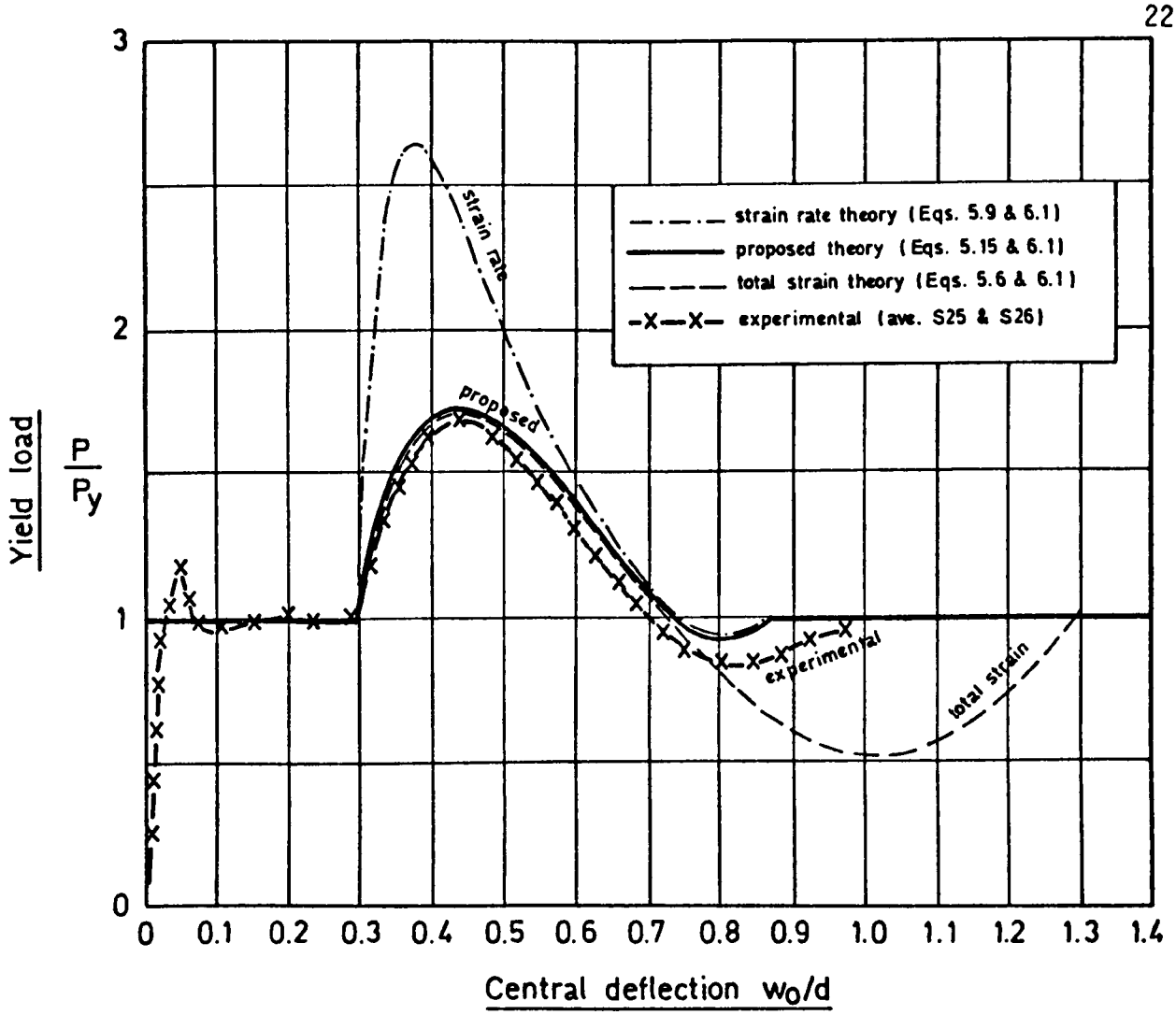

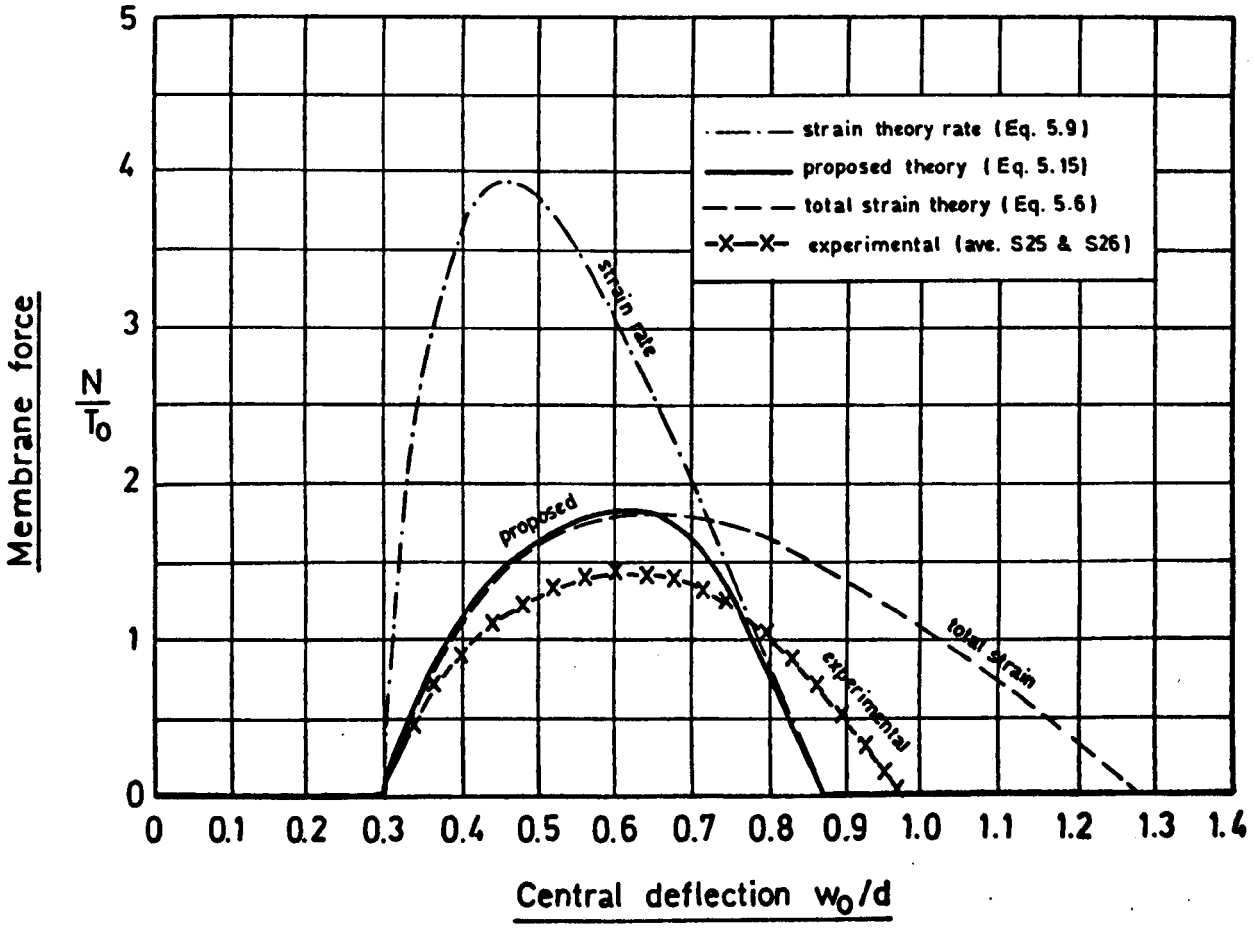

FIG. (6.11) Comparison Between Experimental Results and Theoretical Predictions ((S25 & S26 - Series II, Reinforced))

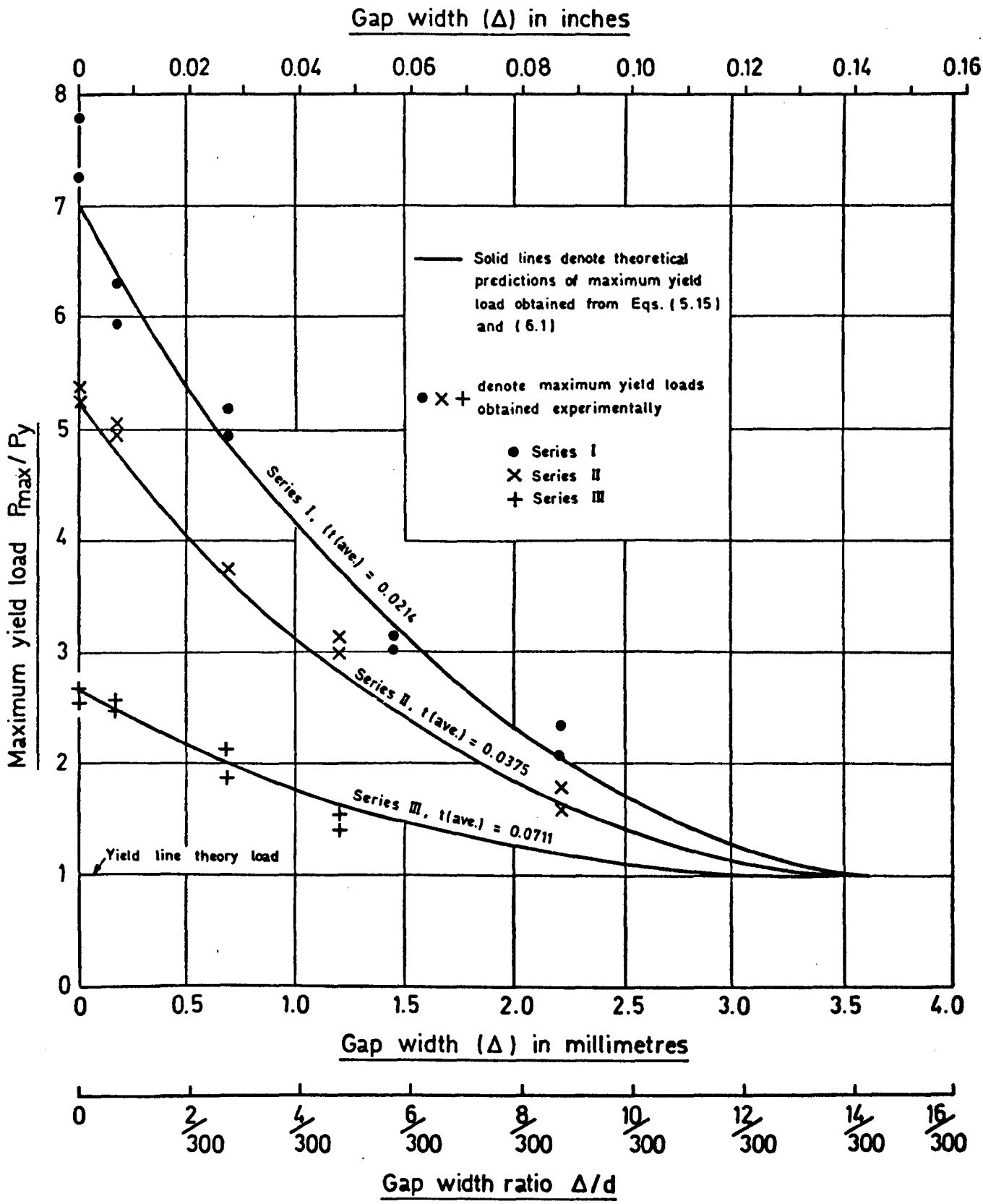

FIG. (6.12) Theoretical and Experimental Relationship Between Maximum Yield Load and Gap Width (Series I, II & III)

the experimental value of the maximum membrane force was less than the corresponding theoretical values, also the membrane force decreased much more rapidly than was predicted. Experimentally, the ratio of the maximum membrane force to the maximum yield load varied from approximately 8 (S41) to 3 (S35). The highest value of the maximum yield load for all the slabs was approximately 20 kN ($\simeq$ 2 tons), slab S2, which produced a maximum membrane force of approximately 100 kN ($\simeq$10 tons). These values relate to the slab with the highest cube strength and with a mortar filled gap.

Results from tests on eight unreinforced slabs confirmed the fact that the load carrying capacity of an axially restrained slab is dominated by the cube strength of the concrete. One unreinforced slab strip [S14 (Photo 6.7), u = 49.7 N/mm^2 (7205 lbf/in^2)] tested with a mortar filled gap carried a maximum yield load identical with the maximum load applied on a heavily reinforced slab [S29, u = 38.8 N/mm^2(5625 lbf/in^2)] tested for similar slab end conditions. The eight unreinforced slab strips failed suddenly in an explosive manner and the strain gauges on the tie bars indicated a high value of membrane forces at failure, as the theoretical analysis predicted.

A summary of the comparison between theory and experiment is given in table (6.5) below for reinforced and unreinforced slab strips.

TABLE (6.5) Summary of the Comparison Between Experimental Results and Theoretical Predictions

I T E M Mean of two identical samples		$\frac{(P_{max})_{Eave}}{(P_{max})_T}$	$\frac{(w_o)_{Eave}}{(w_o)_T \text{ @ } P_{max}}$	$\frac{(N_{max})_{Eave}}{(N_{max})_T}$	$\frac{(w_o)_{Eave}}{(w_o)_T \text{ @ } N_{max}}$
Mean Value for All Tests	Reinforced slab strips	1.00	1.11	0.82	0.79
	Unreinforced slab strips	0.97	1.25	0.80	0.76
Extreme Upper Value	Reinforced slab strips	1.09 (S1&S2)	1.76 (S17&S18)	0.93 (S17&S18)	1.01 (S25&S26)
	Unreinforced slab strips	1.00 (S15&S16)	1.35 (S13&S14)	0.87 (S41&S42)	0.83 (S41&S42)
Extreme Lower Value	Reinforced slab strips	0.89 (S35&S36)	0.83 (S35&S36)	0.66 (S35&S36)	0.65 (S19&S20)
	Unreinforced slab strips	0.92 (S41&S42)	1.15 (S15&S16)	0.77 (S13&S14) (S39&S40)	0.67 (S13&S14)

This table shows that the mean value of the maximum experimental yield load is very well predicted by the proposed theory, fortunately for reinforced slab strips with no error at all but for unreinforced strips with an error of -3% only; the extreme upper and lower differences being respectively +9% and -11% for reinforced slabs and +3% and -5% for unreinforced slabs.

The mean value of the maximum membrane force, however, was for reinforced slab strips 18% lower than that obtained theoretically, with the extreme upper and lower values being respectively 7% and 34% lower. For unreinforced slabs, the mean value of the maximum membrane force was 20% lower than the corresponding theoretical value; the extreme upper and lower values being respectively 13% and 23% lower. The lack of agreement is not altogether unexpected since the maximum membrane force, in all the slabs tested, occurred at a later stage of deformation than that of the maximum yield load. The theoretical analysis was based on the stress distribution of the concrete compressive block defined by the parameters given by Hognestad, Hanson and McHenry (25). These parameters were derived at a state where the maximum yield load and maximum axial force were reached simultaneously. However, the analysis of the previous chapter has shown that in partially restrained slabs the maximum yield load is usually reached at an earlier stage of deformation than that of maximum membrane force. In this case, Hognestad's parameters could be expected to give reasonable estimates of the maximum yield load. For states of stress after the maximum yield load, the use of these parameters leads to overestimation of the compressive force on concrete. It must be noted that for all deformation stages except that corresponding to the ultimate load, the theory overpredicts the load carrying capacity of the slab because at these stages the integral sum of the stresses occurring on the fibres of the compressive block is less than that represented by Hognestad's equivalent rectangular block. For all stages of deformation occurring prior to ultimate load the discrepancy can be predicted to be small since the stress on the concrete increases rapidly with initial increments of strain but for large deflections the concrete disintegrates and its strength declines rapidly which results in large discrepancies between experimental results and theoretical predictions. Nevertheless, the error in the value of the maximum membrane force is not excessive for such a non-homogeneous material as

concrete. Concrete is clearly not a perfectly plastic material as assumed in the theoretical model.

The ratio of the experimental to theoretical central deflections at the corresponding maximum yield load for the reinforced slab strips tested is shown in table (6.5) to have a mean value of 1.11, the extreme upper and lower values being 1.76 and 0.83 respectively. For the unreinforced strips tested, the corresponding ratio is 1.25, with the extreme upper and lower values being 1.35 and 1.15. For that corresponding to the maximum membrane force, the ratio is 0.79 as a mean value for the reinforced slabs, the extreme upper and lower limits are 1.01 and 0.65; and as a mean of the unreinforced slabs the ratio is 0.76, the extreme upper and lower values being 0.83 and 0.67 respectively. The discrepancies are undoubtedly due to the negligence of the elastic bending curvature of the slab member in the theoretical analysis and to perfectly plastic assumptions for the concrete.

6.10 SUMMARY

36 simply supported concrete slab strips (28 reinforced and 8 unreinforced) restrained axially against longitudinal expansion by a surround of low stiffness were tested under two point loading. The main object of these tests was to examine the validity and reliability of the proposed hypothesis regarding relevance of total strain and strain rate theories in cracked sections.

The tests formed five series of experiments, the slab strips of each series having a similar concrete cube strength, the same amount of reinforcement and tested for different gap widths at their restrained ends. The experimental results compared favourably with the corresponding predictions obtained from the proposed theoretical model. The maximum values of the yield load and the membrane force showed a much closer agreement with total strain theory than with strain rate but the values at large deflections agreed much better with the latter. For the reinforced slab tests the average maximum applied load was fortuitously identical with the theoretical collapse load, the extreme differences varied between +9% and -11%, but for unreinforced slabs the mean value of the maximum experimental load was 3% lower than the corresponding

theoretical load with extreme errors of +3% and -5%. These errors are well within the discrepancies that can be expected for concrete slabs.

Results of the tests confirmed the beneficial effect of compressive membrane action in increasing the load carrying capacity of axially restrained slabs beyond those suggested by the simple yield line theory. The ratio of the maximum applied load to Johansen's yield line theory load varied from 7.79, for a slab with a high concrete cube strength and a low percentage of reinforcement, to 1.40 for a slab strip with a low concrete cube strength and a high percentage of reinforcement. The experimental tests had also shown that compressive membrane action delays the development of the first visible crack. The ratio of the yield load at which first cracking occurred to yield line theory load was found to increase with the concrete cube strength, and with decreasing gap widths and percentage of steel.

The slabs at test behaved wholly as expected. With physical gaps at the slab ends the membrane action did not start before the slab had deflected a certain distance. The development of the membrane force, the increments in the yield load at the early stage of increasing membrane force as well as the value of the peak load were all very well predicted. Thus, the experimental results provided a firm support to the theoretical model presented in which the value of the maximum yield load is associated with total strain theory as is the whole stage of increasing membrane force. At later stages of deformation the yield load and the membrane force were found to fall more rapidly than expected but then showed some recovery and started to coincide with the theoretical predictions at larger deflections. This supports the validity of the strain rate theory at the stage of decreasing membrane force. The final stage of pure flexure was well defined and was reasonably close to the theoretical estimations.

The effect of gap in reducing the values of both the ultimate load and the maximum membrane force was apparent. The reduction in these values was high when only small gap widths were present at the restrained ends of the slabs. A gap width as small as 0.01 x slab depth can reduce the ultimate load by one third.

Tests on eight unreinforced slab strips restrained axially against longitudinal expansion showed that ultimate loads are dominated by the cube strength of the concrete.

CHAPTER 7

DISCUSSION AND GENERAL CONCLUSIONS

7.1 SUMMARY OF THE STUDY AND CONCLUSIONS

Intensive previous studies have been carried out during the last two decades in an attempt to understand and utilise the considerable reserves of strength obtained in reinforced concrete slabs in which membrane action can occur. These studies have shown that due to 'compressive membrane action' in slabs restrained axially against longitudinal expansion very high ultimate loads, many times greater than the yield line theory load, can be sustained for very small deflections. 'Tensile membrane action' in axially unrestrained slabs has been found to occur only when a collapase mechanism forms that has a non-developable surface and does not greatly influence the load at which the yield mechanism forms but it raises the load necessary for continuing deflection.

In the present work, the diverse existing methods of approach were reviewed, closely examined and criticised. The limits of application of each method, the assumptions upon which it is based and the method of analysis were carefully outlined. The equations for the ultimate loads obtained were given in a unified form to enable comparisons to be made.

The existing methods of approach can be broadly classified as approximate and rigorous. Each of the approximate methods is based on completely different assumptions such as assuming that the membrane force developing in the slab due to axial restraint against longitudinal expansion is constant along yield lines, or the neutral axes at yield sections lie on the same horizontal level, or membrane forces and moments do not change with deformation, ...etc. The rigorous methods were found to be based on one of two fundamental assumptions concerning plastic flow behaviour, namely, total strain and strain rate. It is perhaps surprising that authors have adopted either of these two assumptions without giving any physical justification for its validity.

In this thesis, a careful examination of total strain and strain rate assumptions with detailed arguments for the correct flow theory to

use has been presented. A new and important study of the plastic behaviour of non-homogeneous materials based on these two assumptions was discussed for cracked reinforced concrete sections. The proposed hypothesis was then applied to problems of axially restrained slab strips where compressive membrane action is present. The study is the first of its kind to be reported and plays a highly significant part in the concept of plasticity in concrete. As is usual with new concepts, questions emerge at the end of the study which were not present at the beginning.

From a physical discussion, it was argued that strain rate theory is always valid in cases of homogeneous ductile materials, but in cases of cracked sections, including gaps at axially restrained ends, the strain rate theory is applicable only when the neutral axis for strain rate moves into the compressive zone for total strain. The total strain theory is valid in cases of uniform stress state (uniform in time) since similar results to those of strain rate theory are then predicted, but more importantly in cracked sections when the neutral axis for strain rate moves into the crack, i.e. the zone of total tensile strains.

These concepts were applied to the study of the problem of compressive membrane action in axially restrained slab strips. Both total strain and strain rate assumptions were separately adopted in the analysis and showed highly significant discrepancies.

Firstly, the slab elements were assumed rigidly restrained at the ends and considered to behave in a rigid - perfectly plastic manner. The theoretical load - deflection relationship for such slabs showed an initial maximum yield load, occurring at zero deflection, which is many times greater than Johansen's yield line theory load. The value of the compressive membrane force corresponding to this load is also a maximum. It was found theoretically that with continuing deflection the load falls off rapidly (taking a parabolic path) due to the value of the compressive membrane force falling linearly. The equilibrium of the slab during this stage is 'unstable'. Eventually the membrane force becomes zero and the value of the load is the yield line theory load. When the deflection increases further the slab shows some recovery in the load with the membrane force becoming tensile. Even when at a later stage the slab is cracked throughout the depth at some

sections of yield it continues to carry increasing load until all the reinforcing bars fracture and the slab reaches its limit of usefulness. The equilibrium of the slab during this stage of recovery in load is 'stable'.

During the whole deformation process of the rigidly restrained rigid-plastic slab strip the neutral axis for strain rate at yield sections moves into the compressive zone for total strain and therefore in this case the strain rate theory is valid. The variation in the stress state due to deflection of such slabs was shown to cover an extensive part of the yield locus ranging from maximum yield moment to minimum. This large variation of the stress state point causes highly significant discrepancies between the predictions of total strain and strain rate theories.

Although the start of collapse showed consistency between these two theories (due to the maximum values of the yield load and the membrane force being the same) the total strain theory was found to overestimate the membrane force and underestimate the yield load for any specific value of deflection when compared to strain rate theory. For total strain theory the values of deflection corresponding to zero membrane force and when the cracks penetrate the whole thickness of the slab were found to be double those obtained by strain rate theory.

It must be emphasized that the rigidly restrained rigid-plastic strip is only a theoretical idealisation. It cannot exist in reality and there is no possible experimental verification for its behaviour.

Within similar theoretical considerations the concepts of total strain and strain rate theories were applied to the study of the behaviour of rigid-plastic simply supported slab strips with physical gaps at their rigid boundaries. In this case the total strain theory was found to predict an initial non-linear increase in the values of the membrane force and the yield load after contact of the bottom surfaces of the slab strip with the surrounds takes place with increasing deflection. The neutral axis at the yield sections during this stage of increasing membrane force moves towards the mid-depth of the slab into the 'crack' or 'zone of total tensile strains'. When the membrane force becomes a maximum, the neutral axis is at its closest position to the mid-depth of the slab and the yield load has passed its

peak point. The equilibrium of the slab strip then becomes unstable due to the values of the membrane force and the yield load becoming smaller. The neutral axis during this stage of decreasing membrane force moves back towards the compressed face of the slab into the compressive zone for total strain.

In contrast to the total strain theory, the strain rate theory, at the start of membrane action (i.e. when the bottom surfaces of the slab strip are just in contact with the surrounds), predicts an abrupt change in the value of the membrane force from zero to a maximum (equal to the value obtained from the rigid plastic - no gap solution at that particular deflection). Also the value of the yield load corresponding to this deflection according to strain rate theory changes suddenly from that of the yield line theory load to a maximum equal to the rigid plastic - no gap load at that particular deflection. Such sudden changes in the values of the yield load and the membrane force demonstrate the invalidity of the strain rate theory during the early stages of membrane action where the neutral axis normally moves into the crack or zone of total tensile strains. For any value of deflection at which membrane action occurs, the strain rate theory gives identical predictions to that of the corresponding rigid plastic - no gap solution because of the disappearance of the gap parameter from the governing equations.

The total strain and strain rate predictions for rigid-plastic slab strips with simple supports and physical gaps at the infinitely stiff boundaries were shown to be identical only at a value of central deflection corresponding to the 'total strain' maximum membrane force. According to the proposed hypothesis the behaviour of such slabs follows total strain theory during the stage of increasing membrane force and strain rate theory for the whole stage of decreasing membrane force, thus the maximum yield load, which always occurs within the stage of increasing membrane force, is associated with total strain theory.

The effect of a gap on the behaviour of infinitely restrained rigid-plastic slab strips was found to lower the values of the maximum membrane force and the peak load and to increase the deflections at which they occur. The differences between the predictions of total strain and strain rate theories increase as the physical gap at the slab boundaries widens.

The most important practical case, however, is that of elastic-plastic strips with elastic restraints and physical gaps. Such slabs were considered in the second part of the research and the elastic shortening of the slab and the outward movement of the surround were taken into account. Again the analysis was performed assuming either a total strain or a strain rate flow rule to apply. In this case the load - deflection relationship consisted of four successive stages. First, an early stage of pure flexure where the yield line theory is valid. Second, a stage of increasing membrane force where the neutral axis for strain rate at the yield sections moves towards the mid-depth of the slab into the 'crack' or 'zone of total tensile strains' in which case the total strain theory is valid. The yield load during this stage increases rapidly (the equilibrium of the slab is 'stable') until it becomes a maximum at a certain value of central deflection and thereafter decreases. The falling part of the load - deflection curve represents a state where the equilibrium of the slab is 'unstable'. The maximum yield load is always attained within the stage of increasing membrane force. The third stage is one of decreasing membrane force where the neutral axis at the yield sections moves back towards the compressed face of the slab. During the early part of this stage of decreasing membrane force, the neutral axis for strain rate was shown to continue to move into the crack so that total strain theory still applies. When the state of stress is reached when both the total strain and strain rate theories predict equal values for the membrane force, yield load and position of the neutral axis at the yield sections, the strain rate theory is applicable since the neutral axis for strain rate then moves into the compressive zone for total strain with continuing deflection. The application of the strain rate theory in the analysis of such slabs covers the major part of the decreasing membrane force stage. The fourth and final stage is pure flexure which starts when the membrane force vanishes at large deflection and yield line theory applies up to the fracture of the steel.

On the yield surface, the stress state moves from the point representing pure flexure (i.e. zero membrane force) to a point of largest membrane force just to the right of the maximum yield moment point and then returns to its original position. This large movement

of the stress state again causes highly significant discrepancies between the predictions of total strain and strain rate theories.

The errors caused by using the strain rate theory in the analysis of the slab during the stage of increasing membrane force instead of total strain theory produce too high values of membrane force and yield load. The errors caused by using the total strain theory in the analysis of the slab during the stage of decreasing membrane force instead of strain rate theory lead to overestimates of membrane force and underestimates of yield load. The differences between the predictions of total strain and strain rate theories are greatest in slab strips with relatively wider physical gaps at the boundaries and restrained laterally by stiffer surrounds. However, it must be emphasized that for these practical cases of slab strips, the maximum yield loads are always associated with total strain theory.

The effect of a gap on the behaviour of these elastic - plastic slab strips with elastic restraints is similar to that of the infinitely restrained rigid-plastic strips; it produces lower values for the maximum membrane and the peak load compared to those corresponding to similar slabs with no gap, and these occur at larger deflection. The degree of the stiffness of the surround was found to have an opposite effect on the behaviour of slab strips compared to the gap parameter; the maximum values of the yield load and the membrane force are higher when slab strips are restrained with stiffer surrounds and they are attained at lower values of deflection.

For a specified geometry of a slab strip, the enhancement in the yield load above the yield line theory load was found to be directly proportional to the cube strength of the concrete and the degree of stiffness of the surround and inversly proportional to the percentage of reinforcement and the width of the gap at the restrained ends. By comparing the results of the analysis with solutions previously found by other investigators it was found that the type of loading does not affect the ratio of the yield load to the yield line theory load but the shape of the collapse mechanism does. The value of the maximum yield load was found to be dominated by the cube strength of the concrete rather than the amount of reinforcement.

A series of experimental tests were carried out on concrete slab strips (both reinforced and unreinforced) to check the validity of the proposed hypothesis and to demonstrate the effect of the important parameters, particularly the gap parameter since it illustrates most vividly the large differences between total strain and strain rate theory approaches. The experimental results showed that the maximum yield loads were very accurately predicted by the new model with fortuitously zero average error for the reinforced strips and an average error of 3% only for the unreinforced strips. The start of membrane action and the final stage of pure flexure also showed very close agreement between theory and experiments. The values of the maximum membrane force and the deflections corresponding to it and the peak load were overestimated by the theory but these errors are considered to be primarily due to the fact that concrete is not a perfectly plastic material as assumed theoretically. The experiments also demonstrated that the appearance of the first visible cracks are delayed when axial restraints are present.

7.2 REMARKS AND FURTHER RESEARCH

Membrane action is a common occurrence in structural concrete slabs since they are frequently restrained against outward movement by surrounding bodies. Due to compressive membrane action, axially restrained concrete slabs can carry ultimate loads which are far beyond those obtained by yield line theory. The enhanced strengths, however, have not yet been taken into account in design codes. Because of the unstable equilibrium at the peak load, care is needed in including membrane action in design and therefore a thorough understanding of the behaviour of axially restrained slabs is required. The work presented here is a contribution to this understanding although restricted to slab strips. The significance of this study of membrane action in slabs arises in providing a better understanding of the higher strengths obtained in restrained slabs which could lead eventually to a more economic use of reinforcement. Certainly more research should be directed towards this aim.

It is to be noted that the elastic-plastic analysis of the slab strips in the present work was based on adopting an equivalent

rectangular compressive stress block for the concrete that does not change with deformation of the slab. The effect of this assumption on the behaviour of the slab strip was demonstrated by comparing theoretical predictions with results obtained from experiments. The theory according to this assumption overestimated the values of the yield loads and the membrane forces at all deflections except that corresponding to maximum yield load. Further investigations need to be made including a more representative stress distribution for the concrete which should be a function of deformation.

The analysis in this research is restricted to elemental strips of slabs having uniform depth. Another field for extending this work in the future will perhaps be by attempting to study the effect of compressive membrane action in axially restrained tapered slab elements. Slabs with bottom surfaces tapered to the shape of pyramids provide both economy in material and attractive appearance.

Also, further investigation is needed to consider the effect of the elastic curvature of the slab strip which would help to give a closer agreement between the theoretical and experimental curves representing the yield load - central deflection and the membrane force - central deflection relationships, especially the early parts of the relations that correspond to initial deformations.

Another point worth considering concerns the analysis of membrane action in doubly reinforced slabs. In such analysis, attention must be given to the conditions at large deflection when the slab cracks throughout the depth at some yield sections and the neutral axis lies outside the slab on the top surface. In this case, the 'compression' reinforcement will not act in compression but will be subjected to tensile strains.

In the present work, new concepts and limits were given for the use of total strain and strain rate plastic flow theories in the study of membrane action in slab strips. A promising field for future research is the application of these concepts to the analysis of various shapes of slabs with different boundary conditions in which membrane action can occur. Two methods of approach may be followed in the analysis of these slabs, the strip method and the slab element method.

In the strip method the slab can be considered as composed of strips running in the longitudinal and transverse directions of the slab. In this case the new theoretical model may be applied directly. Thus for the analysis of rigidly restrained - rigid plastic slabs the strain rate theory is applicable for the whole deformation process of the slab whereas in elastic-plastic slabs with physical gaps at partially stiff surrounds the total strain theory must be used for the whole stage of increasing membrane force and the early stage of decreasing membrane force up to the stress state where the membrane force, yield load and position of the neutral axis at sections of yield are equally predicted by both total strain and strain rate theories. The strain rate theory then applies for the remaining part of the decreasing membrane force stage.

For slabs axially restrained on all sides, this approach should give reasonable predictions of behaviour but for slabs restrained on some sides and the remaining sides free to move laterally, the solution will have limitations similar to those of Park's (12) strip method. Park's method neglects any membrane action developing in the slab in the direction perpendicular to an unrestrained edge and so predicts an ultimate load equal to the yield line theory load. If however the slab is considered to be composed of strips running in the diagonal directions, membrane action will be developed in some strips which will enable the slab to carry ultimate loads higher than Johansen's load. The predictions of strip theory therefore depend on the directions chosen for the strips.

In the second method of approach (slab element method), the slab can be considered as composed of elements or portions bounded by yield lines (for example triangular elements in square slabs or trapezoidal and triangular elements in rectangular slabs). In this method and for rigidly restrained - rigid plastic slabs the strain rate theory is predicted to apply for the whole stages of slab deformation, but for elastic-plastic slabs with physical gaps at partial lateral restraints the new theoretical model should be applied. It is matter for future research to decide how this can be done, especially the way the elastic shortening of the slab element, the outward movement of the surround and the existence of physical gaps at the boundaries of the slab, can be considered in the analysis. One possible approach in

this case will perhaps be by attempting to solve the problem numerically by using the finite element technique, but this is likely to be demanding in computer time. As a first step it would certainly be of interest to compare a finite element elastic plastic analysis of slab strips with the method presented in this thesis.

In conclusion, it is recognised that much more research is required before it will be possible to include membrane action in design methods for restrained slabs. It is hoped that this study is a useful contribution towards this end.

REFERENCES

1. Johansen, K.W., "Yield-Line Theory". Cement and Concrete Association, London, 1962. pp. 181.

2. British Standard Codes of Practice CP110 (1972) and CP114 (1957), "The Structural Use of Reinforced Concrete".

3. Wood, R.H., "Plastic and Elastic Design of Slabs and Plates". Thames and Hudson, London, 1961. pp. 334.

4. Kemp, K.O., "Yield of a Square Reinforced Concrete Slab on Simple Supports, Allowing for Membrane Forces". The Structural Engineer. Vol. 45, No.7. July 1967. pp. 235-240.

5. Thomas, F.G., "Studies in Reinforced Concrete, Part VIII, The Strength and Deformation of Some Reinforced Concrete Slabs Subjected to Concentrated Loading". Technical Paper No.25. H.M.S.O. London.

6. Ockleston, A.J., "Load Tests on Three Storey Reinforced Concrete Building in Johannesburg". The Structural Engineer, Vol. 33, October 1955. pp. 304-322. (Discussion in Vol. 34, 1956. pp. 360-369).

7. Ockleston, A.J., "Arching Action in Reinforced Concrete Slabs". The Structural Engineer, Vol. 36, June 1958. pp. 197-201.

8. Powell, D.S., "The Ultimate Strength of Concrete Panels Subjected to Uniformly Distributed Loads". Thesis presented to the University of Cambridge for the degree of Ph.D. 1956.

9. Gamble, W.L., Sozen, M.A. and Siess, C.P., "An Experimental Study of a Reinforced Concrete Two-Way Floor Slab". Civil Engineering Studies, Structural Research, Series No.211, University of Illinois, 1961.

10. Morley, C.T., "Yield-Line Theory for Reinforced Concrete Slabs at Moderately Large Deflections". Magazine of Concrete Research. Vol. 19, No.61. December 1967. pp. 211-222.

11. Timoshenko, S.P. and Woinowsky - Kreiger, S., "Theory of Plates and Shells". 2nd Edition, McGraw-Hill, New York, 1959. pp. 580.

12. Park, R., "The Ultimate Strength of Uniformly Loaded Laterally Restrained Rectangular Two-Way Concrete Slabs". Thesis presented to the University of Bristol for the degree of Ph.D. 1964.

13. Park, R., "Tensile Membrane Behaviour of Uniformly Loaded Rectangular Reinforced Concrete Slabs with Fully Restrained Edges". Magazine of Concrete Research. Vol. 16, No.46. March 1964. pp.39-44.

14. Park, R., "Ultimate Strength of Rectangular Concrete Slabs Under Short-Term Uniform Loading with Edges Restrained Against Lateral Movement". Proceedings of the Institution of Civil Engineers. Vol. 28, June 1964. pp. 125-150.

15. Park, R., "The Ultimate Strength and Long-Term Behaviour of Uniformly Loaded Two-Way Concrete Slabs With Partial Lateral Restraint At All Edges". Magazine of Concrete Research. Vol. 16, No. 48. September 1964. pp. 139-152.

16. Park, R., "The Lateral Stiffness and Strength Required to Ensure Membrane Action At the Ultimate Load of a Reinforced Concrete Slab-and-Beam Floor". Magazine of Concrete Research. Vol.17, No.50. March 1965. pp. 29-38.

17. Sawczuk, A. and Winnicki, L., "Plastic Behaviour of Simply Supported Reinforced Concrete Plates At Moderately Large Deflections". International Journal of Solids and Structures. Vol.1, 1965. pp. 97-111.

18. Hayes, B., "Allowing for Membrane Action in the Plastic Analysis of Rectangular Reinforced Concrete Slabs". Magazine of Concrete Research. Vol.20, No.65. December 1968. pp. 205-212.

19. Taylor, R., "A Note on a Possible Basis for a New Method of Ultimate Load Design of Reinforced Concrete Slabs". Magazine of Concrete Research. Vol.17, No.53. December 1965. pp. 183-186.

20. Maher, D.R.H., "A Study of the Ultimate Load of Reinforced Concrete Slabs". Thesis submitted to the University of Manchester for the degree of M.Sc. 1965.

21. Hayes, B., "Computer Programme for the Strength-Deflection Characteristic of Reinforced Concrete Slabs Allowing for Tensile Membrane Action". University of Manchester, Simon Engineering Laboratories, 1965.

22. Janas, M., "Large Plastic Deformations of Reinforced Concrete Slabs". International Journal of Solids and Structures. Vol.4, 1968. pp. 61-74.

23. Christiansen, K.P., "The Effect of Membrane Stresses on the Ultimate Strength of the Interior Panel in a Reinforced Concrete Slab". The Structural Engineer, Vol.41, August 1963. pp.261-265.

24. Roberts, E.H., "Load-Carrying Capacity of Slab Strips Restrained Against Longitudinal Expansion". Concrete 3. September 1969. pp. 369-378.

25. Hognestad, E., Hanson, N.W. and McHenry, D., "Concrete Stress Distribution in Ultimate Strength Design". Journal of the American Concrete Institute, Vol.27, No.4. December 1955. pp. 455-479.

26. Janas, M., "Arching Action in Elastic-Plastic Plates". Journal of Structural Mechanics. Vol.1, No.3. 1973. pp. 277-293.

27. Yee, T.P., "Compressive Membrane Action in Slabs With Non-Rigid Lateral Restraint". Journal of the Faculty of Engineering - University of Singapore - Singapore. Vol.1, December 1973. pp. 15-24.

28. Datta, T.K. and Ramesh, C.K., "Some Experimental Studies on a Reinforced Concrete Slab-Beam System". Magazine of Concrete Research. Vol.27, No.91. June 1975. pp. 111-120.

29. Jones, L.L., "Ultimate Load Analysis of Reinforced and Prestressed Concrete Structures". Chatto and Windus, London, 1962. pp. 248.

30. Wood, R.H., Discussion on "Ultimate Strength of Rectangular Concrete Slabs Under Short-Term Uniform Loading With Edges Restrained Against Lateral Movement". by Park, R., Proceedings of the Institution of Civil Engineers. Vol.32, September 1965, p.97.

31. Road Research, "Design of Concrete Mixes". D.S.I.R. Road Note No.4. London, H.M.S.O., 1950.